UTS UNIVERSITY OF TECHNOLOGY SYDNEY

Membrane Capacitive Deionization Using Ion-exchange Polymer Coated Electrodes for Resource Recovery from Wastewater

by David Kim

Thesis submitted in fulfilment of the requirements for the degree of

Doctor of Philosophy

under the supervision of Hokyong Shon

University of Technology Sydney
Faculty of Engineering and Information Technology

November 2020

Certificate of Original Authorship

Required wording for the certificate of original authorship

CERTIFICATE OF ORIGINAL AUTHORSHIP

I, David Kim declare that this thesis, is submitted in fulfilment of the requirements for the award of Doctor of Philosophy, in the School of Civil and Environmental Engineering/ Faculty of Engineering and Information Technology at the University of Technology Sydney.

This thesis is wholly my own work unless otherwise referenced or acknowledged. In addition, I certify that all information sources and literature used are indicated in the thesis.

This document has not been submitted for qualifications at any other academic institution.

This research is supported by the Australian Government Research Training Program.

Signature: Production Note:
Signature removed prior to publication.

Date: 14 November 2020

Collaborative doctoral research degree statement

I certify that the work in this thesis has not previously been submitted for a degree nor has it been submitted as part of the requirements for a degree at any other academic institution except as fully acknowledged within the text. This thesis is the result of a Collaborative Doctoral Research Degree program with Korea University.

ACKNOWLEDGEMENTS

First of all, I really appreciate my beloved wife, Gimun Gwak, for her sacrifice in support of my PhD study at UTS. Also, I would like to truly thank my parents, Dr. Kyunghoon Kim and Mrs. Haekyung Park, for their support and encouragement. I also Thanks also to my sister Dr. Johanna Inhyang Kim Kim. Without their support, I could not achieve a successful Ph.D. study outcome. My dear son, Haon Kim, I love you all from the bottom of my heart.

I would also like to thank my colleagues, Pema Dorji and Jade Jiaxi Jiang, for their sincere co-operation. Besides, I would like to appreciate the invaluable time and memories that I shared with my friends, Ralph Rolly Gonzales, Seongchul Ryu, Federico Volpin, Dr. Jungeun Kim, Dr. Myoung Jun Park, Dr. Yunchul Woo, Dr. Youngkwon Choi, Yunju Jo, Dr. Sungil Lim, Nawsahd Akther, Van Huy Tran, Syed Muztuza Ali, Minwei Yao, Ugyen Dorji, Dr. Nirenkumar Pathak, Jiawei Ren, Dr. Mohammed Johir, Dr. Leonard Tijing, and Dr. Laura Chekli.

I would like to express my heartfelt appreciation to my principal supervisor Prof. Ho Kyong Shon for giving me the opportunity to work with him at University of Technology Sydney. I also am very thankful to my co-supervisor Dr. Sherub Phuntsho for his encouragement, mentorship, and support. The thesis could not be completed without their supervision

Thanks to all the people I have met during my PhD career at University of Technology Sydney. The journey of my life in Sydney for a year and a half was truly unforgettable.

Book chapters and Journal Articles Published or Submitted**

1. Min Zhan, Gimun Gwak, **David Inhyuk Kim**, Kiho Park, Seungkwan Hong, Quantitative analysis of the irreversible membrane fouling of forward osmosis during wastewater reclamation: Correlation with the Modified Fouling Index, ***Submitted to Journal of Membrane Science***.
2. Pema Dorji, **David Inhyuk Kim**, Seungkwan Hong, Sherub Phuntsho, Ho Kyong Shon, Pilot-scale membrane capacitive deionisation for effective bromide removal and high water recovery in seawater desalination, ***Submitted to Desalination***.
3. HyunJun Chung, Jungbin Kim, **David Inhyunk Kim**, Gimun Gwak, Kyeongil Kim, Seungkwan Hong, Feasibility study of reverse osmosis–flow capacitive deionization (RO-FCDI) for energy-efficient desalination using seawater as the flow-electrode aqueous electrolyte, ***Submitted to Desalination***.
4. ***David Inhyuk Kim**, Ralph Rolly Gonzales, Pema Dorji, Sherub Phuntsho, Seungkwan Hong, Hokyong Shon, Efficient Removal and recovery of nitrate from wastewater in MCDI using a nitrate selective resin/anion-exchange polymer coated activated carbon electrode, ***Submitted to Separation and Purification Technology***.
5. Gimun Gwak, **David Inhyuk Kim**, Seungkwan Hong, Draw solutes for FO: Model, polymer hydrogels, and nanoparticles, Current Trendsand Future Developments on (Bio-) Membranes: Reverse and Forward Osmosis: Principles, Applications, Advances, (2019) 37-56.
6. ***David Inhyuk Kim**, Pema Dorji, Sherub Phuntsho, Seungkwan Hong, Hokyong Shon, Reuse of municipal wastewater via membrane capacitive

deionization using ion-selective polymer-coated carbon electrodes in pilot-scale, ***Chemical Engineering Journal***, 372 (2019) 241-250.

7. Gimun Gwak, **David Inhyuk Kim**, Seungkwan Hong, An integrated system for CO2 capture and water treatment by forward osmosis driven by an amine-based draw solution, ***Journal of Membrane Science***, 581 (2019) 9-17.
8. ***David Inhyuk Kim**, Pema Dorji, Gimun Gwak, Sherub Phuntsho, Seungkwan Hong, Hokyong Shon, Effect of brine water on ion discharge in membrane capacitive deionization and its implication on nitrogen recovery from wastewater, ***ACS Sustainable Chemistry & Engineering***, 7(13) (2019) 11474-11484.
9. Pema Dorji, **David Inhyuk Kim**, Sherub Phuntsho, Hokyong Shon, Bromide and iodide selectivity in membrane capacitive deionization, and its potential application to reduce the formation of disinfection by-product in water treatment, ***Chemosphere***, 234 (2019) 536-544.
10. *Jiaxi Jade Jiang[1], **David Inhyuk Kim[1]**, Pema Dorji, Sherub Phuntsho, Seungkwan Hong, Hokyong Shon, Phosphorus removal mechanisms from domestic wastewater by membrane capacitive deionization and system optimization for enhanced phosphate removal, ***Process Safety and Environmental Protection***, 126 (2019) 44-52.
11. **David Inhyuk Kim**, Gimun Gwak, Seungkwan Hong, Sustainable dewatering of grapefruit juice through forward osmosis: Improving membrane performance, fouling control, and product quality, ***Journal of Membrane Science***,578 (2019) 53-60.
12. Pema Dorji, Jongmoon Choi, **David Inhyuk Kim**, Sherub Phuntsho, Seungkwan Hong, Ho Kyong Shon, Membrane capacitive deionisation as an alternative to

the 2nd pass for seawater reverse osmosis desalination plant for bromide removal, ***Desalination***, 433 (2018) 113-119.

13. Gimun Gwak, **David Inhyuk Kim**, Seungkwan Hong, New industrial application of forward osmosis (FO): Precious metal recovery from printed circuit board (PCB) plant wastewater, ***Journal of Membrane Science***, 552 (2018) 234-242.
14. ***David Inhyuk Kim**, Gimun Gwak, Pema Dorji, Di He, Sherub Phuntsho, Seungkwan Hong, Hokyong Shon, Palladium recovery through membrane capacitive deionization (MCDI) from metal plating wastewater, ***ACS Sustainable Chemistry & Engineering***, 6 (2018) 1692-1701.
15. **David Inhyuk Kim**, Jongmoon Choi, Seungkwan Hong, Evaluation on suitability of osmotic dewatering through forward osmosis (FO) for xylose concentration, ***Separation and Purification Technology***, 191 (2018) 225-232.
16. Jungwon Kim, **David Inhyuk Kim**, Seungkwan Hong, Analysis of an osmotically-enhanced dewatering process for the treatment of highly saline (waste)waters, ***Journal of Membrane Science***, 548 (2018) 685-693.
17. Byeong Gyu Choi, **David Inhyuk Kim**, Seungkwan Hong, Fouling evaluation and mechanisms in a FO-RO hybrid process for direct potable reuse, ***Journal of Membrane Science***, 520 (2016) 89-98.
18. **David Inhyuk Kim**, Jungwon Kim, Seungkwan Hong, Changing membrane orientation in pressure retarded osmosis for sustainable power generation with low fouling, ***Desalination***, 389 (2016) 197-206.
19. Jungwon Kim, Bongchul Kim, **David Inhyuk Kim**, Seungkwan Hong, Evaluation of apparent membrane performance parameters in pressure retarded

osmosis processes under varying draw pressures and with draw solutions containing organics, ***Journal of Membrane Science***, 493 (2015) 636-644.

20. **David Inhyuk Kim**, Jungwon Kim, Ho Kyong Shon, Seungkwan Hong, Pressure retarded osmosis (PRO) for integrating seawater desaliniation and wastewater reclamation: Energy consumption and fouling, ***Journal of Membrane Science***, 483 (2015) 34-41.
21. Eunjeong Mun, Sangyoup Lee, **Inhyuk Kim**, Boksoon Kwon, Heedueng Park, Seungkwan Hong, Measurements of assimilable organic carbon (AOC) in high saline conditions using P17, ***Water Science & Technology: Water Supply***, 13 (2013) 265-272.

** Publications made during the PhD candidature include articles not related to the thesis.

* Articles related to the thesis.

Conference papers and presentation

1. Gimun Gwak, Jungwon Kim, **David Inhyuk Kim**, Seungkwan Hong, "Integrating system for carbon dioxide (CO2) capture and water reuse: Application of forward osmosis (FO) with amine-based draw solution", The 11th Conference of the Aseanian Membrane Society (AMS 11), July 3-6, 2018, Brisbane, Australia.
2. **David Inhyuk Kim**, Gimun Gwak, Seungkwan Hong, "Sustainable dewatering of grapefruit juice by forward osmosis (FO): FO performance, fouling control and product quality", The 11th Conference of the Aseanian Membrane Society (AMS 11), July 3-6, 2018, Brisbane, Australia.
3. Gimun Gwak, **David Inhyuk Kim**, Seungkwan Hong, "New Industrial Application of Forward Osmosis (FO): Precious Metal Recovery from Printed Circuit Board (PCB) Plant Wastewater", International Environmental Engineering Conference (IEEC), November 15-17, 2017, Jeju, Korea.
4. Gimun Gwak, **David Inhyuk Kim**, Jihoon Alex Lim, Seungkwan Hong, "New industrial application of forward osmosis: precious metal recovery", 8th IWA Specialist Conference on Membrane Technology for Water and Wastewater Treatment, November 05-09, 2017, Singapore, Singapore.
5. **David Inhyuk Kim**, Gimun Gwak, Sherub Phuntsho, Seungkwan Hong, Ho Kyong Shon, The potential of CDI for recovery of precious metals: Palladium from plating industry wastewater, International Conference on Capacitive Deionization, Electrosorption & Electrodialysis (CDI&E 2017), July 3-6, 2017, Seoul, Korea.
6. **David Inhyuk Kim**, Jongmoon Kim, Seungkwan Hong, "Feasibility of forward osmosis (FO) for food processing: A comparison to nanofiltration (NF)", 5th

IWA Regional Conference on Membrane Technology (IWA-RMTC), August 22-24, 2016, Kunming, China.

7. **David Inhyuk Kim**, Jungwon Choi, Seungkwan Hong, “A hybrid process of PRO-RO for sustainable water production with low fouling: Changing membrane orientation in PRO”, 5th IWA Regional Conference on Membrane Technology (IWA-RMTC), August 22-24, 2016, Kunming, China.
8. **David Inhyuk Kim**, Jungwon Kim, Junghyun Kim, Seungkwan Hong, "A hybrid process of pressure retarded osmosis and reverse osmosis (PRO-RO) for sustainable water-energy generation with low fouling, The 8th International conference on separation science and technology, July 5-8, 2016, Tianjin, China.
9. Byeonggyu Choi, **David Inhyuk Kim**, Seungkwan Hong, “Sustainability of forward osmosis-reverse osmosis (FO-RO) hybrid process: Water quality and membrane fouling", The 8th International Desalination Workshop, November 18-21, 2015, Jeju, Korea.
10. **David Inhyuk Kim**, Byeonggyu Choi, Seungkwan Hong, "Changing membrane orientation for pressure retarded osmosis (PRO) with low fouling”, The 8th International Desalination Workshop, November 18-21, 2015, Jeju, Korea.
11. **David Inhyuk Kim**, Seungkwan Hong, "Effect of pressure on performance of pressure assisted osmosis (PAO) membrane processes", International Environmental Engineering Conference (IEEC 2015), October 28-30, 2015, Busan, Korea.
12. Byeonggyu Choi, **David Inhyuk Kim**, Seungkwan Hong, "Innovation of osmosis membrane technology for the direct potable reuse of wastewater”, The 6th IWA-ASPIRE Conference &Exhibition, September 20-24, 2015, Beijing, China.

13. **David Inhyuk Kim**, Jungwon Kim, Junghyun Kim, Seungkwan Hong, " PRO for wastewater reclamation and seawater desalination with low energy consumption", 4th International Conference on Environmental Engineering, Science and Management, May 27-29, 2015, Chiang Mai, Thailand.
14. Jungwon Kim, Bongchul Kim, **David Inhyuk Kim**, Seungkwan Hong, "Evaluation of RSF in PRO prcess at the presence of organic matters", 7th International Desalination Workshop, November 5-8, 2014, Jeju, Korea.
15. **David Inhyuk Kim**, Jungwon Kim, Seungkwan Hong, "Pressure retarded osmosis (PRO) for seawater desalination and wastewater reclamation with low energy consumption", The 10th International Congress on Membranes and Membrane Processes, July 20-25, 2014, Suzhou, China.
16. Yoontaek Oh, Younggil Ju, **David Inhyuk Kim**, Jungwon Kim, Seungkwan Hong, Sangho Lee, Seukhun Lee, Menachem Elimelech, “Effect of externally induced hydraulic pressure on water flux in pressurized forward osmosis (PFO) with different membrane orientations", The 7th IWA Specialized Membrane Technology Conference and Exhibition for Water and Wastewater Treatment and Reuse, August 25-29, 2013, Toronto, Canada.
17. Jungwon Kim, Bongchul Kim, **David Inhyuk Kim**, Seokheon Lee, Seungkwan Hong, "Membrane fouling and analysis in pressure retarded osmosis", The 8th conference of the Aseanian Membrane Society, July 16-19, 2013, Xian, China.
18. **David Inhyuk Kim**, Bongchul Kim, Seungkwan Hong, “Developing the methods for evaluating FO membrane performance", The 5th International Desalination Workshop, October 28-31, 2012, Jeju, Korea.

Presentation made during the PhD candidature including proceedings, oral and poster presentations.

Abstract

In the face of major global challenging issues of water scarcity, the water industry has been undergoing a paradigm shift. The limited availability of nutrients resources, such as nitrogen and phosphorus, and their oversupply as fertilizer are projected to risk the global demands for food production. Therefore, the global needs of renewable resources have driven the wastewater facilities to recycle nutrients. Wastewater has been considered an important source of recoverable nutrients and other valuable materials, and thus, resource recovery from wastewater has become attractive where technological innovation is being used to provide additional social, environmental, and economic benefits.

Membrane capacitive deionization (MCDI), driven by an electrochemical potential between two electrodes across ion-exchange membranes (IEMs), has been shown to be an effective system for recovering valuable nutritional resources dispersed in wastewater via the enrichment and selective collection of the ions present in small amounts in low salinity wastewater resources. In particular, the recovery of nitrogen and phosphorus from municipal wastewaters has been noted as one of the most feasible targets to prevent environmental issues, such as the eutrophication of water resources and procuring these biological nutrients essential for food production. However, the application potential of MCDI for the resource recovery has not been verified due to lack of its full investigation from practical perspectives.

In this study, the application potential of MCDI was explored to recover nutrient resources present in wastewater, especially converging the ion selectivity and performance efficiency during electrosorption and electrode regeneration. Carbon electrodes coated with a thin cation- or anion-exchange polymer layer which acted as an

IEM in the conventional MCDI have been mainly used as an advanced configuration for the electrosorptive process with both inducing lower membrane electrical resistance and inhibiting the electrosorption of the counter-ions during regeneration of electrodes.

The ion transport during resource recovery via MCDI, from feed water to a carbon electrode in electrosortpion and then from the carbon electrode into highly enriched brine solution in regeneration, was examined. The ion discharge was retarded by a reverse-ionic strength gradient induced by the enriched brine solution. The regeneration was further hindered when a dilute feed solution concentration was used (<10 mM), attributing to the enhanced resistance of the ion-exchange (IX) layer. Energy-efficient regeneration methods, such as short-circuiting, were constrained owing to lack of electrochemically repulsive force capable of overcoming the reverse gradient. The preferential desorption order under a mixture of cations was $K^+ > Na^+ > Mg^{2+}$, as mainly determined by their physiochemical properties, whereas the permselectivity through the cation-exchange membrane (CEM) was insignificant.

The application potential of MCDI using IX layer coated electrodes was systematically explored demonstrating its effective performance in resource recovery from wastewater, and the operating conditions were optimized considering the complex nature of the characteristics of real municipal wastewater. A higher salt adsorption capacity and charge efficiency could be attained owing to the lower resistance induced by the thinly coated layer facilitating faster ionic transport. The organic substances had an insignificant impact on the electrodes' performance in a longer operation, as the fairly adsorbed negatively charged organic compounds were well released in the consequent desorption stage. The fouling-free operation was attributed to the flat morphology of the coated IX layer surface

with low roughness offering a smaller chance for the impurities to accumulate on the electrode surface.

The electrosorption selectivity followed the permselectivity through the IX layers, and was impacted by the change in their mobility under different applied potential. The selective electrosorption of NO_3^- can be enhanced by decreasing applied potential to increase relative ion mobility and by increasing water flow rate to reach faster electrode saturation. The recovery of phosphate has been examined considering the effect of phosphate speciation reactions at a typical pH range in wastewater (between 6.5 and 8.5). The overall P adsorption capacity was apparently higher in the lower pH, where $H_2PO_4^-$ dominantly presents in wastewater, owing to the smaller hydrated radii monovalent ions occupying less space within the electric double layer (EDL) for charge neutralization. However, the effect of phosphate speciation on selective phosphorus removal from wastewater was insignificant, as in reality it presents in a low amount compared to the other anions.

One of the major disadvantages of MCDI for resource recovery is the inability of electrodes to selectively remove target ions. Therefore, a nitrate selective composite electrode coated with an anion-exchange polymer with A520E resins was fabricated for enhanced recovery of nitrate. The low-contact resistance of the coated IX layer enhanced the electrosorption capacity, whereas the granular nitrate—selective resin incorporated in the IX layer rather increased the electrical resistivity. The adsorbed mole fraction of NO_3^- kept increased even after saturation, attributing to the ion exchange between Cl^- on the resin coating layer and NO_3^- contained in the bulk feed solution. However, its desorption efficiency for NO_3^- was lowered as the NO_3^- were temporarily intercepted by being

exchanged with Cl^- ions in the resin at the IX layer during the ion migration towards the bulk brine solution.

The possible application of MCDI was further tested on the recovery of palladium from metal plating wastewater. The highly efficient adsorption of Pd from a single Pd solution, higher than 98.38% even at 0.3 V of low applied potential, was driven by both electrosorptive and physical adsorption. Its removal was remained to be high even under co-existence of different cations present in the metal plating wastewater, since the Pd species with high initial concentration and ionic charge valency competitively took place within the EDL. High concentration of Pd was obtained after five successive operation cycles (925.48 mg/L) from a 100 mg/L Pd catalyst solution. However, an apparent decrease in Pd removal and desorption in the successive cycles implied the deterioration of electrodes attributing to physisorption or complexation of Pd metal ions within the porous structure of electrode, resulting in reduced available surface of area of electrode for additional electrosorption.

This thesis finally concludes with recommendations to provide future insights into realizing the practical use of MCDI for the recovery of resources from wastewater. The operating conditions of MCDI are important in order to achieve selective and highly efficient resource recovery. Enriching the target resource above a desired amount could be limited due to the reverse-ionic strength gradient. Reversing polarity is expected work best for discharging ions into brine, but however, its optimized condition has to be determined carefully as its energy demand could compensate the feasibility of MCDI. Employing lower potential and higher flow rate for selective nitrate removal may rather result in poor total removal of ions in the wastewater, whereas selective collection of phosphate at the current technological level is likely to be challenging due to its low

amount present in wastewater and low permselectivity through the IEM. The carbon electrodes can be customized for the enhanced extraction of target species by coating IX polymer solution. New coating techniques for a thinner selective layer incorporating micro-fine resins will further improve the charge efficiency and ion selectivity. The application of MCDI on recovery of precious metals requires preventive maintenance or cleaning strategies to inhibit the physisorption, complexation or crystal formation of the metallic species on the IX layer surface.

Table of Contents

List of Figures

List of Tables

CHAPTER 1

Introduction

1.1 Research background

Supplying fresh water has become one of the most challenging issues worldwide because of the over-exploitation and extensive pollution of conventional water resources (Miller 2006; Shannon et al. 2008). The global demand for potable water augmentation is therefore being increasingly promoted to allow exploration of new water resources. Reuse of wastewater resources has been proposed to relieve the imposed pressures of fresh water supply (Asano & Levine 1996; Elimelech & Phillip 2011; Gude, Nirmalakhandan & Deng 2010). Reusing wastewater resources can elicit both significant environmental and economic benefits by increasing water resource availability and by reducing the over-extraction of freshwater, thus, reducing discharged wastewater volume. However, the current practices of wastewater treatment remain at a basic level simply satisfying the water discharge regulations.

Apart from the significance of reuse of wastewater resources to solve the global challenges of water scarcity, the water industry has been undergoing a paradigm shift to resource recovery. Reclaiming valuable resources such as nitrogen, phosphorus, and other minerals from different wastewater sources is another important environmental and social issue because of the rising global demand for vastly depleting natural resources and nutrients (Penuelas et al. 2013; Prior et al. 2012; Tilton 2003). Apart from its use in desalination of low-salinity water resources, membrane capacitive deionization (MCDI) has been studied for possible applications targeting on resource recovery (Huang & He 2013; Huang et al. 2014; Huang, Fan & Hou 2014; Kim & Choi 2012; Kim, Kim & Choi 2013; Macías et al. 2014; Ryu et al. 2015; Ryu et al. 2013; Tang et al. 2015; Wang & Na 2014; Wang et al. 2017; Yang, Shi & Yang 2014; Yeo & Choi 2013).

MCDI, driven by electrochemical potential, extracts charged species from water by applying an electrical potential difference over two porous carbon electrodes across ion-exchange membranes (IEMs). It has been considered a potential alternative for reclamation of low-saline wastewater for removing charged ionic species, because of its energy-efficiency and eco-sustainability. As shown in Figure 1.1, the MCDI process comprises two steps: electrosorption to purify the water, where ions are immobilized on electrode pairs and followed by the desorption of ions, thus regenerating the electrodes. Its use in water treatment industry has reached to the early stages of commercialization leaded by Atlantis (USA), Voltea (Netherlands), AquaEWP (USA), Enpar (Canada), etc. This technology has been an important alternative and one of the most feasible technologies developed recently for sustainable freshwater production from unconventional water resources such as wastewaters (Porada et al. 2013a; Zhao, Porada, et al. 2013). Previous studies on the development of advanced materials of electrodes, effective process designs, and energy recovery have now improved this process drastically, making this technology a practical method for production of potable water. MCDI has been acknowledged potentially effective in the recovery of charged species by selectively collecting valuable ions present in small amounts in low salinity water. However, the potential of MCDI for possible resource recovery has not been demonstrated because of the lack of studies on resource recovery as most of the existing applications have focused on water production.

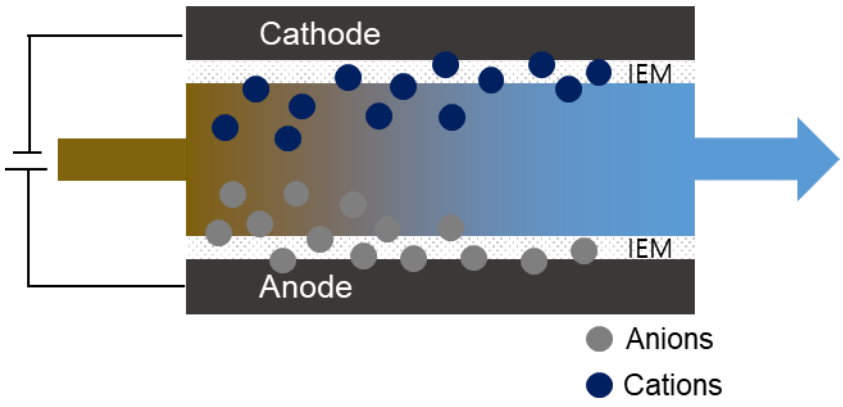

Figure 1.1. Schematic of an MCDI process. Upon an applied electrical potential between two porous carbon electrodes, ions attract toward the electrodes: cations toward the cathode (on top) and anions toward the anode (bottom).

Therefore, the main goal of this study was to explore the application potential of MCDI to recover resources from wastewater. Activated carbon electrodes coated with a thin ion-exchange (IX) membrane layer were used to induce lower electrical resistance, resulting in improved electrosorptive and regenerative performances. The ion transport in MCDI during resource recovery, from feed water to a carbon electrode in electrosortpion and then from the carbon electrode into a highly enriched brine solution in regeneration, under different solution compositions were examined. The applicability of IX layer coated MCDI as a resource recovery (i.e., nitrogen and phosphorus) process was assessed. The optimization of operating conditions for enhanced recovery has been carried out considering the complex nature of the characteristics of real municipal wastewater. Enhanced selective recovery of nutrients has been achieved by developing an ion selective electrode. The application of MCDI was expanded to the recovery of palladium waste from metal plating wastewater, which can be an economically viable precious metal that can be feasibly recovered.

1.2 Objectives and scope of the research

This study aimed to explore the potential application of MCDI for selective resource recovery from wastewater. The details of the research objectives are described as follows:

1. To investigate the fundamentals of selective electrosorption and ion discharge in MCDI during resource recovery (Chapter 4).
2. To evaluate the ion recovery performance of MCDI, especially in terms of ion selectivity and adsorption/desorption efficiency, and to optimize the operating parameters for enhanced selective removal of nutrient resources from municipal wastewater (Chapter 5 and 6).
3. To examine the effect of operating conditions and wastewater characteristics on resource recovery performance and improve the system design to improve the performance in pilot-scale (Chapter 5 and 6).
4. To develop an ion-exchange membrane layer coated electrode to increase its targeted selectivity of nutrients incorporating nitrate selective resins in an anion-exchange membrane layer on the surface of carbon electrode (Chapter 7).
5. To validate the potential applicability of MCDI on different target ionic resources, such as palladium from metal plating wastewater (Chapter 8).

1.3 Structure of the thesis

This dissertation contains nine chapters, some of which include published journal papers. Research backgrounds, objectives and scope of the study, and structure of the thesis are addressed in Chapter 1.

Chapter 2 covers literatures of fundamental theories in (M)CDI, progress of the electrosorptive technology, and previous studies on resource recovery.

Chapter 3 provides detailed information of materials and methods used in this studies.

Chapter 4 examines the ion transport behavior during resource recovery in MCDI under different solution compositions, especially the ion discharge into a high concentration brine during electrode regeneration. The findings were then utilized to explain the adsorption of nitrogen ions from wastewater effluent and their discharge into a high concentration brine. The results of this chapter was published on ACS Sustainable Chemistry & Engineering, which is entitled as "*Effect of Brine Water on Discharge of Cations in Membrane Capacitive Deionization and its Implications on Nitrogen Recovery from Wastewater"*.

Chapter 5 covers the MCDI for selective nitrate recovery from wastewater using ion-exchange polymer coated electrodes at both lab- and pilot-scales using synthetic and real wastewater effluents. The electrosorptive performance of the advanced electrodes, removal performance of different charged species from wastewater, influence of operating conditions on adsorption efficiency and ion selectivity for NO_3^-, and performance degradation in long-term operations were investigated in this study. The results from this study were published on Chemical Engineering Journal entitled "*Reuse of municipal wastewater via membrane capacitive deionization using ion-selective polymer-coated carbon electrodes in pilot-scale*".

Chapter 6 investigates the mechanisms of phosphorus removal in MCDI from domestic wastewater, considering the equilibrium system of phosphate under different pH, and optimized the system for its enhanced recovery. This work closely investigated the key mechanisms such as phosphate speciation and competitive sorption, and adjusting

operating conditions and solution compositions considering the complex nature of the characteristics of real domestic wastewater. The results from this work was published on Process Safety and Environmental Protection ("*Phosphorus removal mechanisms from domestic wastewater by membrane capacitive deionization and system optimization for enhanced phosphate removal*").

Chapter 7 introduces a NO_3—selective activated carbon electrode, by coating an anion-exchange polymer layer on the electrode surface with embedded A520E nitrate selective resins, for enhanced selective removal and recovery of NO_3^-. The electrosorptive performance of the coated electrodes, preferential electrosorption and desorption of major anionic species, and recovery of NO_3^- from real municipal wastewater effluent was investigated in this study. This chapter has been submitted to Desalination ("*Selective nitrate recovery from municipal wastewater for water reuse via membrane capacitive deionization*").

Chapter 8 expands the possible application of MCDI on recovery of palladium from metal plating wastewater to verify the potential of MCDI for the recovery of different charged resources from industrial wastewater. The experiments were carried out under various operating conditions and solution compositions. The long-term performances were measured in terms of the adsorptive and desorptive behaviors during multiple cycles of MCDI operations for enrichment of the Pd concentrate. The results from this chapter was published on ACS Sustainable Chemistry & Engineering ("*Palladium recovery through membrane capacitive deionization from metal plating wastewater*").

Chapter 9 provides a summary of major outcomes from the research to highlight the contribution of this work to knowledge, and includes recommendations to further improve resource recovery from wastewaters through the MCDI.

CHAPTER 2

Literature Review

2.1 Introduction

The present chapter provides a review of the MCDI process related to resource recovery from wastewater. This chapter introduces the background of the application of MCDI for resource recovery from wastewater sources. Various studies on different technologies for resource recovery are reviewed. The basic principles for introducing MCDI, studies on its potential applications, and its economic feasibility in terms of energy efficiency and energy recovery are also described in this chapter.

2.2 Water scarcity

The growth of world population, rapid climate change, massive urbanization, expanding agriculture, and higher standards of living have driven the global need for freshwater (Vörösmarty et al. 2000). The global population is increasing by 80 million per year, and is predicted to reach up to 9.1 billion people by 2050 (Nations 2015b). More than 50% of the world population is currently living in cities, and the accelerating urbanization is predicted to attract 6.3 billion people to cities by 2050 (WWAP 2012). The agriculture industry accounts for 70% of the consumption of world's freshwater withdrawals, whereas 15% of the total water in the world is extracted for energy production (Water 2014).

Thus, the continuously increasing demand for water supply has led to water scarcity (**Figure 2.1**), which recently has been perceived as one of the most concerning global risks (Mekonnen & Hoekstra 2016). In 2015, the World Economic Forum expressed sincere concerns over the potential global impact of water crisis (Forum 2015). A recent

study on water scarcity found that 4 billion people, which accounts for two-thirds of the global population, experience severe water shortage for at least a month every year (Mekonnen & Hoekstra 2016). Promoting sustainable use of water resources while meeting the growing demand for freshwater is now an important mission to perform (Hoekstra & Wiedmann 2014).

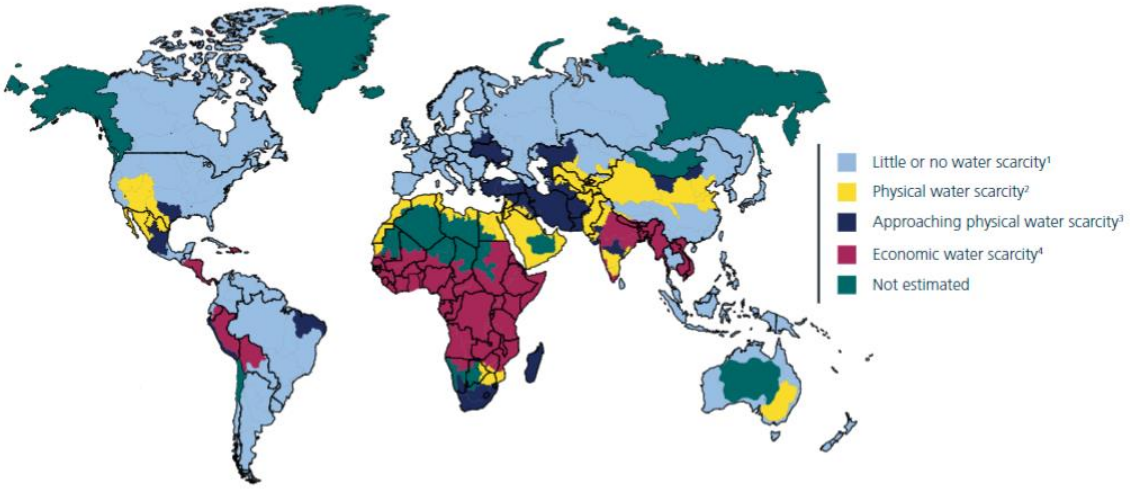

Figure 2.1. Global economic and physical water scarcity (Molden 2013).

2.3 Sustainable development of wastewater

The growing pressure on sustainable water development is a driving force to settle the wastewater challenge. Because of the depletion of accessible freshwater resources , 40% global water deficit by 2030 has been predicted (Connor 2015). In 2015, the United Nations adopted the 2030 Agenda for Sustainable Development to achieve 17 Sustainable Development Goals (SDGs) (Connor 2015) (**Figure 2.2**). The establishment of SDG 6, namely "Ensure availability and sustainable management of water and sanitation for all," reflects a particular interest for protection of eco-systems and

sustainable water management. A Target of SDG 6, Target 6.3, addresses the importance of wastewater management by minimizing pollution, improving water quality, and increasing sustainable water reuse.

Figure 2.2. 17 Sustainable Development Goals to be achieved by 2030 (Connor et al. 2017).

The world has been focusing beyond conventional water sources, and attempts are being made to seize the opportunity for exploiting new resources for supply. As depicted in **Figure 2.3**, 56% of 3928 km^3 of freshwater sources each year is discharged back to the environment in the form of wastewater (Mateo-Sagasta, Raschid-Sally & Thebo 2015). Wastewater, which has been regarded as an underestimated resource, is now considered a key element that must be efficiently managed for sustainable development of the aquatic ecosystem (Connor et al. 2017). The strong pressure on water resources is now driving

the desire for an improved approach for the management of wastewater (Bixio et al. 2008). Development of wastewater resources is expected to support the transition to a circular economy by drawing considerable environmental and economic and environmental values, such as procuring water availability, by reducing the over-discharge of wastewater, and ensuring wastewater quality.

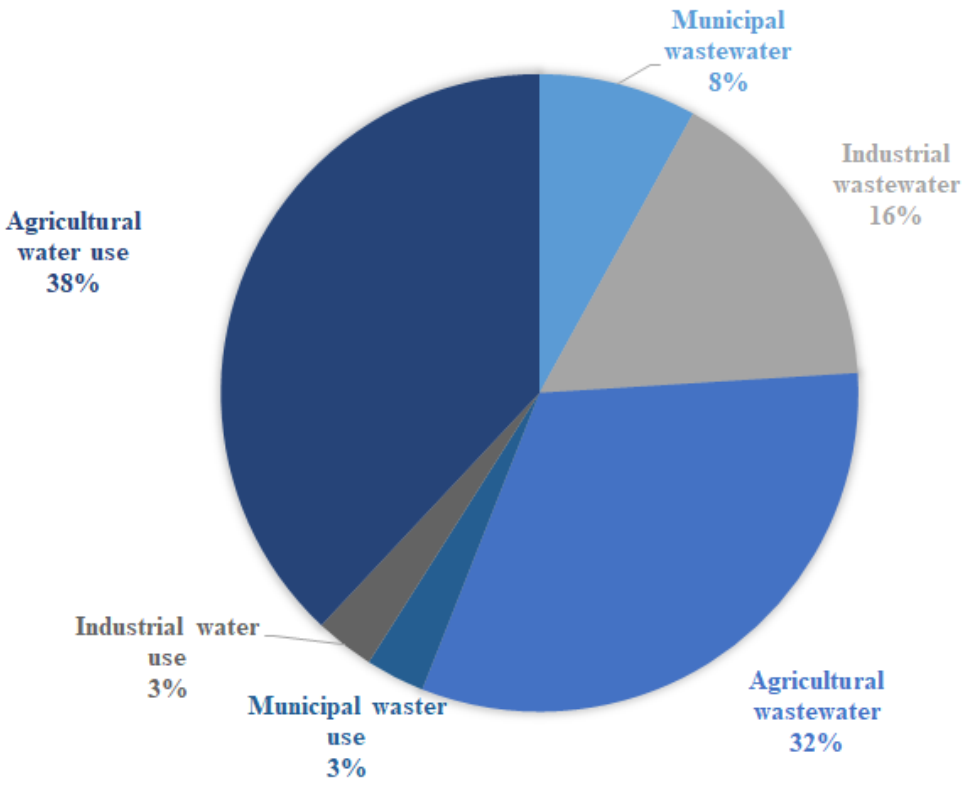

Figure 2.3. Global consumption of freshwater resources (Mateo-Sagasta, Raschid-Sally & Thebo 2015).

2.4 Municipal wastewater

Municipal wastewater is a by-product influenced by human use, especially from domestic, commercial, or agricultural activities (Connor 2015). Its composition varies depending on the range of pollutants released by any combination of the sources listed above. The specific constitution of wastewater varies and is determined by several factors, such as the degree of urbanization and industrialization and domestic water use. Suspended solids, bio- and non-bio-degradable organic compounds, nutrients, pathogens, inorganic dissolved solids, and heavy metals are the most common pollutants found in different wastewater sources (Hanjra et al. 2012).

The increasing release of municipal wastewater is a critical challenging issue that has to be overcome in the developing world. Therefore, the municipal wastewater sources offer opportunities for both securing stable resources for human use and minimizing the risks of water pollution to human and environmental health. The potential for municipal wastewater reuse can be evaluated by the level of wastewater contamination, water scarcity, water cost, and application target (Connor et al. 2017). Reuse of wastewater is principally driven by its economic feasibility (Haruvy 1998). Optimizing the cost for re-utilizing used water to lower than the cost of using traditional freshwater sources will drive wastewater reuse to become popular. Therefore, developing an advanced reusing technology that can be both economically feasible and eco-sustainably operated is strongly needed for the extensive application of an eco-friendly water reuse system.

2.5 Advanced wastewater treatment technologies

2.5.1 Adsorption

Adsorption is a developed technology that is generally utilized in wastewater treatment. Various materials have been developed and commercialized as absorbents, but most of the adsorption processes for wastewater treatment plants (WWTPs) adopt activated carbon because of its economic advantage. Numerous research works have applied activated carbon in various forms (e.g., powder (powered activated carbon; PAC), granules (granulated activated carbon; GAC), or granules with a biofilm (biological activated carbon; BAC)) to real WWTPs for water reuse. Therefore, it has been demonstrated that activated carbon is a feasible option at the large scale for municipal WWTPs because of its reasonable cost and performance (high removal of TSS, bacteria, coliphages, DOC, phosphorus, NH_4, and BOD_5). Sufficient removal of micro-contaminants can be achieved by adjusting the operating conditions such as the dose of activated carbon and contact time (Maurer et al. 2007) because various compounds can be adsorbed in activated carbon. Notably, however, the adsorption capacity of activated carbon needs to be continuously monitored. When the adsorption capacity is depleted, only biological degradation is performed by activated carbon, resulting in poor removal of micro-contaminants. Besides the cost for the regeneration of carbon or its replacement needs to be considered to demonstrate its feasibility.

2.5.2 Ozonation

Ozonation is one of the most widely applied technologies for reutilization of wastewater resource, and thus, various attempts have been made to utilize it in wastewater treatment. Several pilot-scale studies level have been conducted to study the removal of micro-contaminants and disinfection of water using ozonation systems after secondary treatment (e.g., biological treatment). A former study reported that compounds with aromatic rings or double bonds are easily eliminated below the detection limits with a dose of 0.8g O_3 g^-

[1] DOC (average value) owing to their high affinity for a direct reaction with ozone under acidic conditions (Duan & Gregory 2003). Effective disinfection of the effluent can also be achieved by the direct ozonation, thus satisfying the European standard for good bathing water quality (i.e., >95% removal of coliphage virus and >97% reduction in the concentration of fecal bacteria) (Maurer et al. 2007).

However, ozonation can unintentionally generate toxic by-products; several researches have shown an increase in toxicity of wastewater effluents owing to the formation of toxic by-products during ozonation (Clara et al. 2005; Kim et al. 2005; Vieno, Tuhkanen & Kronberg 2005). Bromate is a genotoxic carcinogen which is generated when wastewater containing bromide is ozonized (Kimura, Hara & Watanabe 2007). Moreover, nitrosamines, highly toxic to the liver, can be directly formed during ozonation (Duan & Gregory 2003).

2.5.3 Advanced oxidation processes (AOPs)

AOPs, including UV/H_2O_2, O_3/H_2O_2, photo-fenton and heterogeneous photocatalysis, can be defined as treatment technologies that utilize a hydroxyl radical for oxidation. The hydroxyl radicals are generated from a less reactive oxidant (i.e., H_2O_2 or O_3), and possess a significantly high standard reduction potential, which can oxidize various organic compounds. These technologies have been thus studied to degrade and mineralize recalcitrant organic matter from wastewater (González et al. 2016). Unfortunately, the practical application of AOPs to WWTPs has not been well-accomplished due to their low economic feasibility caused by the high costs for chemical use and/or intense energy consumption. Moreover, AOPs generally involve incomplete mineralization of micro-contaminants similar to the ozonation process, thus forming oxidation by-products.

2.5.4 Membrane-based technologies

Pressure-driven membrane-based processes, such as microfiltration (MF), ultrafiltration (UF), nanofiltration (NF), and reverse osmosis (RO), are widely utilized for the advanced treatment of municipal wastewater (González et al. 2016). In MF and UF, the governing separation mechanism is the sieving of contaminants; these processes have been applied to effectively remove turbidity of wastewater, but because of the relatively large size of membrane pores, the removal efficiency of micro-contaminants is generally moderate or low. Therefore, the MF/UF-based systems need to be integrated with other membrane processes such as NF or RO to achieve higher rejection of micro-pollutants. In NF and RO, the hydraulic pressure difference across the semi-permeable membrane drives the solution/diffusion-based ion and water separation mechanisms. NF and RO are generally used for further treatment of MR or UF permeate for surface water supply or potable water reuse from unconventional water source.

Although NF and RO membrane processes are considered the most advanced water treatment technology for removing various micro-pollutants, the generation of large volumes of brine stream constrains the eco-sustainability of this technology. Proper treatment and management strategies of brine are required to alleviate the detrimental impacts on the ecosystem (Nghiem, Tadkaew & Sivakumar 2009). The high energy demand caused by the high hydraulic pressure applied for operation is another challenging issue that needs to be solved. Lastly, membrane fouling can lead to concerns of the exacerbation of sustainable operation of the membrane process because an irreversible fouling layer is formed on the membrane surface which intensifies the membrane resistance.

2.5.5 Overall comparison

A comprehensive comparison of the four different technologies for advanced treatment of wastewater is presented in **Table 2.1**. All processes have been proved to be feasible at the pilot- and/or plant-scale WWTPs as demonstrated from previous studies, but each technology has certain strengths and weaknesses. For example, NF and RO Exhibit excellent performance in the rejection of various contaminants, but they inevitably generate concentrates. AOPs, likewise, present a high potential to remove micro-contaminants but further studies should be conducted at the full-scale level to sufficiently demonstrate their applicability.

Table 2.1. Comparison of different technologies for wastewater treatment for advanced wastewater treatment (González et al. 2016).

Technology	Strength	Weakness	Easily removed compounds	Hardly removed compounds
Adsorption (activated carbon)	• Adsorption of a wide range of contaminants • Easy operation and application • High removal of DOC	• Non-destruction of contaminants • Periodic regeneration required	Hydrophobic (Kow < 2.5) or positively charged micro-contaminants	Hydrophilic (Kow > 4) or negatively charged micro-contaminants
Ozonation	• No waste stream generation • Excellent disinfection • Excellent disinfectant • Oxidation of micro-contaminants	• Potential generation of toxic by-products • Poor removal of DOC	• Hydrophobic or positively charged micro-contaminants • Micro-contaminants with electron-rich moieties	Micro-contaminants with low affinity to O_3 direct reaction and HO
AOP	• No waste stream generation • Non-selectivity of OH • Rapid reaction rates	• Potential generation of toxic by-products • High chemical and/or energy consumption	Most target compounds due to the non-selectivity of OH	N.A.
Membranes (NF/RO)	• Reduction in labor requirement	• Non-destruction of contaminants	Hydrophobic, ionic compounds	Hydrophilic, non-ionic, and low molecular weight compounds

• Excellent removal of most inorganic and organic compounds and microorganisms	• Generation of concentrate • High energy consumption • High investment required

2.6 Wastewater-based resource recovery

Phosphorus is one of the most essential elements for growth of animals and plants (Filippelli 2002). Under natural conditions, phosphorus is the limiting nutrient in surface water because it prevents the growth of both algae and aquatic plants in water bodies. With the rising demand for food production, the need for fertilizers including phosphorus is consequently increasing (van der Salm, Kros & de Vries 2016). However, exhaustion of phosphorus and the fluctuation of economic feasibility for its production have been extensively addressed (Cordell, Drangert & White 2009). Phosphate rocks, which are the remaining phosphorus sources, are not renewable and are predicted to be exhausted within the next 30 to 300 years. The world population is facing critical risks of food supply as phosphorus cannot be replaced by other materials for the development of fertilizers (Matsubae et al. 2016; Mew 2016).

Nitrogen, which is one of the most important nutrients for growth of bio-organisms, exists in the N-cycle in forms of nitrate, nitrite, ammonium, and nitrogen gas (Smith & Smith 2015). The high amount of nitrogen gas in the air cannot be taken up by bio-organisms because of the stable chemical form of N_2. Therefore, N_2 is processed by biological nitrogen fixation and transferred to a reactive form of ammonium to be adsorbed by plants. Ammonium undergoes nitrification, which is the process of transformation from ammonium to nitrite, and a subsequent conversion from nitrite to nitrate. However,

because the consumption of ammonia for industrial use has exceeded N-sources from biological nitrogen fixation, concerns have been raised regarding the N-cycle being impaired, which can pose a potential risk to environmental and human health (Fowler et al. 2013).

The limited availability of nutrients resources, such as nitrogen and phosphorus, and their oversupply as fertilizers is projected to threaten the global demands for food generation. The current consumption of nutrients has been reported to be 19 million tons as phosphorus-P and 111 million tons as nitrogen-N (Batstone et al. 2015). Ledezma et al. (2015) suggested that for the development of fertilizers, a 1.8% increase in phosphorus supply is required to ensure stable food production (Ledezma et al. 2015). The massive consumption of these resources arouses concerns of the collapse of the circular food cycle and to encourage sustainable practices for the regeneration of nutrients (Cordell & White 2015).

Recently, the importance of reclamation of phosphorus and nitrogen from wastewater has been recognized because wastewater contains high amounts of those nutrients (Musfique et al. 2015). The current wastewater treatment practices including sedimentation, filtration, and oxidation processes are at the primary level of simply meeting the regulations for discharge of wastewater effluents. Normally, waste water treatment aims to remove phosphate, nitrate, and ammonium ions rather than recover the ions. Various open water sources are currently experiencing excess inflow of phosphate, ammonium, and phosphorus originated from human activities, which can cause concerns of accelerated eutrophication in aquatic systems, water quality impairment, aquatic species biodiversity decrease, and risk to human health. Nitrate, which is formed from the oxidation of ammonia, is regarded as a hazardous contaminant and can cause health issues

if consumed, such as reduced fertility, increased levels of methemoglobin in infants, stillbirths, and even death (Kim & Choi 2012). Strict removal of nutrients has been performed in previous studies various advanced water treatment technologies: biological treatment (Watsuntorn et al. 2019), electrocoagulation (Karamati-Niaragh et al. 2019), catalysis (Mendow et al. 2019), ion exchange (Johir et al. 2011; Liberti et al. 1981), ultrafiltration (Bahmani et al. 2019; Gao et al. 2019), RO (Epsztein et al. 2015; Schoeman & Steyn 2003), electrodialysis (Menkouchi Sahli et al. 2008), and adsorption (Senthil Kumar, Yaashikaa & Ramalingam 2019).

Rapid urbanization has seriously increased the municipal wastewater generation. However, this growth also provides opportunities for the water industry shift from its traditional role of purifying wastewater to advance roles by adopting innovative approaches. The potential of wastewater as a source of nutrients has remained under-exploited. However, the importance of nutrient recovery from domestic wastewater has been recognized nowadays. It was reported that 45-90% of phosphorus can be recovered, whereas 5 to 15% of the available nitrogen can be captured from wastewater (Mayer et al. 2016). To widen the accessible nutrient resources in an efficient manner, new approaches have been suggested to reclaim nutrients present in municipal wastewater (Chrispim, Scholz & Nolasco 2019). The global needs of renewable resources have driven wastewater facilities to recycle nutrients, such as nitrogen and phosphorus. Wastewater is now considered a potentially important source of recoverable nutrients and other valuable materials, and thus, resource recovery from wastewater has become a field where technological innovation is being used to provide additional social, environmental, and economic benefits (Connor et al. 2017).

Reclaiming inorganic nutrients in wastewater provides opportunities not only for the recovery of highly valuable nutrient compounds but also for reducing potential risks on human health and contamination of the aquatic ecosystem caused by the disposal of such compounds. Recovering nutrient resources from domestic wastewater can reduce the risks of eutrophication to some degree. Thus, the global warming issues can be relieved through their recovery (Bradford-Hartke et al. 2015). However, the technologies currently employed to recycle nitrogen and phosphorus from wastewater are still in the early phases of development because of economic barriers for application (Batstone et al. 2015).

2.7 Review of membrane-based technologies for resource recovery

This section provides a review of advanced technologies for attaining resource recovery by collecting valuable nutrients. Emerging membrane processes have been highlighted because they can possibly advance nutrient recovery from municipal wastewater. This is because they are well suited to solve the issues of low concentration of target nutrients present in wastewater by enriching the wastewater feed solution. Here, membrane-based technologies that enable resource recovery are extensively reviewed, and the future opportunities in this field are elucidated. **Table 2.2** summarizes the previous studies on future membrane technologies on the recovery of valuable nutrients. An overview of each resource recovery technology is described in the following sections along with discussions of their benefits and concerns in application on the wastewater industry.

Table 2.2. Literature of nutrient recovery from wastewater resource by membrane-based processes.

Driving force	Target nutrient	Wastewater source	Membrane technology	Removal	Driving energy
Pressure-driven	Urea, nitrogen, phosphorus (Pronk et al. 2006)	Synthetic wastewater	NF	Urea 10%; ammonium 55%; phosphate 94%	Pressure of 20 bar
	Phosphorus, potassium (Niewersch et al. 2014)	Digested sludge	NF	Phosphoric acid; 50%; potassium 30%	Pressure of 12 bar
	Phosphorus (Blöcher, Niewersch & Melin 2012)	Synthetic urine	NF	Phosphate 50%	Pressure of 25 bar
	Nitrogen, phosphorus, potassium (Maurer, Pronk & Larsen 2006)	Urine	RO	Ammonium 70%; phosphate; 73%, potassium 71%	Pressure of 50 bar
Osmotically-driven	Nitrogen, phosphorus, potassium (Zhang et al. 2014)	Urine	FO	Ammonium 50-80%; phosphate >90%; potassium >90%	N.A.
	Nitrogen, phosphorus (Hancock et al. 2013)	Secondary treated effluent	FO-RO	Nitrate> 72%; phosphate >99%	N.A
	Nitrogen (Xie et al. 2013)	Raw sewage	FO-MD	T-N >99%	Draw temperature 40°C
	Nitrogen, phosphorus (Hau et al. 2014)	Activated sludge	FO-NF	Ammonium >97%, phosphate >99%	Pressure of 80 psi
	Nitrogen, phosphorus (Xie et al. 2014)	Anaerobic sludge	FO-MD	Ammonium >90%; phosphate >97%	Draw temperature 40°C
Thermally-driven	Nitrogen (Zhao, Xu, et al. 2013)	Urine	Vacuum MD	Ammonia 41-75%	Feed temperature 50-70°C; vacuum pressure 9.5 kPa
	Nitrogen (Xie et al. 2009)	Synthetic wastewater	Sweep gas MD	Ammonia >96%	Feed temperature 65°C; sweep gas flowrate 3 L/min
	Nitrogen (El-Bourawi et al. 2007)	Synthetic wastewater	Vacuum MD	Ammonia >90%	Feed temperature 50°C; vacuum pressure 6.3 kPa

	Nitrogen (Ahn, Hwang & Shin 2011)	Synthetic wastewater	Direct contact MD	Ammonia >92%	Feed temperature 35°C; ammonia stripping solution 1M H_2SO_4
	Nitrogen (Qu et al. 2013)	Synthetic wastewater	Direct contact MD	Ammonia >99%	Feed temperature 55°C; ammonia stripping solution 0.1 M H_2SO_4
Electrically-driven	Nitrogen, phosphorus, potassium (Pronk, Biebow & Boller 2006)	Urine	ED with IEM	Concentration factor: ammonia 2.9; potassium 3.1; phosphate 2.7	Current density 22.5 mA/cm^2; current efficiency 50%
	Phosphorus (Zhang et al. 2013)	Municipal wastewater	ED with IEM	Concentration factor: phosphate 6.5	Current density 31.25 mA/cm^2; current efficiency 72%; energy 16.7 kWh/(kg PO_4^{3-})
	Phosphorus (Wang et al. 2013)	Synthetic wastewater	ED with IEM	Concentration factor: phosphate 4.2	Current density 71.5 mA/cm^2
	Phosphorus (Wang et al. 2013)	Excess sludge	ED with bipolar membrane	Concentration factor: phosphate 16	Current density 50 mA/cm^2; current efficiency 75%; energy 29.3 kWh/(kg H_3PO_4)

2.7.1 Pressure-driven membrane processes

Pressure-driven membrane processes, where water molecules diffuse from the feed side to the permeate through a mechanically stable membrane, have been widely used in the desalination of brine water and seawater industry. This technology is driven by hydraulic pressure higher to overcome the osmotic potential of the feed solution. High performance membranes with high salt rejection and water permeability, such as RO and NF, have shown significant potential for use in nutrient reclamation from wastewater (**Figure 2.4**). NF membranes have a pore size in the range of 0.2 to 2 nm with molecular weight cut-off from 200 to 1000 Da (Chuntanalerg et al. 2019). In general, multivalent ions that are larger in size than monovalent ions are mostly rejected by the NF membrane. The

molecular weight cut-off for RO membranes ranges from 0.1 to 1nm, at which all dissolved matters including most monovalent ions can be removed. RO membranes are normally driven at an operating pressure of 1.5 to 12 MPa. This membrane-based technology has been extensively studied for decades and is now widely applied for practical application in water treatment and wastewater treatment.

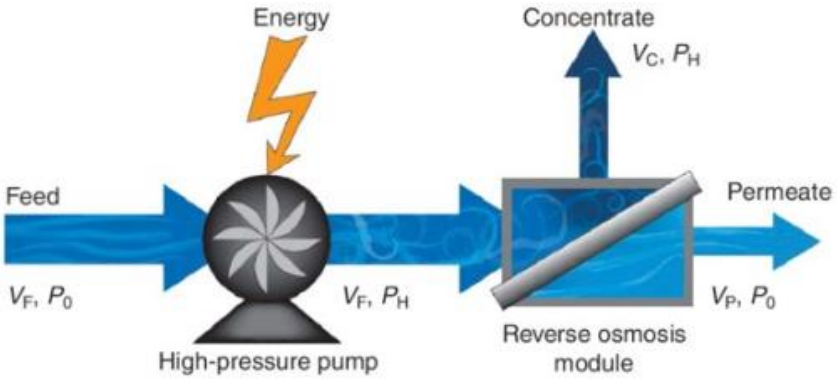

Figure 2.4. Schematic illustration of RO with a high-pressure pump (Elimelech & Phillip 2011).

The NF process for nutrient recovery from urine can achieve highly selective removal of phosphate with removal of 10% of urea, 55% of ammonium and 94% of phosphate (Pronk et al. 2006). Phosphate nutrients from wastewater and digested sludge were also collected, and 50% removal of phosphoric acid and phosphate was achieved with applied pressure ranging from 12 to 25 bar. The RO process for the recovery of valuable nutrients from urine successfully concentrated the feed solution by 5-fold.

However, RO and NF membranes are prone to membrane fouling caused by contaminants in wastewater, such as organic compounds, suspended solids, microbial growth, and precipitation of inorganic species. Hence, an extensive pretreatment to rule out those undesirable species may be required for the sustainable operation of pressure-driven membrane processes in nutrient recovery. Apart from pretreatment, these membranes also require frequent cleaning steps, which produces significant volumes of cleaning waste solutions that require further management.

2.7.2 Osmotically-driven membrane processes

The osmosis-based membrane processes, such as forward osmosis (FO), has been acknowledged as a suitable technological system to facilitate nutrient recovery from municipal wastewater. This technology, where pure water flows through a semi-permeable membrane from low-salinity water to high-salinity water, ensures a low concentration to be achieved with significantly low energy consumption due to the lack of hydraulic pressure (**Figure 2.5**). The early studies on FO also showed its strength in sustainable operation because FO is less prone to membrane fouling and a fouling layer is much more reversible (Lee et al. 2010), whereas the following works on membrane fouling during FO countered the ruling by demonstrating high fouling tendency (Lay et al. 2010; Nguyen et al. 2019; Zou et al. 2013). Several studies have demonstrated the capability of osmosis-based technologies to improve the efficiency of nutrient reclamation from various wastewater sources. This process can also simultaneously attain advanced wastewater treatment when integrated with a subsequent draw solution recovery stage.

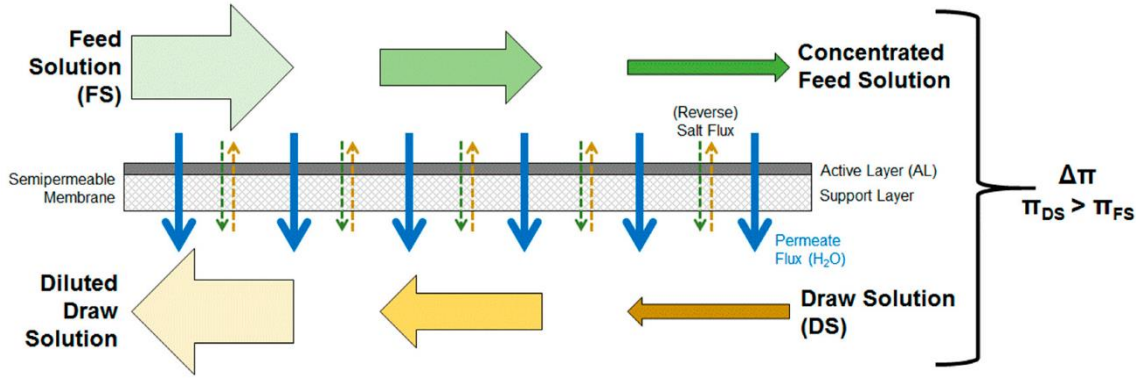

Figure 2.5. Schematic illustration of osmosis-based FO process (Haupt & Lerch 2018).

Reverse draw solution diffusion, the transport of draw solutes toward the feed wastewater stream, is expected to benefit the precipitation of struvite nutrient minerals. Xie et al. (2014 verified this concept by concentrating an anaerobic sludge by employing $MgCl_2$ as the draw solution and enriched the activated sludge to 5-fold higher concentrations, resulting in high nutrient concentration in the feed with 1210 mg/L of ammonium, 615 mg/L of phosphate, and some amount of magnesium which reversely diffused from the draw side (**Figure 2.6**) (Xie et al. 2014). These mass transfer characteristics of FO can drive nutrient reclamation for different wastewater feeds, such as urine, wastewater effluent, raw sewage, and sludge (Hancock et al. 2013; Hau et al. 2014; Xie et al. 2013; Zhang et al. 2014). The osmosis-based membrane process also demonstrated its merits of low fouling propensity during nutrient recovery. The nutrient-rich feed wastewater sources were well enriched in the long term, thus providing high concentration factors, even when activated and anaerobic sludges and raw sewage, which imply very high fouling potential, were concentrated (Hau et al. 2014; Xie et al. 2013, 2014). However, it

has to be noted that the technical limitations of FO such as low membrane performance and cost for draw solution recovery constrains its industrial application in recovery of resources from wastewater (Gwak et al. 2015).

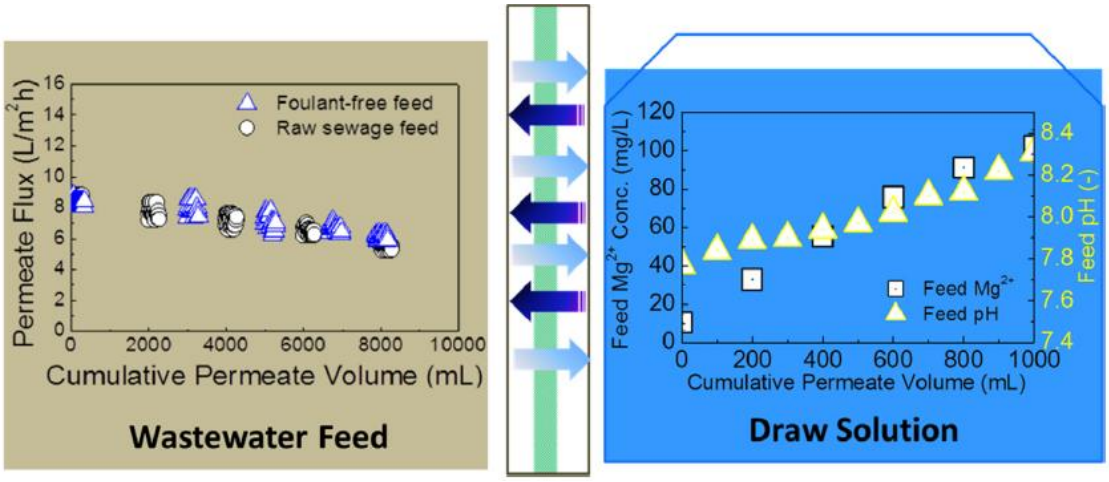

Figure 2.6. Beneficial reverse diffusion of draw solutes in FO promoting nutrient recycle from wastewater (Xie et al. 2014)

2.7.3 Thermally-driven membrane processes

Membrane distillation (MD) is a non-isothermal process where water permeates through a hydrophobic and microporous membrane driven by vapor pressure differences between two different phases across the membrane (Alklaibi & Lior 2005) (**Figure 2.7**). The aqueous water phase cannot pass through the membrane pores because of the hydrophobic nature of the MD membrane, whereas the increased partial vapor pressure caused by the increased temperature drives the transport of water vapor through the micropores of the membrane. This thermal-based membrane technology can achieve high amounts of

recovered water because the effect of feed osmotic pressure on the membrane process is not significant, unlike RO and FO. Furthermore, non-volatile contaminants and impurities are completely removed in the permeate as the transportation of water through the membrane is conducted only in the vapor phase.

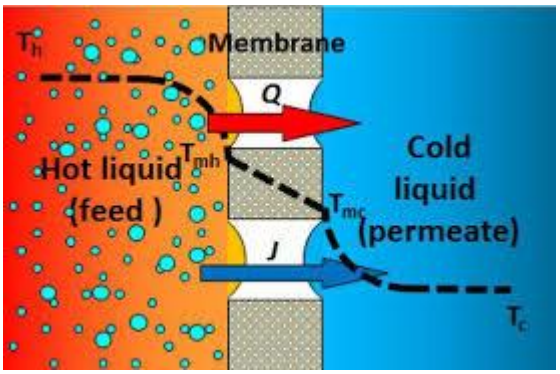

Figure 2.7. Schematic illustration of the basic principles of MD process (Shirazi, Mahdi & Kargari 2015).

The required installation size of an MD system is much smaller than other membrane-based technologies, whereas the heating energy needed is not too high because the desired operating temperature is below the liquid's boiling temperature.

Because of these unique features of MD, this thermally driven process has been studied for the recovery of valuable nutrients in wastewater. Phosphate was concentrated by MD in the feed side to enhance subsequent struvite precipitation. Ammonia recovery in wastewater has mainly been explored as one of the most possible applications of MD, where highly volatile ammonia can be selectively enriched on the permeate side (Zhao,

Xu, et al. 2013) (**Figure 2.8**). Each different configuration of the MD process, direct contact MD, vacuum MD, and gas sweeping MD has been utilized for the recovery of ammonia from varying wastewater sources, such as urine and municipal wastewater (El-Bourawi et al. 2007; Qu et al. 2013; Xie et al. 2009; Zhao, Porada, et al. 2013). Up to 99% of ammonia nutrients were reclaimed through the configuration of direct contact MD, when H_2SO_4 was employed as a stripping solution.

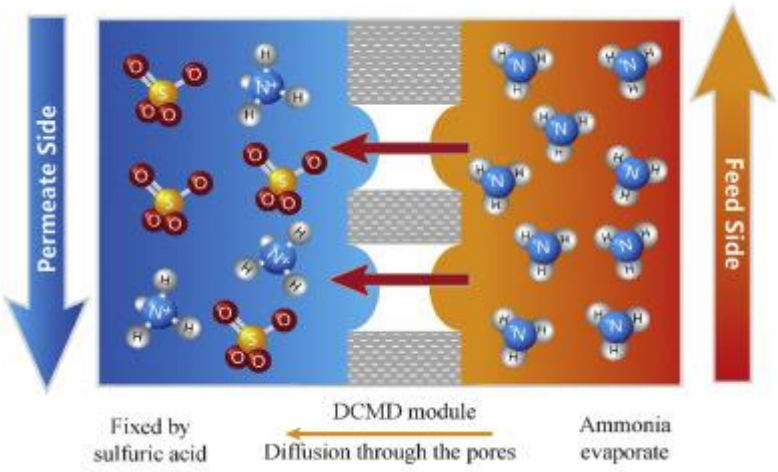

Figure 2.8. A direct contact MD process for the recovery of ammonia from wastewater using H_2SO_4 as stripping solution (Guo et al. 2019).

Controlling volatile organic impurities that can jeopardize the quality of enriched ammonia permeate stream is one of the most challenging issues in practical application of MD for ammonia recovery. Furthermore, wetting of the hydrophobic membrane pores by certain contaminants could lower the tension between the interfaces of liquid and vapor near the pores and hence could risk the sustainability of MD operation. Lastly, membrane fouling of MD caused by protein-like substances and peptides during ammonium

recovery, which reduces the hydrophobicity of the membrane surface, needs to be effectively controlled by implementing proper anti-fouling strategies (Zarebska et al. 2014).

2.7.4 Electrically-driven membrane processes

Electrodialysis (ED), in which charged species are migrated from a feed solution through ion-exchange membranes (IEM) to another solution under a direct current field driven by an applied potential difference, can be used to selectively collect nutrients from wastewater to produce high quality nutrient products. The separation of ionic species in the ED system is carried out by IEMs, anions passing through an anion-selective membrane, and cations through a cation-selective membrane. The characteristics of ion separation in ED offers an opportunity of selective nutrient recovery from wastewater (**Figure 2.9**).

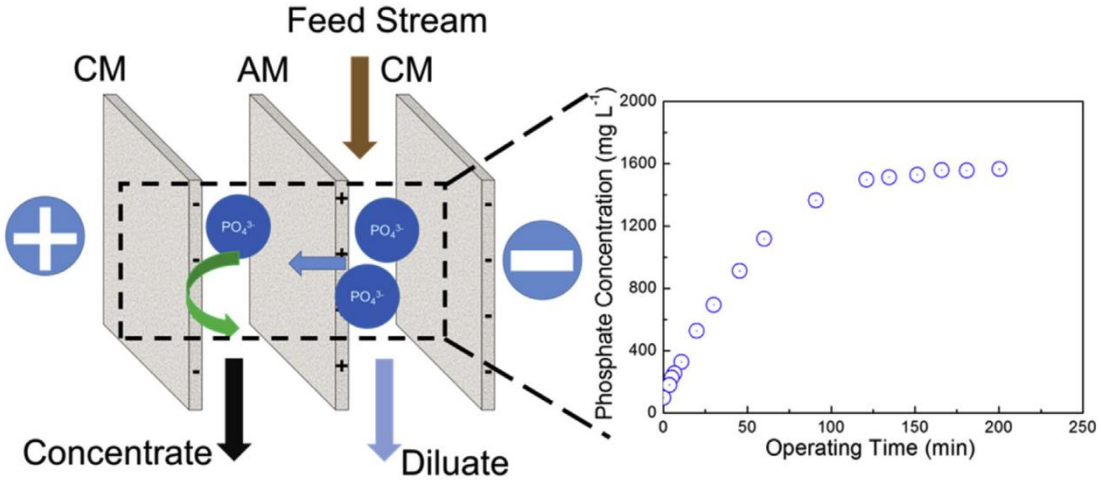

This ED system was studied for the recovery of phosphate from municipal wastewater

effluent, and an enriched solution containing phosphate with a concentration factor of 6.5 was obtained (Zhang et al. 2013). Enrichment of ammonium, phosphate, and potassium was also initiated from a urine feed solution, and the target minerals were concentrated by 3-times higher (Pronk, Biebow & Boller 2006). The selectivity of phosphate removal from urine under co-existence of different minerals can be enhanced by increasing the pH of the feed urine stream or increasing the applied potential difference (Tran et al. 2015). This is because slow ion transport of multivalent $H_2PO_4^{2-}$ and HPO_4^{3-}, which are the governing phosphate ions at high pH, widens the gap of diffusion rate of different ions through the IEM, leading to higher selectivity of ions. Adjusting the current density is also an efficient strategy for partitioning the different ions and achieving selectrodialysis for phosphate collection (Zhang et al. 2012). Besides a bipolar membrane, which is an IEM composed of both of cation- and anion-exchange layers through a junction layer, has been employed in the ED system. ED with bipolar membranes, named bipolar membrane ED, is a combined process of ED where the splitting of water into protons and hydroxide ions can be enhanced through the bipolar membranes (Tanaka 2007). This process can be differed from conventional ED, as ED transfers ions from one solution stream to another through IEMs where bipolar electrodialysis splits water into OH^- and H^+, generating acid and caustic streams. The bipolar membrane ED process has been used to enhance the efficiency of phosphate recovery from excess sludge, and a significantly high concentration factor of 16 was achieved for phosphate ions, which was more than 2-times higher than the concentration factor when using IEMs (Wang et al. 2013).

Even though nutrients from wastewater can be extracted with high selectivity and purity, the ED process is significantly prone to membrane fouling during resource recovery. The fouling layers on the IEM surface intensify the electric resistance, leading to current drop

and consequently exacerbated ED performance (Mondor et al. 2009). Specifically, the cation-exchange membrane was severely deteriorated by cationic calcium scaling, whereas organic fouling was found to be more problematic on the anion-exchange membrane because of the negatively charged organic compounds, such as protein and humic materials, attracted and accumulated on the membrane surface (Ayala-Bribiesca et al. 2006; Lindstrand, Sundström & Jönsson 2000).

2.8 Historical background theory in capacitive deionization

Several technologies, such as distillation, RO, and electrodialysis, have been studied recently and have been found to efficient for production of fresh water from unconventional water resources (Anderson, Cudero & Palma 2010; Zhao, Porada, et al. 2013). An electrochemical process called CDI, where ions are driven by the applied electrical potential over two porous electrodes to be transported from the bulk aqueous solution toward a porous carbon electrode surface, is one of the most feasible alternative technologies for sustainable demineralization.

CDI as an electrochemical desalination process was studied by Blair and Murphy in 1960 (Blair & Murphy 1960). Ions were initially assumed to be removable from water only when specific chemical groups on the carbon surface could undergo reduction/oxidation, followed by the formation of ionic binds between the ions in the electrolyte solution and the functional group on the carbon surface.

Evans and Hamilton followed up by clarifying the mechanism of electrochemical desalination using coulometric and mass balance analysis (Evans & Hamilton 1966). Their studies discussed ion adsorption on electrodes where an external potential is present

in the system and also attempted to elucidate the fundamental ion removal mechanism in CDI (Evans, Accomazzo & Accomazzo 1969; Evans & Hamilton 1966). They claimed that ion adsorption was mainly driven by Faradaic reactions, which is no longer considered to be the governing mechanism in driving the CDI system. Murphy and Caudle first described the desalination process using a mathematical method based on a capacitive mechanism in 1967 (Murphy & Caudle 1967). The integrated ion transport equations and mass balance of ions to describe the ion concentration as a function of operation time and the model results matched their experimental data under different operating conditions. Then, the electric double layer (EDL) theory was revealed to be the actual dominating mechanism of ion sorption in electrochemical deionization process (Johnson et al. 1970). In a further study (Johnson & Newman 1971a), a porous electrode model was developed to identify ion adsorption in porous carbon electrodes. They showed that the ion absorptive capacity of carbon electrodes can be determined by the electrical capacity of the EDL, surface area of the electrode, and the applied potential.

2.9 Electric double layer

In this section, the theoretical concepts to describe the electrochemical properties of ion transport for CDI are discussed. EDL has been used to explain the adsorption of salts and their charge storage in the pores within the carbon electrode particles. The EDL theory begins with the Helmholtz-model which describes charge separation across an interface between the carbon surface and electrolyte solution, with some excess charge in the carbon electrode surface being locally charge-compensated by its counter-charge (Helmholtz 1853). Considering that the EDL theory is an ideal situation for CDI, cations can be transferred to the cathode to compensate for the negatively charged carbon surface, whereas anions are transferred to the anode to compensate for the positively charged

electrode. Consequently, salt ions in the bulk solution passing through the spacer channel are removed.

However, the Helmholtz-model fails to completely explain that ions remain diffusively distributed in the EDL layer close to the carbon surface rather than condensing right next to the surface. Furthermore, an inner thin and compact Stern layer exist between the electrically charged surface and the diffuse layer, where charge is not contained (Stern 1924). The widths of the diffuse layer cannot be precisely defined; however, the ion concentrations in the layer progressively decrease with increasing distance from the electrode surface. This approach was made assuming that the diffuse layer within a micropore of a single carbon particle does not overlap with a nearby opposite carbon particle's. However, as the EDL layers formed within porous carbon particles' surfaces are almost placed close and be overlapped to each other, the diffuse layer has a finite extension, which is half of the distance between the two surfaces. At equilibrium, in the Gouy–Chapman model, the ion concentration profiles can be described by the Boltzmann distribution (Chapman 1913; Gouy 1910). The Gouy–Chapman theory describes that two options are available to compensate for charges on the carbon surface. The first is the adsorption of counter-ions on the diffuse layer, and the second is co-ion repulsion for the same charge built up at the surface.

2.10 Membrane capacitive deionization: Basics and principles

MCDI is a modified configuration of conventional CDI, which employs ion-exchange membranes (IEM) in front of two oppositely placed porous carbon electrodes (Biesheuvel & Van der Wal 2010a). Here, a non-conductive mesh spacer separates the two IEM-electrode assemblies with opposite charges. During the electrosorption stage, the ions in

the aqueous stream passing between the two opposite electrodes are removed and stored on the surface of the porous electrodes. During electrosorption, IEMs inserted directly in front of the porous carbon electrodes block the co-ions from exiting the electrodes. Because only the counter-ions can freely migrate into and out of the EDL and co-ions are blocked from the IEMs, a better salt removal efficiency can be expected in the MCDI process. In contrast, in conventional CDI without IEMs, the expulsion of co-ions leads to reduced salt removal efficiencies (Bazant, Thornton & Ajdari 2004). Consequently, the adsorbed ions can be freed from the EDL into the solution during electrode regeneration by reversing the applied potential, producing a concentrated brine stream. During regeneration, when a reversed polarity is employed for ion release in MCDI, the IEMs let the system to more fully deplete the regions of the counter-ions, thereby improving the salt adsorption capacity in the subsequent electrosorption cycle.

The electrosorption of ions in MCDI is dynamic, in which the physiochemical properties of carbon electrode and IEMS, as well as the flow profiles through the system, are significant. The design factors influencing the MCDI process mentioned above are not fully reflected yet in the developed models, and future studies need to consider the multi-dimensions of the Navier–Stokes equation for bulk stream flow, the Nernst–Planck equation for the ions' molecular transport, Poisson's equation for the electrical field, modifications for non-ideal behavior in the MCDI system (Biesheuvel 2009), electrostatic boundary conditions, and Faradaic charge transfer processes (Biesheuvel, Van Soestbergen & Bazant 2009).

A previous study developed a model for the MCDI process by modifying the model for conventional CDI without IEMs (Biesheuvel, Van Limpt & Van der Wal 2009). This model reflected the most significant parameters of the process such as channel volume,

flow rate, ion concentration, electrode area, and applied the potential to obtain the results of electrical current and effluent ion concentrations. The MCDI study presented a model considering the effects of IEMs such as the formation of stagnant diffusion layers (SDLs) on the surface of the membranes (Biesheuvel, Fu & Bazant 2012; Levich 1962). The Donnan equilibria for counter-ions on the internal and external membrane interfaces were also included in the model. The IEMs were assumed to be ideally permselective, i.e., they excluded co-ions perfectly. The MCDI model described both ion transport through the membrane and the EDL by steady-state description based on an assumption of local electroneutrality (Levich 1962).

An advantage of the MCDI over the conventional CDI process is that the co-ions repelled from the EDL during the electrosorption step lead to further adsorption of ions inside the macropores of the electrodes (Porada, Bryjak, et al. 2012a; Zhao, Satpradit, et al. 2013; Zhao et al. 2012). This implies that charge efficiency, which can be defined as the ratio between the ions removed from feed water and electrical charge applied, is close to unity in MCDI (Zhao, Biesheuvel & Van der Wal 2012). However, the minimum energy required to separate ionic species from the feedwater stream is greater than the thermodynamic minimum because of the additional energy loss caused by movement of ions. The energy used for the removal of charged species from the feed solution during MCDI is to a certain extent stored in the EDLs, and the stored energy is released back during electrode regeneration, when the adsorbed ions are freed from the carbon electrode to the bulk aqueous solution (Hou et al. 2008a, 2008b). It was reported that the energy released during electrode regeneration in MCDI can be recovered using the Capmix technique (Bijmans et al. 2012) and (Sales et al. 2010). Dlugolecki and van der Wal evaluated the recoverable energy values under different operational settings in MCDI and

verified that highly conductive IEMs may lead to a dramatically lowered electrical resistance (Długołęcki & van der Wal 2013). New electrodes with fast charge and discharge kinetics with higher capacity can also greatly enhance the performance of MCDI with lower overall energy consumption (Porada, Weinstein, et al. 2012; Suss et al. 2012).

2.11 Preferential order of electrosorption of ions

Because of the complex nature of the characteristics of real water and wastewater resources, ion selectivity in electrosorption and electrode regeneration in MCDI needs to be understood for efficient removal and recovery of target ions from the feed water stream. Several studies have investigated the effect of feed stream chemistry on the electrosorption where different ions are simultaneously present in the feed solution to determine the preferential order of ions (Liang et al. 2013). Experimental works on ion selectivity during electrosorption in conventional CDI have revealed that the preferential adsorption order can first be determined by the initial concentration of the ions present in the bulk solution, followed by the charge valency and the diffusion kinetics of the ions (Chen et al. 2015). Porous carbon electrodes favorably attract ions present at a higher concentration. In particular, ions with a higher charge valency are energetically more favorable for compensating the charge of the electrode surface. If the molar concentrations need to be the same, multivalent charge ionic species would be more electrosorbed on the carbon electrode surface than monovalent ions. Finally, if two different ions possess similar molar concentrations and yield the same charge valence, ions with smaller hydration radii are more preferentially adsorbed by the EDL because they diffuse faster toward the carbon pore EDL surface.

The selective electrosorption of different ions described above can be numerically explained by the extended Nernst-Planck equation. In the quantitative theoretical consideration of ion transport in IEMs, the ionic flux, *Ji*, can be described as follows (Luo, Abdu & Wessling 2018a):

$$J_i = J_{i,conv} - J_{i,diff} - J_{i,migr} = vc_i - D_i\nabla c_i - D_i c_i \frac{z_i F}{R_g T}\nabla\varphi, \quad i = 1, \dots, N_c \qquad (2.1)$$

Where v is the convective flow velocity and $J_{i,conv}$, $J_{i,diff}$, and $J_{i,migr}$ are the parts of the ion flux intensity of the ith component J_i, C_i, D_i, and z_i the concentration, diffusion coefficient, and ion valency of ion i, respectively,and φ the electrical potential. The equation shows the ion diffusion are significantly influenced by the ions' concentration and valency.

Based on a modified Donnan model which describes the micropores in the carbon particle by a single electrostatic potential, the concentration of ion i adsorbed within the micropore volume is then given by:

$$C_{i,mi} = C_{mA} \cdot \exp(-z_i \cdot \Delta\emptyset_d + \mu_{att}) \qquad (2.2)$$

Where $C_{i,mi}$ is the concentration of ion i in the micropores,C_{ma} the concentration in the macropores, z_i the ion valency, $\Delta\emptyset_d$ the Donnan potential difference, and u_{att} the terms for non-electrostatic adsorption (Biesheuvel et al. 2011a).

Because the electrosorption mechanisms in terms of selectivity in the diverse CDI processes have been extensively studied, many suggestions to optimize the selectivity and performance during resource recovery have been provided. However, only few experimental and theoretical studies on the preferential ion discharge during electrode regeneration during mineral recovery have been performed.

Several studies on CDI also developed theoretical models to predict the ion selectivity during electrosorption in a quantitative manner. A dynamic two-dimensional model based on non-linear theory was developed to present the time-dependent selectivity of different ions from a mixed solution in a conventional CDI process (Zhao et al. 2012). The dynamic transport model and the improved modified Donnan model were combined to illustrate the preferential order of electrosorption from multiple monovalent charged ions, especially targeting the selective adsorption of potassium over sodium (Dykstra et al. 2016). Suss suggested a size-based selectivity model reflecting the size of spherical counter-ions by explaining the ion volume exclusion interactions in the EDL (Suss 2017).

2.12 Energy efficiency and recovery in CDI

CDI has emerged as an alternative to the conventional desalination, wastewater treatment, and dewatering processes owing to its energy-efficient performance. To better understand the energy-efficiency of CDI, Zhao et al. (2013) compared the specific energy consumptions of MCDI and RO processes (Zhao, Porada, et al. 2013). MCDI was studied in a series of experiments using an MCDI stack containing 13 electrode cells, and NaCl was used at a concentration range of 0.4-5.2 g/L as feed solution. The results shown in **Figure 2.14** demonstrated MCDI can be economically competitive over conventional RO only if the initial feed solution concentration is lower than 2 g/L. This was attributed to the lack of high hydraulic pressure in MCDI. It has to be noted that this study did not optimize the MCDI system for practical use in the large scale; thus, the energy requirement can likely be further reduced by reducing the resistance and optimizing the system.

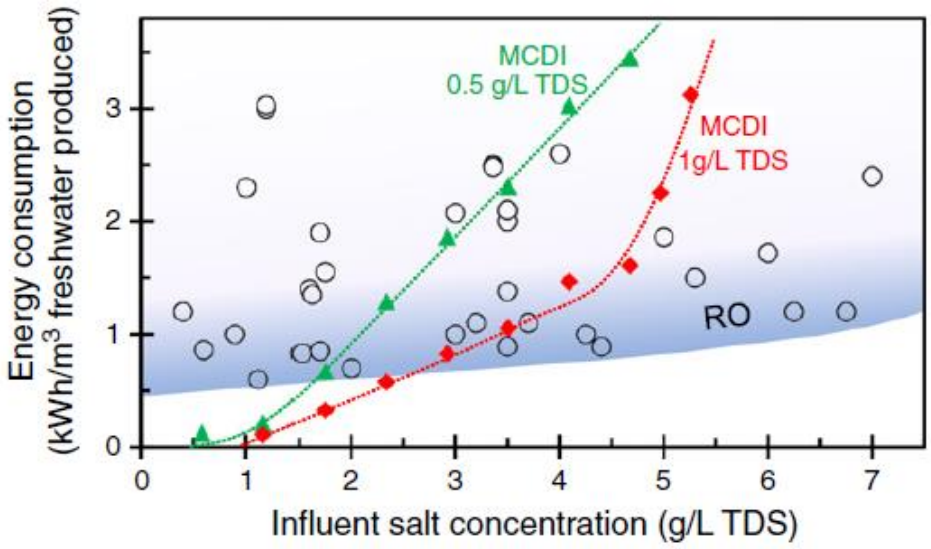

Figure 2.9. Comparison of energy consumption between RO and MCDI (Zhao, Porada, et al. 2013).

Dorji et al. (2018) compared the energy consumption between MCDI and RO during the 2nd-pass treatment of SWRO permeate within a TDS range of 25-300 mg/L (Dorji et al. 2018). The energy consumption of the 2nd pass BWRO unit in a desalination plant located in Perth, Australia, was reported to be 0.35 kWh/m^3, whereas the energy demand of MCDI for treatment of a feed with 300 mg/L TDS was 0.21 kWh/m^3 (40% lower than the BWRO stage). Furthermore, notably, further energy savings in MCD can be realized because up to 83% of the energy used during electrosorption was reported to be recoverable during electrode regeneration using an energy recovery device (Długołęcki & van der Wal 2013).

Palakkal et al. (2018) developed a thin sulfonated poly(ether ether ketone) CEM and a quaternary benzyl ammonium chloride poly(2,6-dimethyl 1,4-phenylene oxide) AEM to induce higher conductance through IEMs and achieved greater than 50% reduction in

energy use per ion removed (Palakkal et al. 2018). This study implied the importance of adopting a rational IEM design for the achievement of high MCDI efficiency.

The practical use of MCDI is expected to be more feasible when an energy recovery system can save the energy released during discharge of ions. Kang et al. (2016) integrated MCDI with a buck-boost converter as the energy recovery system and investigated the energy recovery ratio under various operating conditions (Kang et al. 2016). Up to 35% of the energy used in electrosorption could be recovered during the electrode regeneration with a higher capacitance and lower reference current of the super-capacitor. Chen et al. (2018) investigated the influence of the operational mode (constant current (CC) and constant voltage (CV)) and charge voltage/current and discharge current values on the consumption and recovery of energy in MCDI. Up to 46.6% energy used for electrosorption could be recovered by electrode regeneration (Chen, Yin, et al. 2018). This work correlated the increase of energy loss with an increase of charge voltage/current and discharge current, thus resulting in increased non-ohmic resistance. A reduction in the internal resistance in the MCDI system was observed to be the key for reducing dissipated energy. The energy recovery ratio was higher in the CC mode, attributed to the higher current in obtained CV mode. The lower energy recovery in the CV mode was likely due to the higher current resulting in an increase in the non-ohmic resistance, thus leading to more loss of resistive energy.

2.13 Applications of capacitive deionization

Apart from its use for saline water desalination, as shown in **Figure 2.10**, the possible application of (M)CDI has been expanded to other water fields. It has also been studied for other applications such as water softening, selective removal of contaminants, and

recovering mineral resources from wastewater (Huang & He 2013; Huang et al. 2014; Huang, Fan & Hou 2014; Kim, Yoon, et al. 2017; Kim & Choi 2012; Kim, Kim & Choi 2013; Macías et al. 2014; Ryu et al. 2015; Ryu et al. 2013; Tang et al. 2015; Wang & Na 2014; Wang et al. 2017; Yang, Shi & Yang 2014; Yeo & Choi 2013). This section reviews the potential of CDI for different applications. This especially focuses on the previous works on (M)CDI for mineral resource recovery.

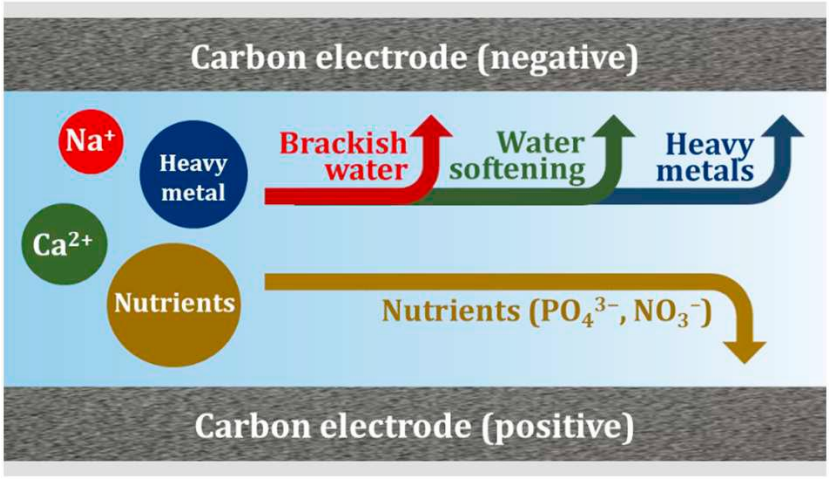

Figure 2.10. Schematic illustration of possible applications of (M)CDI (Choi et al. 2019).

2.13.1 A RO-CDI hybrid system for brackish water desalination

RO technology, which has been extensively used in the desalination field owing to its high desalting efficiency, has limitations of critical membrane scaling/fouling and high energy demand. Integrating RO with (M)CDI (RO-CDI process) is expected to compensate for the current limitations that RO is facing and achieve enhanced desalination performance with high energy efficiency. The hybrid process can be

categorized into two different configurations: a two-pass RO-CDI process for production of ultrapure water, and a two-stage RO-CDI system for enhanced water recovery (**Figure 2.11 and 2.12**).

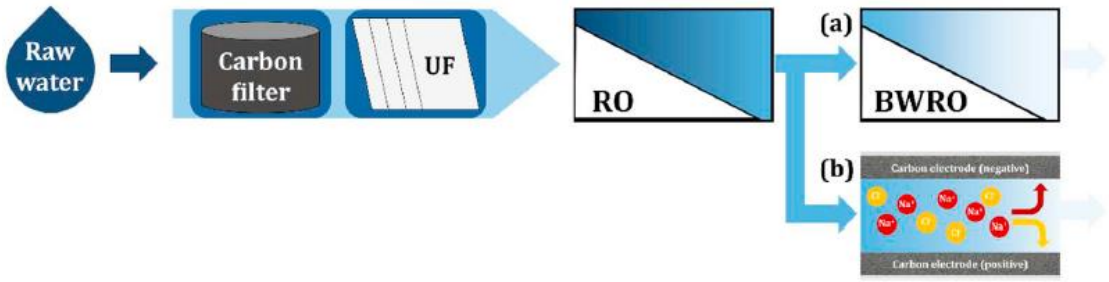

Figure 2.11. Schematic illustration of the two-pass (a) RO-RO system and (b) RO-CDI system for the production of high quality water (Choi et al. 2019).

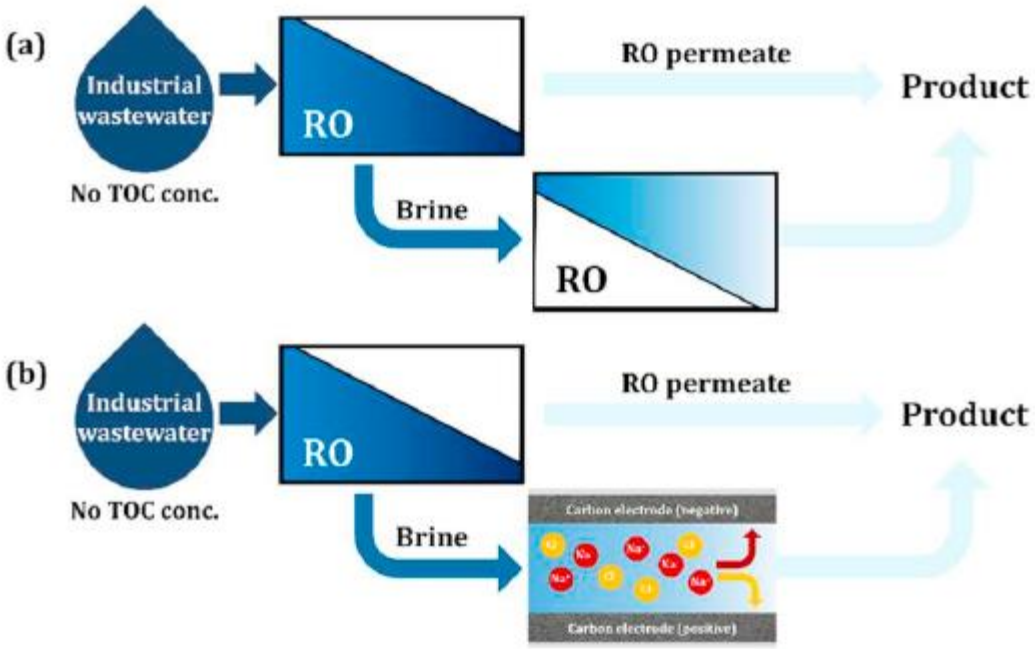

Figure 2.12. Schematic illustration of the two-stage (a) RO-RO system and (b) RO-CDI system for enhanced water recovery (Choi et al. 2019).

With the increasing demand for higher quality water, the RO permeate from various unconventional water resources needs to be treated further. Specifically, with the rising demand for ultrapure water (UPW), the two-pass RO process is widely used in current water industries to meet the high water quality standards. However, its significantly high energy use has led to the development of new alternatives, and a RO-CDI two-pass system has been delineated as one of the most possible technologies. The CDI process subsequent to RO was shown to be an energy-efficient polishing stage from previous studies (Jande, Minhas & Kim 2015; Minhas, Jande & Kim 2014). By optimizing this hybrid two-pass system, the resistivity of the final permeate reached 18.8 MΩ/cm, whereas another study adopting this configuration was able to produce pure water with a resistivity ranging from 2 to 9 MΩ/cm. CDI as a polishing stage for the purified water can be compared with electrode deionization (EDI), which is the standard approach used at industrial scale for production of pure water. EDI can be seen as an improved ED process for generation of ultrapure water. Its conventional module involves ion-exchanger resins and IEMs. Here the cations migrate towards cation-exchange resins passing through cation-exchange membrane, whereas the anions move towards anion-exchange resins passing through anion-exchange membrane.

The other possible hybrid configuration of RO and CDI, two-stage RO-CDI, has been proposed to meet the needs for enhanced overall water recovery of the current RO systems (Yu et al. 2013). The previous work on this hybrid system aimed at extracting more water

from RO brine and implemented various pretreatment processes for the removal of high amounts of organic matters present in the brine solution. The 497 mg/L TDS of permeate water was obtained from RO brine (1686 mg/L) via CDI, meeting the drinking water regulations of WHO. The energy consumption was 19% less than that for the two-stage RO-RO system, demonstrating the economic feasibility of the two-stage RO-CDI process.

2.13.2 Water softening through CDI process

Another possible application of CDI is water softening, a water harness reduction process that involves removing calcium and magnesium ions to prevent scaling issues (**Figure 2.13**). Ion-exchange, ED, and pressure-driven membrane processes have been widely studied as possible technologies for water softening (**Table 2.3**). CDI has been explored as a new process for water softening because the previously investigated technologies required high energy (Johnson & Newman 1971b; Pan et al. 2009; Seo et al. 2010).

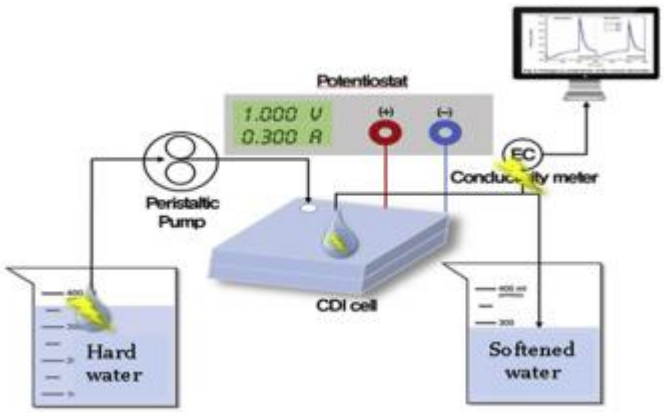

Figure 2.13. Schematic illustration of CDI for hardness removal (Tuan et al. 2015).

Table 2.3. Hardness removal via CDI under various operating conditions and electrode types ((Choi et al. 2019)).

Hardness concentration	Voltage (V)	Flow rate (mL/min)	Removal efficiency	Electrode type
350 mg/L, $CaCO_3$	1.5	4	73%	CDI with carbon cloth electrode (Seo et al. 2010)
10 mM, $CaCl_2$	1.2	2	14.2 mg Ca^{2+}/g	CDI with Ca-alginate coated electrode (Yoon et al. 2016)
35mg/L, $CaCO_3$	2	10	3.5 $CaCO_3$/g	CDI with reduced GO electrode (Tuan et al. 2015)
46 mg/L, Ca^{2+}	1.2	28,000	74%	MCDI with porous carbon electrode (van Limpt & van der Wal 2014)
5.1 mg/L, Mg^{2+}	1.2	28,000	71%	MCDI with porous carbon electrode (van Limpt & van der Wal 2014)
1.45 mM, Ca^{2+}	2	10	58%	CDI with activated carbon electrode (Hou & Huang 2013)
2.41 mM, Mg^{2+}	2	10	47%	CDI with activated carbon electrode (Ayala-Bribiesca et al. 2006)
2.5 mM, $CaCl_2$	1.5	-	98%	CDI with SiO_2 coating electrode (Wouters et al. 2018)
3 mM, $CaSO_4$	1.2	110	4.38 mg, $CaSO_4$/g	CDI withSiO_2 coating electrode(Lado et al. 2014)

Ca-alginate, an eco-friendly cation-exchange polymeric material forming a gel layer on the carbon electrode's surface in a gel form via Ca^{2+} substitution reaction (Aslani & Kennedy 1996; Sata 2007), attained more than 14.2 mg Ca^{2+}/g of salt adsorption owing to their significantly increased charge efficiency (from 55% of conventional CDI to 85% of Ca-alginate CDI) (Yoon et al. 2016). Nearly 44% of Ca^{2+} was removed by SiO_2-coated activated electrode (Wouters et al. 2018). Apart from coating materials dramatically improving the hardness removal efficiency, modifying the carbon electrode material can also greatly impact Ca^{2+} removal. The removal of Ca^{2+} reached up to 98% when SiO_2 was coated on carbon foam or nanofoam type electrode materials, whereas the Ca^{2+} removal by SiO_2-coated carbon remained at 16% (Wouters et al. 2018). In addition, better Ca^{2+} removal was reported for a carbon cloth material over composite electrodes because of

the higher wettability of carbon cloth (Seo et al. 2010). In this work, improved ion selectivity for divalent ions through optimizing the pore size of the electrode carbon material was observed.

Earlier studies on CDI have demonstrated the distinct advantages of CDI for its use in water softening. Currently, a commercial modular-based CDI unit, fabricated by Voltea, Netherlands, is now practically used for water softening. However, its sustainable use is hindered by scaling on the spacer within the flow channel and on the IEM. Further long-term operation is needed for the demonstration of CDI in real-scale.

2.13.3 CDI for resource recovery

Reclaiming mineral sources such as nitrogen, phosphorus, and metal ions from wastewater and saline water has been suggested as an environmentally sustainable solution to the rising global need for mineral resources and nutrients which are being depleted (Penuelas et al. 2013; Prior et al. 2012; Tilton 2003). CDI, which is an electrochemically driven process based on the separation of charged species, has been shown—in the past—to be an effective system for recovering mineral resources via the enrichment and selective collection of ions present in minute amounts in low salinity water resources.

Heavy metals dissolved in wastewater resources also have been studied as possible target mineral ions to be reclaimed via CDI (**Table 2.4**). The experimental studies on copper removal showed CDI to be a useful process for extraction of Cu^{2+} from wastewater with high preferential adsorption over natural organic matters (NOM) and NaCl in a

competitive environment (Huang & He 2013; Huang, Fan & Hou 2014). The studies on the recovery of lithium ions via CDI showed high removal performance with faster adsorption and desorption kinetics over several cycles than a conventional lithium reclamation process (Kim, Yoon, et al. 2017; Ryu et al. 2015; Ryu et al. 2013). A binder-free carbon nanotube porous electrode was found to offer increased electrochemically adsorptive surface area, leading to higher removal of chromium ions (Wang & Na 2014), whereas lead ions present in aqueous solution were more easily collected by an air-plasma treated carbon nanotube electrode (Yang, Shi & Yang 2014).

Table 2.4. Removal of heavy metals via MCDI under various feed chemistries and electrode types.

Heavy metal	Concentration	Electrode type	Removal	Ref.
Arsenic	0.02-0.1 mg/L	Activated carbon	86-98%	(Zhang et al. 2016)
	0.1-200 mg/L	Activated carbon	0.01-0.025 mg, As(V)/g	(Fan et al. 2016)
Lead	5-100 mg/L	3D graphene	60-99%	(Liu et al. 2017)
Cadmium	0.5 mM	Activated carbon	32%	(Huang et al. 2016)
Chromium	0.5 mM	Activated carbon	52%	(Huang et al. 2016)
	2mg/L	Carbon aerogel	99.6	(Rana-Madaria et al. 2005)
	0.035 mg/L	Carbon aerogel	94%	(Farmer et al. 1997)
Copper	50 mg/L	Activated carbon	>90%	(Huang, Fan & Hou 2014)

Several studies on CDI have investigated its suitability for recovering nutrients and minerals (**Table 2.5**). In particular, the recovery of nitrogen (Kim & Choi 2012; Kim, Kim & Choi 2013; Tang et al. 2015; Wang et al. 2017; Yeo & Choi 2013) and phosphorus (Huang et al. 2014; Macías et al. 2014) from municipal wastewaters has been noted to be one of the most feasible targets for reclamation to prevent environmental issues such as

the eutrophication of water resources; furthermore, procuring these biological nutrients is essential for food production (Conley et al. 2009; Majumdar & Gupta 2000).

Table 2.5. Recovery of nutrient resources via MCDI under various feed chemistries and electrode types.

Nutrient	Concentration	Electrode type	Removal	Ref.
Phosphate	50 mg P/L	Conventional CDI	86.5%	(Huang et al. 2014)
	300 mg P/L	Conventional CDI	77.4%	(Huang et al. 2014)
	500 mg P/L	MCDI	17.5 mmol	(Huang et al. 2017)
	3.2 mg P/L	Activated carbon cloth	80.7%	(Ge et al. 2018)
	81.5 mg P/L	LDHs/AC composite electrodes	26.2 mg P/g	(Zhu et al. 2019)
Nitrate	300 mg/L	Conventional CDI	90%	(Tang et al. 2015)
	100 mg N/L	Charge-barrier CDI	98%	(Broséus et al. 2009)
	2.0 mM	Ion selective electrodes	19 mmol/m^2	(Kim & Choi 2012; Yeo & Choi 2013)
	1.6 mM	SiO_2 and Al_2O_3 coated asymmetric electrodes	50%	(Lado et al. 2017)

A pilot-scale CDI process was tested to evaluate its removal capacity, and 86.5% and 77.4% of phosphate ions were recovered from feed waters containing 50 and 300 mg/L phosphate, respectively (Huang et al. 2014). Huang et al. (2017) investigated the impact of pH on the phosphate removal and suggest to lower the pH for optimum P removal where monovalent P species is more dominant (Huang et al. 2017). The effective removal and recovery of phosphate was demonstrated by Ge et al (2018) (Ge et al. 2018). This study pointed out the limitations of conventional CDI systems for targeted recovery of phosphate due to its poor selectivity. Another study of CDI developed LDHs/activated carbon composite electrodes to examine the influence of various experimental parameters on the electrosorptive removal of phosphate (Zhu et al. 2019). The collection of phosphate by Mg-Al LDHs/AC electrodes reached 80.43 mg PO_4^{3-}/g carbon, under cirucmneutral

pH and low ionic strength. The co-existing anions hindered the lowered the adsorption of phosphate mainly due to the occurrence of a compressed electrical double layer.

A series of pilot-scale studies used the same system to test the CDI performance for a mixture of nitrate and NaCl solutions (Tang et al. 2015). A commercial CDI test unit was used to evaluate its capability for removal of nitrate from wastewater, which resulted in 88-98% removal (Broséus et al. 2009). Nitrate removal was further studied by coating carbon electrodes with anion-exchange resins, attaining high nitrate selectivity (BHP 55) (Kim & Choi 2012; Yeo & Choi 2013). The resin used for coating the electrodes enhanced nitrate selectivity over selectivity for other anions from synthetic wastewater solutions. Another study employed asymmetric electrodes coated with SiO_2 and $Al_2O_3^-$ and attained higher nitrate removal compared to the uncoated symmetric electrodes, owing to the faster ion transport induced by the decreased hydrophobicity and increased specific area of the carbon surface. (Lado et al. 2017). Besides, Hu et al. (2018) developed a Pd/NiAl-LMO coated electrode which effectively captured nitrate and converted nitrate to nitrogen during electrode regeneration (Hu et al. 2018).

2.14 Conclusion

Recently, (M)CDI has emerged as one of the most promising alternative desalination processes to obtain fresh water from low salinity brackish water resources. While the current practices in wastewater management mainly focus on water treatment technologies, new innovative solutions are emerging for future trends in wastewater management that increasingly focus on resource recovery. Apart from desalting ions from wastewater to produce fresh water, the electrosorptive process has good potential for reclaiming mineral resources from aqueous solutions. Although replacing the current

recovery technologies is challenging, M(CDI) is an attractive option considering its low energy consumption during ion capture from low salinity water. However, the feasibility of MCDI still remains to be demonstrated in practice, and the mechanisms of ion discharge into brine solutions for enriching charged ionic species have not been fully investigated yet. In this thesis, experimental work systematically addressed these challenges for solutions with different chemical compositions, electrode characteristics, and operating conditions. This chapter demonstrates the significance of this thesis, investigating the mechanisms of ion desorption in MCDI and its implication on mineral recovery from wastewater resources by providing a brief review of the studies on M(CDI) conducted to date.

CHAPTER 3

Materials and Methods

3.1 Introduction

The experimental works made in the thesis cover performance evaluation of MCDI for use in resource recovery via bench-scale CDI/MCDI and pilot-scale MCDI set-ups, surface modified activated carbon electrodes, and characterization techniques. The details of the experimental methods are described in this chapter.

3.2 Experimental materials

The porous activated carbon electrodes supplied by Siontech Co. (Republic of Korea) were made of a graphite body sheet with coating a carbon slurry composed of activated carbon (P-60, Kuraray Chemical Com., Japan) and PVDF binder (Inner Mongolia 3F-Wanhao Fluorine Chemical Co. Ltd., China). The total carbon mass topped on the 10 x 10 cm^2 sized graphite body sheet was reported to be 0.8 g. Cation and anion exchange membranes (Neosepta CMB and AFN, respectively) used in the experiments were obtained from Astom Corporation (Japan). Cation- and anion-selective polymers were provided by Siontech Co. (Republic of Korea) for electrode coating by mixing with N-methyl-2-pyrrolidone (NMP, Sigma-Aldrich, USA). NO_3-selective A520E resin, which has a polymer structure of a macroporous polystyrene cross-linked with divinylbenzene with quaternary ammonium functional groups (in chloride form; particle size: 300–1200 μm) were used for fabrication of NO_3-selective carbon porous electrode. A Millipore Milli-Q water system (United States) was used for production of deionized (DI) water. All the chemicals used for preparation of synthetic solutions were purchased from Sigma Aldrich (United States). All chemicals were used as received.

3.3 Fabrication of ion-exchange polymer coated carbon electrode

A cation-exchange polymer solution with a sulfonic acid group was used for the fabrication of cation-exchange polymer coated electrode. The IX capacity of the polymer solution was reported to be 1.7 meq/g. A 20 wt% solution of the cation—selective polymer blended with NMP by vigorously stirring at 20 ºC for 24 hr. An anion-exchange polymer was prepared by introducing tertiary amine groups after the chloromethylation of polystyrene. The IX capacity of the dry anion-exchange polymer was 1.5 meq/g in average. For the preparation of the NO_3—selective anode, A520E resin was firstly dried at 80 ºC for 24 hr followed by pulverization with a ball mill. The ground resin powders were then sieved with a 50 um sized stainless-steel mesh, consequently mixed with the 12 wt % anion-exchange polymer solution with a 1:1 polymer-to-resin weight ratio. The cation- and anion-selective electrodes were coated with the uniformly mixed coating solutions using a casting machine (Elcometer 4340, Elcometer (Asia) Pte Ltd, Singapore), as shown in **Figure 3.1**, and dried at 50 ºC for 12 hr. The surface of the ion-selective electrodes was completely covered by a 50 μm thick polymer layer.

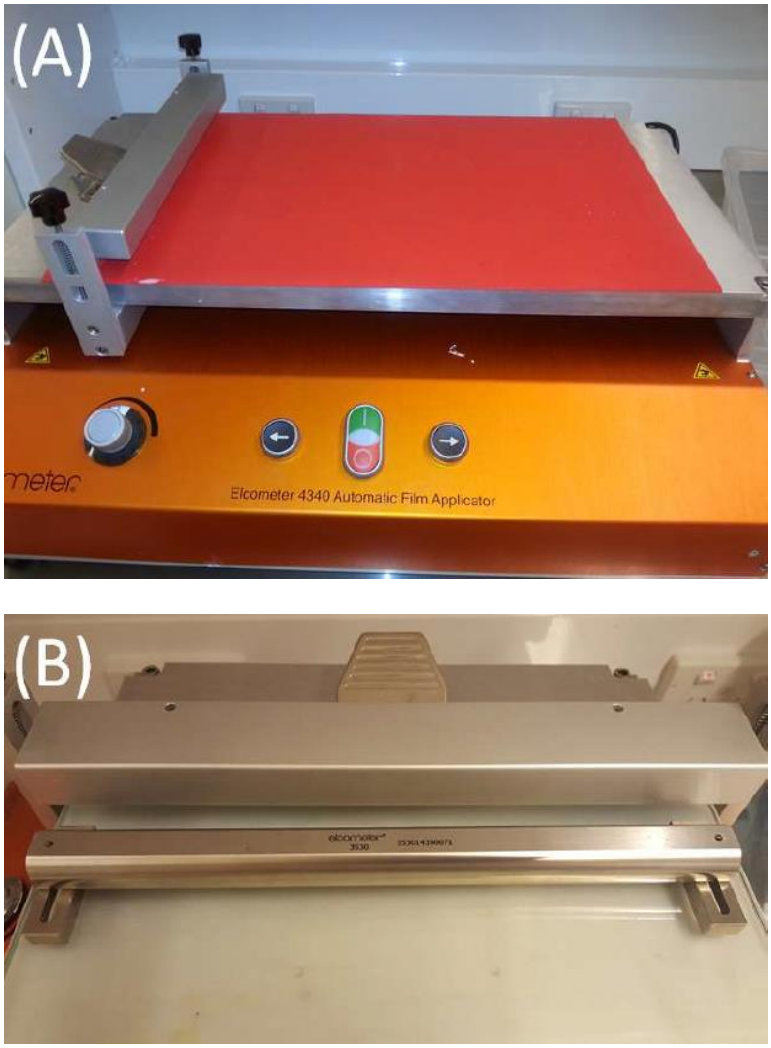

Figure 3.1. (a) Automatic film applicator (Elcometer 4340, Elcometer Aisa Pte. Led.) and (b) casting blade for coating of ion-exchange polymer coated carbon electrodes.

3.4 Membrane capacitive deionization tests

3.5.1 Bench-scale MCDI experiments

The MCDI tests were performed using at a bench-scale unit as depicted in **Figure 3.2**. In the conventional MCDI configuration, a pair of carbon electrodes were inserted within the test cell, whereas the anion and cation exchange membranes were placed between those two electrodes. The porous carbon electrodes and IEMs were replaced to a pair of

anion- and cation-selective electrodes when using the ion-exchange polymer solution coated electrodes. A non-electrically conductive nylon mesh type spacer was placed between the two IEMs for ensuring the water flow and preventing short-circuit. The dimensions of the rectangular flow channel of the MCDI test cell were 10 cm in length and 10 cm in width, providing an effective area of 100 cm^2 for electrosorption. In the center of the electrodes and IEMs placed in the flow channel, a 1 cm diameter sized hole was punched to enable the feed solution to be entirely in contact with the carbon electrodes and provide full flow within the system cell unit. The feed water was fed throughout the test unit using a peristaltic pump (Cole–Palmer, USA). A potentiostat, WPG–100 (WonATech Co., Republic of Korea), was used to supply an electrical potential on the carbon electrodes. System stabilization prior to the tests was carried out by flushing the feed water through the system under single-pass mode at 0 V until the reads of pH and conductivity of the permeate water were the same as those of the influent. The conductivity data of the permeate water were logged on an electrical conductivity meter (Hach, USA) to calculate the salt adsorption capacity of the carbon electrode. All the experiments were run at 20 ^oC in duplicate.

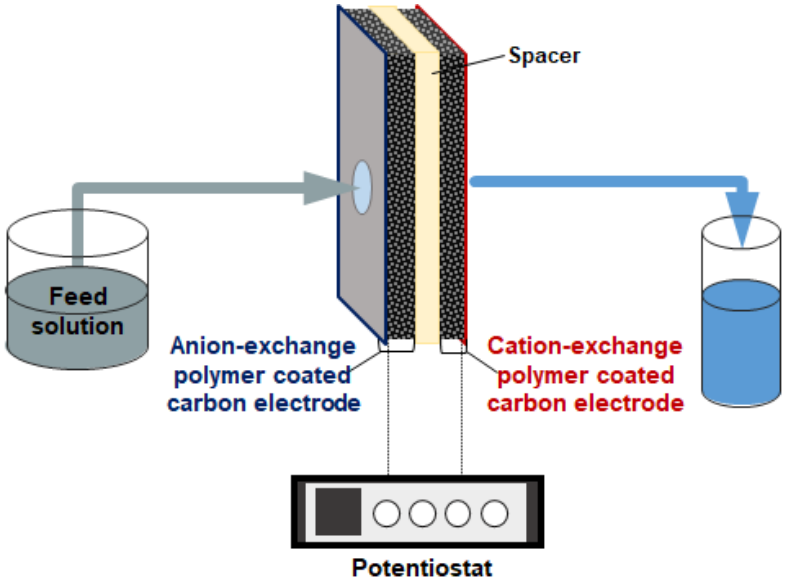

Figure 3.2. Schematic illustration of the bench-scale MCDI test units.

3.5.2 Pilot-scale MCDI experiments

We installed a single-pass pilot-scale MCDI test system at a decentralized wastewater reuse plant located in Sydney, Australia (**Figure 3.3**). The wastewater effluent from the reuse plant was fed through the MCDI module using a high-pressure pump (Walrus Pump Co., Taiwan). The effluent water after electrosorption and electrode regeneration (2 min for each), which was charged by a direct current power supply, was then separately collected from the permeate and concentrate lines. The voltage and current loads on the electrode module were monitored using a digital data logger. Electrical conductivity, temperature, and pH data in the inlet, permeate and concentrate lines were measured using in-line probes, and saved on the logger. The pressure drop between the inlet and outlet along the module also was checked by placing hydraulic pressure meters. The applied voltage on the electrode module was at 0.6–1.5 V, whereas the flow rate was at 0.5–2.5 L/min. The system was firstly stabilized prior to the run of each test by flushing the

wastewater effluent throughout the pilot-scale system at a desired applied voltage with at least five repetitive electrosorption and electrode regeneration cycles.

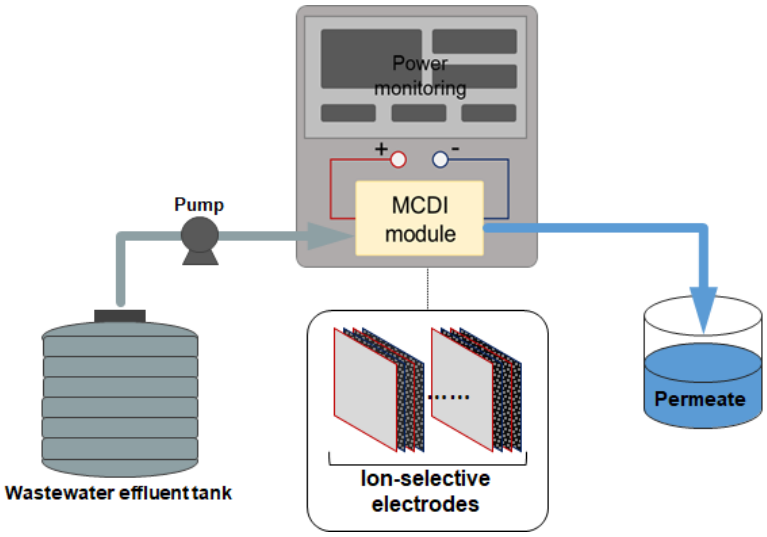

Figure 3.3. Schematic illustration of the pilot-scale MCDI test unit for wastewater reuse.

3.5 Analytical methods

3.5.1 Scanning electron microscope

A scanning electron microscopy (SEM, Zeiss Supra 55VP, Germany) was used to observe the top vies of the raw and coated carbon electrodes. The coupon of the samples was first coated with Au/Pd, and then was imaged at an accelerating voltage of 10 kV with different image magnifications.

3.5.2 Atomic force microscopy

The electrodes' and IEMs' surface roughness was characterized by atomic force microscopy (AFM) imaging. AFM roughness measurement was done under in non-contact mode with silicon probes (Dimension 3100 Scanning Probe Microscope, Bruker,

United States). All the electrodes and IEMs' analysed were scanned more than twice with a randomly selected scanning position.

3.5.3 Measurement of water quality

The cation concentrations of feed, permeate and concentrate streams were measured by inductively coupled plasma-mass spectrometer (ICP-MS), NExon 300D ICP-MS (Perkin Elmer Co., MA), and microwave plasma atomic emission spectrometer (MP-AES), 4100 MP–AES (Agilent Technologies, USA). Ammonium (NH_4^+) was quantified using a UV/VIS spectrophotometer (Spectroquant NOVA 60, Sigma–Aldrich, USA) with an NH_4^+ photometric test kit (Merck Millipore, USA). The anions, such as chloride (Cl^-), sulfate (SO_4^{2-}), nitrate (NO_3^-), nitrite (NO_2^-), and ortho-phosphate (PO_4^{3-}) were analyzed using ionic chromatography (IC), (IC Thermo Fisher Scientific, Australia). Total organic carbon (TOC) values were measured using a multi N/C 3100 TOC analyzer (Analytik Jena, Germany). All the samples were diluted properly and filtered by a 0.45 μm filter (Merck Millipore, USA) before characterization.

CHAPTER 4

Investigation of Ion Transport During Electrode Regeneration and Its Implications on Mineral Recovery from Wastewater

The results of this chapter was published on ACS Sustainable Chemistry & Engineering, which is titled as "*Effect of Brine Water on Discharge of Cations in Membrane Capacitive Deionization and its Implications on Nitrogen Recovery from Wastewater"*.

Research highlights

- This work explored the ion transport behavior in MCDI during mineral recovery.
- The enriched brine formed a reverse ionic strength gradient and constrained discharge.
- Short-circuiting lacked a repelling force to overcoming the reverse ionic strength.
- The discharge selectivity was inconsistent with the permselectivity through CEM.
- Pseudo kinetic models help understanding desorption kinetics of ions in MCDI.

4.1 Introduction

In the face of major global issues, including water scarcity and uncertainties surrounding the acquisition of mineral resources and effective energy generation, the water industry is currently undergoing a significant paradigm shift. Besides its traditional role of conducting water purification with low energy consumption, a new role has been assigned to conventional wastewater treatment plants. There has been a global trend toward utilizing treatment plants for mineral resource recovery, especially nutrients such as nitrogen and phosphorus. Wastewater is now considered a potentially important source of recoverable nutrients and other valuable materials, and thus, resource recovery from wastewater has become a field where technological innovation is being used to provide additional social, environmental, and economic benefits (Connor et al. 2017). However, the technologies currently employed to recover nitrogen and phosphorus from wastewater are still in progress of development due to the economic challenges associated with them (Batstone et al. 2015).

Capacitive deionization (CDI) has the potential to deionize saline water to harvest potable water by capturing charged impurities through the application of electrical potential

difference over two porous carbon electrodes. This electrosorptive technology is one of the most promising technologies for producing sustainable, fresh water from low saline, unconventional water resources (Tang, He, Zhang & Waite 2017; Uzun & Debik 2019). CDI has been significantly improved by research on the development of advanced electrode materials, and enhanced energy recovery. In particular, the techniques that are based on effective process designs, has enabled this process to be feasible for potable water production (Oladunni et al. 2018; Suss et al. 2015). In addition to the generation of purified water, CDI is also a potential method for recovering mineral resources during wastewater reuse (Jiang et al. 2019b; Kim et al. 2019c). Using this technology, the charged species can be reclaimed through adsorption onto the electric double layers formed at the interface between an electrode and the wastewater solution. As the electrosorption of the CDI process is rooted in ion separation from water, it effectively recovers the charged nutrient compounds by gathering the ions in minute amounts from low-salinity water.

Several studies have explored CDI, also membrane CDI (MCDI) and flow-electrode CDI (FCDI), for recovering mineral resources such as nitrogen, which is considered the most probable nutrient for reproduction from municipal wastewater (Fang et al. 2018; Wang et al. 2017). Previous studies of conventional CDI for mineral recovery conducted basic tests to evaluate the adsorption capacity and selectivity of the target species. The ionic ammonium (NH_4^+), which is faradaically separable, was shown to be stably stored in the pores of carbon electrodes by the non-faradaic electrochemical CDI process (Ge et al. 2018). A NH_4^+ recovery rate of 65% was achieved by using a hybridized MCDI and an ion-exchange process in three successive operating cycles (Wang et al. 2017). The NH_4^+ concentration of up to 322 mg/L in the brine solution was achieved through FCDI,

allowing the simultaneous removal and concentration of ammonia from the influent stream (Fang et al. 2018). The concentration of NH_4^+ in the brine solution was further enhanced using an integrated FCDI membrane stripping system (Zhang, Ma, et al. 2018). As the adsorption mechanisms in the diverse CDI process have been widely studied, many solutions to optimize the performance and selectivity during nutrient removal in CDI have been suggested. However, in the meantime, there are very few theoretical and experimental studies on the behavior of ion discharge into high-concentration brine during the regeneration process for mineral recovery.

The primary aim of this study is to understand the cation desorption behavior in the regeneration stage of MCDI during mineral resource recovery, which is presently one of the most widely used systems in this field (Biesheuvel & Van der Wal 2010a; Kim & Choi 2010b). Considering that the ions adsorbed onto the carbon electrode surface are discharged into a high-concentration brine passing through an ion-exchange membrane (IEM) for mineral enrichment, the effect of brine solution chemistries on cation desorption was probed by changing the ionic compositions and strengths of the synthetic feed and brine solutions. Additionally, the desorption efficiency of cations through reverse polarity and short-circuiting was evaluated while releasing the adsorbed ions into the brine. The cation selectivity in electrode regeneration and the role of IEM in preferential desorption were also studied using a mixture of different ions in the feed solution. Lastly, the electrosorption and electrode regeneration stages in MCDI were repeatedly run to attain a high concentration of NH_4^+ from synthetic wastewater; methods for improving this recovery process are discussed in this work based on these findings.

This chapter is an extension of the research article published by the author in ACS Sustainable Chemistry & Engineering.

4.2 Experimental

4.2.1 Synthetic and wastewater solutions

ACS-graded sodium, potassium, and magnesium chlorides (NaCl, KCl, and $MgCl_2$, Sigma-Aldrich Co., USA) were used as both the feed and brine solutions for the experiments examining ion discharge behavior under different ionic compositions (0.1−10.0 mM). A synthetic wastewater effluent was used during the tests that examined nitrogen recovery from municipal wastewater. The ionic composition of the synthetic wastewater was based on the water quality of the secondary effluent from selected wastewater treatment plants in California, USA (**Table 4.1**) (Huertas et al. 2008). The enriched synthetic wastewater was prepared by dissolving all ACS-graded chemicals (Sigma-Aldrich Co., USA) in DI water. Potassium phosphate and magnesium sulfate were replaced with KCl and $MgCl_2$, respectively, to prevent any possible scaling formation caused by the chemicals in the synthetic wastewater (Kim, Kim & Hong 2016). The total ionic strength of the modified synthetic wastewater was adjusted to align with that of the original wastewater. The organic matters originally contained in the wastewater were not factored into the test to rule out the potential effect of the adsorption of negatively charged organics or possible fouling onto the surface of the carbon electrode.

Table 4.1. Chemical compositions of the synthetic wastewater feed.

	Constituent	Molecular weight (g/mol)	Concentration(mM)	Note
Ionic composition	Sodium citrate	294.09	1.16	

Ammonium chloride	53.49	0.94	
Potassium phosphate	136.09	0.45	Replaced to 0.45 mM of KCl
Calcium chloride	147.01	0.5	
Sodium bicarbonate	84.01	0.5	
Sodium chloride	58.44	2.0	
Magnesium sulfate	246.47	0.6	Replaced to 0.45 mM of $MgCl_2$

4.2.2 Carbon electrodes and ion-exchange membranes

The two, symmetric, porous carbon electrodes provided by Siontech Co. (Republic of Korea) were composed of a graphite body sheet coated with a carbon slurry blended with activated carbon, P-60 (Kuraray Chemical Co., Japan) and PVDF (Inner Mongolia 3F-Wanhao Fluorine Chemical Co., China). The dimensions of the carbon electrodes were 10 x 10 cm^2, and the total carbon mass of each electrode was 0.8 g. Commercial anion-exchange membrane (AEM) and cation-exchange membrane (CEM) (Neosepta AFN and CMB, respectively) purchased from Astom Co. (Japan) were used for inhibiting the adsorption of the counter-ions during electrode regeneration.

4.2.3 Bench-scale MCDI setup

The MCDI experiments were carried out in a lab-scale flow-by system as described in our previous study (Kim, Gwak, et al. 2017a). The dimensions of the rectangular feed channel of the test cell were 10 x 10 cm^2—an effective electrosorption area of 100 cm^2. Two carbon electrodes were inserted symmetrically within the test cell, and the AEM and CEM were placed between them. The membranes were separated by a non-electrically

conductive nylon spacer to ensure water flow and prevent short-circuiting (Dorji et al. 2018). The feed water was brought completely into contact with the carbon electrodes by punching a hole with a diameter of 1 cm in the center of the carbon electrodes, IEMs, and nylon spacer.

A peristaltic pump (Cole-Palmer, USA) was placed to pump the feed solution throughout the MCDI system with a constant flow rate of 15 mL/min. A constant level of electrical potential was supplied through the MCDI unit by a potentiostat, WPG-100 (WonATech Co., Republic of Korea). The MCDI system was stabilized prior to the electrosorption and regeneration experiments by flushing out the feed solution through the MCDI system under the single-pass mode at 0 V, until the values of conductivity and pH were the same as those of the influent. All tests were duplicated at 20ºC.

4.2.4 Investigation of ion desorption behavior

The experimental procedure for MCDI operation is presented in **Figure 4.1**. A 100 mL feed solution containing 0.1, 1.0, or 10.0 mM of NaCl, $MgCl_2$, or KCl was fed into the lab-scale MCDI system for 8 min at a 1.0 V applied potential under the batch mode. The ions adsorbed onto the carbon electrodes were then discharged under the single-pass mode in the following regeneration step. In this step, a solution with 0 to 10 mM of NaCl, $MgCl_2$, or KCl (the brine solution used in the regeneration) flowed through the system at -1.0 V for 8 min, and the concentrated water that passed through the MCDI unit was collected each minute. A mixture of NaCl, $MgCl_2$, and KCl solutions (0 to 10 mM in total) was also used for investigating the cation desorption behavior under the co-existence of different ionic conditions.

After each test, complete discharge of ions from the carbon electrodes was ensured by employing an additional regeneration stage using DI water for longer than 30 min at -1.0 V. Thus, no discharge of ions was detected through the conductivity measurement of the flushing effluent, confirming that there were no remaining ions that could be released by electrical force. The mass balance on the amount of adsorbed and desorbed salts was roughly calculated to make sure that the electrode was completely regenerated at the end of flushing.

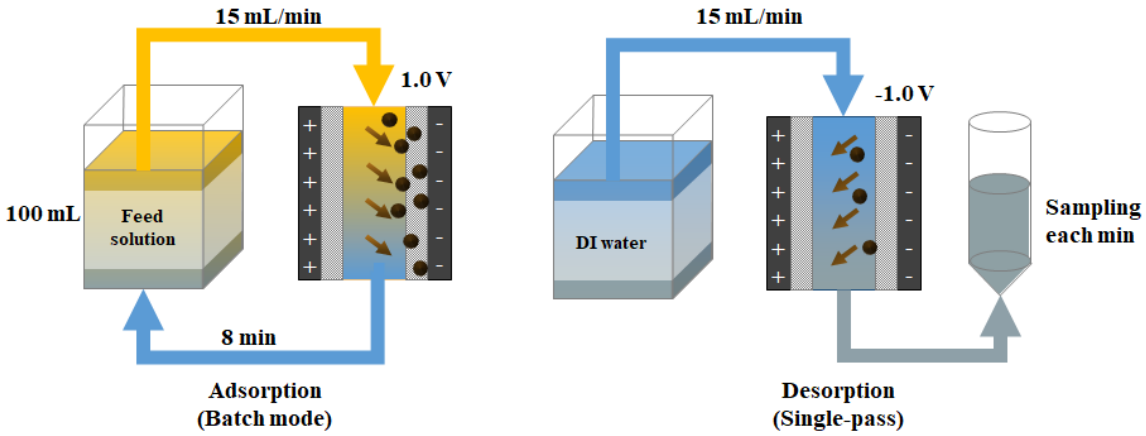

Figure 4.1. Experimental procedure of MCDI tests for the investigation of ion discharge into a high-concentration brine solution.

4.2.5 Successive, five-cycle operation for concentrating ammonium

A 100 mL portion of synthetic wastewater effluent was fed under the batch mode through the MCDI system for 8 min under a 1.0 V adsorption condition. The same volume of fresh DI water was then circulated through the system under the same condition as electrosorption by reversing the potential. The desorbed ions, including NH_4^+, were kept collected in the brine solution after regeneration for all cycles. This batch mode

adsorption and desorption process was run for five cycles using 100 mL of fresh synthetic wastewater solution and 100 mL of concentrated brine solution for each test.

4.2.6 Measurement of water quality

Microwave plasma atomic emission spectrometry (MP-AES) (4100 MP-AES, Agilent Technologies Co., USA) was used to quantify the concentrations of Na^+, Mg^{2+}, and K^+, whereas NH_4^+ was measured using a UV/VIS spectrophotometer (Spectroquant NOVA 60, Sigma-Aldrich Co., USA) with an ammonium photometric test kit (Merck Millipore, USA). The solution samples were effectively diluted before analysis by the measurement devices. The analyzed results of water quality were used to calculate the MCDI desorption performances.

4.3 Results and discussion

4.3.1 Effect of brine water concentration on cation desorption

The target cations for recovery are to be highly enriched through successive MCDI operational cycles to achieve a high–ionic–concentration brine. To explore the effect of the brine water's ionic strength on the cation desorption during electrode regeneration, the MCDI adsorption and desorption operations were carried out under various ionic compositions of the feed and brine solutions under various ionic compositions.

The desorption rate in MCDI was first evaluated using different NaCl feed and brine solution concentrations to observe the effect of the concentration difference at the

interface between the carbon electrode surface and brine solution through the IEM, without the influence of other co-ions. **Figure 4.2** shows the desorption rate of MCDI under the single-pass mode operated under various NaCl feed concentrations (0.1, 1, and 10 mM) followed by desorption using varying concentrations (0, 1, and 10 mM of NaCl) of brine solution. As expected, the ion desorption rate was initially high during the first minute of desorption time and then decreased as most of the Na^+ ions were released into the DI water. The average initial desorption rate of electrode regeneration for electrodes operated using 0.1, 1, and 10 mM NaCl as feed solution was 0.24, 2.37, and 23.79 mM/min, respectively, when DI water was used to collect the discharged ions. However, when a 10 mM NaCl solution was used as brine water, the desorption rate further decreased to 0.01, 1.27, and 22.29 mM/min for electrodes operated with 0.1, 1, and 10 mM NaCl feed, respectively. The influence of brine water concentration on the retardation of ion desorption was clearly more significant when the electrodes were operated at lower feed concentrations. For example, for electrodes operated with 0.1 mM feed, the desorption rate decreased by 35% and 96% when 1 and 10 mM solutions (10- and 100-fold of feed) were used as brine water, respectively, compared to that of DI water.

The results showed that the desorption performance, particularly in the initial stage, was retarded by the concentration difference between the two solutions. This was likely due to the relative concentration difference between the two different phases across the CEM (i.e. the electrode surface and the aqueous brine) (Choy, Evans & Cussler 1974). The decrease in the desorption rate when more concentrated brine water was used can be explained by the increased ionic concentration gradient across the IEMs, as elucidated by the Gouy-Chapman theory (Delahay 1965). A high electrolyte concentration in the brine solution results in a low-or reverse-ion concentration gradient between the two phases (i.e., the water media and carbon electrode surface) across the IEM, as the ions are

interrupted from being freed from the porous carbon surface.

The transport of cations during electrode regeneration was likely further retarded by enhanced resistance of the CEM at low feed concentration near the electrode surface which leads to a lower membrane conductance. The IEM resistance which was strongly dependent on the concentration of the dilute stream (particularly for <10 mM of NaCl) significantly increased, thereby resulting in a lowered desorption efficiency (Długołęcki et al. 2010; Zhu et al. 2018). Besides, the increase in CEM resistance was likely more intensified as the concentration gradient between the brine bulk solution and electrode surface across the membrane increased. Galam et al. (2014) revealed that the conductance of an IEM is largely determined by both sides of the membrane, and its resistance increases more where the ion concentration difference becomes greater (Galama et al. 2014).

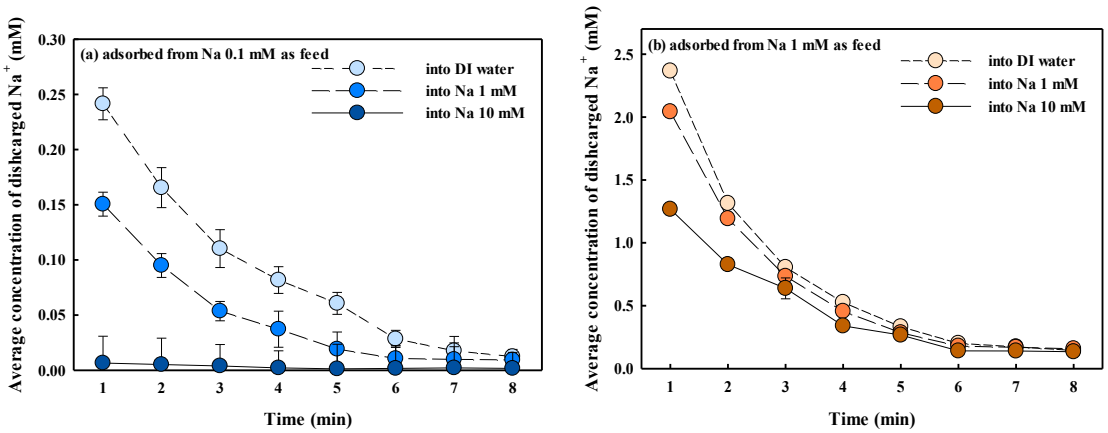

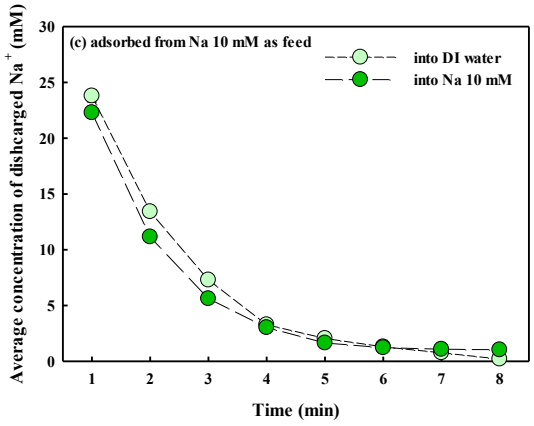

Figure 4.2. Average concentration of Na^+ desorbed into brine solution (0 to 10 mM of NaCl). The samples were collected every minute and Na^+ was collected on the electrode from a 100 mL feed solution containing (a) 0.1, (b) 1, and (c) 10 mM of NaCl. The average Na^+ adsorption capacity after the electrosorption stage from the 0.1, 1, and 10 mM NaCl feed solution was 0.24, 2.47, and 10.81 Na^+ mg/carbon g, respectively.

4.3.2 Desorption rate change in electrode regeneration with different ions in brine

The Na^+ desorption performance of MCDI using various brine solutions presented in **Figure 4.3** shows that the ion desorption efficiency varied with the type of electrolyte used as desorption water. The desorption capacity during the regeneration of the cations into brine, depicted in **Figure 4.3c**, was calculated using the following equation.

$$\text{Desorption efficiency (mg/g)} = \frac{m_{desorbed,t}}{m} = \frac{Q \times \int_0^t (C - C_0) dt \times M}{m} \qquad (4.1)$$

where $m_{desorbed,t}$ is the total amount of desorbed ions after time t (mg), m the mass of carbon on the electrode (g), Q the volumetric flow rate during regeneration, C the

concentration of the effluent at time t (mmol/L), C_0 the initial concentration of the brine solution (mmol/L), and M the molar mass of salt (mg/mmol).

The average Na^+ desorption rate early in the first minute was 2.04 and 1.27 mM/min as 1 and 10 mM of NaCl were present in the brine, respectively. However, the average Na^+ desorption rate decreased when the brine solution was replaced with KCl or $MgCl_2$ solution. The desorption efficiency of Na^+ into the KCl brine was slightly lower than that of NaCl, which may be considered insignificant. Nevertheless, the KCl electrolyte formed a stronger reverse–ionic-strength gradient, resulting in a lower ion desorption rate. A decrease in desorption performance could be observed more clearly for $MgCl_2$ brine, which induced a much higher ionic strength.

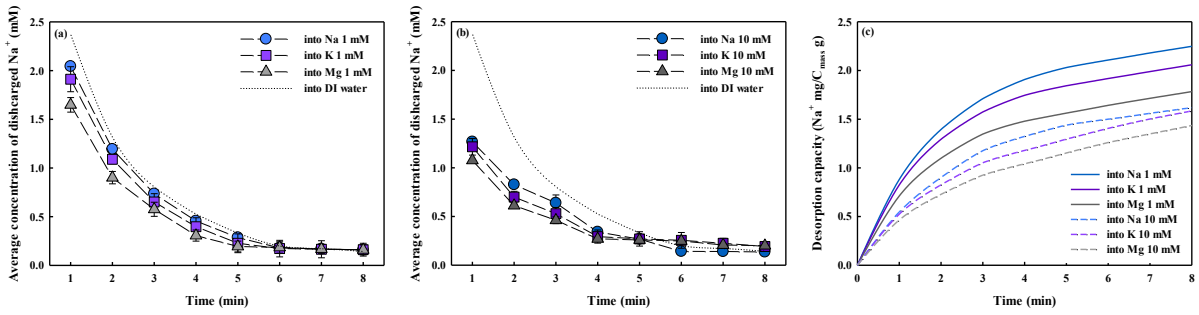

Figure 4.3. Average concentration of Na^+ desorbed into the brine solution: ((a) 1 mM and (b) 10 mM of NaCl, KCl or $MgCl_2$) and (c) the corresponding desorption capacity of the used carbon electrode. Na^+ was adsorbed on the electrode from a 100 mL feed solution containing 1 mM of NaCl, and the Na^+ adsorption capacity after the electrosorption stage was 2.47 Na^+ mg/carbon g.

In summary, the ionic strength gradient (or the relative ionic strength difference) between the carbon electrode surface and the aqueous brine solution across the IEM affects the ion discharge kinetics. The slowed desorption kinetics are consistent with the findings from previous studies that explored the effects of brine composition on ion discharge in MCDI. Hassanvand et al. (2017) first verified the effect of the brine to feed concentration ratio on the desorption time for electrode regeneration (Hassanvand et al. 2017b). A reduced discharge efficiency due to the high–ionic-strength of the disposal water was also found in a study on palladium recovery from plating wastewater, which reported a constrained palladium discharge efficiency due to an enriched palladium brine solution (Kim, Gwak, et al. 2017a).

4.3.3 Comparison of reverse polarity and short-circuiting for mineral resource recovery

The efficiency of the MCDI process for mineral resource recovery was hampered by a reduced desorption efficiency due to an intensified ionic-strength gradient. In this study, two different ion discharge methods were examined to further investigate the reduced desorption efficiency caused by high-concentration brine during mineral recovery.

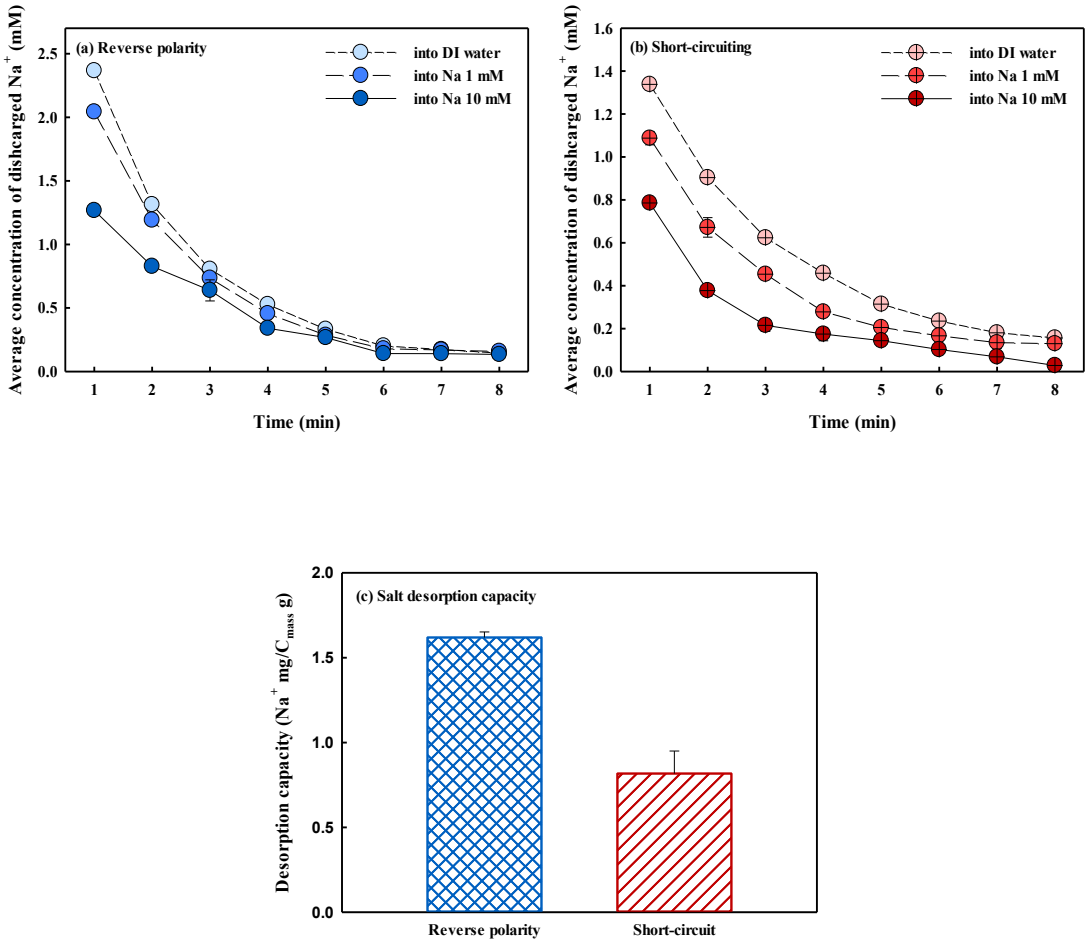

Figure 4.4. Effect of desorption methods on the ion discharge performance in MCDI. The average concentration of desorbed Na^+ driven by (a) reverse polarity and (b) short-circuiting, and (c) the corresponding desorption capacity when disposed into 10 mM of NaCl brine. Na^+ was adsorbed onto the electrode from a 100 mL feed solution containing 1 mM of NaCl; the Na^+ adsorption capacity after the electrosorption stage was 2.47 Na^+ mg/carbon g.

Figure 4.4 presents the discharged Na^+ concentration after reversing polarity or short-circuiting in the highly enriched brine solutions. The ions were released under high brine

concentration by short-circuiting at desorption rate of 1.09 and 0.79 mM/min under 1 and 10 mM of NaCl in brine, respectively, as the electrostatic energy holding the ions was quickly dissipated (**Figure 4.4b and c**) (Yao & Tang 2017). The retarded desorption rate during short-circuiting was likely because the ion diffusion was hindered by the concentration gradient between the phases of electrode surface and highly concentrated brine bulk solution across the CEM (Jeon et al. 2014). The ion desorption rate by reversing polarity was higher than that by short-circuiting, though the brine solution involved high total dissolved solids as the ions were strongly expelled from the carbon electrode by the electrostatic driving force (2.04 and 1.27 mM/min where 1 and 10 mM NaCl were used as brine, respectively (as shown in **Figure 4.4a**).

In this study, the ion discharge efficiency via short-circuiting was shown to be constrained during mineral recovery due to a lack of electrochemical force capable of overcoming the reverse-ionic-strength gradient between the electrode surface and the bulk brine water across the CEM. Reversing polarity was expected to shorten the duration of the regeneration stage by quickly releasing counter-mineral ions from the carbon electrode, consequently resulting in better adsorption capacity in the next operation cycle (Biesheuvel et al. 2011b; Liang et al. 2013). However, increasing the discharging voltage may rather lead to intensified energy loss caused by the increase in the resistances at high recovery of the target minerals (Zhao, Porada, et al. 2013).

A pilot-scale study of MCDI performed by Biesheuvel and van der Wal reported that reversing the voltage during ion discharge well concentrated the ions stored on the carbon electrode into brine (Biesheuvel & van der Wal 2010b). Besides, reversing polarity was advantageous for the consequent electrosorption stage in MCDI as the counter-ions were expelled from the electrode surface, which therefore became depleted, whereas the

concentration of counter-ions simply released from the EDL near the surface became equal to the inlet concentration after short-circuiting. The repulsion of counter-ions by reversed polarity led to a stronger attraction for the counter-ions toward the electrode in the following electrosorption stage.

4.3.4 Competitive ion desorption under the co-existence of different ions

As different ions are simultaneously present in wastewater, electrode regeneration tests were carried out using a mixture of different cations in the feed solution to understand how the different co-existing cations migrate from the carbon electrode to the brine water through the membrane. The experiments were performed using a feed solution containing 0.33 mM of NaCl, KCl, and MgCl each. Across all of the tests, the average charge efficiency of the MCDI system during electrosorption was 63.6%, while the average removal efficiencies of Na^+, K^+, and Mg^{2+} from the feed solution were 73%, 95%, and 97%, respectively, showing that the preferential ion sorption has a sequence of $Mg^{2+} > K^+ > Na^+$. The consequent separation factors in terms of meq, K^+/Na^+ and Mg^{2+}/Na^+, obtained from our experimental data were 1.30 and 0.67, respectively. Experimental studies on the preferential adsorption in conventional CDI have revealed that the selectivity of electrosorption can first be determined by the initial concentration of the feed, followed by the ionic charge valency and the hydrated radius of the ions (Chen et al. 2015). First, the carbon electrode preferentially adsorbs the ions present in higher amount. Specifically, the cations of a higher valence are energetically more favorable to screen the surface charge of the electrodes. Thus, divalent charged species would be more

electrochemically adsorbed on the electrode surface than monovalent ions if the molar concentrations of both are the same. Finally, possessing similar concentrations, cations with smaller hydration radii diffuse faster toward the pores, and thus, are more favorably adsorbed by the electrostatic field.

Several works have developed theoretical models to predict the mechanisms of the observed ion selectivity in a quantitative manner. Zhao et al. (2012) used a two-dimensional dynamic model based on the non-linear theory to illustrate the time-dependent selectivity of multivalent ions in a conventional CDI system (Zhao et al. 2012). Dykstra et al. (2016) combined two different models, improved modified Donnan model and dynamic transport model, to explain the preferential adsorption among multiple monovalent ionic species in CDI and well described the selective removal of K^+ over Na^+ (Dykstra et al. 2016). Suss developed a size-based ion selectivity model considering the size of spherical counter-ions by accounting for the ion volume exclusion interactions in the EDL (Suss 2017).

The cation selectivity trend in MCDI was consistent with that in the conventional CDI. This is likely because that the permselectivity of cations through the CEM placed between the carbon electrode and the bulk solution, which can significantly influence the electrosorption selectivity, is determined by the cation's charge valence and Stokes radius, same as the selectivity trend in the conventional CDI (Luo, Abdu & Wessling 2018b).

Figure 4.5 presents the results of competitive desorption of Na, K, and Mg ions. The desorption efficiency of the cations disposed into DI water, which can be defined as **Equation 4.2**, is shown in **Figure 4.5b**, whereas the ion discharge selectivity in **Figure 4.5c** can be expressed as **Equation 4.3**.

$$\text{Desorption efficiency} = \frac{m_{d,t}}{m_a} = \frac{Q \times \int_0^t (C - C_0) dt \times M}{m_a} \quad (4.2)$$

$$\text{Discharge selectivity} = \frac{m_{i,d,t}}{m_{total,d,t}} \quad (4.3)$$

where m_a indicates the adsorbed amount of ions (mmol) on the carbon electrode, and $m_{i,d,t}$ and $m_{total,d,t}$ represent the desorbed amount of the specific salt, i, at time t and those of all the ionic species at time t, respectively. At the beginning of the regeneration stage, K^+ was quickly freed from the electrode surface, followed by Na^+, while Mg^{2+} was the least favored species for discharge (**Figure 4.5a**). This trend is clearly confirmed by **Figure 4.5b**, which presents the desorption percentage of the ions adsorbed on the cathode. K^+ took the shortest time to be disposed among the three cations, while the maximum time was needed to release all of the adsorbed Mg^{2+}. The rapid desorption of K^+ can be explained by its fast diffusion kinetics and hydrated ionic radius over Na^+ and Mg^{2+} (**Table 4.3**). In addition, the slow desorption of Mg^{2+} is likely due to its large size and the low diffusion rate that results from it. Unlike the electrosorption selectivity, the desorption preference order during regeneration was inconsistent with the permselectivity trend of the cations through the CEM. Therefore, the ion discharge selectivity was likely related more to the diffusion transport of the adsorbed cations near the electrode pore rather than the ion mobility (permselectivity) through the CEM.

A previous MCDI study explained the discrepancies between the desorption rates of different ions based on the diffusion kinetics and the strong electrostatic force between divalent ions and the fixed charged groups within an IEM (Hassanvand et al. 2018). The monovalent ion with higher diffusivity rapidly escaped from the carbon pore, but the divalent ion left the electrode pore passed through the membrane much faster, despite its slow diffusion rate. Unlike the earlier study, the trend of desorption preference in our

study was primarily governed by the diffusion kinetics, whereas the influence of electrostatic force induced by the charge valence was insignificant. However, Mg^{2+} ions could be preferentially retained within the IEM during adsorption, due to Donnan exclusion (Strathmann 2004). This may be a result of different operating conditions or the system configuration of the lab-scale experiment, as the preferential order of adsorption found in the previous work also differed from our results and those of other adsorption selectivity studies (Hou & Huang 2013; Zhao, Wang, et al. 2013).

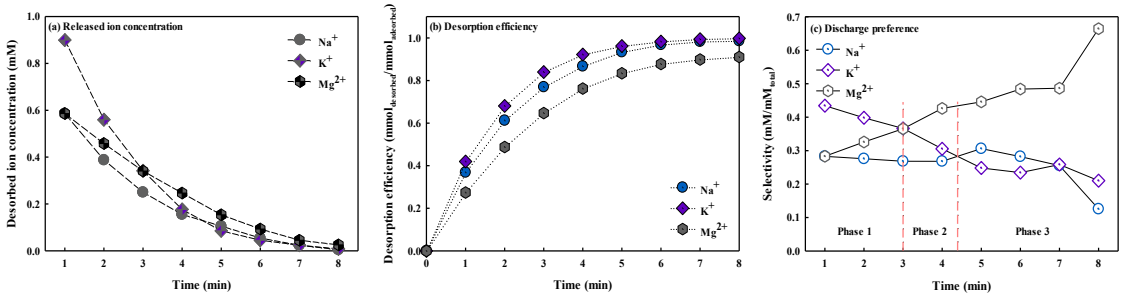

Figure 4.5. Competitive desorption among Na, K, and Mg ions. (a) The average concentration of desorbed ions, (b) desorption efficiency, (c) and discharge selectivity of three different cations. The electrosorption tests were run using a mixed feed solution containing 0.33 mM of NaCl, KCl, and $MgCl_2$ for each. The average removal efficiency of Na^+, K^+, and Mg^{2+} from the feed solution was 71%, 96%, and 97%, respectively. The adsorbed ions were then desorbed in to DI water during regeneration.

In our results, the cation discharge selectivity was defined by three distinct phases (**Figure 4.5c**). K^+ was quickly released at the start of electrode regeneration, followed by Na^+, due to its fast diffusion. In the mid-phase, after many K^+ ions were desorbed, Mg^{2+} became

the most desorbed. Last, K^+ turned out to be the least preferentially desorbed ion in the final phase as it was almost entirely discharged from the electrode. During the mid- and end-phases, Na^+ was the slowest-released species as its number of adsorbed ions on the electrode surface was fewer than that of the other two ions. Further test results investigating the discharge selectivity in different concentrations of brine solution (1 and 10 mM) in **Figure 4.6** confirmed that the trend of desorption preference was consistent regardless of the ionic strength gradient.

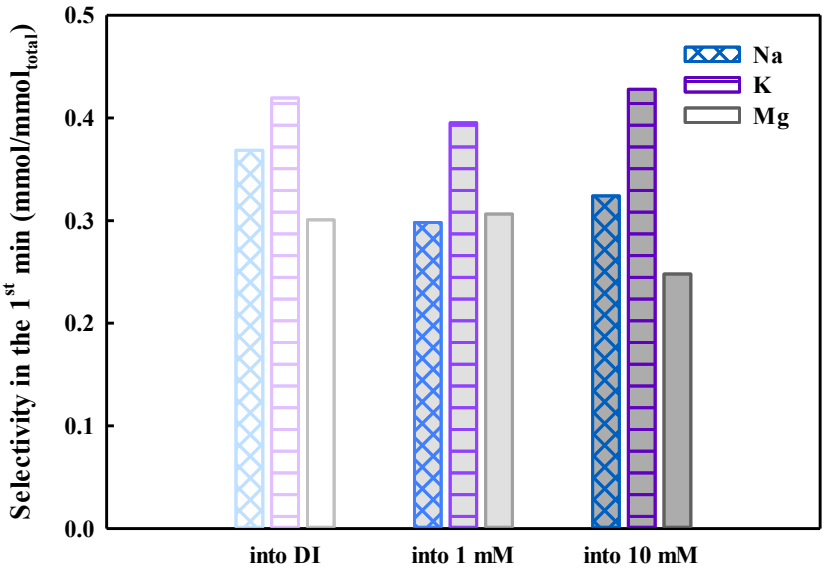

Figure 4.6. Discharge selectivity of Na, K, and Mg in the 1st min of electrode regeneration. The ions were discharged into 0, 1, and 10 mM NaCl brine solutions. The average removal efficiency of Na^+, K^+, and Mg^{2+} from the feed solution was 71%, 96%, and 97%, respectively.

4.3.5 Desorption kinetics using pseudo-first-order and pseudo-second-

order models

Several studies on CDI have evaluated the kinetics of electrosorption using pseudo-first and -second order models (Wimalasiri, Mossad & Zou 2015; Zornitta & Ruotolo 2018). In this study, kinetic models were also developed to quantitatively determine preferential desorption of the cations in MCDI. The desorption data were fitted using pseudo-first- and pseudo-second-order kinetic models to obtain numeric information from the kinetic constants.

The linearized pseudo-first-order and -second-order model equations can be described as:

$$\log(q_e - q_t) = log q_e - \frac{k_1 t}{2.303} \text{ for pseudo-first-order} \quad (4.4)$$

$$\frac{t}{q_t} = \frac{1}{k_2 {q_e}^2} + \frac{t}{q_e} \quad \text{for pseudo-second-order} \quad (4.5)$$

where q_e and q_t (mg/g) indicate the adsorbed and desorbed amounts of salt at time t (min) during regeneration, respectively, and k_1 and k_2 (g/mg-min) are the desorption rate constants of the pseudo-first- and -second-order equations.

Figure 4.7 shows the linear fitting between the model equations and experimental data. The desorption rate constants were obtained from the slopes and intercepts of the fitting lines (listed in **Table 4.2**). Evidently, both the first- and second-order models could approximate the experimental data. All the regression coefficients R^2 for each fitting were > 0.94, displaying compatible features. However, even though the isotherm-based model can predict the adsorption performance by extracting the parameters of q_e and k, it has to be noted that the fitted isotherms cannot reflect the impact of electrochemical

characteristics, such as applied potential and charge efficiency (Porada et al. 2013b). Besides, the doubt of the pseudo kinetic model as a quantitative model remains if it can be extended to describe different MCDI configurations, such as asymmetric electrodes (Porada, Bryjak, et al. 2012b).

Herein, however, we adopted the linearized pseudo models as an indicator for approximately deriving the kinetic parameters to express the preferential order in desorption of different cations. The order of k_1 and k_2 values for Na^+, K^+, and Mg^{2+} corresponded to the experimental results, indicating that the preferential desorption trend is $K^+ > Na^+ > Mg^{2+}$. However, the q_e values estimated using both the pseudo-first- and -second-orders were higher than the actual number of adsorbed ions. The fitting results suggested that the pseudo kinetic models can be used to understand and roughly predict the desorption kinetics in MCDI, particularly the preferential desorption order of different cations in the system.

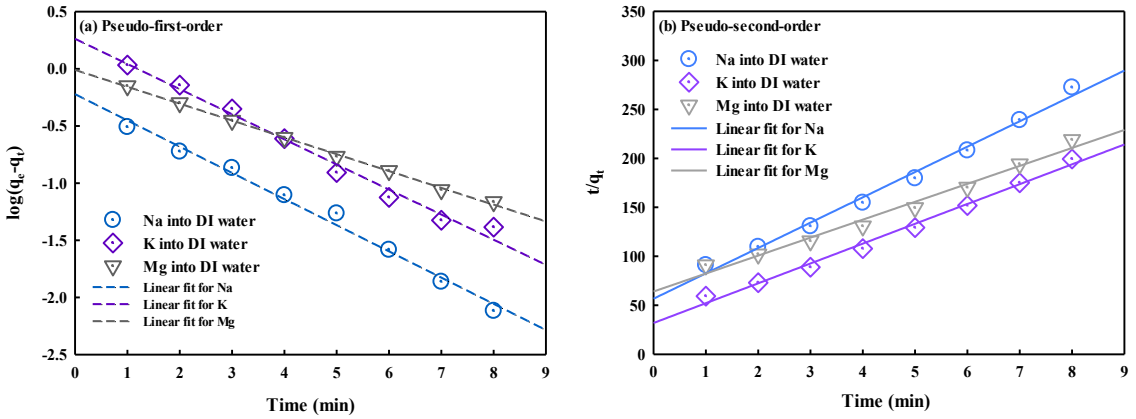

Figure 4.7. Linearized (a) pseudo-first- and (b) -second-order kinetics fitting for the results of discharged Na, K, and Mg ions.

Table 4.2. Parameters derived by the fitting of pseudo-first- and -second-order kinetics for the desorption performance.

Kinetics	Parameter	Value		
		Na^+	K^+	Mg^{2+}
First-order	q_e (mmol/g x10^{-2})	6.5781	3.5992	3.6291
	k_1 (1/min)	0.5801	0.7971	0.3130
	R^2	0.9818	0.9781	0.9581
Second-order	q_e (mmol/g x10^{-2})	3.3865	4.9385	5.4573
	k_2 (g/mg-min)	11.7984	12.8332	5.2398
	R^2	0.9689	0.9410	0.9612

4.3.6 Implications for the recovery of ammonium from wastewater

The results of this study can be utilized for understanding the desorption behavior of minerals during their recovery. In this study, NH_4^+, which is considered a valuable nitrogen source, was recovered from synthetic wastewater effluent through the MCDI system. The hydration size and diffusion coefficient of the cations, and their removal and desorption efficiencies from the wastewater feed, are listed in **Table 4.3**. NH_4^+ was the second most competitively adsorbed species following Na^+. The effective collection of NH_4^+ under the employed operating conditions is likely due to its high concentration (which holds the second largest portion of cations in the feed solution), and fast diffusion rate.

The captured ions were then successively discharged into brine for several cycles to enrich the NH_4^+ concentration. As presented in **Figure 4.8**, the NH_4^+ concentration in the

brine solution exhibited a nearly linear increase after each cycle and reached 3.92 mM after the five-cycle operation (4.17-fold compared to its initial concentration in the wastewater feed) suggesting that nitrogen resources in wastewater can be successfully reclaimed through MCDI. Assuming its fixed removal (89.68%), however, all the NH_4^+ adsorbed onto the electrode in each cycle were supposed to be fully desorbed. Its concentration after five cycles was consequently supposed to be 4.22 mM as opposed to 3.92 mM (as shown in **Figure 4.8**). This slight discrepancy in the amount of NH_4^+ collected was likely due to the constrained ion discharge rate that occurs when the reverse-ionic-strength gradient across the CEM increases.

In addition, the portion of NH_4^+ among all cations in the brine solution was increased by disposing of the ions in the brine successively. As the diffusion coefficient of Na^+ was lower than that of the other monovalent ions, this competitively adsorbed species was less discharged than NH_4^+ and K^+. As a result, the Na^+ was less preferentially released, leading to its lower portion in the brine solution, whereas NH_4^+ was comparatively well discharged. The results imply that NH_4^+ can be recovered through MCDI, achieving high concentration with good selectivity; however, its incomplete discharge must be improved by optimizing the operating conditions of the electrosorptive system.

Recovering the energy released during electrode regeneration, where the ions migrate toward the brine solution, is expected to significantly lower the energy consumption during NH_4^+ recovery from wastewater. Długołęcki and van der Wal demonstrated that up to 83% of the energy used for electrosorption can be recovered during regeneration (Długołęcki & van der Wal 2013). However, the energy recovery could be hampered during ion discharge into high-salinity brine during regeneration, owing to the energy loss caused by the ohmic and non-ohmic resistances (Jeon et al. 2014). In this regard,

increasing the reverse current for enhanced recovery of NH_4^+ from wastewater generates a higher ohmic drop, attributing to the energy dissipated by internal resistances. Thus, more energy will be needed to overcome the internal resistances in the MCDI system during electrode regeneration (Zhao, Porada, et al. 2013). Adjusting the operating conditions, such as lowering flow rate or water recovery, could improve the energy recovery (Zhao, Porada, et al. 2013). However, it has to be noted that more total electrode area is needed to achieve the same total NH_4^+ collection capacity, which results in more cost for electrodes and IEMs. Therefore, the practical application of the MCDI system for NH_4^+ recovery could be possible only after solving the issue of its economic feasibility by delicately designing the mineral recovery process.

Table 4.3. Ionic compositions of the feed and brine solutions after successive cycles of operation (Hertz & Franks 1973; Nightingale Jr 1959; Picioreanu, Van Loosdrecht & Heijnen 1997).

Solution		Constituent					
		Na^+	NH_4^+	K^+	Ca^{2+}	Mg^{2+}	pH
Ionic radius (Å)		0.95	1.48	1.33	0.99	0.65	-
Hydrated radius (Å)		3.58	3.31	3.31	4.12	4.28	-
Diffusion coefficient (m^2s^{-1} x 10^{-9})		1.33	1.86	1.96	0.79	0.71	-
Feed	Concentration (mM)	3.66	0.94	0.45	0.5	0.6	6.5

Permeate	Removal (%)	69.32	89.68	89.76	90.14	89.68	-
	SAC (mmol/g)	0.317	0.105	0.050	0.056	0.067	-
Brine	1st cycle (mM)	2.49	0.84	0.41	0.45	0.54	6.7
	3rd cycle (mM)	6.80	2.42	1.20	1.33	1.60	6.9
	5th cycle (mM)	10.39	3.92	1.97	2.18	2.63	6.9
	Concentration factor after 5 cycles	2.84	4.17	4.37	4.36	4.38	

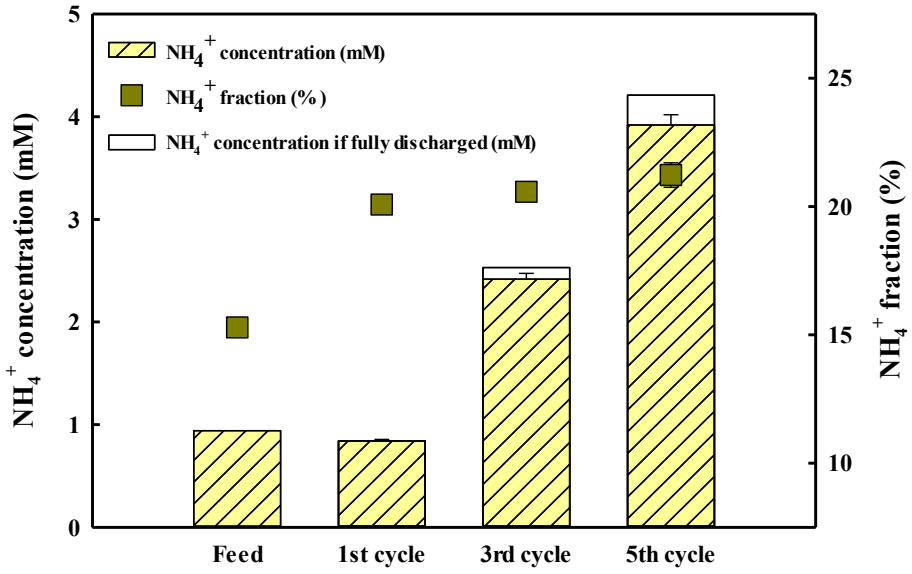

Figure 4.8. Concentration and portion of NH_4^+ in synthetic wastewater feed and brine solutions after the 1st, 3rd, and 5th operation cycle.

4.4 Concluding remarks

To better understand the desorption behavior of ionic species in MCDI during mineral recovery, the migration of cations from a carbon electrode to a high concentration brine through the IEM has been explored in a lab-scale MCDI system. The findings were then utilized to explain the discharge of ammonium ions collected from wastewater effluent. The major outcomes of this study are summarized below:

- The ionic strength gradient between the carbon electrode surface and the bulk brine solution across the IEM greatly influences ion desorption efficiency. The stronger ionic strength of brine, induced by a higher concentration and ion valency, and a smaller hydration radius, retards the ion desorption rate. The desorption rate can be lowered when the adsorbed number of ions on the electrode surface is small, as its low concentration leads to stronger resistance of the membrane.
- Energy-efficient regeneration methods, such as short-circuiting and power disconnection, yields limited performance for highly concentrating the mineral resources due to their weak repulsive force. The electrochemically adsorbed ions are well discharged by applying reverse polarity, however require more energy to attain higher ion concentration of brine.
- The selective desorption experiments confirmed that the preferential sequence of ion discharge was $K^+ > Na^+ > Mg^{2+}$, determined by the hydration size and the ion diffusion rate. The ion discharge order was inconsistent with the ion permselectivity trend through the CEM, implying that the desorption preference cannot be determined only by the membrane during electrode regeneration in MCDI.
- NH_4^+ from wastewater was well recovered by MCDI due to its high removal from the wastewater effluent and stable discharge into the brine solution. However, its lowered

desorption efficiency into brine with a high concentration may raise concerns about poor recovery performance. This should be improved by establishing proper strategies, such as applying higher energy potential during electrode regeneration.

Lastly, it should be stated that practical application of the MCDI system for mineral recovery could be possible only after solving the issue of its economic feasibility with optimizing the energy demand and brine concentration during electrode regeneration.

CHAPTER 5

Selective Nitrate Recovery from Municipal Wastewater for Water Reuse via Membrane Capacitive Deionization

The results from this chapter was published on Chemical Engineering Journal, which is titled as "*Reuse of municipal wastewater via membrane capacitive deionization using ion-selective polymer-coated carbon electrodes in pilot-scale*".

Research highlights

- MCDI was probed for mineral recovery from wastewater using IX layered electrodes.
- The coated electrodes showed better performance attributing to its low resistivity.
- NO_3^- was selectively removed attributing to its high permselectivity through AEM.
- Faster flow rate and lower potential enhanced NO_3^- selectivity in single-pass mode.
- The flat coated layer kept organic substances from accumulating on the surface.

5.1 Introduction

The depletion of freshwater resources has been attributed to the large demands for water due to rising population and global urbanization. Accordingly, the world is projected to face a 40% global water deficit by 2030 (Connor 2015). Given the worldwide depletion of the available water resources, wastewater, which has been perceived as an undervalued resource, has now become a must-have component that needs to be properly managed to enhance the economic sustainability (Connor et al. 2017). The increased demand for water resources is now driving the need for reclaiming wastewater resources to alleviate the impact of some of the imposed pressures attributed to this growing demand. Therefore, water reuse is gaining momentum as a reliable alternative source of freshwater (Bixio et al. 2008). The reuse of wastewater is expected to elicit significant economic and environmental benefits by increasing water availability and by reducing the over-abstraction of freshwater, thereby diminishing the volume of discharged wastewater, and ensuring the quality of wastewater.

The United Nations established the 2030 Agenda for Sustainable Development with a set of 17 sustainable development goals (SDGs) (Nations 2015a). The establishment of SDG

6, namely “Ensure availability and sustainable management of water and sanitation for all,” reflects the critical interests based on water scarcity and the needs of procuring water resources. Recycling, reusing, and recovering wastewater resources are expected to alleviate water stress and offer environmental and economic benefits. Additionally, wastewater is an important source of recoverable nutrients and other valuable materials which can be recovered and reutilized (Batstone et al. 2015).

However, the management of wastewater resources has been constrained by the current practices of wastewater treatment, which remain at a basic level and only satisfying the regulations for water discharge into natural streams. The quality of wastewater effluent treated by conventional practices needs to be refined by advanced water treatment technologies. Given that only a small fraction of wastewater effluent undergoes advanced treatment processes, the installation of tertiary water treatment facilities to obtain high quality reclaimed water is crucial (Gwak, Kim & Hong 2018; Gwak et al. 2019). In addition, the strict regulatory standards for wastewater effluent are mandating the water industry to develop new technologies that are suitable for sustainable wastewater reuse. Specifically, domestic and municipal wastewaters are characterized by their increased loads of nitrogen and phosphorus, which are associated with limited removal and economically unfeasible processes based on the adoption of conventional treatment technologies, such as biological treatments that ultimately cause high-toxicity levels, oxygen depletion, and eutrophication issues (Ruiz et al. 2013).

Capacitive deionization (CDI), an electrostatically driven process, has been acknowledged as an energy-efficient and eco-sustainable technology for removing charged species from saline water resources because it does not require any chemicals or hydraulic/thermal energy (Porada et al. 2013a). A typical CDI system consists of two

electrodes at which an electrical potential is applied. Consequently, the charged ions in the feed solution are attracted within the electrical double layer (EDL) formed between the electrode and feed solution interface. This process is exceptionally energy-efficient compared to other possible desalting technologies for desalinating low-concentration salt water below 5000 ppm (Anderson, Cudero & Palma 2010) because it readily removes relatively few salts from low-saline water compared to the removal of water molecules through the extensively used technique of reverse osmosis (Liu et al. 2015). Hence, this technology is expected to have strong potential applicability in advanced wastewater treatment processes attaining enhanced removal of salinity, especially for problematic species, such as nitrates, to obtain reclaimed water (Hu et al. 2018).

Several studies on CDI for reusing municipal wastewater have been explored thus far as means of removing charged impurities, including high loads of nitrate (NO_3^-) and phosphate, which must be removed as they pose a risk to human health. Garcia-Quismondo et al. (2016) provided a comprehensive look at CDI demonstrating its environmental and socio-economic benefits as a technology for wastewater reclamation (García-Quismondo et al. 2016). The effects of the operational conditions and feed solution chemistry on the electrosorption performance of adjusting the sodium chloride (NaCl) concentration to match it with the ionic concentration of wastewater have been investigated (Liang et al. 2013). The degraded performance of the fouled electrode after longer operations in CDI was revealed to be caused by the physically and electrochemically adsorbed organic matters, such as humic- and protein-like substances, and was well-recovered by implementing proper fresh water flushing and chemical cleaning strategies (Wang et al. 2015). Membrane CDI (MCDI) attained better desalination rates than those of typical CDI in wastewater treatment with higher charge

efficiencies (Jiang et al. 2019a; Liang et al. 2013), whereas flow electrode CDI was used to conduct simultaneous wastewater reclamation and ammonia recovery during continuous operation (Fang et al. 2018). Integrating the electrosorption process with microbial fuel cells as the prior stage by applying an overpotential on the system to generate chlorine were initiated as a method of overcoming the weak organic removal capability of CDI (Feng et al. 2017). Palko et al. (2018) suggested a hybrid system of CDI where no potential was needed for adsorption to the electrode and the captured ions were consequently expelled through capacitive regeneration (Palko et al. 2018).

However, the majority of the studies on CDI for the advanced treatment and reuse of wastewater remained in theory and lab-scale investigations. The assessment of MCDI for its application in wastewater reuse is necessary to understand its fluctuating performance owing to the complex nature of the characteristics of real municipal wastewater inflow and operating conditions of a scaled-up system. The selectivity of the charged species that are harmful to human body and their total removal from wastewater under different operating conditions using real wastewater must be probed through a pilot-scale demonstration.

This study explored MCDI, which is considered one of the most efficient systems in practice, for wastewater reclamation at a pilot-scale using real wastewater effluent. The main goal in this work was to demonstrate the suitability of the MCDI process for practical wastewater reuse. We used carbon electrodes coated with a thin anion- or cation-exchange polymer layer that acted as an ion-exchange layer in the MCDI instead of using separate ion-exchange membranes (IEMs) for inhibiting the electrosorption of the counter-ions during electrode regeneration, which was expected to induce better electrosorption efficiencies and higher packing densities for the MCDI module. The

performance of the coated carbon electrodes was first evaluated at a lab-scale under different flow rates and applied potentials (i.e., adsorption capacity and charge efficiency). The pilot-scale unit used an MCDI module that involved 50 pairs of anion/cation selective electrodes, which was employed to desalinate the charged species from the wastewater effluent. The operating conditions were then optimized to ensure high total ion removal and to enhance the selectivity of problematically charged species, such as nitrates. Last, the electrosorption/regeneration stages were repeatedly run for 15 consecutive days to examine the long-term sustainability of the pilot system, and the findings were then utilized to discuss improvements in this process for real use in wastewater reclamation.

This chapter is an extension of the research article published by the author in Chemical Engineering Journal.

5.2 Experimental methods

5.2.1 Activated carbon electrodes coated by ion-selective polymers

The activated carbon electrodes were coated by cation- and anion-selective polymers containing a functional group with an ion-exchange capacity, and were provided by Siontech Co. (Republic of Korea). The carbon electrodes consisted of a graphite body sheet coated with a carbon slurry blended with activated carbon P–60 and polyvinylidene fluoride obtained from Kuraray Chemical Co. (Japan) and Inner Mongolia 3F–Wanhao Fluorine Chemical Co. Ltd. (China), respectively (Dorji et al. 2018). Both sides of each electrode were then coated by ion-selective solutions using an automatic casting machine, thereby forming a thin polymer layer that acted as an IEM. Thus, no separate IEM was needed for inhibiting the sorption of the counter-ions during electrode regeneration in our

MCDI system. The dimensions of each activated carbon electrode were 10 L × 10 W cm^2, and the total carbon mass covering the graphite body was 0.8 g.

Fifty pairs of the coated electrodes were stacked in an acrylic rectangular MCDI module used in the pilot-scale unit. The cation- and anion-selective electrodes were alternately inserted in the module. All the electrodes were separated by an electrically nonconductive nylon mesh spacer, thereby ensuring the availability of space for water flow and preventing short-circuiting. The feed solution that passed through the MCDI system was entirely in contact with the carbon electrodes by punching a hole with a diameter of 1 cm in the center of the electrodes and nylon spacers. The graphite bodies of each cation- and anion-selective electrode were connected by a conductive copper pole to let the electrical energy pass through the system.

5.2.2 Experimental protocol of lab-scale MCDI

The MCDI tests were performed using a lab-scale unit as described in our previous work (**Figure. 5.1(a)**) (Kim, Gwak, et al. 2017b). A pair of cation- and anion-selective electrodes was symmetrically inserted within the test cell, and a non-conductive spacer was placed between these two electrodes. The feed water was completely in contact with the carbon electrodes by punching a 1 cm diameter sized hole in the center of the carbon electrodes and nylon spacer. The feed solution was fed throughout the unit using a peristaltic pump made by Cole–Palmer (USA). An electrical potential was supplied to the electrodes by a potentiostat, WPG–100 (WonATech Co., Republic of Korea). Stabilization prior to the experiments was conducted by flushing the feed solution through

the system under single-pass at zero voltage until the conductivity and pH of the permeate solution were the same as those of the influent.

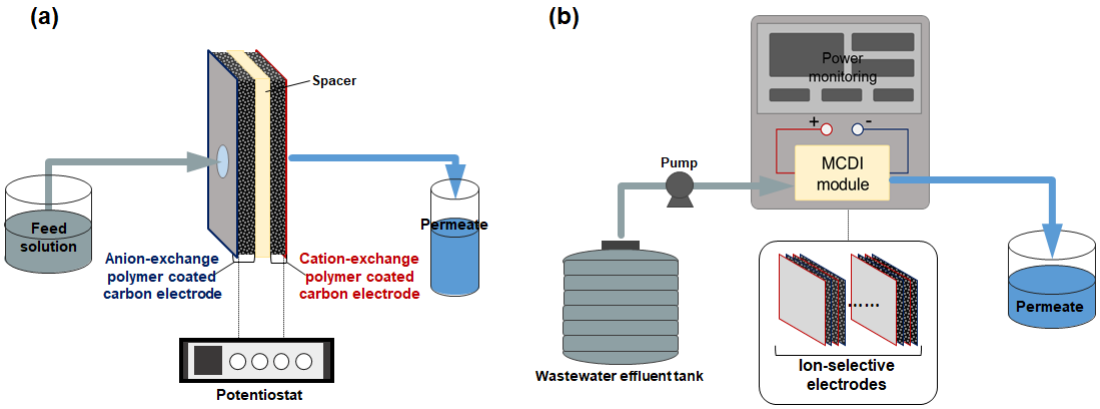

Figure 5.1. Schematic diagram of the (a) lab- and (b) pilot-scale MCDI test units using ion-selective electrodes for wastewater reuse.

Single-pass mode experiments were performed to evaluate the adsorption capacity and charge efficiency of the cation/anion-selective electrodes. The feed solution was 10 mM of NaCl, whereas the adjusted flow rate and applied potential varied from 10 to 40 mL/min and 0.6 to 1.2 V, respectively. The conductivity data of the permeate solution were recorded on an electrical conductivity meter (Hach, USA) to calculate the adsorption capacity of the electrode. All the tests were run in duplicate at 20°C.

5.2.3 Configuration of the pilot-scale MCDI unit

A single-pass pilot-scale MCDI system was installed at a decentralized wastewater treatment plant located in Sydney, Australia (**Figure. 1(b)**). The wastewater effluent from

the treatment plant was pumped out through a 10 μm pre-filter followed by the MCDI module with the use of a high-pressure pump (Walrus Pump Co., Taiwan). The effluent water after adsorption and desorption of ions (2 min for each), which was charged by a direct current power supply, was then separately collected from the permeate and concentrate line. The voltage and current loads on the module were monitored. Electrical conductivity, temperature, and pH in the inlet from the cell and in the permeate and concentrate lines were measured using in-line probes, and the data were saved on a data logger. The hydraulic pressure drop along the electrode module was also monitored by placing pressure meters in the inlet and outlet. The applied potential on the module in this study ranged from 1.2–1.5 V, whereas the flow rate was at 0.5–2.5 L/min. Prior to the run of each test, the system was stabilized by flushing the wastewater throughout the module at a desired applied voltage with at least five electrosorption and regeneration cycles.

5.2.4 Measurement of water quality

The cationic compositions of the raw and processed wastewater samples, such as sodium (Na^+), potassium (K^+), calcium (Ca^{2+}), and magnesium (Mg^{2+}), were quantified using a microwave plasma atomic emission spectrometer (MP–AES), (4100 MP–AES, Agilent Technologies, USA), while a UV/VIS spectrophotometer (Spectroquant NOVA 60, Sigma–Aldrich, USA) was used to measure ammonium (NH_4^+) with an NH_4^+ photometric test kit (Merck Millipore, United States SA). The anionic species, such as NO_3^-, nitrite (NO_2^-), chloride (Cl^-), sulfate (SO_4^{2-}), and ortho-phosphate (PO_4^{3-}), were measured using ionic chromatography (IC), (IC Thermo Fisher Scientific, Australia). Total organic carbon (TOC) values of the wastewater and permeate were measured using a multi N/C 3100 TOC analyzer (Analytik Jena, Germany). The solution samples were diluted

properly and filtered using a 0.45 μm filter (Merck Millipore, USA) before they were analyzed by the measurement devices. The calibrations of MP–AES and IC were carried out before the analyses of the samples based on external calibrations with deionized water and standard synthetic solution (1.25, 2.5, 5, 10, and 20 mg/L of each ion in the mixed solution).

The salt adsorption capacity (SAC) of the electrode at time *t* was calculated using **Equation. 5.1**:

$$\text{SAC (mg/g)} = \frac{m_t}{m} = \frac{Q \times \int_0^t (C_0 - C)dt \times M}{m} \qquad \textbf{(Equation 5.1)}$$

where m_t is the total amount of adsorbed ions at time *t* (mg), *m* is the mass of carbon on the electrode (g), *Q* is the volumetric flow rate (mL/min), C_0 is the initial concentration of feed solution (mmol/L), *C* is the concentration of permeate at time *t* (mmol/L), and *M* represents the molar mass of salt (mg/mmol).

The charge efficiency Λ, which is the ratio of salt adsorption to applied charge in the MCDI system, can be derived by **Equation. 5.2**:

$$\Lambda = \frac{\text{total n} \times \text{F} \times \int (\text{C}_0 - \text{C})\text{dt} \times \text{Q}}{\int \text{Idt} \times \text{A}} \qquad \textbf{(Equation 5.2)}$$

where *n* is the number of electrons needed for electrosorption of one charged ion, *F* is the Faraday's number (96485.3 C/mol), *I* is the current density (A/m^2), and *A* represents the effective surface area of the electrode (0.01 m^2).

The electrosorption removal efficiency from the wastewater effluent after pilot operation was calculated using **Equation 5.3**:

$$\text{Removal efficiency (\%)} = \frac{(C_0 - C)}{C_0} \times 100 \qquad \textbf{(Equation 5.3)}$$

where C_0 and C (mg/L) are the initial and permeate concentrations of wastewater, respectively.

The electrosorption selectivity of ion *i* at time *t* can be expressed by **Equation 5.4**:

$$\text{Adsorption selectivity of i} = \frac{C_{i,t,b}}{C_{total,t,b}} \qquad \textbf{(Equation 5.4)}$$

where $C_{i,t,p}$ denotes the molar concentration of *i* and $C_{total,t,p}$ is the total molar concentration in the permeate solution at time *t*. Larger values of the adsorption selectivity imply that the ion *i* is more preferentially adsorbed from the carbon electrode over other co-existing ions.

5.3 Results and discussion

5.3.1 SEM analysis of the ion-selective carbon electrodes

The carbon electrodes covered by ion-selective polymer layers provide effective regenerability by screening the attraction of counter-ions during electrode regeneration (Kim & Choi 2010c; Liang et al. 2013). Apart from this, the coated electrode was expected to induce a high adsorption capacity owing to the low resistivity of the thin ion-selective polymer-coated layer compared to the placement of a separate thick IEM. The basic electrosorption performance of the ion-selective electrodes was first tested at the lab-scale, and the results were compared with those that employed a typical MCDI configuration, which was carbon electrodes integrated with separate IEMs.

The scanning electron microscope (SEM) images of the top views of the cation- and anion-selective electrodes, and the conventionally used activated carbon electrode are shown in **Figure 5.2**. The original carbon electrode consisted of relatively large particles that appeared to have a granular surface (**Figure 5.2(a)**). Unlike that of the raw carbon electrode, the surface of the ion-selective electrodes coated by a 50 μm thick cation- or anion-selective polymer layer was apparently smooth, thereby confirming the fact that the carbon surface was completely covered by the polymer solution. In addition, the carbon particles did not detach from the coated surface by hand rubbing, thereby yielding better mechanical strength attributed to the film coating on the surface. From the observation of the SEM images, the smooth surface was expected to mitigate the degradation of the electrode performance caused by the physical adsorption of organic and inorganic contaminants involved in wastewater because it provides less opportunity for the contaminants to be in contact with and be absorbed onto the electrode surface. The mitigation of performance degradation caused by the impurities is explained more in detail in the following sections.

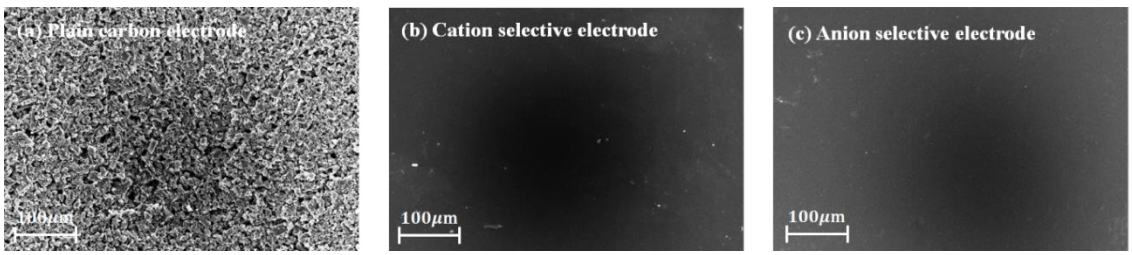

Figure 5.2. SEM images of the surface of (a) the original, (b) cation-selective, and (c) anion-selective carbon electrodes.

5.3.2 Lab-scale performance of the coated electrodes

Figure 5.3 presents the SACs in the MCDI using ion-selective carbon electrodes. The results using conventional MCDI consisting of raw carbon electrodes and separate IEMs are also outlined for a better understanding. The SAC reached values up to 0.160, 0.188, 0.214, and 0.248 mmol/g in the ion-selective layer-coated MCDI using the respective voltage values of 0.6, 0.8, 1.0, and 1.2 V, whereas the respective SAC values in the conventional MCDI operation were 0.103, 0.134, 0.181, and 0.234 mmol/g. This was likely owing to the lower membrane resistance induced by the thinly coated ion-selective layer, which played a role as an IEM. The other possibility could have been the low contact resistance between the coating layer and the carbon surface that led to the reduction in energy use and enhanced ion adsorption, whereas high contact resistance was induced by the weak contact adhesion between the separated IEM and the original carbon electrode (Lee et al. 2011).

The low resistance through the coated layer also facilitated faster ionic transport reaching electrosorption equilibrium after approximately 210 s compared to that of the IEM in a conventional MCDI system, which attained adsorption equilibrium at approximately 300 s (Kang et al. 2013). However, the amount of adsorbed salts decreased in minute amounts after the ion-selective electrode reached saturation, which was probably owing to the co-ion expulsion from the EDL near the pores and the neutral salt discharge from the electrode (Biesheuvel et al. 2014).

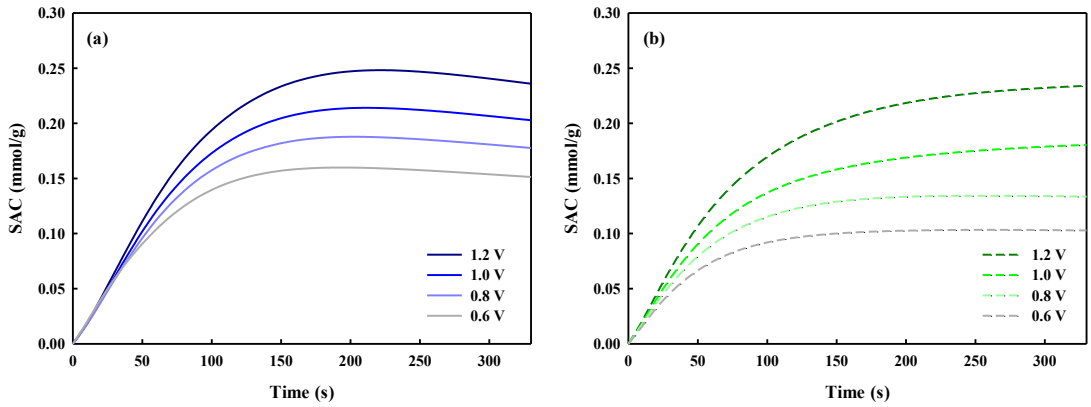

Figure 5.3. SAC of the (a) ion-selective and (b) conventional MCDI systems at different potentials (0.6–1.2 V).

Charge efficiency is a functional tool to evaluate the energy efficiency of the MCDI system. The average charge efficiency of the ion-selective electrode and the original electrode in the conventional MCDI system was estimated at voltage value of 1.2 V, as shown in **Figure 5.4**. The average charge efficiency for the conventional MCDI system was 63.6%, while that of the ion-selective electrode was enhanced to 73.3%, which was attributed to the reduced interfacial resistance between the ion-selective polymer layer and carbon electrode caused by their improved contact adhesion (Liu et al. 2014).

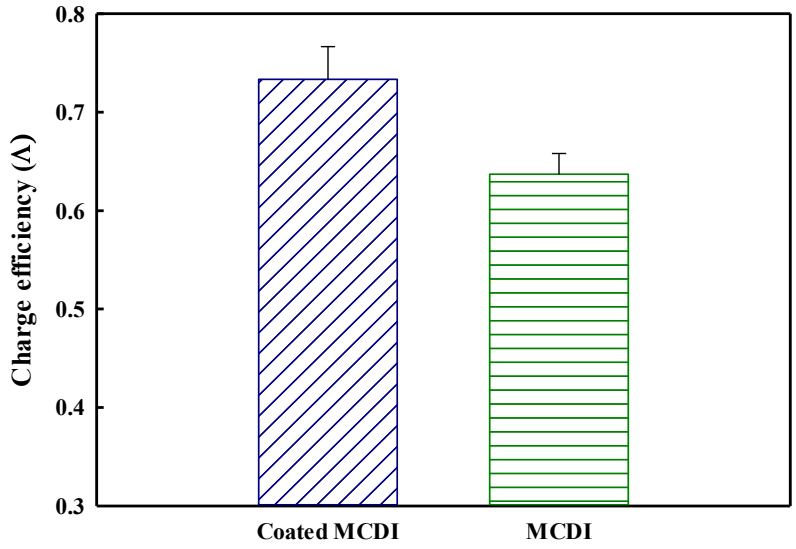

Figure 5.4. Average charge efficiency for ion-selective and conventional MCDI systems at 1.2 V.

5.3.3 Removal efficiency of ions during wastewater reuse

The competitive removal of ionic species in real municipal wastewater effluent was investigated using a pilot-scale unit under a flow rate of 2 L/min and an applied power of 1.2 V. Several studies of preferential electrosorption in (M)CDI revealed that the carbon electrode preferentially trapped the ions present in high concentrations (Chen et al. 2015; Hou & Huang 2013). To be specific, the ions with higher valence would be more electrochemically adsorbed compared to the lower valence ions on the carbon surface if their respective molar concentration were the same. Last, possessing similar concentrations and the same charge valence allowed smaller hydrated ions with a faster diffusion rate to rapidly migrate toward the carbon surface (Hassanvand et al. 2018).

Table 5.1. Average removal of ionic species in wastewater effluent during pilot-scale layered-MCDI operated at 1.2V for 2 min.

Ion	Feed (mM)	Removal efficiency (%)	Adsorption capacity (mmol/g)	Adsorption capacity (meq/g)
Na^+	4.08	50.8	0.377	0.377
K^+	0.46	67.4	0.031	0.031
Ca^{2+}	0.27	84.1	0.023	0.046
Mg^{2+}	0.15	79.4	0.012	0.024
NH_4^+	0.007	64.3	0.000	0.000
TP	0.03	37.5	0.001	0.001
NO_3^-	0.76	75.7	0.058	0.058
NO_2^-	0.003	48.7	0.000	0.000
Cl^-	2.26	52.6	0.119	0.119
SO_4^{2-}	0.46	21.3	0.010	0.020

As shown in **Table 5.1**, Na^+ was the most adsorbed ion on the cathode, which was owing to its high initial concentrations in the wastewater feed. However, the removal efficiency of Na^+ in terms of percent removal was the lowest, even though the number of adsorbed Na^+ ions on the electrode outnumbered that of other cations. Given that K^+ diffused faster and Ca^{2+} had stronger electrochemical attraction toward the electrode surface, the portion of their adsorbed ions was relatively higher than that of Na^+ (Hassanvand et al. 2018). Unlike the ion adsorption selectivity in terms of the number of adsorbed ions, which was primarily determined by the initial concentration of the ions (specific selectivity in the expression of $mmol/mmol_{total}$ in **Figure 5.5(a)**), the ion selectivity in terms of removal efficiency was rather governed by the feed solution characteristics, such as the diffusion rate and charge valence (specific selectivity in units of $\%/\%_{total}$ in **Figure 5.5(a)**).

Interestingly, the total amount of removed cations was greater than that of the anions. The asymmetry of the anion and cation removals was likely due to the electrosorption of the negatively charged organic substances present in the wastewater. These results implied that the organics were attracted near the EDL, and the space for the anions to be adsorbed became limited as the electrode was saturated. More specific discussions regarding the removal of organic compounds are provided in the following sections. Changes in the electrode surface chemistry attributed to Faradaic reactions and the selective electrosorption of H^+ and OH^- may also have accounted for the imbalance in anion and cation removals (Tang, He, Zhang, Kovalsky, et al. 2017). However, the likelihood of a significant reaction of carbon oxidation was low owing to the stability of MCDI from the presence of IEMs (Yu et al. 2018).

The preferential electrosorption sequence of the major anions present in wastewater, in terms of the adsorption capacity, was in the order of $Cl^- > NO_3^- > SO_4^{2-}$, as mainly determined by their initial concentrations (**Figure 5.5(b)**). The removal efficiency of the three major ions was in accordance with the order of $NO_3^- > Cl^- > SO_4^{2-}$. Unlike the trend in electrosorption of cations from wastewater, the order of removal efficiency was less compliant with the charge valence and diffusion kinetics. In addition, the removal efficiency of NO_3^- was much higher than that of Cl^-, even though their hydrated ionic sizes and diffusion coefficients were similar. The hydrated radii of Cl^- and NO_3^- were 0.332 nm and 0.335 nm, respectively (Nightingale Jr 1959), whereas the diffusion coefficients both near 1.7×10^{-9} m^2/s (Picioreanu, Van Loosdrecht & Heijnen 1997; Poisson & Papaud 1983). Several studies attributed the better selectivity of NO_3^- to its strong hydrophobicity over the other major anions (Chen et al. 2015; Hassanvand et al. 2018), thus, its stronger affinity to the hydrophobic electrode surface (97.86±0.67°

contact angle) allowed it to replace the Cl^- and SO_4^{2-} ions. Besides its hydrophobicity, the planar molecule structure of NO_3^- with weak bonding to water molecules was reported to lead to its preferential adsorption within ultramicroporous structure of carbon electrodes (Hawks et al. 2019).

The removal efficiency of divalent SO_4^{2-} was expected to be higher than that of the monovalent ions owing to its affinity to screen the surface charge of the electrode caused by its higher valence. The selectivity of SO_4^{2-}, which is the representative divalent anion in wastewater, was controversial in several studies. Li et al. (2016) reported that the activated carbon electrode in conventional CDI accepted more SO_4^{2-} than NO_3^- primarily owing to the higher electrostatic attraction of SO_4^{2-}, which was mainly determined by its higher valence (Li et al. 2016). For MCDI, Tang et al. (2017) and Yeo et al. (2013) both reported that the competitive removal of SO_4^{2-} could be determined as a function of the applied electrical current (Tang, He, Zhang & Waite 2017; Yeo & Choi 2013). These works observed a higher selectivity for SO_4^{2-} compared to that for Cl^- as the applied constant current increased. However, the adsorbed amount of SO_4^{2-} from a mixture solution that consisted of Cl^-, NO_3^-, and SO_4^{2-} was similar to that of the other ions in a MCDI study conducted by Hassan et al. (2018) (Hassanvand et al. 2018). The percent removal of SO_4^{2-} from water obtained from the Colorado River was much lower than that of the other two anions during electrosorption, as reported by Gabelich et al. (2002) (Gabelich, Tran & Suffet 2002), despite the fact that the initial concentrations were in the order of $SO_4^{2-} \cong Cl^- >> NO_3^-$.

Our results of the order of removal efficiency for both the cations and anions followed the general permselectivity trend through the IEMs. Especially for the anions, their permselectivity through anion-exchange membranes (AEMs) correlated with the Gibbs

hydration energy of anions and Hofmeister anion series (Luo, Abdu & Wessling 2018b; Sata 2000). The anion permselectivity was dependent on the affinity of the anions to the membrane. In addition, their selectivity was also affected by the change in their mobility through the AEM (Luo, Abdu & Wessling 2018b; Sata 2000). As shown in the results (**Table 5.1** and **Figure 5.5(b)**), the preferential adsorption of the major anions, in terms of removal efficiency, in the wastewater was likely determined by the permselectivity trend in IEMs. Furthermore, the change in the order of preferential adsorption of the anions in MCDI with different applied potentials could also be explained by the change in ion mobility through the IEM (Dong et al. 2019).

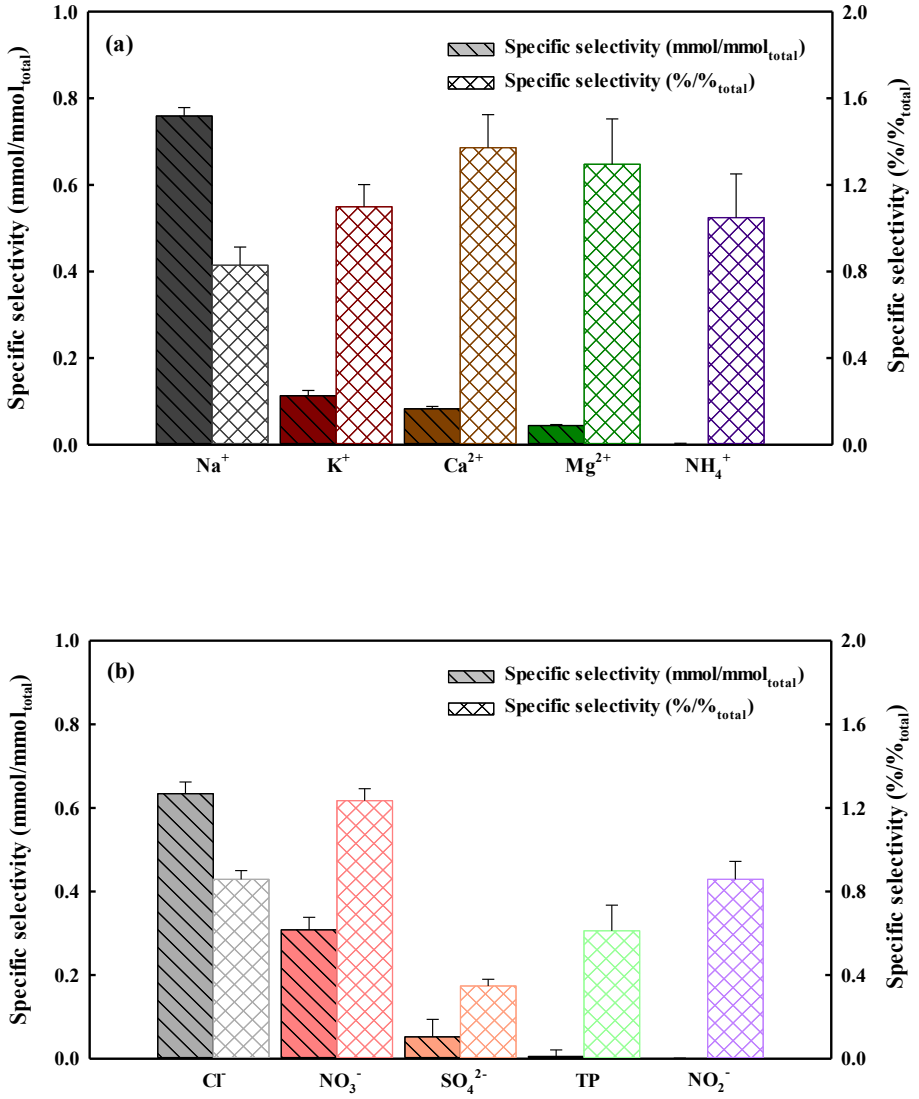

Figure 5.5. Specific selectivities of (a) cations and (b) anions on ion-selective polymer-coated electrodes in wastewater. The left axis shows the selectivity derived by the number of adsorbed ions divided by the total number of removed cations or anions. The right axis shows the selectivity derived by the ion removal efficiency divided by the average removal of the total number of ions (61.3% total removal efficiency).

5.3.4 Enhancing water quality by changing electrosorption time

The influence of the operating conditions in the MCDI system on the electrosorption performance during wastewater reuse was investigated. For the cations, the adsorption rates of Na^+ and K^+ dramatically decreased as a function of time, whereas the divalent species (Ca^{2+} and Mg^{2+}) were adsorbed on the electrode at a steady rate for 2 min (**Figure 5.6**). This was likely owing to the high affinity of the divalent ions on the EDL, which replaced the monovalent ions adsorbed on the surface. Therefore, shorter operation of MCDI led to the better removal of monovalent cations.

Among the anions (**Figure 5.6(b)**), the NO_3^- concentration in the effluent was maintained at a low level, whereas those of Cl^- and SO_4^{2-} increased. This could be explained by the high affinity of NO_3^- to the carbon electrode owing to its hydrophobicity, as discussed in Section 5.3.3. Accordingly, this resulted in the substitution of Cl^- and SO_4^{2-} by NO_3^- in longer operations. Therefore, we could expect high and selective removal of NO_3^- during longer operation, which is one of the most problematic species for the reuse of wastewater.

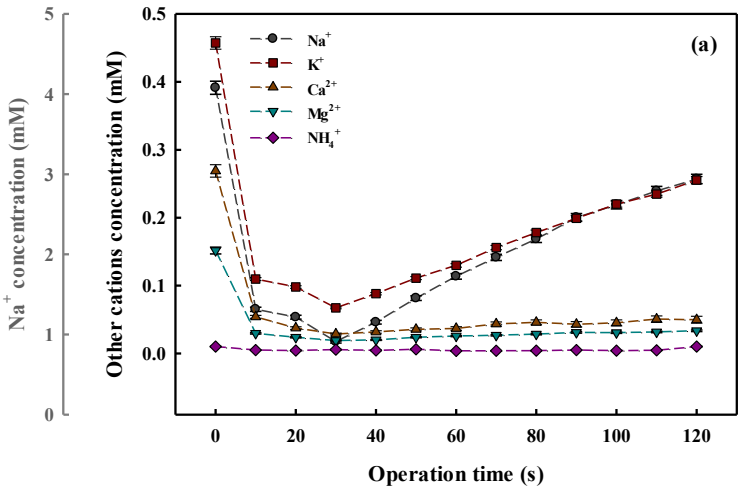

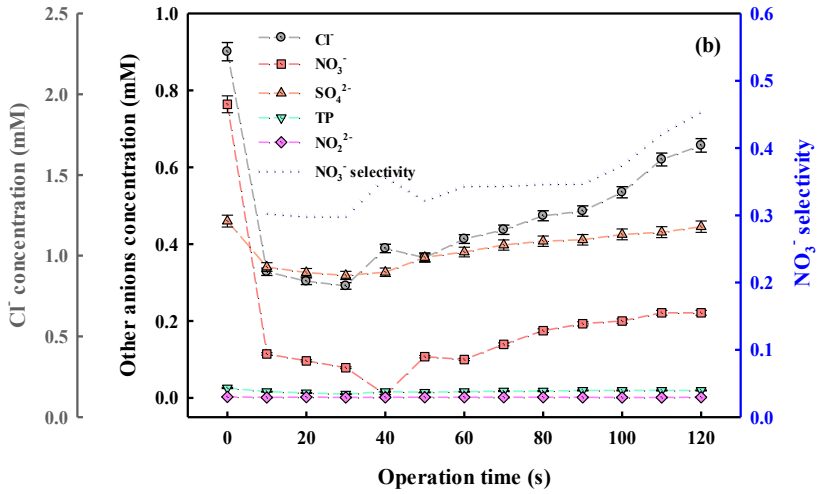

Figure 5.6. Changes in permeate (a) cation and (b) anion concentrations obtained from ion-selective MCDI cells during the treatment of wastewater.

5.3.5 Changing applied potential and flow rate for selective NO_3^- removal

The permeate that passed through the MCDI pilot unit based on a single-pass continuous flow regime was collected during a 2-min period at different flow rates and applied potentials. **Figure 5.7** shows the variation in the average removal and selectivity of NO_3^- of the sampled water.

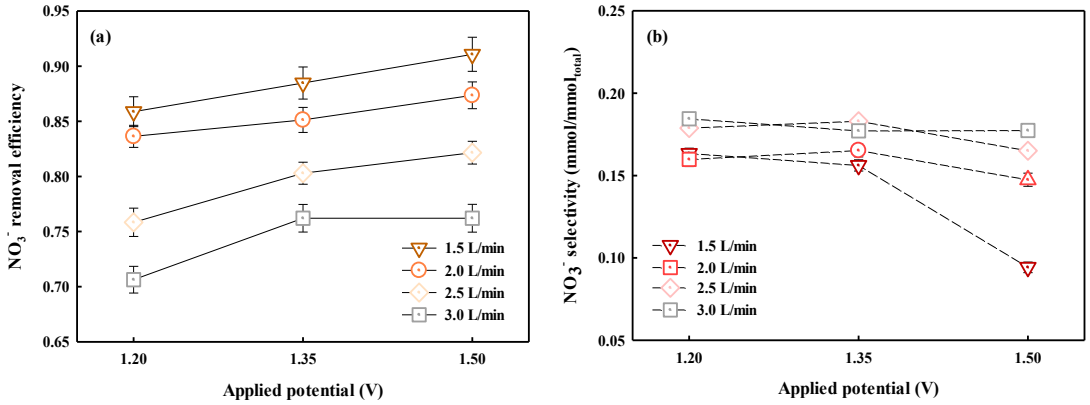

Figure 5.7. (a) Removal efficiency and (b) selectivity of NO_3^- at different potentials and flow rates.

The results elicited in **Figure 5.7(a)** implied that a larger applied voltage and a lower flow rate contributed to a reduced permeate NO_3^- concentration. The removal efficiency of NO_3^- reached up to 91.08% at a flow rate of 1.5 L/min and at an applied potential of 1.5 V. In single-pass operation, a lower flow rate is preferred to provide sufficient contact time for better electrosorption of the ions in wastewater.

As shown in **Figure 5.7(b)**, the selectivity of NO_3^- was worsened by raising the potential and lowering the flow rate, thereby showing an inverse trend with the NO_3^- removal efficiency. In contrast with the earlier batch-mode studies, which showed that the flow rate barely affected the preferential adsorption, the NO_3^- selectivity slightly decreased at lower flow rates in our single-pass tests (Choi, Lee & Hong 2016). This was likely due to the fact that increasing the flow rate gave rise to shorter time for saturation of the electrode, and the adsorbed ions, such as Cl^- and SO_4^{2-}, were quickly replaced by the supplemented NO_3^- from the continually supplied feed stream owing to its high affinity to the carbon

electrode. This was also supported by our results in **Figure 5.6(b)**. As the space of the carbon electrode surface becomes saturated with ions in longer operations, NO_3^- tends to replace the other ions that have been already adsorbed by the carbon surface (Chen et al. 2015; Hassanvand et al. 2018). Yeo et al. (2013) and Kim et al. (2013) ascribed the worse selectivity of NO_3^- at higher voltages to a significant increase in the ion mobilities of Cl^- and SO_4^{2-} through the AEM compared to that of NO_3^- (Kim, Kim & Choi 2013; Yeo & Choi 2013). Therefore, NO_3^- passes through the ion-selective layer slower than the other anions at higher voltages, and consequently fewer ions are adsorbed on the electrode surface. Therefore, it could be concluded that applying a lower potential and supplying feed water at a faster rate are recommended to enhance the removal selectivity of NO_3^- with low energy consumption, which is one of the most problematic ionic species in wastewater, especially if high total ion removal is not necessary for reusing the wastewater.

5.3.6 Successive operation of the pilot-scale MCDI system in a 15 d period

A long-term operation of the pilot-scale MCDI system was conducted to assess the effect of organic and inorganic contaminants present in wastewater, which potentially risk the sustainability of the wastewater reuse process by exacerbating the electrode's performance. Several studies investigated the fouling and scaling issues by considering the fact that CDI and MCDI are being extensively used in practice (Xu et al. 2008). A significant reduction in the ion removal efficiency in CDI was observed when the TOC concentration was increased up to 3.1 mg/L (Mossad & Zou 2013). The high organic

loads in the brackish water led to the accumulation of organic matters within the pores of the carbon electrode, which was not able to be detached, thereby leading to a lowered energy efficiency of the system. Zhang et al. (2013) carried out a 15 d CDI pilot operation and confirmed the physical adsorption of organic compounds at 2 mg/L of dissolved organic carbon (DOC), which caused a greater reduction in the salinity removal efficiency (Zhang, Mossad & Zou 2013). IEMs provided a protective function for electrodes from the physical adsorption of organic substances in the MCDI system by shifting the fouling potential from the electrode to the IEM (Chen, Wang, et al. 2018). In the MCDI system, the negatively charged nature of organic matters migrated toward the IEM, partially accumulated on the membrane surface, and hence raised its electrical resistivity and gradually hampered the salt sorption performance.

However, unlike the earlier findings, the degradation of electrosorption caused by the organic compounds involved in the wastewater effluent was insignificant during the 15 d operation period (**Figure 5.8**). As shown in **Figure 5.9**, the negatively charged organic compounds in the wastewater effluent were fairly adsorbed on the electrode surface during electrosorption (29.1%). However, the conductivity profile in the 15 d operation showed no significant degradation in the electrosorption/regeneration performance even though the organic loads in the wastewater were very high (12.4 mg/L DOC). These results implied that the electrochemically adsorbed organic species were well discharged during the regeneration stage, thereby leading to sustainable operation of the MCDI for wastewater reuse.

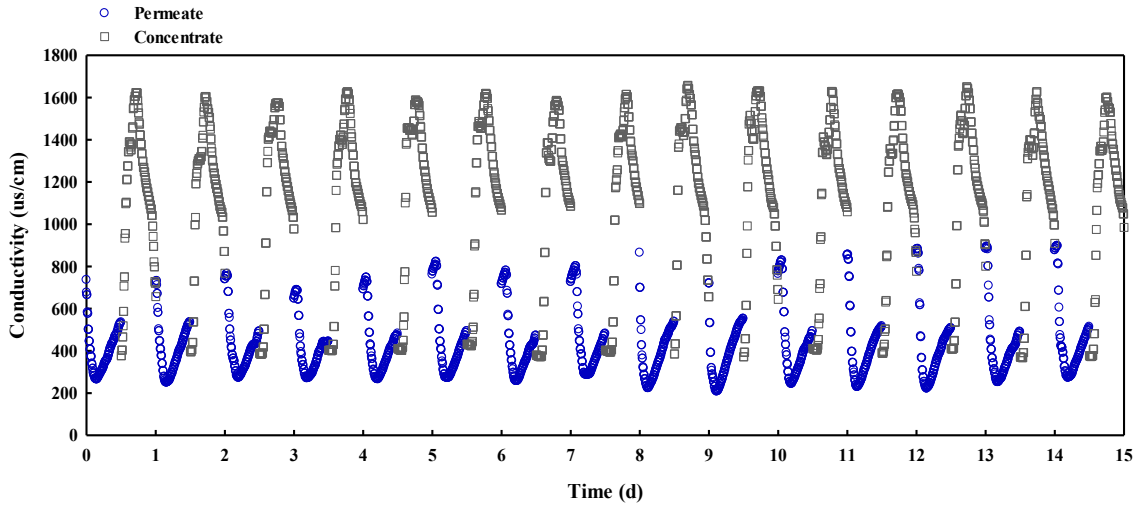

Figure 5.8. Average conductivity profile of the permeate (blue) and concentrate (gray) for 2-min adsorption/desorption cycles on each day. The long-term MCDI operation was carried out for a period of 15 d.

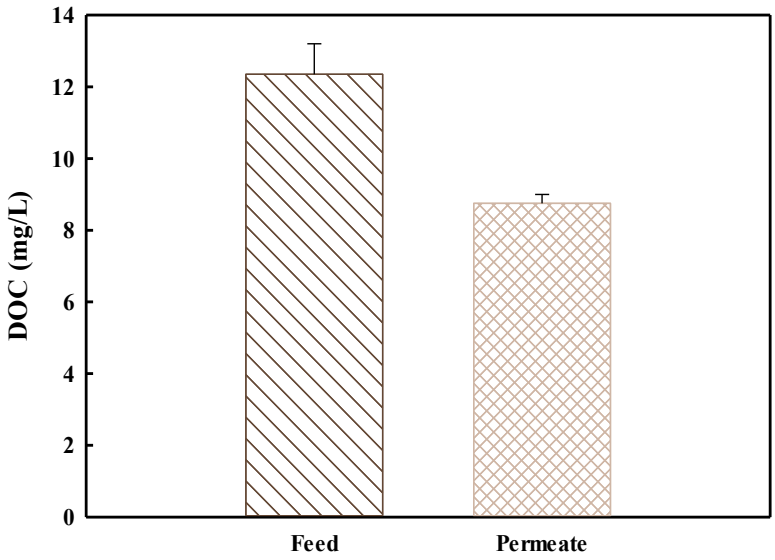

Figure 5.9. Removal of DOC from the feed and permeate of the wastewater.

The fouling-free MCDI operation could be partially explained by the roughness of the ion-selective electrodes used in the pilot-scale system. In general, the roughness of the IEM and carbon electrode surfaces is a significant factor affecting severe physical adsorption and accumulation of organics (Zhao et al. 2018). The root-mean-square roughness values of the activated carbon electrode and AEM in the conventional MCDI configuration were 756 and 159 nm, respectively, whereas that of the surface of the anion-selective electrode tested in the pilot-run was 36 nm (**Figure 5.10**) (Zhao et al. 2016). The flat surface of the coated layer offered a smaller opportunity for the organic particles to attach on the surface, thereby leading to less accumulation of the negatively charged organic species. Apart from the roughness, it was noted that the other surface properties of the IEM and electrode surfaces, such as the surface charge and hydrophobicity, also influenced the accumulation of organic species, which must be further studied for an in-depth discussion of the fouling-free surface of the anion-selective carbon electrode (Xiao et al. 2011).

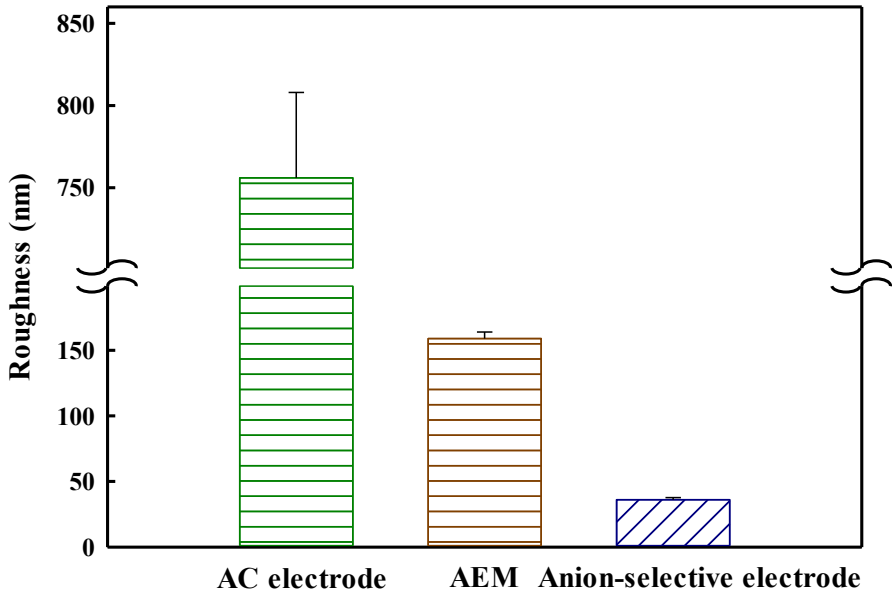

Figure 5.10. Root-mean-square roughness of the originally activated carbon electrode, AEM (Neosepta AMX), and anion-selective electrode.

5.4 Concluding remarks

Our work systematically explored MCDI for the demonstration of its practical use in wastewater reclamation at a pilot-scale using real wastewater effluent. The electrosorptive performance of electrodes, removal of charged species from wastewater, influence of operating conditions on ion removal, such as for NO_3^-, and performance degradation in long-term operations were investigated in this study.

The lab-scale tests confirmed rapid electrosorption and better SAC and charge efficiency of the ion-selective polymer-coated electrode. In a more practical view, installing the wastewater reuse system is expected to be more space-efficient by using the thin coated electrode rather than the conventional MCDI configuration, which as attributed to the

high packing density of the electrodes in the module. The removal efficiency of the major anions from municipal wastewater via the pilot-scale MCDI unit was in the order of $Cl^{-}>NO_3^{-}>SO_4^{2-}$, thereby showing high removal of NO_3^{-}, which is one of the most problematic ionic species in wastewater. The preferential anion removal was likely determined by the anion permselectivity through the AEM, which was dependent on the affinity of the anions to the membrane and on the change in the ion mobility through the AEM. The selectivity of NO_3^{-} could be enhanced in longer operations as it replaces the other anions adsorbed on the electrode. Supplying water at higher flow rates led to faster saturation of the electrode, and resulted in the swift replacement of Cl^{-} and SO_4^{2-} by the fast supply of NO_3^{-} from the wastewater feed. However, increasing the voltage worsened its selectivity owing to the significantly increased ion mobility of Cl^{-} and SO_4^{2-} through the AEM. The deterioration of MCDI performance caused by the contaminants present in the wastewater was insignificant during the 15 d pilot-scale operation. The smooth morphology of the ion-selective electrode surface contributed to sustainable wastewater reuse in the long-term CDI operation by providing a small effective area for the physical accumulation of organic substances.

To sum up, the results from our study demonstrated that wastewater could be well reclaimed by achieving selective removal of the un-welcoming impurities. It was also shown that sustainable operation of MCDI in the long-term can be realized owing to the fouling-free properties of the ion-selective electrodes.

CHAPTER 6

Phosphorus Removal Mechanisms from Domestic Wastewater and System Optimization for Selective Phosphate Recovery

The results from this work was published on Process Safety and Environmental Protection, which is titled as "*Phosphorus removal mechanisms from domestic wastewater by membrane capacitive deionization and system optimization for enhanced phosphate removal*".

Research highlights

- This work investigates the suitability of MCDI for P recovery from wastewater.
- Phosphate speciation was reflected in understanding P removal mechanisms.
- Phosphate speciation under different pH impacts the degree of P adsorption.
- The effect of pH was insignificant on P removal due to the competing anions.
- Selectivity of P was improved by increasing potential and lowering flow rate.

6.1 Introduction

Phosphorus (P) is an essential nutrient for the growth of plants and animals (Filippelli 2002). Under natural conditions, P is the limiting nutrient in surface water because it prevent the growth of algae and aquatic plants in water bodies. The natural background level of total phosphorus (TP) and phosphate are typically less than 0.03 mg/L and range between 0.005 and 0.05mg/L, respectively (Kotoski 1997). However, many open water sources such as lakes, streams, oceans and reservoirs, are currently experiencing excess of P from human activities, which can speed up eutrophication in aquatic system and cause water quality impairment, aquatic species biodiversity decrease, adverse human health impacts, and increase the cost of water treatment, etc. (Chislock et al. 2013; Wilkinson 2017).

To mitigate or prevent the risk of eutrophication, the P concentration in the wastewater effluent from the wastewater treatment plants (WWTPs) is regulated by the environmental authorities globally to control the effect of discharges on water quality and aquatic species biodiversity. Current WWTPs treatment methods used for P removal include physical, chemical and biological processes (Mohammed & Shanshool 2009; Strom August 2006). In contrast, the above nutrient removal methods, to some extent,

have drawbacks in terms of life-cycle costs, operation complexity, safety, portability, and further maintenance requirements.

Capacitive deionization (CDI), on the other hand, is a promising technology that uses electrophoretic driving forces to remove charged ions from an aqueous solution (Pekala et al. 1998). It was shown to have great application potential for seawater and brackish water desalinations (Biesheuvel et al. 2017; Dorji et al. 2018), water softening (Tuan et al. 2015), selective removal of specific ions (Choi, Lee & Hong 2016), resources removal and recovery (Huang et al. 2017; Kim et al. 2018), and water reclamation (Anderson, Cudero & Palma 2010). CDI operates at a low voltage, generally less than 1.23 V, to avoid faradaic reactions that can result in water electrolysis (Liang et al. 2017; Shanbhag et al. 2017; Zhang, He, et al. 2018). Unlike other wastewater treatment measures, CDI process functions as an electrosorbent without requiring any additional chemical. Benefits of applying CDI technology include: higher water recovery, lower operation cost, lower energy requirements, higher removal efficiency of charged ions, high portability, and no water softening requirement prior to purification. (Anderson, Cudero & Palma 2010; Porada et al. 2013b; Zarzo & Prats 2018).

CDI technology has been receiving increased attention for P removal and recovery. Huang et al. (2014) was the first to evaluate the feasibility of applying a commercial CDI unit to treat phosphate-containing wastewater using single salt feed solution (Huang et al. 2014). Huang et al. (2017) subsequently studied the pH-dependent phosphate (P) electrosorption capacity in MCDI under both constant voltage (CV) and constant current (CC) mode of operations (Huang et al. 2017). However, the earlier works on CDI for P removal which fundamentally investigated the P removal has failed to reflect the very nature of phosphate ions in wastewater. So far, very few studies have been focused on understanding the effect of phosphorus speciation reactions particularly at pH between

6.5 and 8.5, which is the typical pH range maintained for the residential raw wastewater. The inorganic phosphate within this pH range mostly exists in the form of dihydrogen phosphate ion ($H_2PO_4^-$) and hydrogen phosphate ion (HPO_4^{2-}) (Mogens Henze 2008), which is predominantly in a weakly acidic and weakly basic conditions, respectively. The proportion of these phosphate species in this pH range (6.5-8.5) is shown in **Table 6.1**, in compliance with following reversible reaction:

Table 6.1. The proportion of different phosphorus species under various pH.

pH	$[H^+]$	$\alpha[H_3PO_4]$	$\alpha[H_2PO_4^-]$	$\alpha[HPO_4^{2-}]$	$\alpha[PO_4^{3-}]$	$\alpha[H_2PO_4^-]$: $\alpha[HPO_4^{2-}]$
6.6	0%	0%	80%	20%	0%	4:1
6.9	0%	0%	67%	33%	0%	2:1
7.2	0%	0%	50%	50%	0%	1:1
7.5	0%	0%	33%	67%	0%	1:2
7.8	0%	0%	20%	80%	0%	1:4

$$H_2PO_4^- \leftrightarrows H^+ + HPO_4^{2-} \quad (6.1)$$

the corresponding acid dissociation constant K_{a2} (mol/L) at 25 °C is:

$$K_{a2} = \frac{[H^+][HPO_4^{2-}]}{[H_2PO_4^-]} \cong 6.2 \times 10^{-8} \quad (pK_{a2} \approx 7.21) \quad (6.2)$$

Generally, the ion selectivity and degree of ion electrosorption capacity mainly depend on the hydrated size, ionic charge, ion concentration, and degree of ion complexation (Hou & Huang 2013). Fan et al. (2017) investigated preferential adsorption sequence of co-existing ions in single-pass-mode (SP-mode) CDI (Fan, Liou & Hou 2017). And they observed that the co-existence of other ions can significantly affect the phosphate removal from the wastewater. However, these reported works did not closely reflect the real ionic

composition present in domestic wasteater considering the complexity of the co-existence of other ions. They conducted their studies in a mixed environment covering different ionic charge and non-equal ion concentration (Fan, Liou & Hou 2017). In another work, Huang et al. (2017) analyzed pH-dependent ion selectivity between P and Cl^- in SP-mode membrane CDI (MCDI) with equivalent ionic strength (Huang et al. 2017). However, more in-depth research is required to fully understand the phosphate electrosorption capacity and competitive ion selectivity in more complex and realistic electrolytes with ionic contents.

The main goal of this work was to explore the suitability of MCDI for effective P removal from domestic wastewater. To do so, the effects of the equilibrium reactions on P adsorption capacity when feed solution contains only $H_2PO_4^-$ and HPO_4^{2-} were firstly investigated. In addition, the phosphate sorption capacity and ion selectivity in the presence of Cl^- and SO_4^{2-} as co-ions were experimentally studied by mimicking the real ionic composition of a domestic wastewater. An overall evaluations of individual operating parameters (different flow rate, pH, voltage, and sorption time) and their corresponding TP removal performance were then covered to achieve optimal P removal via this electrosorptive technology and study the potential of applying MCDI - as one of the alternative WWTPs treatment option - for effective P removal from domestic wastewater.

6.2 Materials and methods

6.2.1 Lab-scale MCDI unit setup

The lab-scale symmetric two-electrode MCDI unit was used for the study purposes. It consists of a pair of commercial composite activated carbon electrodes coated by anionic

and cationic exchange solutions which are manufactured by Siontech Co., Republic of Korea. Each single composite carbon electrode has a mass of 0.8 g with a dimension of 100 mm x 100 mm. A same-sized non-electrically conductive nylon spacer was placed between them to prevent the occurrence of short circuit.

The feed solution was pumped into the cell by a peristaltic pump which is made by Cole-Parmer Co., Ltd. The constant electrical voltage was appplied by a potentiostat WPG-100 (Wonatech Co., Republic of Korea). The equilibrium status prior to the electrosorption stage was attained by flushing out the entire MCDI unit with feed solution under single-pass, at zero volts, until the reading of effluent conductivity and pH were to be the same to that of in influent. All experiments were performed in triplicate to provide a relatively sound basis for statistical analysis. **Figure 6.1** shows a schematic diagram of the proposed single-pass mode (SP-mode) lab-scale MCDI unit set up.

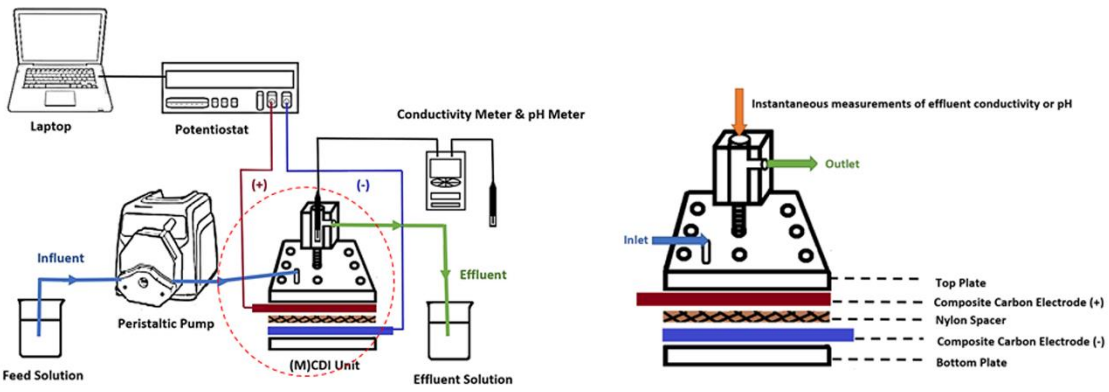

Figure 6.1. Schematic diagram of the proposed single-pass lab-scale MCDI unit setup

2-column fitting image

6.2.2 Feed solution preparation

Sodium phosphate buffer solution was used in preparing a synthetic solution for the investigation of the impact of phosphate buffer on P removal. As it can maintain the feed

solution at a relatively constant pH without additional acid/base needed, which can cause the increase of feed total dissolved solid (TDS). $NaHPO_4$ and Na_2HPO_4 were used in making buffer solution because they are commonly available and affordable. The desired pH value could be achieved by adjusting the ratio between these two chemicals. The proportions of $H_2PO_4^-$ On HPO_4^{2-} at pH equals to 6.6, 6.9, 7.2, 7.5 and 7.8 are 4:1, 2:1, 1:1, 1:2 and 1:4, respectively.

Synthetic wastewater solution was used in experiments to examine the ion selectivity of phosphate over co-existing ions and optimizing operating conditions for enhanced TP removal. As it simulates the major chemical compositions and their mass concentrations, solution pH, and conductivity in typical raw domestic wastewater; but is free of organic pollutants, solid particles, and the like. Literature formulations for the synthetic wastewater developed by researchers were aimed to simulate the conductivity and TDS content, match concentrations and range of particle sizes of suspended solids and achieve a longer storage life (Boeije et al. 1999; O'Flaherty & Gray 2013). Toifl et al. (2014) also discussed that the characteristics of the desirable composition should be commonly available, affordable, non-volatile and non-biological. The desired synthetic wastewater recipe was then developed, shown in **Table 6.2** (Toifl et al. 2014). Few drops of HCl was added to adjust synthetic wastewater solution pH between 7 and 8 without significantly increasing the TDS in the feed solution.

Table 6.2. Composition of synthetic wastewater feed solution. HCl was added to adjust pH between 7 and 8.

Constituents		Molar Weight (g/mole)	Concentration (mM)
Sodium citrate	$Na_3C_6H_5O_7$	258.06	1.16
Ammonium chloride	NH_4Cl	53.49	0.90
Sodium phosphate dibasic	Na_2HPO_4	141.96	0.40
Calcium chloride dihydrate	$CaCl_2 \bullet 2H_2O$	147.01	0.50
Potassium bicarbonate	$KHCO_3$	100.12	0.50
Magnesium sulphate heptahydrate	$MgSO_4 \bullet 7H_2O$	246.47	0.32

6.2.3 Experimental operating conditions

The SP-mode lab-scale MCDI system which is more relevant to actual wastewater treatment measures was used in this study in order to obtain reliable experimental results. The details of proposed experimental conditions and control parameters are described in **Table 6.3**. Experiment 1, corresponding to section 6.3.1 in this paper, studied the effects of equilibrium reactions on P adsorption capacity when feed solution contains only $H_2PO_4^-$ and HPO_4^{2-}. Experiment 2, corresponding to section 6.3.2 in this paper, investigated the phosphate electrosorption capacity and ion selectivity in the presence of Cl^- and SO_4^{2-}. Moreover, an overall evaluation of individual operating parameters and their corresponding TP removal performance was covered in Experiment 3, corresponding to section 6.3.3 in this paper. All the experiments under different operating conditions were carried out at more than three times.

Table 6.3. Proposed experimental conditions and control parameters.

Section	Objective	Feed	Test	Operating Conditions						
				Initial ionic strength (mM)			Initial influent	Flow rate (mL/min)	Voltage (V)	Time (min)
				TP	Cl^-	SO_4^{2-}	pH			
3.1.	Equilibrium	Sodium phosphate buffer	1.1	4			6.6,6.9,7.2,7.5,7.8	8	1.2	10
			1.2	0.4			6.6, 7.2, 7.8			
			1.3	0.4	3.6		6.6, 7.2, 7.8			
3.2	Electrosorption capacity and ion selectivity	Synthetic wastewater	2	0.4	1.9	0.32	7.2	8	1.2	10
3.3	Optimization of operating parameters	Synthetic wastewater	3.1	0.4	1.9	0.32	7.2	8	1.2	10
			3.2					8	1.2	8
			3.3					8	0.6	10
			3.4					24	1.2	10

6.2.4 Sample analysis

The validity of experimental results was guaranteed by performing triplicate experiments and carefully collecting samples in every 30 seconds. All the samples that had been digested by phosphorus test kit (Phosphate Test (o-phosphate) 114842) were measured by Merck Millipore UV/VIS Spectrophotometer (Spectroquant Nova 60, USA) for effluent TP concentration.

The salt adsorption capacity (SAC) (mg/g) in SP-mode was calculated using **Equation (6.3)**:

$$\text{SAC (mg/g)} = \frac{\text{Q}\times\int_0^t \Delta\text{C}\, dt \times \text{M}}{m} \quad (6.3)$$

where Q is the volumetric flow rate (mL/min); ΔC is the concentration difference (mM) at time t; M is the molar mass of the salt (mg/mmol); and m represents the total electrode mass (g).

The average salt adsorption rate (ASAR) (mg/g-min) in SP-mode was determined according to **Equation (6.4)**:

$$\text{ASAR (mg/g-min)} = \frac{\text{SAC}}{\Delta t} \tag{6.4}$$

where Δt is the time difference from start to any time t.

The average ion removal efficiency (E) (%) in SP-mode was determined as follows:

$$\text{E (\%)} = \frac{\int_0^t \Delta C \, dt}{C_0 \times t} \times 100\% \tag{6.5}$$

where C_0 is the influent concentration.

The relative ion removal ratio (RE) in SP-mode was expressed by **Equation (6.6)**:

$$\text{RE} = \frac{E(A)}{E(B)} \tag{6.6}$$

where RE represents the selectivity of salt A compared to salt B. RE value greater than 1 means salt A has higher selectivity than salt B, which means salt A will be more preferentially removed from aqueous solution over salt B.

6.3 Results and discussion

6.3.1 Speciation of phosphate

As indicated previously, the major composition of influent total phosphorus in domestic wastewater is inorganic phosphorus, often in the form of orthophosphate. Henze and Comeau reported it constitutes around 75% of total phosphorus concentration with concentration ranging from 5 to 15mg/L (Henze & Comeau 2008).

To probe the effects of equilibrium system on degree of P adsorption capacity, highly concentrated sodium phosphate buffer solution ($[P]_0$ = 4 mM) was fed through the MCDI system. The experimental results, as shown in **Figure 6.2**, suggested that the TP was most quickly removed under about neutral pH from the synthetic water at the beginning of

adsorption stage. For instance, at end of 90s, the instantaneous effluent TP concentration in neutral solution (pH 7.2) dropped from 4.0 to 2.2 mM, while the TP concentrations with the initial solution pH at 6.6, 6.9, 7.5, and 7.8 is declined to slightly higher levels at 2.5, 2.8, 3.0 and 2.6 mM, respectively. It implies that such system, constituted by equal amount of monovalent and divalent phosphate ions, is likely to quickly respond to reversible reactions at equilibrium. At the beginning of adsorption stage, speciation of phosphate continuously provides system sufficient amount of HPO_4^{2-} to screen carbon electrode surface charge. Meanwhile, adequate amount of $H_2PO_4^-$ to be adsorbed inside the carbon electrode pores.

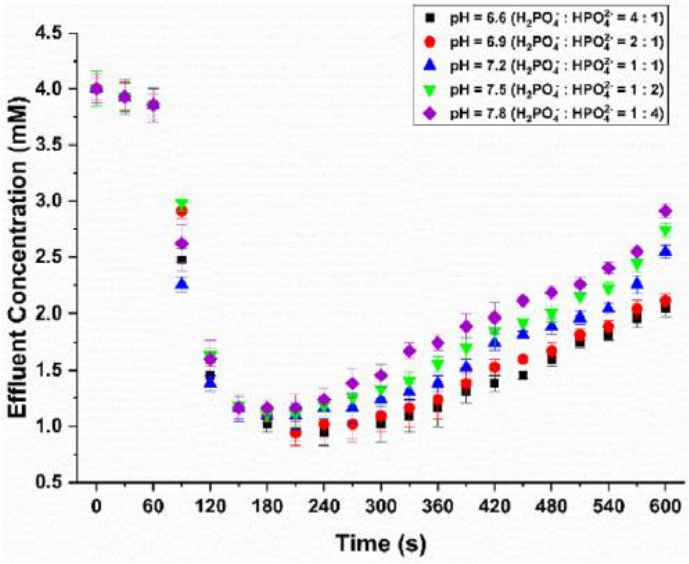

Figure 6.2. Effects of equilibrium system on variation of the effluent TP concentration for highly concentrated feed streams when feed solution containing phosphate salt only, during electrosorption process operated at 1.2 V (Experimental conditions: $[P]_0$ = 4 mM, Flow rate = 8 mL/min.).

Interestingly, however, the overall P removal capacity is more efficient in the lower range of initial pH than that is in higher initial pH. This is likely due to the fact that the adsorption capacity also depends on the ionic radius - smaller hydrated radius ions taking less space within and near the carbon electrode pores and preferentially removed from aqueous solution (Hassanvand et al. 2017a; Huang et al. 2017). Since the concentrations of $H_2PO_4^-$ (0.302 nm) with smaller hydrated radius is higher compared to HPO_4^{2-} (0.327 nm) at lower pH range, it resulted in higher removal rate of the TP. Besides many more ions are needed for charge neutralization near the carbon electrode surface when the monovalent $H_2PO_4^-$ outnumbers the divalent HPO_4^{2-}.

The above experimental results are consistent with findings from a previous study by Huang et al. (2017) in which they concluded that, for solution containing only $H_2PO_4^-$ and HPO_4^{2-}, the optimal TP removal performance is observed under acidic solution (initial pH valued at 5 and 6) where dihydrogen phosphate ion ($H_2PO_4^-$) is predominant (Huang et al. 2017). The results in **Figure 6.2** show that, at the beginning of adsorption stage, phosphate speciation system has a great influence on TP removal. Due to the reason that the quick swift between the divalent and monovalent ions in order to maintain the system at equilibrium state increases amount of divalent ions inside the system. However, in phosphate only solutions, the overall TP sorption capacity is also greatly varied with solution pH, as it directly determines the types and proportions of various P species.

However, the equilibrium system of phosphate may have a negligible effect on TP removal as in reality the phosphate concentration in the real domestic wastewater is generally much lower and hence the 4.0 mM of P used in this study does not reflect the real composition of wastewater. Therefore, further CDI tests with an initial P concentration of 0.4 mM was carried out to more closely simulate the P concentration

present in a typical domestic wastewater. The experimental results in **Figure 6.3(a)** show that at a low phosphate concentration of 0.4 mM, the equilibrium reactions during adsorption stage and types of P species is unlikely to significantly affect the TP removal performance. Another set of experiments were run in which 0.4 mM TP was present together with the 3.6 mM NaCl solution to reflect the background TDS of a real wastewater. It is noticeable from **Figure 6.3(b)** that the trends in the TP removal in the presence of background TDS were consistent as observed in **Figure 6.2** earlier. In other words, effluent TP concentration curves in both highly concentrated feed streams (**Figure 6.2**) and high TDS feed solutions (**Figure 6.3(b)**) reflected an identical trend.

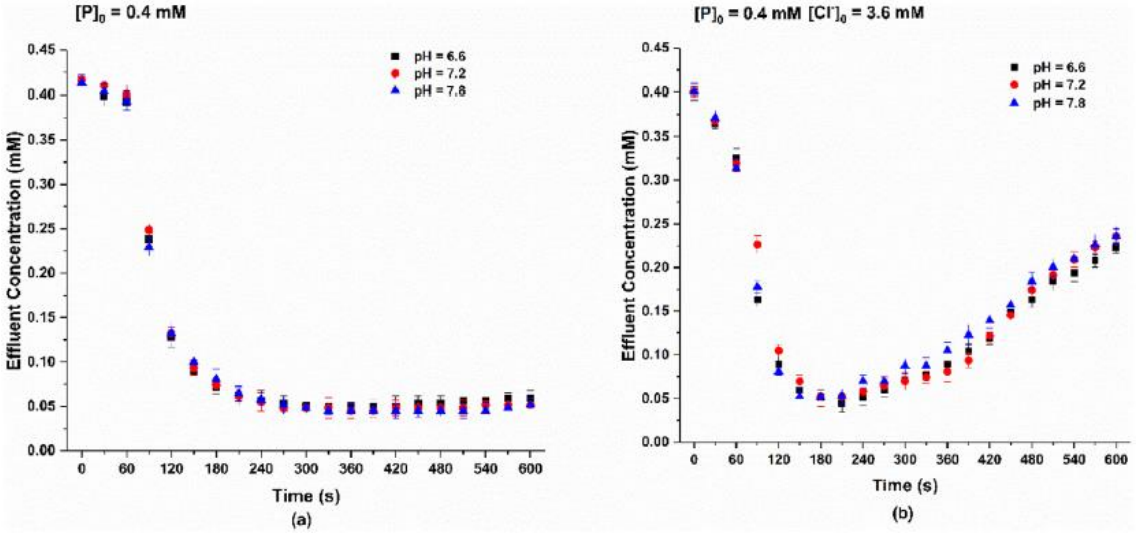

Figure 6.3. Effects of equilibrium system on variation of the effluent total phosphorus concentration for feed simulating P concentration in real domestic wastewater at (a) low concentration of TDS, $[P]_0$ = 0.4 mM (b) high concentration of TDS, $[P]_0$ = 0.4 mM, $[Cl^-]_0$ = 3.6 mM (Experimental conditions: Flow rate = 8 mL/min; Voltage = 1.2 V).

Figure 6.4 shows that, the SAC of TP using 4 mM phosphate as feed solutions ranged from 5.9 to 7.1 mg/g, which are around 6.5 to 7.5 times higher than that when 0.4 mM phosphate solutions (0.93 – 0.94 mg/g) was used as feed solution under the three different pH conditions. In contrast, the SAC of TP in high TDS mixed solution (0.4 mM phosphate in 3.6 mM NaCl) is less than that of a low TDS phosphate feed solution (0.4 mM phosphate) among all pH values, ranged from 0.76 to 0.79 mg/g. These results demonstrate that a higher initial P concentration makes more TP preferentially removed from the aqueous solution by MCDI process. The co-existence of Cl^- in the phosphate containing feed solution reduces the TP removal performance by MCDI process due to competing co-ions. Therefore, a more in-depth studies were conducted to understand the phosphate electrosorption capacity and the preferential adsorption sequence of co-existing ions in more complex electrolyte according to the typical ionic contents in domestic wastewater.

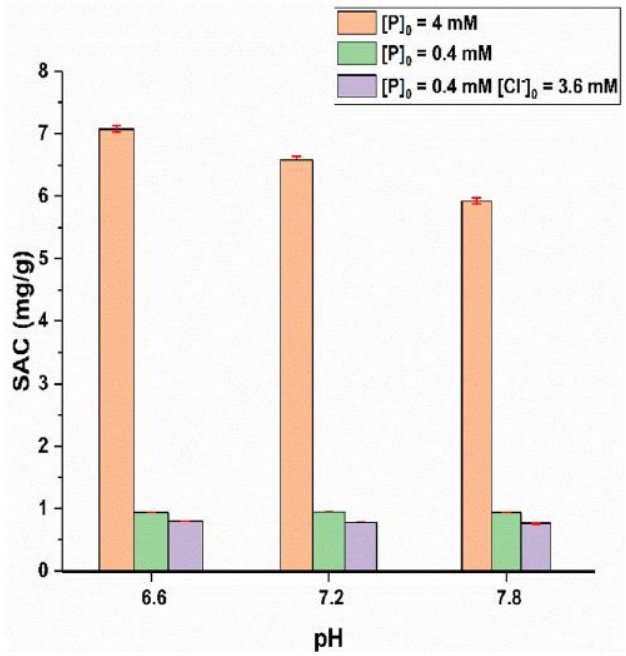

Figure 6.4. Experimental salt adsorption capacity for both concentrated feed streams ($[P]_0$ = 4 mM), low TDS feed streams ($[P]_0$ = 0.4 mM), and high TDS feed streams ($[P]_0$ = 0.4 mM, $[Cl^-]_0$ = 3.6 mM) (Experimental conditions: Flow rate = 8 mL/min; Voltage = 1.2 V).

6.3.2 The influence of co-existing anions in domestic wastewater on T-P removal

By using the synthetic wastewater as feed solution, it has been observed that the presence of co-existing anions can have a significantly negative impact on the degree of phosphate adsorption capacity in a mixed electrolyte solution due to their competitive adsorption onto the carbon electrode. **Figure 6.5** illustrates that, for a feed solution containing mixed of different ionic species, the overall TP removal efficiency was 57% which is lower than the 74% TP removal efficiency observed in **Figure 6.3a** using similar TP concentration of 0.4 mM but only phosphate was feed solution. The overall salt adsorption capacity of Cl^-, SO_4^{2-} and TP observed were 5.2 mg/g, 1.6 mg/g, and 0.7 mg/g, respectively (**Figure 6.5**) resulting in a preferential electrosorption sequence of the competitive anions as: $Cl^- > SO_4^{2-} >$ TP, while their initial ion concentration in the synthetic feed solution were Cl^- (1.09 mM) > TP (0.40 mM) > SO_4^{2-} (0.32 mM). The highest electrosorption capacity of Cl^- among all the co-existing anions is mainly because it had the highest initial concentration amongst all the anions present in the synthetic wastewater (Fan, Liou & Hou 2017). Similar to the results shown in **Figure 6.4**, ions with higher concentration gradient is likely to have a stronger diffusive force to overcome solution resistance, thus faster ion transportation across the electrode pores (Fan, Liou & Hou 2017; Hassanvand

et al. 2018). Interestingly, a preferential electrosorption of SO_4^{2-} over that of TP was observed although its initial concentration of 0.32 mM was 20% less than the initial TP concentration of 0.40 mM. This preferential adsorption of SO_4^{2-} is likely due to the larger charge effect of divalent ions (Tang, He, Zhang & Waite 2017). Specifically, due to the tendency to achieve electroneutrality at the charged electrode surface, divalent sulphate ions are more favourably removed to screen the electrode surface charge. As the pH of the feed solution is 7.2, it contains equal concentrations of $H_2PO_4^-$ and HPO_4^{2-} ions and since their sum of concentrations is still lower compared to SO_4^{2-}, the removal of phosphate underperformed that of SO_4^{2-}. These results show that the co-existence of other anions in the wastewater solution can be a significant challenge for effective removal of TP by the MCDI process, and hence the MCDI process has to be systematically optimized such as increasing the pH or adjusting operating conditions to achieve highly efficient TP removal.

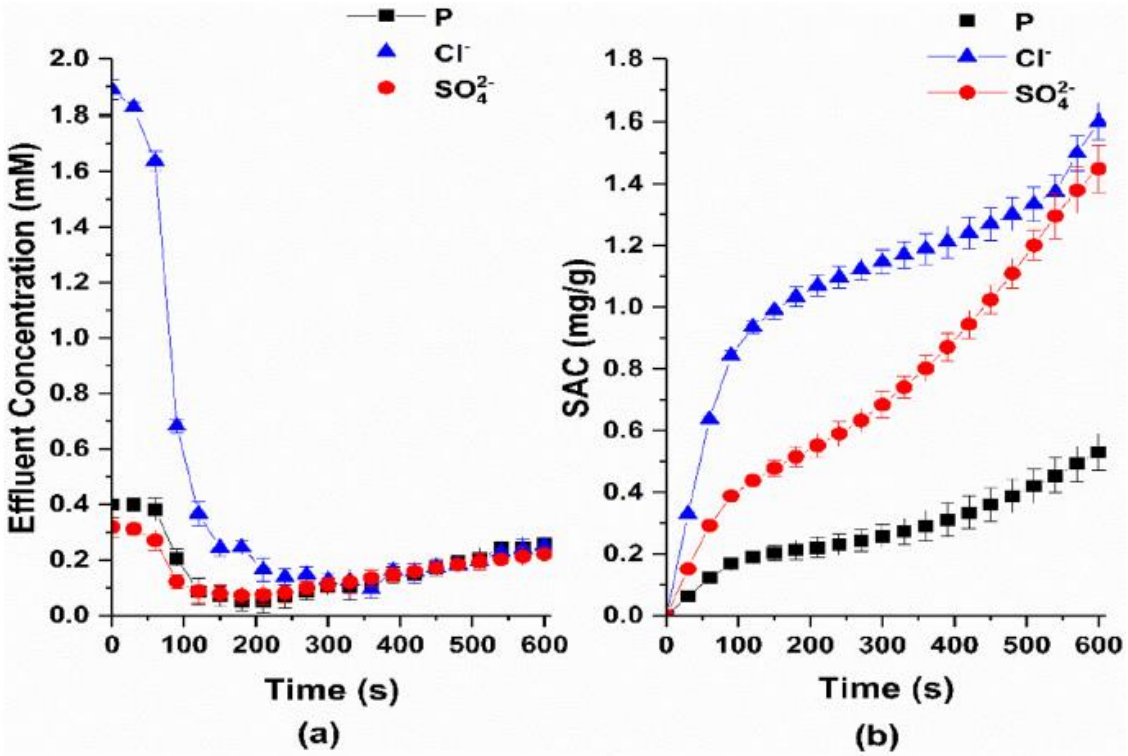

Figure 6.5. The electrosorption competition of Cl^-, SO_4^{2-} and TP in terms of (a) effluent concentration, and (b) salt adsorption capacity in MCDI in a mixed electrolyte at 1.2 V (Experimental conditions: Flow rate = 8 mL/min, Feed solution pH = 7.2).

6.3.3 Optimization of MCDI system for highly efficient total phosphorus removal

Controlled experimental operating conditions such as adsorption time, applied potential, and flow rates were studied using a lab-scale SP mode MCDI unit as shown in **Table 6.2**. The reference experiment was conducted under the following operating conditions: synthetic wastewater feed solution at pH 7.2, applied constant voltage at 1.2 V, pumped flow rate at 8 ml/min, and 10 min adsorption duration. The desalination performance of

controlled experiments was evaluated in accordance with its average salt adsorption rate (ASAR), overall ion removal efficiency (E), and relative ion removal ratio (RE).

In order to find the optimal applied potential for the maximum ASAR and RE of TP over chloride and sulphate, a series of CV controlled experiments were performed. Compared to the results in Experiments 3.1 and 3.2, the effect of electrode saturation over time is negligible to the overall TP removal performance (**Figure 6.6(a)**). However, there was little variation in the relative ion removal ratio of TP over Cl^- - 0.7 for RE($\frac{TP}{Cl^-}$) at 8 min versus 0.73 at 10 min. The relative ion removal ratio of TP over SO_4^{2-} in both the cases were same, all reaching 1.11. By contrast, comparing results Experiments 3.1 and 3.3, **Figure 6.7** illustrates that the overall removal efficiency of TP increased from 37 to 57%, when the applied potential was raised from 0.6 to 1.2 V. This indicates that, approximately 25% more total phosphorus has been selectively removed per minute at 1.2 V (0.07 mg/g-min) compared to 0.6 V (0.05 mg/g-min). As can be inferred from **Figure 6.6(b)**, relative ion removal ratio of TP over Cl^- increased with increase in adsorption voltage: 0.55 for RE($\frac{TP}{Cl^-}$) at 0.6 V versus 0.73 for that at 1.2 V. However, the relative ion removal ratio of TP over SO_4^{2-} dropped from 1.48 at 0.6 V to 1.12 at 1.2V applied voltage. Moreover, comparing results of Experiments 3.1 and 3.4 the relative ion removal ratio of TP over SO_4^{2-} and Cl^- at flow rate of 24 mL/min share the same proportion at 0.92. It is suggested that the co-existing ions in this case have a similar selective removal. It is also worth mentioning that the effluent concentration of all studied ions under the flow rate of 8 mL/min were raised more than double that operated under a flow rate of 24 mL/min, an increase from 24 to 57% (**Figure 6.8**). This suggests that the overall removal efficiency of TP was hampered by the increased feed solution flow rates, which reduces the residence time for ion adsorption. The fact that relatively small amount

of ions would be potentially transported into activate carbon electrodes at higher flow rates, leads to the observation of more concentrated effluent streams (Biesheuvel & Van der Wal 2010a; Dorji et al. 2018; Kim et al. 2015; Zhao, Satpradit, et al. 2013). In summary, the above experimental results demonstrated that the optimal adsorption of total phosphorus over chloride and sulphate may be achieved to some extent by conducting adsorption process with lower feed flow rates, higher applied potentials (less than 1.2 V) and shorter adsorption duration.

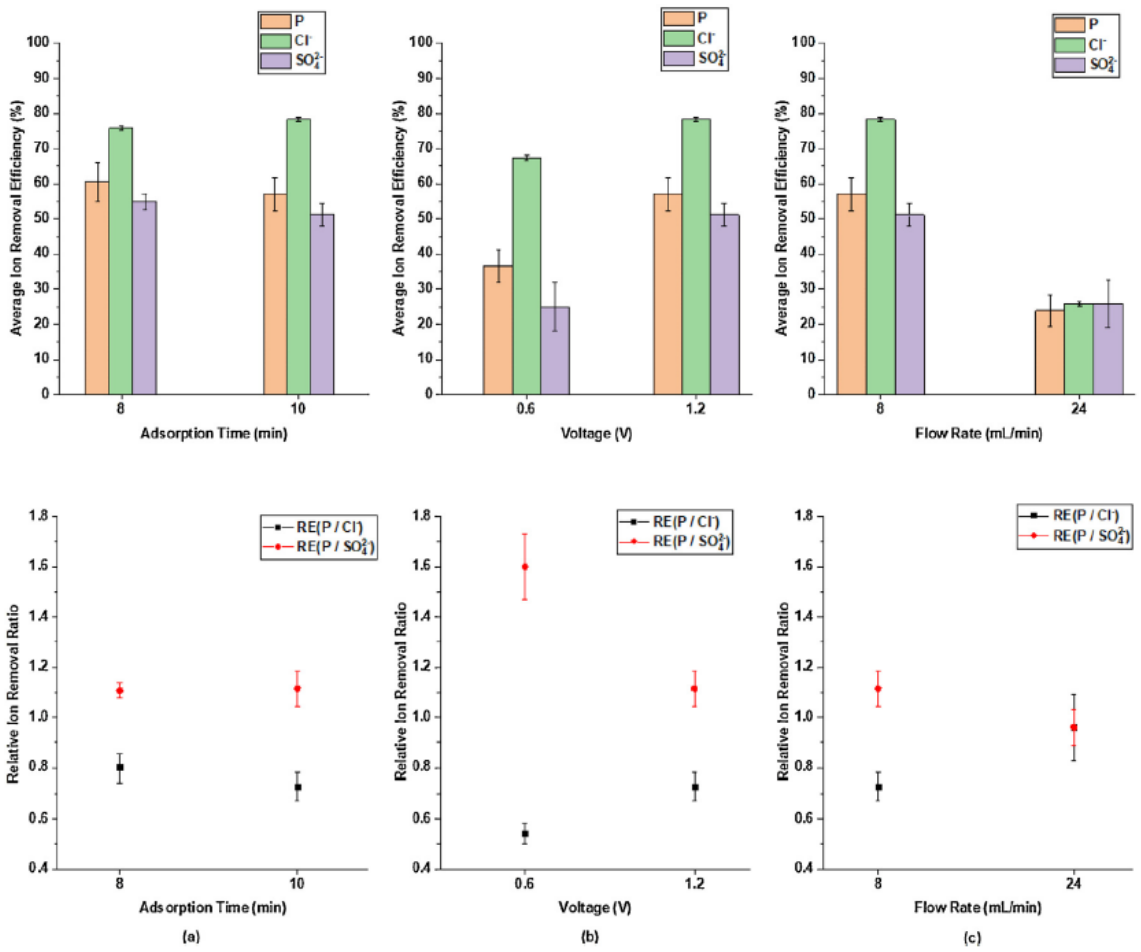

Figure 6.6. Experimental average ion removal efficiency (E) and relative ion removal ratio (RE) results for SP mode MCDI operated at various (a) adsorption time, (b) voltage, (c) flow rate. The details of individual control parameters are described in **Table 6.2**.

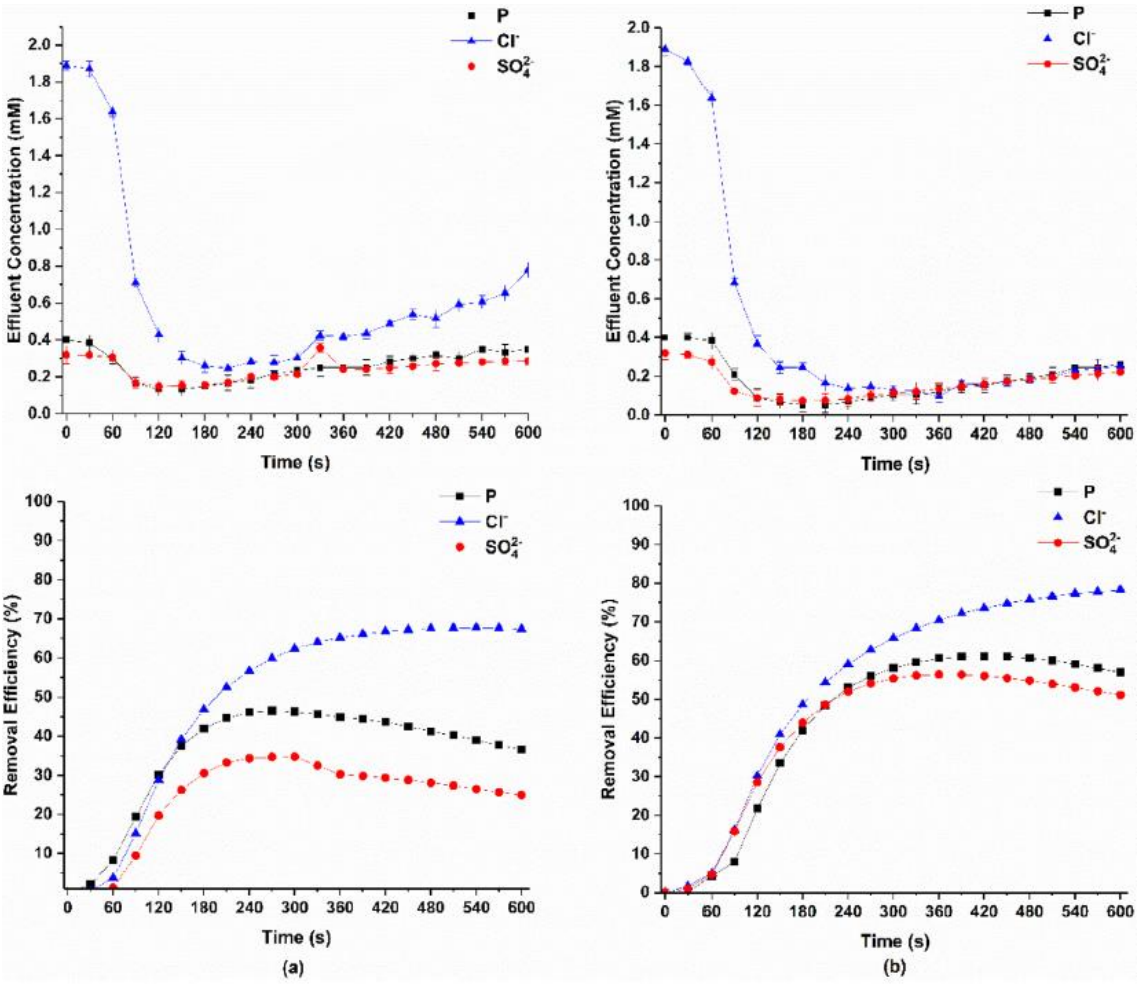

Figure 6.7. The effect of applied voltage on the variation of removal efficiency of phosphorus and other anions for MCDI electrosorption process operated at (a) 0.6 V, and (b) 1.2 V (Experimental conditions: Flow rate = 8 mL/min, Feed solution pH = 7.2).

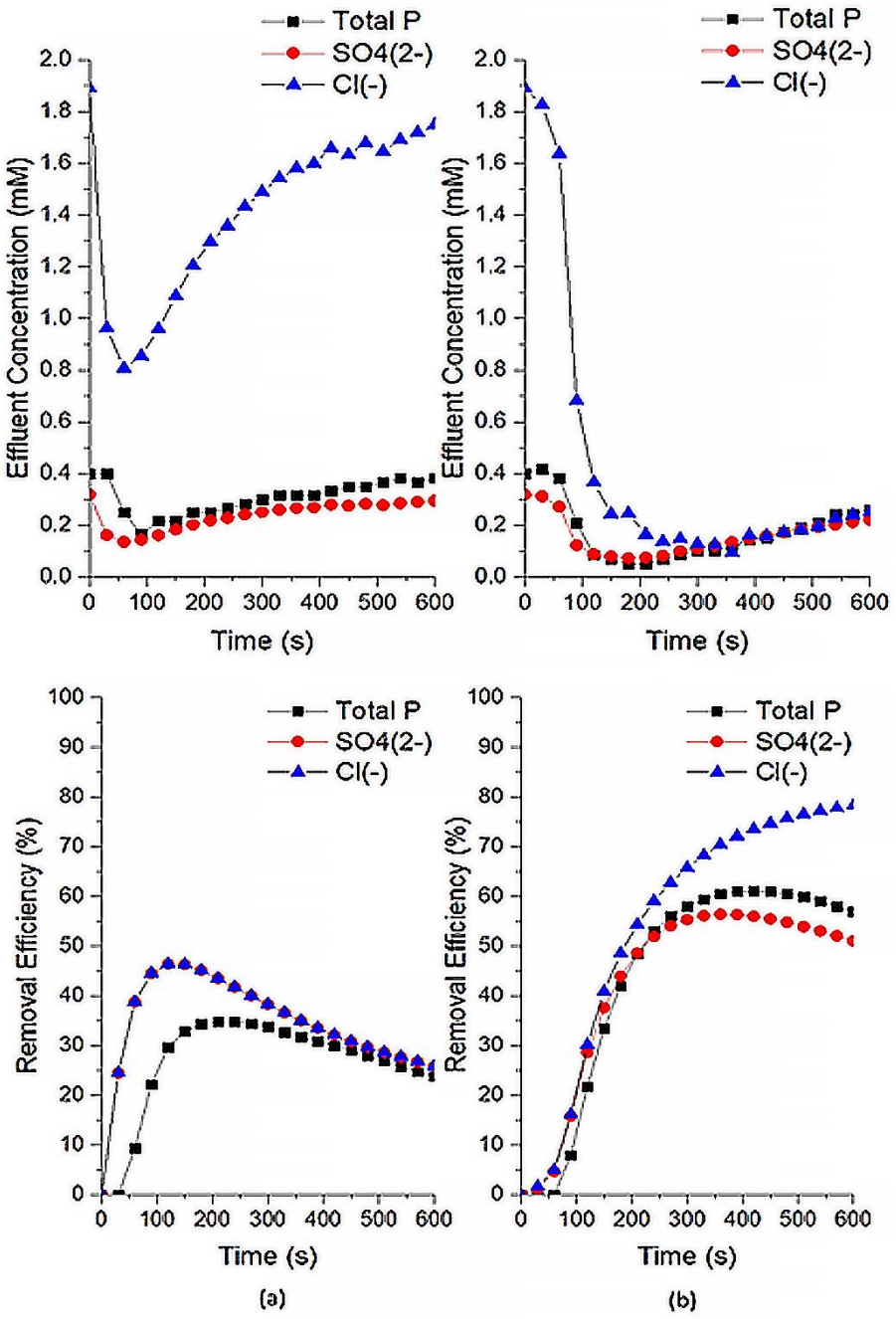

Figure 6.8. The effect of supplied flow rate on the variation of removal efficiency of phosphorus and other anions for adopted flow rate at (a) 24 mL/min, and (b) 8 mL/min (Experimental conditions: Voltage = 1.2 V, Feed solution pH = 7.2).

6.4 Concluding remarks

The removal of phosphate from the domestic wastewater using MCDI and its system optimization for enhanced TP removal has been explored by closely investigating the key mechanisms such as phosphate speciation and competitive sorption, and adjusting operating conditions and solution compositions. This study has shown that the single-pass mode MCDI process has a great potential for effective phosphorus removal from the municipal wastewater. The following are the key findings of the study:

1) In the early stage of adsorption phase, transformation of phosphorus in speciation has a significant impact on the degree of total phosphorus (TP) adsorption capacity and hence its removal. Because the phosphorus speciation reactions continuously provide system sufficient amount of HPO_4^{2-}which is quickly being adsorbed onto the electrode surface to achieve charge neutrality. However, the overall TP removal is more efficient in the lower range of the initial solution pH as the $H_2PO_4^-$ (0.302 nm) with smaller hydrated radius takes less space within and near the carbon electrode pores and preferentially removed from aqueous solution.
2) From the co-existing anions selectivity study, it can be concluded that in the presence of higher Cl^- ion concentrations, it is more favorably removed compared to TP from the mixed electrolyte due to its stronger diffusion force; divalent ion such as sulphate showed higher electrosorption capacity among similar concentrated monovalent ion due to higher electrostatic force. The preferential electrosorption sequence of the competitive anions present in the wasetwater was: $Cl^- > SO_4^{2-} >$ TP, while the initial ion concentration in the feed water was with the order: $Cl^- >$ TP $> SO_4^{2-}$.
3) The optimal adsorption of total phosphorus over chloride and sulphate may be achieved with lower feed flow rates, higher applied potentials (less than 1.2 V)

and shorter adsorption duration.

The above findings summarized in this study may contribute to the enhanced understanding of the application of MCDI as an alternative treatment measure for the effective phosphorus removal from the wastewater effluent.

CHAPTER 7

Enhanced Recovery of Nitrate from Municipal Wastewater using Anion-exchange Polymer Coated Electrode Embedded with Nitrate Selective Resins

The results from this chapter will be submitted for publication as "*Efficient recovery of nitrate from municipal wastewater via MCDI using anion-exchange polymer coated electrode embedded with nitrate selective resin*"

Research highlights

- A NO_3—selective electrode was developed for enhanced NO_3^- recovery.
- The AC electrode was coated with an IX polymer solution containing A520E resins.
- The coated electrode kept collecting NO_3^- even after the electrode reached saturation.
- The selective resins embedded in the coating layer increased electric resistance.
- NO_3^- repelled from the electrode was likely to be temporarily trapped at the IX layer.

7.1 Introduction

There is a currently increasing demand for clean water brought about by the continuous growth of the world's population and economy, as well as industrialization (Chung et al. 2012; Park et al. 2019; Shannon et al. 2008). Among the solutions in augmenting, the clean water supply are desalination and wastewater reuse. Wastewater reuse does not only mitigate water scarcity, but also address problems with environmental pollution and resource recovery (Ansari et al. 2017). In fact, resource recovery is highly important in meeting the strict effluent discharge standards prior to disposal of wastewater (Batstone et al. 2015).

Among these substances present in wastewater is nitrate (NO_3^-), one of the inorganic forms of nitrogen, which is formed from the oxidation of ammonia. This ion is mostly considered as a pollutant whose effect, when consumed, can cause health problems such as reduced fertility, increased levels of methemoglobin in infants, stillbirths, and even death (Kim & Choi 2012). Removal of NO_3^- has been performed in literature through a number of various methods: biological treatment (Watsuntorn et al. 2019), ion exchange (IX) (Bae et al. 2002), electrocoagulation (Karamati-Niaragh et al. 2019), catalysis

(Mendow et al. 2019), ultrafiltration (Bahmani et al. 2019; Gao et al. 2019), reverse osmosis (Epsztein et al. 2015; Schoeman & Steyn 2003), electrodialysis (Menkouchi Sahli et al. 2008), and adsorption (Senthil Kumar, Yaashikaa & Ramalingam 2019). While these processes can remove or recover NO_3^-, each process has its own limitations and challenges. Biological treatment requires microorganisms that are highly sensitive to various stimuli and conditions, as well as large bioreactors that offset its relatively low cost (Park & Yoo 2009). IX may be able to efficiently remove NO_3^-; however, this process results to a huge amount of waste generated from the IX resin required (Bae et al. 2002). Treatment of such wastewater solutions is considered non-economic using conventional pressure driven membranes processes.

Capacitive deionization (CDI), the adsorption of ions of opposite charges onto a porous carbon electrode after the application of electric potential, is an emerging process for desalination of low salinity water and resource recovery (Oren 2008b; Porada et al. 2013b). Among the reasons, this process has attracted research attention for its ability to remove ions from a feed solution by means of electrosorption without the extensive use of energy and the generation of brine waste during operation. Not only CDI is an efficient process in desalting and resource recovery, it is also environmentally friendly. CDI has particularly gained a niche application with the treatment of low salinity water, such as brackish water (which contains 2000 to 10000 ppm of solutes) (Koparal & Öğütveren 2002). Treatment of such wastewater solutions is considered non-economical using conventional membrane processes, due to the energy expenditure associated with these processes.

A particular topic of interest in the study of CDI is the development of various carbon-based electrodes to improve the adsorption capacity of the electrodes and the charge

efficiency (Jia & Zou 2012; Li et al. 2010; Nie et al. 2012). This particular interest has led to the development of the membrane capacitive deionization (MCDI), a process involving a pair of carbon electrodes coupled with ion exchange membranes (IEMs) (Biesheuvel & van der Wal 2010b; Kim & Choi 2010c). MCDI has shown to improve the electrosorption and regeneration efficiencies significantly due to the presence of the IEMs, which adsorb either cations or anions, regardless of the ion type, charge, and size. While the presence of IEMs has significantly enhanced the performance of MCDI, a better application of MCDI electrode development is custumization of the electrodes targeted for specific ion/s that can be used for treatment of a multi-component solution.

Selective removal of NO_3^- using MCDI has been done a few times in previous studies. Batch mode CDI was attempted by Tang et al. (2015), wherein they used CDI to remove NO_3^- and F^- present in a synthetic brackish groundwater solution (Tang et al. 2015). To demonstrate that MCDI operation can be varied to selectively remove NO_3^-, the applied current during MCDI operation was varied in another study (Kim, Kim & Choi 2013). The researchers found out that the mole fraction of NO_3^- relative to all the other ions adsorbed by the MCDI electrode were inversely proportional to the applied current, i.e. less applied current showed lower NO_3^- adsorption.

Development of NO_3—selective electrode for MCDI has also been a topic of interest in recent. Yeo and Choi in 2013 fabricated a NO_3—selective carbon electrode using an anion exchange resin with high NO_3^- selectivity (Yeo & Choi 2013). While the amount of adsorbed ions was similar compared to a nascent electrode, the amount of NO_3^- ions adsorbed on the developed electrode was twice higher. Kim and Choi developed the first reported nitrate-selective composite carbon electrodes for CDI. In their study, the carbon electrode surface was coated with highly NO_3—selective BHP55 anion exchange resin

(Kim & Choi 2012). The resultant electrode's NO_3^- removal was compared with that of the conventional MCDI electrode, and it was found that the NO_3^- adsorption was 2.3 times higher than the conventional MCDI electrode. Despite the improvement of NO_3^- removal performance, selectivity could have been further improved with the use of another resin. Another recent NO_3—specific MCDI study was conducted by Gan et al. (2019) (Gan et al. 2019), wherein they developed a double-layer composite electrodes after coating activated carbon electrodes with A520E anion exchange resin on one side and carboxyl-functionalized multi-walled carbon nanotubes on the other. The asymmetric nature of the electrode showed enhanced NO_3^- selectivity, despite the use of other binary anion solutions, such as those containing SO_4^{2-}, F^-, and Cl^-. Another issue in these studies is that the improved selectivity for NO_3^- was demonstrated using synthetic solutions of high NO_3^- concentrations, when in fact NO_3^- only exists in low concentrations compared to other anions in wastewater. Another problem in the development of electrodes for MCDI is the use of organic polymers, such as PVDF, as binders. These polymers are known to have high electrical resistance, which then hampers the deionization process (Yeo & Choi 2013).

In this study, a NO_3—selective activated carbon electrode with enhanced selective adsorption of NO_3^- in a multi-component solution was developed for effective NO_3^- recovery during an MCDI wastewater reclamation process. The activated carbon electrode was coated with an IX polymer solution containing A520E NO_3—selective resin. The electrosorption performance of the coated electrode was first tested at a lab-scale MCDI unit. Its performance was also compared with an electrode coated by the IX solution only. The selectivity of NO_3^- from a mixture of selected anions during electrosorption and electrode regeneration was then investigated. Lastly, the applicability

of the used electrodes was discussed based on the results of the five successive cycle operation of MCDI using real municipal wastewater.

7.2 Materials and methods

7.2.1 Fabrication of the ion-exchange polymer coated carbon electrode with embedded A520E

The carbon electrodes provided by Siontech Co. (Republic of Korea) were composed of a graphite body sheet coated with a carbon slurry blended with activated carbon, P-60 (Kuraray Chemical Co., Japan) and polyvinylidene fluoride (Inner Mongolia 3F-Wanhao Fluorine Chemical Co., China).

The cathode used for the experiments was coated with a cation-exchange polymer solution containing sulfonic acid group. The IX capacity of the dry cation-exchange polymer was reported to be 1.7 meq/g in average. A 20 wt % solution of the cation—selective polymer with N-methyl-2-pyrrolidone (NMP, Sigma-Aldrich, USA) was vigorously stirred at 20 ºC for 24 hr.

Then, two electrodes coated with different anion-exchange layers were used as anodes to compare their performance. An anion-exchange polymer was prepared by introducing tertiary amine groups after the chloromethylation of polystyrene (Kim & Choi 2012). The IX capacity of the dry anion-exchange polymer was reported to be 1.5 meq/g in average. The anion-exchange polymer was mixed with NMP and stirred at 20 ºC for 24 hr to produce a 17 wt % solution. The control anode (IX layered electrode) was activated carbon electrode coated with this anion-exchange polymer solution. Prior to the

preparation of the other anode, NO_3—selective A520E resin, which has a polymer structure of a macroporous polystyrene cross-linked with divinylbenzene with quaternary ammonium functional groups (in chloride form; particle size: 300–1200 μm) was dried at 80°C for 24 hr, pulverized with a ball mill and was then sieved with a 50 um stainless-steel mesh, and mixed with the 12 wt % anion-exchange polymer solution with a polymer-to-resin weight ratio of 1:1. Another activated carbon electrode was coated with the anion-exchange polymer solution containing A520E NO_3—selective resin to produce A520E/IX layered electrode. The anion-selective electrodes were coated with the uniformly mixed coating solutions using a casting machine (Elcometer 4340, Elcometer (Asia) Pte Ltd, Singapore), and dried at 50°C for 12 hr. The dried samples were then stored in DI water at 4 °C. Surface morphology of the coated electrodes was characterized using a field emission scanning electron microscopy (FE-SEM) (Zeiss Supra 55VP, Carl Zeiss AG, Germany) (Park et al. 2018).

7.2.2 Bench-scale MCDI using ion-exchange layer-coated electrodes

The MCDI experiments were carried out using a lab-scale system as described in our previous work (Kim, Gwak, et al. 2017a). The dimensions of the rectangular flow channel of the test cell were 10x10 cm with an effective adsorption area of 100 cm^2. A pair of cation- and anion-exchange electrodes was symmetrically placed within the test cell, separated by a non-conductive nylon spacer between these two electrodes ensuring flow of water and preventing short-circuiting (Dorji et al. 2018). The influent water was brought entirely into contact with the IX layer-coated electrodes by punching a 1 cm diameter sized hole in the center of the electrodes and mesh spacer. A peristaltic pump (Cole-Palmer, USA) was used to circulate the influent throughout the MCDI unit with a

constant flow rate of 30 mL/min. A constant level of electrical potential was applied through the MCDI unit by a potentiostat, WPG-100 (WonATech Co., Republic of Korea). The system was stabilized prior to the test runs by flushing out the feed solution through the system under single-pass mode at 0 V, until the readings of conductivity and pH were to be the same to those of in feed. All the tests were duplicated at 20 ^{o}C.

.

7.2.3 Investigation of preferential electrosorption and discharge of nitrate using A520E/IX electrode

A synthetic mixed solution containing 3.3 mM each of NaCl, Na_2SO_4, and $NaNO_3$ was flowed into the lab-scale system for 450 s at a 1.2 V applied potential under single-pass mode. The electrodes were then regenerated by reversing polarity under single-pass mode. During the regeneration, DI water was fed through the system at -1.2 V for 450 s, and the effluent was collected each 30 s. After each run, complete regeneration of the carbon electrodes was ensured by employing an additional regeneration stage using DI water for 30 min at -1.2 V, and thereby no discharge of ions was detected by the reading of conductivity of the flushing effluent. The mass balance on the amount of adsorbed and desorbed ions was also roughly calculated to confirm that the electrodes were completely regenerated at the end of flushing.

7.2.4 Successive five-cycle operation for concentrating nitrate

A 120 mL portion of real municipal wastewater effluent was fed under batch mode through the unit for 450 s under a 1.2 V electrosorption condition. The wastewater

effluent was sampled from a decentralized wastewater treatment plant located in Sydney, Australia. Electrode regeneration was consequently performed circulating a fresh DI water with the same volume through the system under the same condition as electrosorption by reversing the potential. The desorbed charged species, including NO_3^-, were kept collected in the brine solution after each regeneration cycle. These electrosorption and electrode regeneration processes were successively repeated for five cycles.

7.2.5 Measurement of concentration of anions and their removal

The major anionic species contained in wastewater, such as NO_3^-, nitrite (NO_2^-), chloride (Cl^-), sulfate (SO_4^{2-}), and ortho-phosphate (PO_4^{3-}), were quantified using ionic chromatography (IC), (IC Thermo Fisher Scientific, Australia). All the samples were diluted properly and filtered using a 0.45 μm filter (Merck Millipore, USA) before their measurement. The calibration of IC was performed before the analyses of the samples based on external calibrations with deionized water and standard synthetic solution.

The electrosorption removal efficiency from the wastewater effluent after pilot operation was calculated using **Equation 7.1**:

$$\text{Removal efficiency } (\%) = \frac{(C_0 - C)}{C_0} \times 100 \qquad \textbf{(Equation 7.1)}$$

where C_0 and C (mg/L) are the initial and permeate concentrations of wastewater, respectively.

The electrosorption selectivity of ion *i* at time *t* can be expressed by **Equation 7.2**:

$$\text{Adsorption selectivity of i} = \frac{C_{i,t,b}}{C_{total,t,b}} \qquad \textbf{(Equation 7.2)}$$

where $C_{i,t,p}$ denotes the molar concentration of *i* and $C_{total,t,p}$ is the total molar concentration in the permeate solution at time *t*. Larger values of the adsorption selectivity imply that the ion *i* is more preferentially adsorbed from the carbon electrode over other co-existing ions.

7.3 Results and discussion

7.3.1 Morphology of the IX and A520E/IX layered electrodes

Since the carbon electrodes were coated with IX polymers, it is expected that the electrodes exhibit high salt adsorption capacity and effective regenerability, due to the low resistivity of the thin IX polymer layer and the inhibition of adsorption of counter-ions during electrode regeneration. Apart from this, the NO_3—selective A520E resin particles embedded in the polymer layer could lead to a more selective removal and recovery of the NO_3^- present in wastewater. The electrosorption and regeneration performances of the A520E/IX layered electrode were initially assessed, and the results were compared with the IX layered coated electrodes.

The SEM images of the surfaces of the conventional activated carbon electrode, IX and A520E/IX layered electrodes are shown in **Figure 7.1**. The nascent activated carbon electrode appeared to have a rough granular surface due to the relatively large-sized activated carbon particles (**Figure 7.1(a)**). In contrast with the virgin carbon electrode, the surface of the IX layered electrode coated with a 50 um thick anion-exchange polymer layer appeared to be smoother, confirming that the electrode surface was entirely covered with the anion-exchange polymer solution (**Figure 7.1(b)**). The NO_3—selective

A520E/IX electrode, where the original carbon surface was covered by an IX layer containing A520E resin, showed a rougher surface morphology compared to the IX layer-containing electrode, due to the presence of the resin particles. It was also observed that the resin particles embedded in the IX polymer layer could not be detached from the surface easily, thus confirming that the IX solution also functioned well.

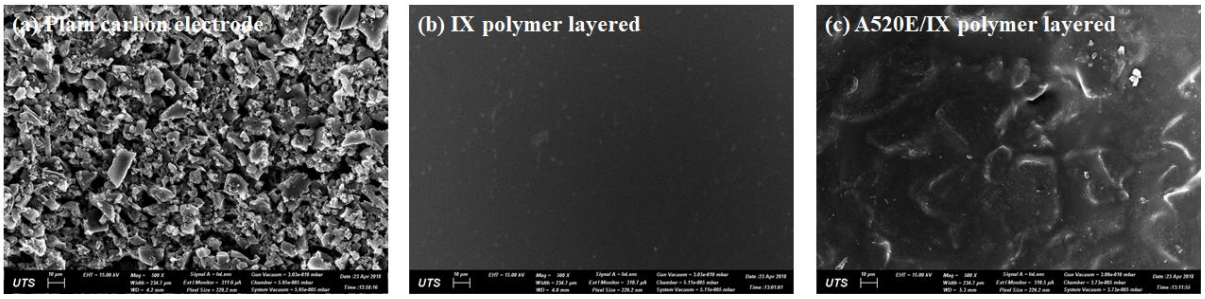

Figure 7.1. SEM images of the surface of (a) the original, (b) IX layered, and (c) A520E/IX layered carbon electrodes.

7.3.2 Electorosorption performance using the nitrate-selective electrode

Figure 7.2 presents the salt adsorption capacities (SAC) of NaCl and $NaNO_3$ in MCDI using the IX and A520E/IX layered carbon electrodes. The SAC of the different electrodes with a function of time t was calculated using **Equation 7.3**:

$$\text{SAC (mmol/g)} = \frac{m_t}{m} = \frac{Q \times \int_0^t (C_0 - C)dt \times M}{m} \qquad \textbf{(Equation 7.3)}$$

where m_t is the accumulative amount of adsorbed ions at time t (mmol), m is the mass of carbon on the electrode (g), Q is the flow rate of feed solution through the MCDI system

(mL/min). C_0 represents the initial concentration of feed solution (mmol/L), C is the concentration of effluent at t (mmol/L), and M is the molar mass of salt (mg/mmol).

The results obtained after employing the conventional MCDI configuration using the virgin activated carbon electrodes with a separate IEM were also outlined for better understanding and comparison. The SAC values of A520E/IX layered-, IX layered-, and conventional-MCDIs were 0.252, 0.286, and 0.235 mmol/g, respectively. The higher adsorption capacity of the IX layered MCDI compared to the conventional MCDI system was likely due to the lower resistance of the screening membrane layer yielded by the thin-coated IX layer, which functioned as an IEM directly attached on the activated carbon electrode (Kim & Choi 2010a; Lee et al. 2011; Liu et al. 2014). The low contact resistance due to the adhesion between the coating layer and the carbon surface in the IX layered MCDI could also contribute to the enhanced electrosorption and reduced energy consumption, whereas a high contact resistance was induced by the weak contact adhesion between the separate IEM and the raw carbon electrode in the conventional MCDI (Lee et al. 2011). However, the membrane layer resistance seemingly increased as the granular NO_3—selective resin particles were incorporated in the IX polymer layer, resulting in lower SAC.

The adsorption capacity for $NaNO_3$ was greater than NaCl for all the three different MCDI configurations. In general, the electrosorption capacity in solution containing single salt species can be explained by size affinity, such that the ions with smaller hydrated size possess a higher salt adsorption capacity with the electrode. Given that the hydrated radii of NO_3^- (0.335 nm) and Cl^- (0.332 nm) are similar to each other (Nightingale Jr 1959), the higher capacity for NO_3^- adsorption cannot be explained by its size-affinity to the electrical double layer (EDL). Li et al. (2016) attributed the high NO_3^- adsorption

performance to its smaller hydration ratio and high electrostatic attraction toward the charged electrode surface (Li et al. 2016). The NO_3^- was therefore likely highly attracted towards the carbon surface as a result of strong non-electrostatic attraction (Tang et al. 2015).

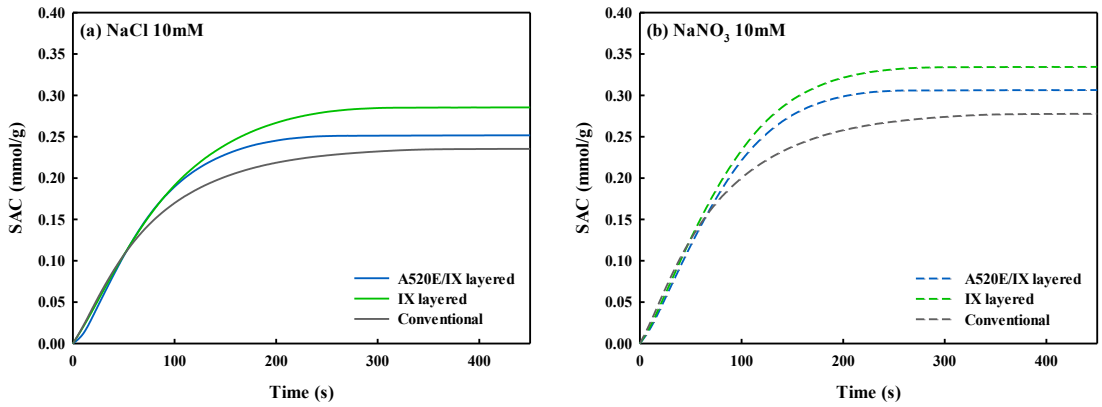

Figure 7.2. Salt adsorption capacities of A520E/IX layered-, IX layered-, and conventional- MCDIs in the removal of (a) NaCl and (b) $NaNO_3$ during experiments involving single salt species. The applied potential and feed solution flow rate during the MCDI tests were 1.2 V and 30 ml/min, respectively, under single-pass mode.

Charge efficiency can be a functional indicator of the energy efficiency of the MCDI system. Ideally, the charge efficiency is expected to be equal to unity when each electron is fully charge-balanced by the adsorption of counter-ions, and the electron transfer from an electrode to the another one is accompanied by the removal of one salt molecule from the feed water (Porada et al. 2013a).

The charge efficiency, Λ, which addresses the ratio of salt electrosorption to a such applied charge in MCDI, can be described as **Equation 7.4**:

$$\Lambda = \frac{total\ n \times F \times \int (C_0 - C) dt \times Q}{\int I dt \times A} \qquad \textbf{(Equation 7.4)}$$

where n is the number of electrons required for electrosorption of one charged ion, F is the Faraday's number (96485.3 C/mol), I is the current density (A/m^2), and A *is* the effective surface area of the electrode (0.01 m^2).

The charge efficiencies of the three different MCDI configurations throughout the single salt electrosorption tests were evaluated, as shown in **Figure 7.3**. The average charge efficiency for the conventional MCDI using the carbon electrodes with separate IEMs was 63.6%, while that of the IX layered MCDI reached up to 73.3%, which could possibly be due to the reduced interfacial resistance between the polymer layer and carbon surfaces, attributing to their strong contact adhesion (Liu et al. 2014). However, integrating the A520E resin in the anion-exchange layer increased its resistance, leading to lowered charge efficiency.

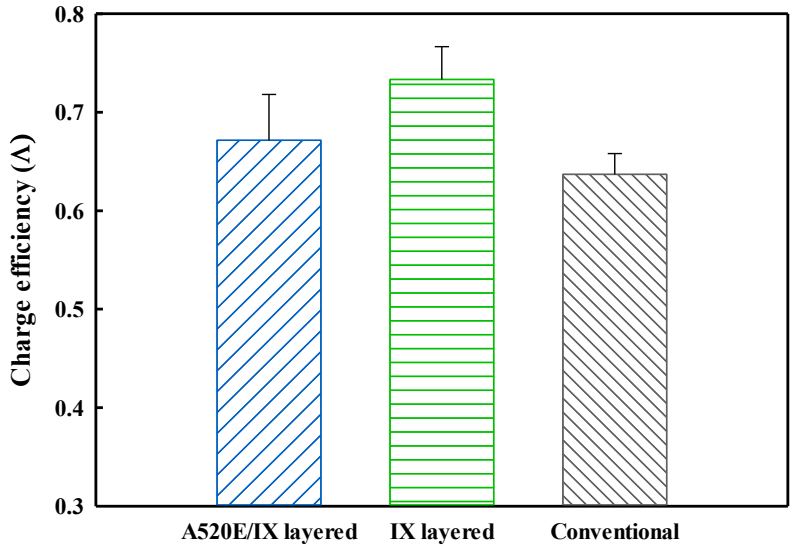

Figure 7.3. Charge efficiency among A520E/IX layered-, IX layered-, and conventional-MCDIs.

7.3.3 Preferential adsorption of anions in MCDI using A520E/IX layered electrodes

The phenomena of competitive removal and discharge of the selected anions in MCDI were investigated in this section using the IX layered and A520E/IX layered electrodes. As shown in **Figure 7.4(a)**, the preferential electrosorption sequence of the anions using the IX layer-coated electrodes was NO_3^- > SO_4^{2-} > Cl^-. The hydrated radii of NO_3^- and Cl^- were 0.335 and 0.332 nm, respectively (Nightingale Jr 1959), whereas their diffusion coefficients were both around 1.7 × 10-9 m^2s^{-1} (Poisson & Papaud 1983). Given the similar hydrated ionic radii and diffusion coefficients between NO_3^- and Cl^-, there has to be a reason why NO_3^- was preferably adsorbed by the IX layer-coated electrode. The better selectivity of NO_3^- was a factor of its strong hydrophobicity, thus its stronger

affinity to the hydrophobic surfaces of carbon electrode allowed it to take more space in the EDL layer (Chen et al. 2015; Hassanvand et al. 2018). Besides, the permselectivity through the IX layer also accounted for the faster electrosorption of NO_3^- (Kim et al. 2019b). NO_3^- showed a better permselectivity through the IX layer, which is highly dependent on the affinity of the anions to the membrane (Luo, Abdu & Wessling 2018a; Sata 2000).

On the other hand, the removal preference between SO_4^{2-} and Cl^- in MCDI remains debatable in a number of previous studies. Kim et al. (2019) observed more selective adsorption of SO_4^{2-} compared to Cl^-, following the order of the general permselectivity trend through the IEM (Kim et al. 2019b). However, no apparent difference of the selectivity of SO_4^{2-} compared to the other NO_3^- and Cl^- could be found in a study of MCDI from Hassanvand et al. (2018) (Hassanvand et al. 2018). Tang et al. (2017) and Yeo et al. (2013) both observed a higher selectivity in SO_4^{2-} over Cl^-, which was in accordance with our results (Tang, He, Zhang & Waite 2017; Yeo & Choi 2013). These studies explained that the preferential electrosorption of SO_4^{2-} onto the electrodes was a function of the applied potential, and a higher selectivity towards SO_4^{2-} can be obtained by increasing the applied current. The gap between our results and the other studies was likely due to the different current applied on the MCDI system.

Compared to the results with the IX layered electrode, the total SAC of the A520E/IX layered electrode became lower due to the increased resistance of the polymer membrane layer, as explained in Section 7.3.1. Using the IX layered electrode, the electrosorption of all salt species appeared to have saturated at around 300 s of operation. However, it was observed that NO_3^- ions were more selectively adsorbed when the A520E resin was embedded in the IX layer coated on the carbon electrode. Furthmore, the adsorption of

NO_3^- using the A520E/IX layered electrode continued to increase even longer than 450 s, whereas the adsorption of the other species (Cl^- and SO_4^{2-}) reached saturation around 300 s when the A520E/IX layered electrode was used in the MCDI tests (**Figure 7.4(b)**). Moreover, the adsorbed amount of Cl^- on the A520E/IX layered electrode decreased with the increased operation time. The mole fraction of NO_3^- with respect to the anions adsorbed on the A52E0/IX layered electrode correspondingly increased with the electrosorption time (**Figure 7.5**). Kim and Choi worked on NO_3^- selective coated with BHP55 resin particles on activated carbon electrodes in conventional CDI and attributed the additional electrosorption of NO_3^- to the exchange between Cl^- on the resin coating layer and NO_3^- contained in the bulk feed solution (Kim & Choi 2012).

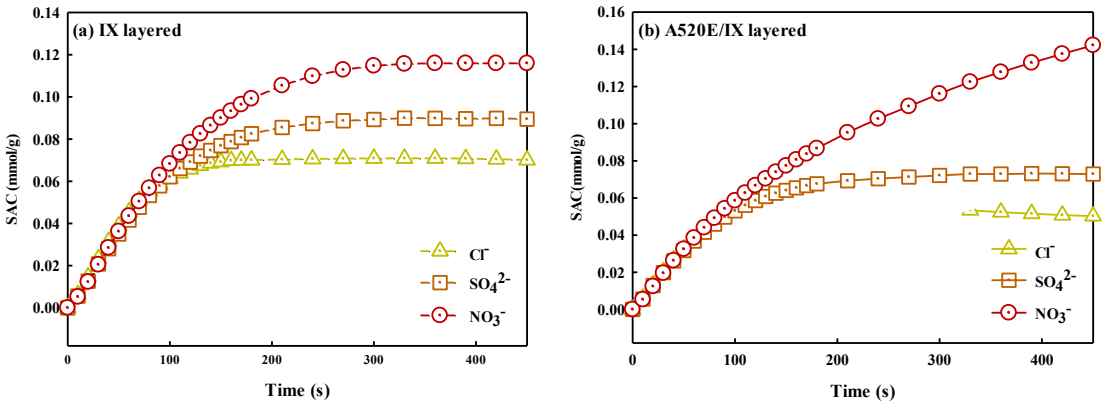

Figure 7.4. Salt adsorption capacity of the (a) IX layered- and (b) A520E/IX layered-MCDIs from a mixture of 3.3 mM of $NaNO_3$, Na_2SO_4, and NaCl, for each.

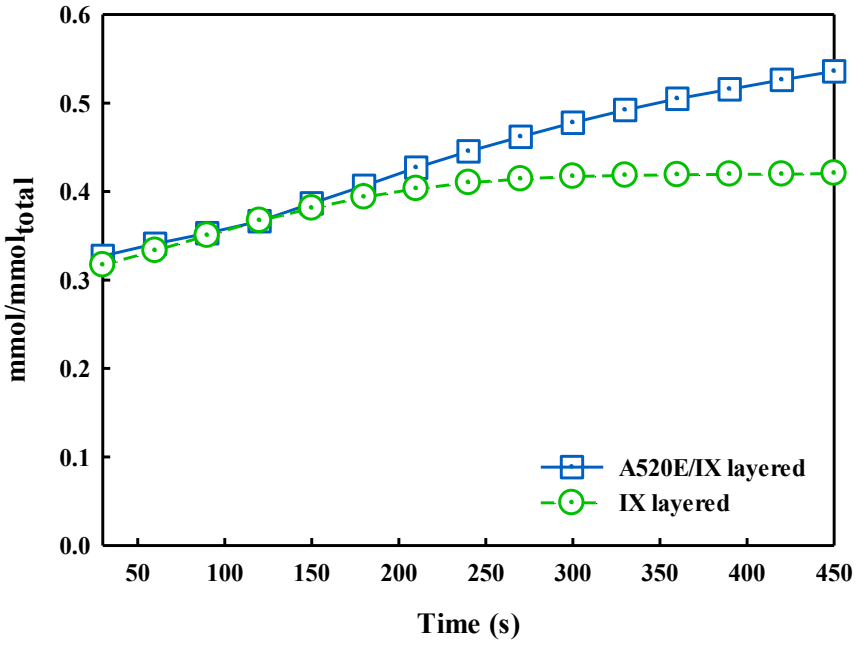

Figure 7.5. Mole fraction of adsorbed NO_3^- in the IX layered- and A520E/IX layered-MCDIs.

7.3.4 Preferential discharge of anions during regeneration of A520E/IX layered electrodes

The electrode regeneration step was employed under single-pass mode after the electrosorption by replacing the influent solution with DI water. The average amounts of anions captured by the IX layered electrodes throughout the experiments were 0.116, 0.090, and 0.071 mmol/g for NO_3^-, SO_4^-, and Cl^-, respectively, whereas 0.142, 0.073, and 0.050 mmol/g of NO_3^-, SO_4^-, and Cl^-, for each, was adsorbed when the A520E/IX layered electrode was used. The desorption efficiency of the anions disposed into DI water, as shown in **Figure 7.6(b) and (c)**, can be defined as the following equation.

$$\text{Desorption efficiency} = \frac{m_{d,t}}{m_a} = \frac{Q \times \int_0^t (C - C_0) dt \times M}{m_a} \quad \textbf{(Equation 7.5)}$$

where m_a indicates the adsorbed amount of ions (mmol) on the carbon electrode, Q is the flow rate of influent (mL/min). C_0 is the initial concentration of the influent (mmol/L), C is the concentration of effluent at time t (mmol/L), and M represents the molar mass of the anion (mg/mmol).

As shown in **Figure 7.6**, NO_3^-, which was the most selectively adsorbed anionic species during electrosorption, was discharged into the DI water stream at the fastest rate for both the IX layered and A520E/IX layered electrodes. The desorption rate of the anions from both the electrodes was in the following order: $NO_3^- > SO_4^{2-} > Cl^-$ (**Figure 7.6(a) and (c)**). However, the desorption efficiencies for the anions adsorbed on the anode show different trends for the IX and A520E/IX layered electrodes. In the MCDI tests using IX layered electrodes, NO_3^- took the shortest time for being disposed among the chosen anions, while the most time was required to completely release the Cl^- (**Figure 7.6(b)**). However, the Cl^- was quickly released from the A520E/IX layered anode (**Figure 7.6(d)**). From the A520E/IX layered electrode, Cl^- took the shortest to be disposed, whereas the longest time for was need for the desorption of NO_3^-. The retarded desorption efficiency of NO_3^- of the A520E/IX layered electrode could most likely be a result of the exchange between the NO_3^- and Cl^- during electrode regeneration (Gan et al. 2019). The reverse polarity repels NO_3^- and Cl^- ions from the EDL passing through the A520E/IX layer. However, the migrating NO_3^- would be exchanged with the Cl^- ions in the resin, thus would be temporarily intercepted at the IX layer. But at the end of the regeneration, the A520E/IX layered electrodes were found to be fully regenerated by applying reverse polarity throughout during all the experimental setups, which was consistent with the results of

Kim & Choi (2012) (Kim & Choi 2012).

From the observations in this section of this study, the mechanism of preferential adsorption and desorption when NO_3^- selective resin is incorporated in the IX layer can be explained better. The A520E resin particles embedded in the IX polymer layer result to additional adsorption of NO_3^- on the resin coating layer, leading to enhanced selectivity of NO_3^-. However, the NO_3^- becomes the least selective species to be desorbed as the A520E resin particles trap the NO_3^- migrating from the electrode surface to the bulk effluent solution during electrode regeneration.

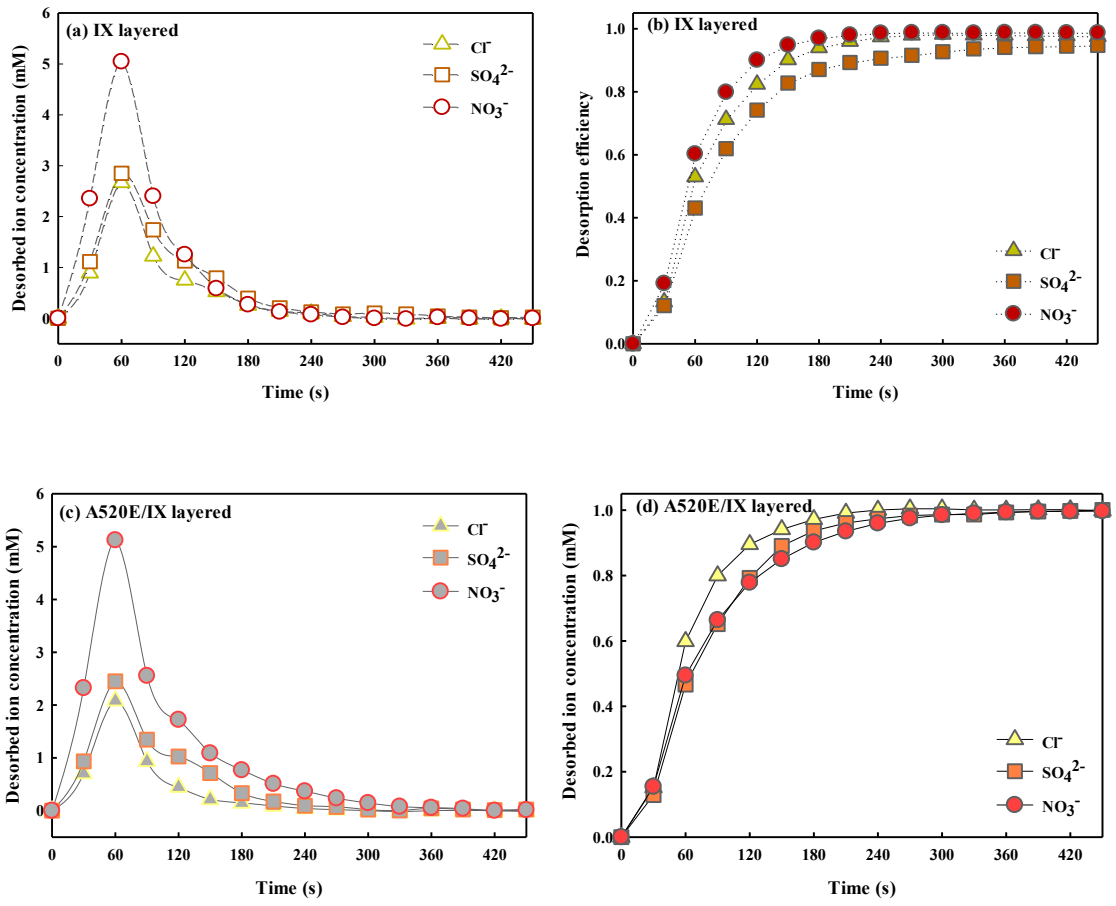

Figure 7.6. Competitive desorption among NO_3^-, Mg^{2+}, and Cl^-. The average concentrations of desorbed ions and corresponding desorption efficiency in (a and b) IX

layered- and (c and d) A520E/IX layered-MCDIs.

7.3.5 Recovery of nitrate from real municipal wastewater effluent with A520E/IX layered electrode

In this section, the competitive removal and discharge of NO_3^- in the real municipal wastewater effluent were assessed using an IX or A520E/IX layered anode under batch mode operation. The same volume of fresh DI water was circulated through the system under the same condition as electrosorption by reversing the potential. The desorbed ions, including NO_3^-, were collected in the brine solution after each regeneration cycle. This batch mode process was operated for five successive cycles using 120 mL of fresh wastewater effluent and 120 mL of concentrated brine solution for each test. As shown in **Figure 7.7(a)** and **Table 7.1**, the A520E/IX layered anode showed a better average removal of NO_3^-, whereas the average removal of Cl^- and SO_4^{2-} was lower than that of the IX layered one. These results imply that the A520E/IX layered electrode can selectively attract NO_3^- more, though the total removal of anionic species from the municipal wastewater was lower. As shown in **Figure 7.7(b)**, the specific selectivity in the expression of $\% / \%_{total}$ using the A520E/IX layered electrode was significantly higher, whereas the SO_4^{2-} was much less preferential than the electrode coated with only the anion-exchange polymer.

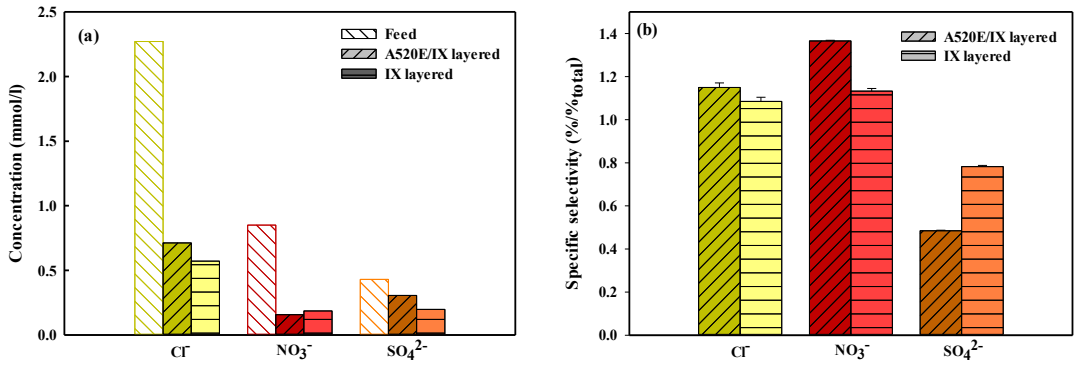

Figure 7.7. (a) Concentration of major anions in wastewater and the effluent, and the corresponding (b) specific selectivity of each ion in terms of removal %/%$_{total}$.

Table 7.1. Ionic compositions of anions in the feed and brine solutions after five successive cycles of operation.

		Anions				
Ion		Cl^-	NO_3^-	SO_4^{2-}	TP	NO_2^-
Feed	Concentration (mM)	2.27	0.85	0.43	0.03	0.004
IX layered	Removal (%)	74.8	78.2	54.0	37.5	48.5
	1st cycle brine (mM)	1.70	0.67	0.23	0.011	0.002
	3rd cycle brine (mM)	4.62	1.91	0.64	0.030	0.004
	5th cycle brine (mM)	7.39	3.01	0.92	0.050	0.005
	Concentration factor after 5 cycles	3.26	3.54	2.14	1.67	1.25
A520E/IX layered	Removal (%)	68.6	81.5	38.9	35.9	47.8
	1st cycle brine (mM)	1.56	0.70	0.17	0.010	0.002

3^{rd} cycle brine (mM)	4.24	1.89	0.48	0.029	0.004
5^{th} cycle brine (mM)	6.94	3.01	0.74	0.047	0.005
Concentration factor after 5 cycles	3.06	3.54	1.72	1.57	1.25

The discharge of the captured anions into brine solution for five cycles was directly followed by the electrosorption to enrich the NO_3^- concentration. As presented in **Table 7.1**, the NO_3^- concentration in the brine solution using IX and A520E/IX layered electrodes exhibited an almost linear increase after each cycle and reached 3.01 mM after the successive operation (3.54-fold compared to its initial concentration in the municipal wastewater feed). These results show that both the IX and A520E/IX layered electrodes can be used for successive reclamation of NO_3^- through MCDI. Given a consistent average removal of NO_3^- (78.2 and 81.5% with IX layered and A520E/IX layered electrodes, respectively) throughout the five cycles; however, incomplete discharge of ions led to the lower brine concentration than expected. The NO_3^- concentration was correspondingly supposed to be 3.35 mM using the IX layered anode and 3.50 mM using the A520E/IX layered anode, as opposed to 3.01 mM (**Figure 7.8**). The discrepancy of the actual amount with the expected amount of NO_3^- collected was most likely a result of the constrained ion discharge efficiency when the ions in the brine solution build up a reverse ionic-strength gradient across the IEM. Previous studies attributed the retarded desorption rate during short-circuiting to the hindered ion diffusion by the concentration gradient between the phases of highly enriched brine solution and electrode surface across the IX layer (Jeon et al. 2014; Kim et al. 2019a).

The fraction of NO_3^- in the brine solution was shown to be higher when the A520E/IX layered anode (**Figure 7.8**). The A520E resin in the IX layer selectively collected more NO_3^- during the electrosorption, as compared to both Cl^- and SO_4^{2-}. However, it can be noted that less of the NO_3^- adsorbed on the A520E/IX layer were less desorbed into the brine solution during electrode regeneration. Assuming the removal of NO_3^- are fixed during electrosorption and its full discharge into brine during electrode regeneration, the NO_3^- concentration in the brine after five cycles operation was supposed to be higher by using the A520E/IX layered electrode (**Figure 7.8**). The lower discharge efficiency of NO_3^- from the A520E/IX layered electrode is likely because NO_3^- was the least preferential anionic species to be desorbed, as aforementioned. These results imply that that coating the A520E/IX layer on the carbon electrode can effectively remove/recover NO_3^- through MCDI, achieving better selectivity; however, its poor selectivity in discharging NO_3^- limits the enrichment of the brine solution when the high concentration brine solution induces reverse ionic-strength gradient.

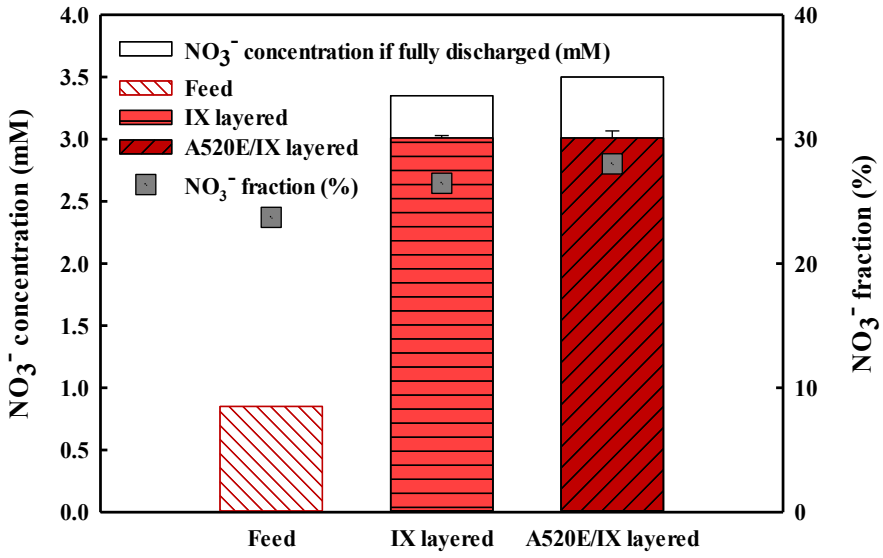

Figure 7.8. Concentration and portion of NH_4^+ in municipal wastewater feed and brine solutions after the 5th operation cycle using IX layered and A520E/IX layered electrodes.

7.4 Concluding remarks

This study systematically explored MCDI for efficient recovery of NO_3^- using a NO_3—selective IX layer coated carbon electrode. The electrosorptive performance of the coated electrodes, preferential electrosorption and desorption of three anionic species (Cl^-, SO_4^{2-}, and NO_3^-, and recovery of NO_3^- from real municipal wastewater effluent were investigated in this study.

- The coated IX polymer layer enhanced the electrosorption capacity and charge efficiency. The thin screening IX layer and tight adhesion between the carbon surface and the coated layer led to a low-contact resistance of the MCDI system. However, the electric resistivity of the electrode was increased when the granular A520E resin particles were incorporated in the IX coating layer.
- The NO_3^- was more selectively collected using the A520E/IX layered electrode. Its adsorption kept increasing even longer than 450 s, whereas the adsorption of salts reached saturation around 300 s. This was likely because the A520E resin embedded in the IX layer continued exchanging NO_3^- with other ions even after the saturation of the electrode.
- The desorption rate in terms of mM/s in the effluent from both the IX layered and A520E/IX layered electrodes was in order of $NO_3^- > SO_4^{2-} > Cl^-$. However, NO_3^- took the longest time for its full desorption attributing to the exchange between the NO_3^- on the EDL and Cl^- within the IX layer during electrode regeneration.

The MCDI process with a A520E/IX layered electrode also recovered NO_3^- well from real municipal wastewater, achieving better selectivity. However, it can be noted that the least selective desorption of NO_3^-, especially when discharging into high concentration brine, was observed to limit the enrichment of the NO_3^- into the brine.

CHAPTER 8

Expanding the Potential Application of Membrane Capacitive Deionization on Recovery of Palladium from Metal Plating Wastewater

The results from this chapter was published on ACS Sustainable Chemistry & Engineering, which is tilted as "*Palladium recovery through membrane capacitive deionization from metal plating wastewater*".

Research highlights

- Application potential of MCDI on Pd removal from industrial wastewater was probed.
- s were competitively removed even under co-existence of other cations.
- An apparent decrease in the desorption of Pd was observed in the successive cycles.
- It was attributed to the Pd complexation or crystal formation on the IX layer surface.

8.1 Introduction

As a result of large-scale exploitation of minerals in contemporary industry and the increasing concerns over environmental issues caused by wastes in electrical and electronic equipment (WEEE), reusing and recycling precious metals from secondary resources (i.e., industrial wastewater) are deemed to be important for those sustainable utilization (Cui & Zhang 2008; Yazici & Deveci 2009). With the significant increase in amount of WEEE and the ever-growing concerns of contamination by toxic and precious metal sources, a "WEEE directive" has been issued by The European Union, forcing WEEE industries to take responsibility for the collection of recovery and recycling of WEEE (EU 2002). Printed circuit board (PCB), which is a key part of electronic devices, has been gaining interests as one of the largest source of heavy metals.

In PCB manufacturing processes, palladium (Pd) complexes are widely used as catalysts to activate electro- and electroless-plating processes, which are regarded as very important steps for fabricating fine products. Electrowinning, the reclamation of used Pd solution from the plating process by electrodepostion of metals from wastewater, is known as the most effective and commonly used metal recovery system (Chen & Lim 2005; Pillai, Chung & Moon 2008). However, recovering the wasted Pd by

electrowinning is unfeasible at low concentration, and a significant amount of low Pd concentration wastes are being disposed. Concentrating the Pd-containing solution prior to electrowinning with an energy-efficient technology could be expected to improve the energy-efficiency and total Pd recovery rate. Therefore, concentrating the Pd containing wastewater from plating industry by means of capacitive deionization (CDI) with low energy use could be done to facilitate feasible and sustainable Pd recovery.

CDI is a technology that has been mainly applied for desalination to produce pure water through the extraction of charged species from water by applying an electrical potential difference over two porous electrodes. It has been one of the most alternative and feasible technology in recent years for sustainable fresh water production from unconventional water resources (Zhao, Porada, et al. 2013). This electrosorption process has especially shown to have better energy-efficiency than RO for deionization at low salt concentration levels water (i.e., salt concentration $\leq$ 30 mM), such as municipal wastewater and brackish water (Zhao, Porada, et al. 2013). Previous researches on development of advanced materials of electrode, effective process designs, and energy recovery have now improved this process drastically, making this technology feasible for potable water production (Liu et al. 2015; Suss et al. 2015; WANG, YU & MA 2017).

Aside from the use of CDI for water production, this technology has also been further studied for other applications including recovery of resources from the water (Huang & He 2013; Huang et al. 2014; Huang, Fan & Hou 2014; Kim, Yoon, et al. 2017; Kim & Choi 2012; Kim, Kim & Choi 2013; Macías et al. 2014; Ryu et al. 2015; Ryu et al. 2013; Tang et al. 2015; Wang & Na 2014; Wang et al. 2017; Yang, Shi & Yang 2014; Yeo & Choi 2013). Since there is a rising global demand for vastly-depleting natural resources and nutrients, reclaiming valuable resources such as nitrogen, phosphorus, and mineral

resources from municipal wastewaters and saline water sources has emerged as a great environmental solution (Penuelas et al. 2013; Prior et al. 2012; Tilton 2003). Since the CDI is based on the principle of ions and charge separation, it has shown to be potentially effective in the recovery of charged resources by highly removing/concentrating or selectively collecting present in minute amounts in low salinity water.

There are several studies that investigated the suitability of CDI for the recovery of nutrients and minerals. Especially, most CDI studies have noted on the recovery of nitrogen (Kim & Choi 2012; Kim, Kim & Choi 2013; Tang et al. 2015; Wang et al. 2017; Yeo & Choi 2013) and phosphorus (Huang et al. 2014; Macías et al. 2014) from municipal wastewaters as one of the most possible applications. Works in the copper removal revealed that CDI can be used to extract Cu^{2+} from wastewater with high selectivity over NaCl and natural organic matter (NOM) in a competitive environment (Huang & He 2013; Huang, Fan & Hou 2014). Studies on lithium recovery using CDI show good removal performance with faster adsorption/desorption than conventional lithium recovery process, and durability over several adsorption and desorption cycles (Kim, Yoon, et al. 2017; Ryu et al. 2015; Ryu et al. 2013). Binder-free carbon nanotube (CNT) electrode was found to provide a much increased electrochemical surface area, leading to enhanced removal of Cr^{VI} and Cr^{III} ions (Wang & Na 2014), whereas Pb^{2+} ions were more easily captured by an air-plasma treated CNT electrode in another study (Yang, Shi & Yang 2014).

The main objective of this work is to investigate the potential application of CDI for the recovery of Pd resources from the plating industry wastewater. The performances of the CDI for Pd recovery under different feed conditions and the influence of various operating parameters were studied using lab-scale membrane CDI (MCDI) unit, which is currently

one of the most advanced system in this field (Biesheuvel & Van der Wal 2010a). The issues of the MCDI performances including the adsorption and desorption efficiencies in long-term operations, and its improvement to attain higher concentration of Pd concentrate were discussed. Following up the long-term runs, the sustainability of CDI as a recovery process has been discussed through investigating the scaling behavior caused by Pd. Lastly, we introduced a new process for the efficient Pd recovery from plating industry wastewater integrating CDI stage, and also suggested improvements of CDI for its enhanced sustainability and feasibility through simplifying the Pd recovery process. This chapter is an extension of the research article published by the author in ACS Sustainable Chemistry & Engineering.

8.2 Materials and methods

8.2.1 Model palladium and palladium catalyst solution for electroless plating

Tetraamminepalladium(II) sulfate (Alfa Aesar, MA) was chosen as representative Pd species, since it can be found in Pd catalyst solutions. Three different concentrations of Pd in model solution were used for the MCDI tests: 1, 10, and 100 mg/L, which are within the range of actual Pd catalyst wastewater concentration observed in the PCB manufacturing process. A bulk palladium catalyst solution for electroless plating was also provided by MSC Co., Ltd (Republic of Korea) to assess the performance of MCDI as a real palladium recovery process. The major compositions of the Pd catalyst solution under different concentrations of Pd species are listed in **Table 8.1**.

Table 8.1. Major characteristics of 1, 10, and 100 mg/L of diluted Pd catalyst solutions.

Parameter	Pd catalyst solution		
	1 mg/L of Pd	10 mg/L of Pd	100 mg/L of Pd
pH	8.22	9.63	10.32
Total dissolved solids (uS/cm)	12.23	46.4	337
SO_4^{2-} (mg/L)	0.90	9.03	90.27
NH_4^+ (mg/L)	4.36	13.93	37.04

8.2.2 Carbon electrodes and ion exchange membranes

Two porous carbon electrodes manufactured by Siontech Co. (Republic of Korea) were used. The electrodes consisted of a graphite sheet body coated with activated carbon P-60 (Kuraray Chemical Co., Japan) and PVDF (Inner Mongolia 3F-Wanhao Fluorine Chemical Co. Ltd., China) blended carbon slurry. The total carbon mass on each 10x10 cm^2 sized electrode was reported to be around 0.8 g. Commercial anion and cation exchange membranes (Neosepta AFN and CMB, respectively) were obtained from Astom Corporation (Japan).

8.2.3 Bench-scale MCDI setup

The MCDI tests were carried out in a bench-scale system as depicted in our previous study (Choi, Lee & Hong 2016). The dimensions of the rectangular feed channel of the test cell were 10 cm in width and 10 cm in length, providing an effective ion adsorption/desorption area of 100 cm^2. There were two carbon electrodes placed within the test cell, whereas the anion and cation exchange membranes were inserted between those two electrodes. A non-electrically conductive nylon spacer was placed between the two ion exchange membranes to ensure the water flow and prevent short circuit. A 1 cm diameter sized hole was punched in the center of carbon electrodes, ion exchange

membranes, and a nylon spacer to enable the solution to be completely in contact with the electrodes and provide flow within the entire system cell (Lee, Bae & Choi 2010).

100 mL of feed solution was recirculated throughout the MCDI system with the flow rate of 30 mL/min by a peristaltic pump (Cole-Palmer, IL). The electrical potential supplied through the MCDI test unit was adjusted at a constant level by a potentiostat, WPG-100 (WonATech Co., Republic of Korea). The MCDI system was stabilized at the desired voltage after the feed water was circulated by repeating 5 cycles of 2 min for ion adsorption followed by 2 min of ion desorption. All the tests were carried out in duplicate.

8.2.4 Multiple cycles operation for concentration of Pd

The five or ten cycles operation procedure of MCDI is depicted in **Figure 8.1**. 100 mL feed solution containing 100 mg/L Pd circulated through the CDI system for 8 min at 0.9 V adsorption condition. To desorb the Pd ions attached onto the carbon electrode, 50 mL of fresh DI water was made to circulate through the system at the same conditions as adsorption. The desorbed Pd ions from the CDI system were collected into the concentrate solution after the primary desorption process for all cycles. To completely remove residual Pd ions remaining on the carbon electrode, an additional desorption step (secondary desorption) in the CDI system was carried out with newly replaced 50 mL fresh DI water at the same time and electric potential conditions. The water containing the residual Pd ions was then discarded. These adsorption, desorption, and secondary desorption processes were performed for five or ten cycles, with 100 mL of fresh feed solution and 50 mL of Pd concentrated water for each test. Complete desorption of ions from the electrodes was ensured by employing a further desorption step for 20 min at 1.2

V after the secondary desorption in each cycle, and thereby no discharge of ions during this step was detected by a conductivity meter confirming that there are no remaining ions that could be released by electrical force. The mass balance on the adsorbed and desorbed Pd ions was also calculated to make sure that ions were completely released at the end of each cycle.

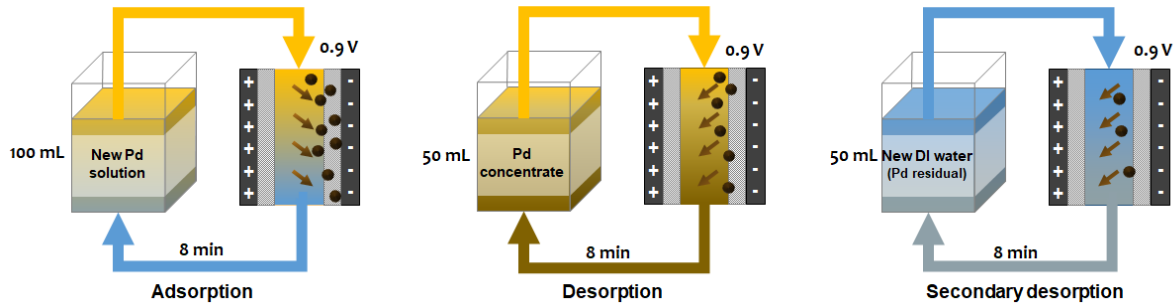

Figure 8.1. The protocol for MCDI test with multiple cycles.

After the long-term operation, both anode and cathode, and anion and cation exchange membranes in the MCDI system were disassembled, pre-rinsed with DI and followed by desiccation for over 24 hr to ensure complete drying of the samples. Then the surface of samples was analyzed by scanning electron microscopy (SEM) and energy-dispersive spectroscopy (EDS) in order to investigate the effect of long-term operation on CDI performances.

8.2.5 Measurement of water quality

The Pd concentrations of feed, permeate and concentrate waters were analyzed by inductively coupled plasma-mass spectrometer (ICP-MS), NExon 300D ICP-MS (Perkin

Elmer Co., MA). The water samples were diluted 100 times for accurate quantification of palladium ion. The calibration of ICP-MS was performed before measurement by external calibration with deionized water and 4 standard palladium solutions (0.625, 1.25, 2.5 and 5 mg/L).

8.3 Results and discussion

8.3.1 Removal of Pd in CDI under different operating conditions

To assess the capacity of CDI in Pd recovery and optimize operating conditions, the removal rate of Pd in this system was tested under varying operating conditions such as applied voltage, duration and Pd concentrations with or without other ions in the adsorption stage.

The basic removal rate of Pd by CDI was first evaluated using the synthetic Pd solution to observe the effect of voltage and time on Pd removal only, without interference of other coexisting ions. **Figure 8.2** shows the Pd removal rates from the 100 mg/L Pd solution at four different potentials during adsorption, ranging from 0.3 to 1.2 V applied voltage. As shown in the results, the CDI process exhibited a very high efficiency for Pd removal throughout all the applied voltages. The removal rate was 98.38% even at a small applied voltage of 0.3 V reaching 99.84% at 1.2 V when the electrosorption stage was carried out for 8 min. The highly efficient adsorption of Pd ions on carbon electrode might be driven by both electrosorptive and physical adsorption, such as the sorption behavior of other heavy metal ions in CDI (Huang et al. 2016). The physisorption mechanism of Pd ions on the carbon surface will be discussed further in the following sections.

It appears that the optimum voltage for Pd removal by MCDI is about 0.9 V achieving a removal efficiency of 99.80% under the operation of CDI for 8 min, and applying voltage

higher than this would not only increase energy input but also contribute to water splitting. This trend of removal rate could be also found in the CDI runs with different charging times. The Pd removal rate at different operation times for 0.9 V applied voltage in Figure 2 shows that the Pd ions were highly extracted by MCDI system achieving 96.76% of Pd removal within just 2 min and above 99.06% in about 4 min. To sum up, the operation of CDI at 0.9 V for 8 min is likely to be the optimum condition for Pd recovery. Similar observations were made in the previous work optimizing the salt adsorption rate in MCDI, which showed similar trends with different operating time and voltage (Zhao, Satpradit, et al. 2013).

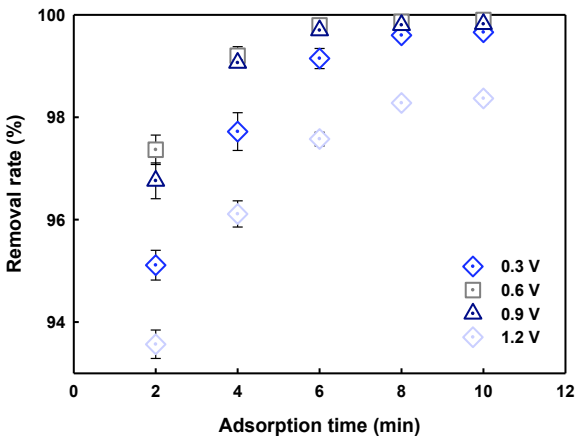

Figure 8.2. Removal rate of Pd using the synthetic solution containing 100 mg/L of palladium under different potentials (0.6 to 1.2 V) operating times (2 to 8 min) in adsorption step.

8.3.2 Enhancing Pd concentration through multiple MCDI adsorption and desorption cycles

The adsorption/desorption in MCDI was repeated for five cycles to capture Pd ions into the concentrate using a mixture of desorbed solution and original Pd feed solution. **Figure 8.4** shows that the Pd concentration increases linearly in the concentrate solution after each cycle for initial feed Pd catalyst solutions containing 1, 10, and 100 mg/L of Pd in **Figures 8.4a, b and c**, respectively. As shown in **Figure 8.4a**, the concentration of collected Pd ions in the concentrate after the 5th CDI cycle reached to 925.48 mg/L, suggesting that CDI could successfully recover and concentrate Pd ions. Theoretically, the Pd concentration in the concentrate was supposed to be 997.76 mg/L assuming a fixed Pd removal rate of 99.78% and the adsorbed ions on the carbon electrodes were completely discharged into the concentrate during the first desorption phase. Perhaps this slightly lower experimentally collected Pd ions in the concentrate is likely due to experimental errors.

Figure 8.4b and c also show the potential of MDCI in concentrating Pd ions from a feed with very low Pd concentrations to achieve higher Pd concentration such as in **Figure 8.4a**, although MCDI has to be operated for significantly more cycles. After five cycles, the Pd concentration in the concentrate reached to 66.28 mg/L for 10 mg/L of Pd catalyst solution (**Figure 8.4b** and 5.95 mg/L for 1 mg/L of Pd containing feed solution). These results show MCDI can adequately recover Pd ions from low feed concentration solutions. However, it is significant to note that the Pd ions in the concentrate did not increase linearly with the MCDI cycles as observed in **Figure 8.4a**. In fact a somewhat logarithmic increase was observed with repeated cycles. For example, when the MCDI was operated with 10 mg/L of Pd catalyst solution, 19.36 mg/L of Pd was desorbed and collected in the 1st cycle, while this reduced to only 4.27 mg/L of Pd in the 5th cycle. Likewise for 1 mg/L of Pd catalyst feed solution, 1.91 mg/L of Pd was desorbed in the 1st cycle against 0.40

mg/L in the 5th cycle. Assuming a stable adsorption and full regeneration in the desorption step throughout the cycles, the Pd concentration in the concentrate was expected to be 99.92 and 9.90 mg/L after the five cycles for 10 and 1 mg/L Pd catalyst feed solutions, respectively. The apparent decrease in the desorption of Pd ions from the electrodes in the successive MCDI cycles shows that the desorption rate was deteriorated and further discussions are made in the subsequent sections.

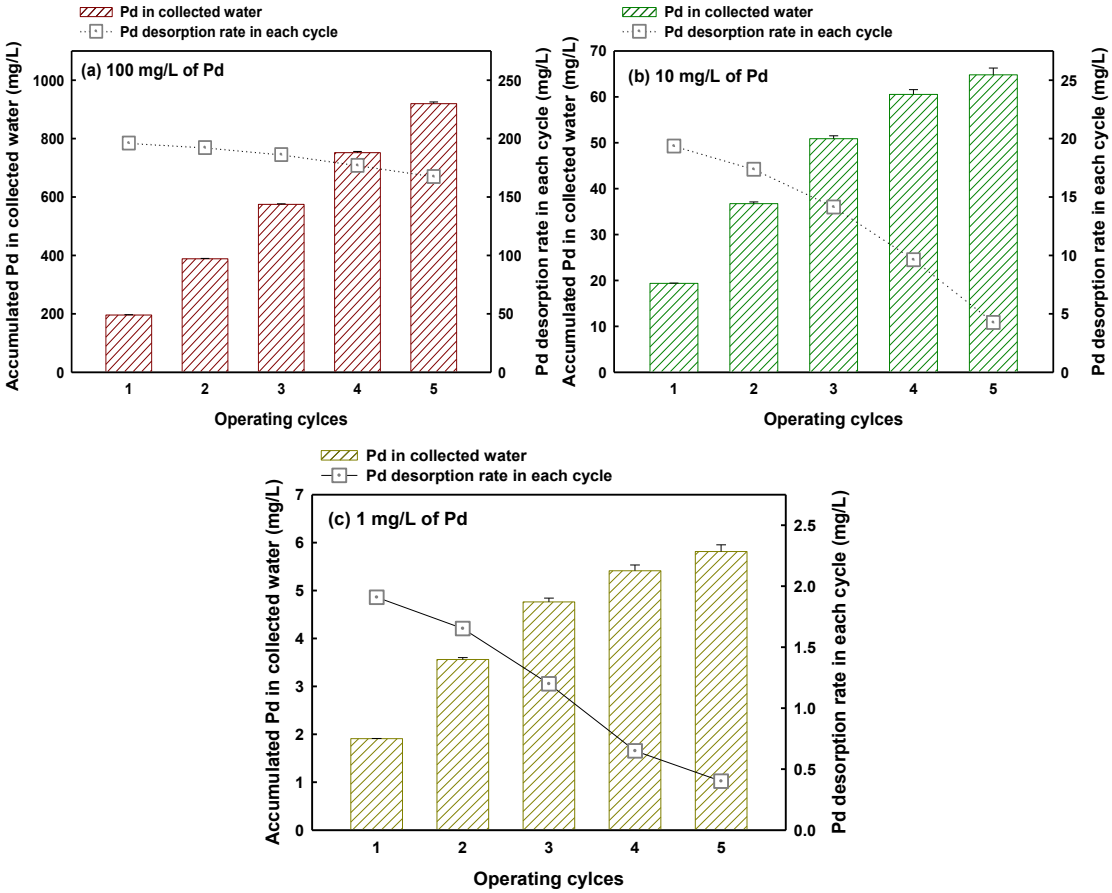

Figure 8.3. Concentration of Pd in concentrate solution after desorption of ions from the carbon electrodes. After adsorption of ions from new catalyst solutions containing (a) 1,

8.3.3 Effect of feed water concentration and composition on Pd

removal rate

Figure 8.3 presents the removal rates of Pd ions from the synthetic Pd and Pd catalyst solutions as a function of Pd concentration in feed water. The Pd removal rates of both the synthetic and catalyst solutions were consistently more than 99.74% for Pd concentration between 5 and 100 mg/L. Meanwhile, the Pd ions indicated slightly lower removal at low feed concentration: 98.65 and 99.49% from synthetic solution and 98.99 and 99.59% from catalyst solution, for feed solutions containing 1 and 2 mg/L of Pd, respectively. This is due to the fact that, lower TDS or Pd concentration has poor electrical conductivity and higher resistance because of which limits the movement and electrosorption of Pd ions but the electrosorption linearly increases with the feed concentrations or feed electrical conductivity (Mossad & Zou 2012; Xu et al. 2008). However, when the feed TDS increases more than 150 mg/L of Pd, the sorption efficiency stabilizes or gradually decreases.

The removal rate of Pd in the catalyst solution was slightly lower than that in the synthetic Pd solution, within the range of 5 to 150 mg/L of Pd in feed solution. The lower Pd removal could be explained due to competitive adsorption from the several other ions present in the plating feed solution, such as ammonium (Hou & Huang 2013; Huang et al. 2016). The ammonium and other minor ions present in the plating solution would competitively occupy the pore space within the carbon electrode, resulting in the decreased rate of Pd removal. However, it should be noted that the Pd ions were still highly removed by CDI even in the presence of other ions in the catalyst solution. This is likely due to the selectivity preference for ions in feed water during CDI (Liang et al. 2013). In general the ion selectivity during the electrosorption process is strongly dependent on the initial concentration, ionic charge valency, and hydrated radius of ions (Liang et al. 2013). Firstly, the ions with high concentration is preferentially adsorbed by

the carbon electrode. More specifically, cations of higher valence are energetically favorable to screen the surface charge of electrodes. On account of the governing number of Pd ions contained in the catalyst solution and those higher charge (divalent) than ammonium and other ions, Pd was the most preferred species to be collected by the carbon electrode.

Furthermore, Pd ions were shown to be more adsorbed in the catalyst solution under low concentration such as 1 and 2 mg/L of Pd. This is because the co-existing ammonium ions increases the total ion mobility toward the carbon surface, leading to higher adsorption capacity under low TDS condition. Since the addition of other ions in Pd catalyst solution offers slightly higher TDS in the low concentration feed water, the adsorption rate reaches higher than that of the synthetic Pd solution. This clearly shows that the co-existence of other ions such as ammonium in the catalyst solution could rather support the Pd removal performance of CDI than competitively taking place of the pore and surface of electrode. Therefore, it can be concluded that Pd could be sufficiently extracted through MCDI, and an outstanding Pd removal could be accomplished even though other co-ions existing in the Pd catalyst solution affect the efficiency of the process by competitive adsorption behavior. It is generally known that the initial pH of feed water influences the electrical potentials by adsorption of hydrogen and hydroxide ions on the surface of electrodes (Elimelech, Gregory & Jia 2013). In our study, however, pH of the feed solution did not play a significant role in the Pd removal though the initial pHs of catalyst solutions involving 10 and 100 mg/L of Pd were 9.63 and 10.32, respectively.

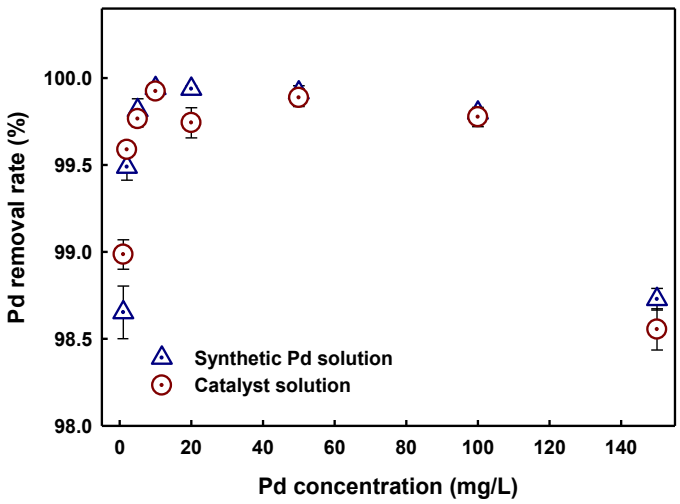

Figure 8.4. Removal rate of Pd in synthetic Pd and Pd catalyst solutions containing 1, 10, and 100 mg/L of Pd in adsorption step. The electrosorption was conducted at 0.9 V for 8 min.

8.3.4 Effect of concentration of concentrate solution on Pd desorption efficiency in MCDI

After every adsorption/desorption cycle at 0.9 V for 8 min, a secondary desorption step was further conducted and ions were released in a newly replaced 50 mL of DI water in each cycle at the same operating condition to unload any residual ionic species that probably still remained on the electrode. **Figure 8.5** presents the concentration of further desorbed Pd into the DI water in each cycle termed in this study as "residual water". The number of additionally discharged Pd ions in the secondary desorption increased with the number of MCDI cycles, clearly indicating that the Pd ions were not completely freed from the carbon electrode during the primary desorption stage, whereas this system showed a fairly stable adsorption performance over every cycle. Earlier studies have indicated that, normally, the carbon electrodes should be totally regenerated after

desorbing the ions under the same conditions with the adsorption step. This incomplete release of the ions in the first desorption phase is presumably owing to the effect of enhanced ionic concentration of the concentrate solution as explained by the Gouy Chapman Theory (Delahay 1965). Theoretically the electrosorptive capacity of the carbon electrodes in CDI is significantly affected by the electrical double-layer (EDL) capacity (Mossad & Zou 2012). Based on the Gouy Chapman Theory, the electrolyte concentration in the aqueous solution is one of the major factors determining the EDL capacity on the carbon electrode surface in CDI (Oren 2008a; Zhao et al. 2009).

Inversely, the increasing electrolyte concentration of the concentrate solution after each successive cycle leads to a lower or reverse ion concentration gradient between the carbon electrode and water media, disturbing the ion desorption from the porous carbon electrode surface. Since the concentration of concentrate solution increased as the operation cycle was repeated, the ions captured from the carbon electrode would be hardly released into the concentrate during the desorption stage, leading the Pd ions adsorbed on the carbon surface to be remained. The concentrate solution approaches saturation, and the lower or reverse concentration gradient is detrimental to desorption. For both desorption and adsorption, a higher concentration gradient is preferred to act as the driving force to overcome resistance to mass transfer of metal ions between the electrode and the solution (Barka et al. 2013).

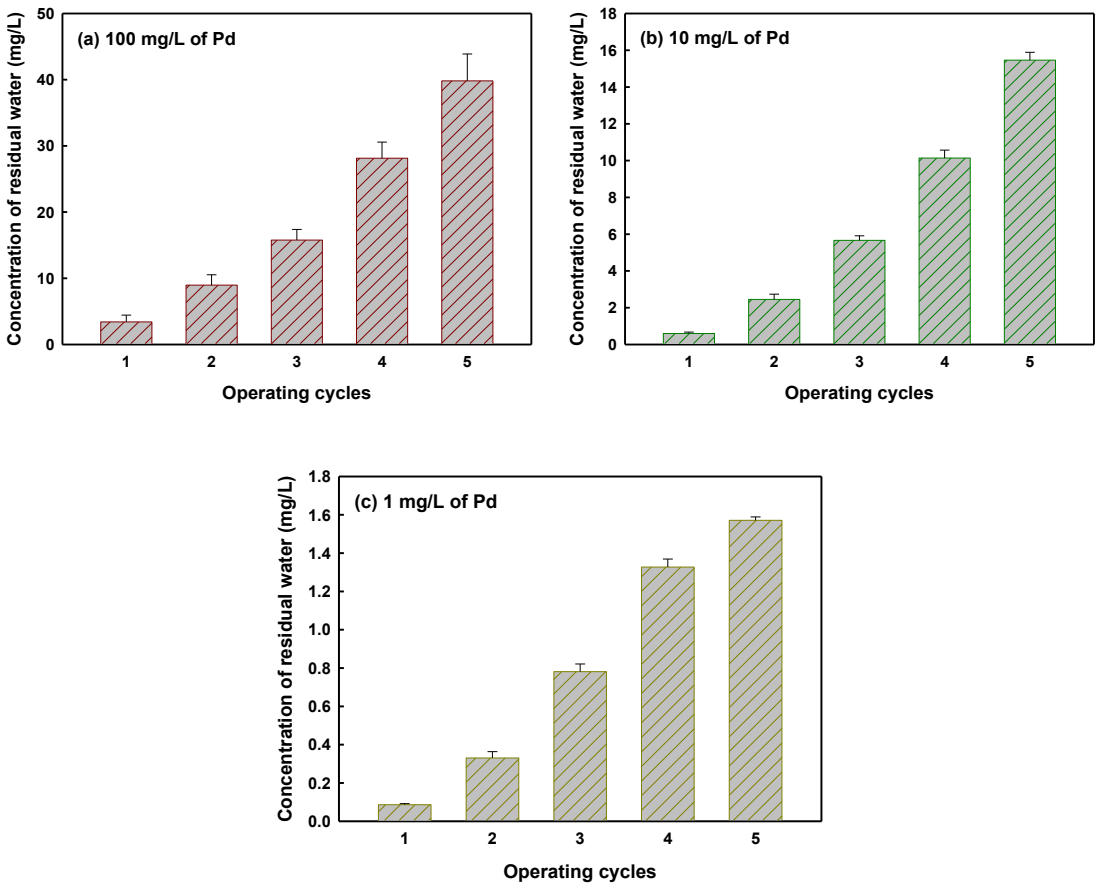

Figure 8.5. Concentration of Pd in residual solution after secondary desorption in each cycle. After adsorption/desorption using new catalyst solutions containing (a) 1, (b) 10, and (c) 100 mg/L of Pd, the remained ions on the electrode surface was further released in a new DI water (residual water) for 8 min at 0.9 V. New feed solution was then replaced to initiate another Pd recovery cycle, whereas the concentrate water was kept being used over every cycles. New DI water was then replaced to measure the concentration of residual water after each cycle.

8.3.5 Enhancing desorption efficiency through increasing desorption time or applied potential for higher Pd concentration

As observed in **Section 8.3.4**, adsorbed Pd ions were not completely released during each primary desorption stage as the Pd concentrations were increased in the successive MCDI

cycles. This section investigates how the two main operating parameters: desorption time and applied voltage affect the concentration rate of Pd ions in the concentrate water (**Figure 8.6**). The results show the final Pd concentration in the concentrate after the 5th cycle using an original catalyst solution of 100 mg/L of Pd where adsorption was performed at 0.9 V for 8 min and desorption was conducted with different potentials (0.8-1.2 V) and times (6-12 min). **Figure 8.6a** shows that, the concentration of Pd in the concentrate increased from 918.2 mg/L at 8 min desorption time to just 920.1 mg/L at 12 min. This indicates increasing desorption time longer than 8 min insignificantly enhances the concentration of Pd. However, a slight increase of Pd concentration in concentrate water was observed when a higher potential is used as shown in **Figure 8.6b** where the Pd concentrate increased from 919.4 at 0.9 V to 929.8 mg/L at 1.2 V. The desorption process generally proceeds rapidly and the majority of the adsorbed ions usually should be desorbed within about 2 min of applying a desorption potential (Lee, Bae & Choi 2010), and thus, the increased desorption time insignificantly improved the efficiency of Pd collection in the concentrate. However, elevating the applied potential raised the desorption current (Lee, Bae & Choi 2010), promoting better desorption rate and resulting in enhanced Pd concentration in the concentrate solution.

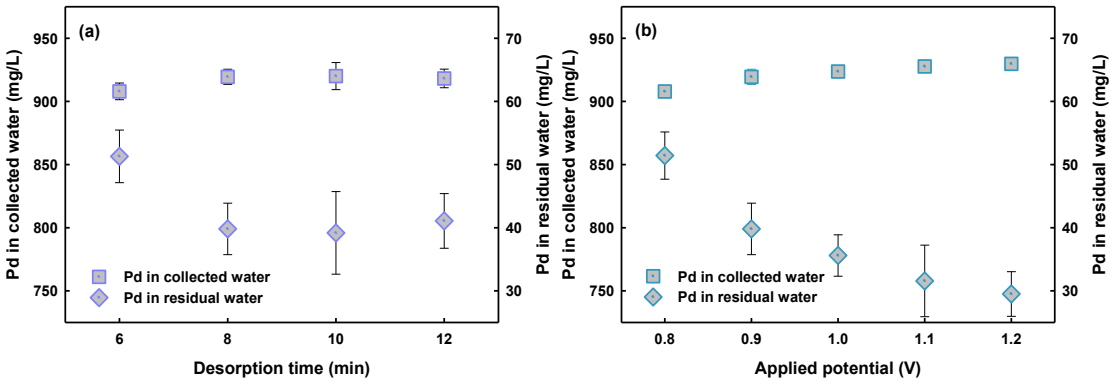

Figure 8.6. The enhanced concentration of Pd concentrate and the corresponding concentration of Pd in residual solutions after secondary desorption with increased (a)

desorption time and (b) applied potential. The secondary desorption to release residual Pd ions from the carbon electrode was performed at 0.9 V and 8 min.

8.3.6 Deterioration of Pd adsorption performance under longer operation cycles

During the CDI operation with five cycles, it was shown earlier that the adsorbed Pd ions were not completely released from the carbon electrode in the primary desorption phase and additional desorption steps were employed in each cycle during the five cycles CDI operation. Therefore, the change of adsorptive capacity of the carbon electrode was investigated in terms of much longer cycles of ten cycles in total. The longer MCDI operation was carried out with adsorption at 0.9 V for 8 min using the initial feed of 100 mg/L Pd solution, whereas the primary desorption process was performed at 0.9 V for 8 min followed by a further desorption phase at 1.2 V for 20 min. No discharge of ions after those two desorption phases were confirmed in each cycle.

Figure 8.7 exhibits the Pd removal rate in each MCDI cycle. The Pd removal rates gradually decreased from 99.8% to 98.0% in the 10^{th} cycle. Although this is a margnial decrease of only 1.7% in 10 cycles and does not appear to be significant, it should be a concern for the long-term operation of MCDI for Pd recovery as this indicates an average 0.2% decrease in the removal rate for every cycle. If this decreasing trend shown in **Figure 8.7** is to continue, it likely that the MCDI removal rate will reach zero after 555 cycles of operations, which is not at all desirable. This decrease in Pd removal rate is likely attributed to physisorption of Pd ions within the porous structure of carbon electrode instead of electrosorption. In common with the adsorption behavior of other metal ions such as Cd^{2+}, Pb^{2+} and Cr^{3+} on activated carbon, the adsorption of Pd ions on

carbon electrode surface would be governed by a complicated adsorption process involving complex formation and surface adsorption mechanisms (Huang et al. 2016). The Pd ions in the aqueous solution migrate into the pores and interact with the interior carbon surface of pores (Corapcioglu & Huang 1987). Those ions that are physically adsorbed and especially within the inner pores of porous carbon electrode are not likely to be easily detached by simply reversing the charges, resulting in reduced available surface area of carbon electrode for further adsorption (Namasivayam & Kadirvelu 1997).

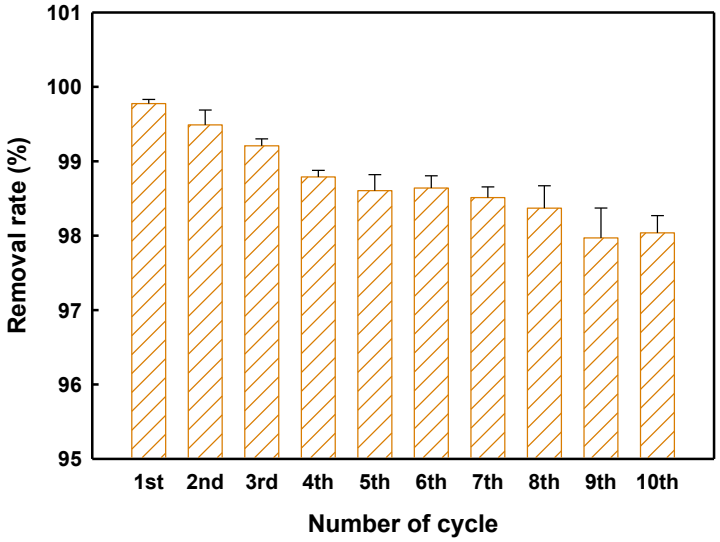

Figure 8.7. Pd removal rate from catalyst solution for ten cycles.

Both the cation exchange membrane and carbon cathode were analyzed by SEM and EDS after the ten cycles of operation to further observe their possible physical deterioration due to repetitive operations. **Figure 8.8c** shows that several deposits were found attached including metallic crystals on the cation exchange membrane. The EDS results in **Figure 8.8c and d** confirm the presence of Pd crystals. These results show that the decline in the

MCDI performances was also likely due to Pd complexation or crystal formation on both the electrode and ion exchange membrane.

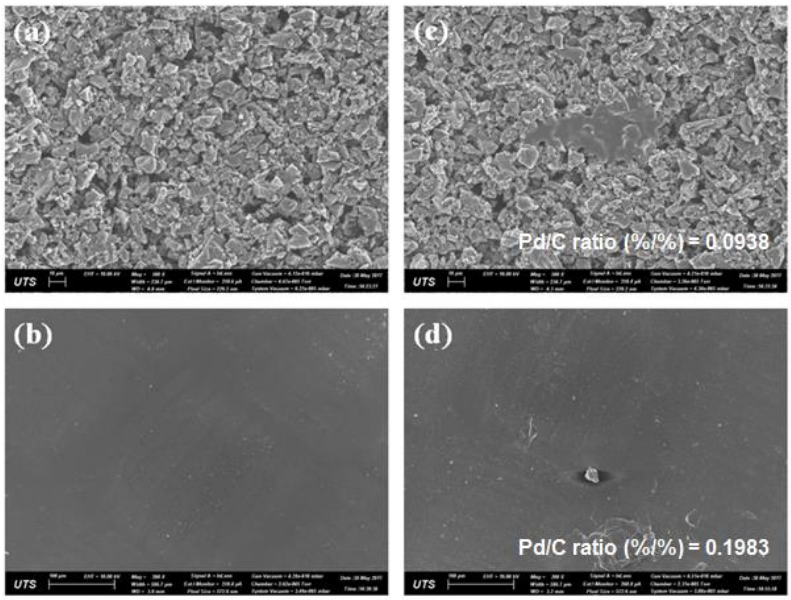

Figure 8.8. SEM images of virgin (a) carbon cathode and (b) cation exchange membrane, and used (c) carbon cathode and (d) cation exchange membrane after ten cycles CDI test. Plus, the Pd/C ratio described in this figure was measured by EDS analysis.

8.3.7 Potential integration of MCDI and ion selective electrode for Pd recovery

Electrowinning, one of the most widely used Pd recovery process from wastewaters, is still regarded as an energy-intensive technology. Especially its energy-efficiency is critically low for water sources with very low Pd concentrations, and because of this reason, the wastewater containing low Pd concentrations are rather disposed. However as shown in **Figure 8.9a**, integrating MCDI with the existing electrowinning process is expected to supplement the technology for concentrating Pd ions in the wastewater. This

integrated process could be feasible by lowering the energy consumption in electrowinning and spending less energy in MCDI. Besides, we can anticipate a more compact Pd recovery process consisting of MCDI only using a Pd selective electrode as presented in **Figure 8.9b** which could significantly enhance the energy efficiency of the Pd concentration.

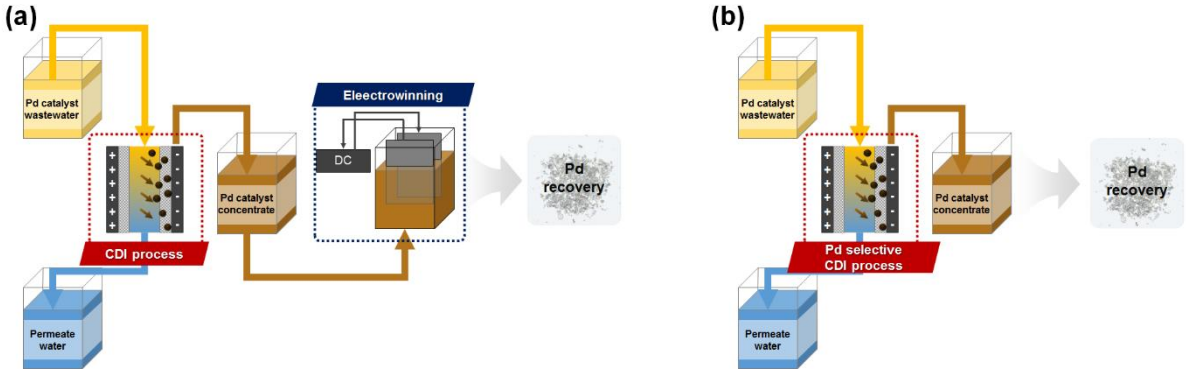

Figure 8.9. Possible application of MCDI: (a) an integrated Pd recovery process consisting of MCDI and electrowinning, and (b) single MCDI process using a Pd selective electrode material.

8.4 Concluding remarks

The potential of MCDI for the recovery of Pd from Pd catalyst wastewater from plating industry has been explored under various operating conditions and solution compositions, and the issues to be overcome are addressed in this work. The performances were measured in terms of the adsorptive and desorptive behavior during multiple cycles of MCDI operations for enrichment of the Pd concentrate. The following are the major findings from this lab-scale study:

- Through adequate process optimization such as operation time and applied potential for a fixed electrode mass, MCDI can be quite effective in the Pd removal from plating wastewater for its recovery and reuse.
- It was demonstrated that Pd can be significantly concentrated through successive cycles of MCDI operation by accumulatively desorbing the ions into the Pd concentrate. However, as the concentrate solution becomes saturated with ions as adsorption cycles are performed repeatedly, incomplete discharge of Pd ions from the electrodes during the primary desorption phase was observed. Applying higher potential slightly enhanced the desorption rate and hence its ability to concentrate the recovered Pd from the feed water.
- The electrosorptive capacity of the MCDI electrode decreased with the increase in the number of operation cycles because of the likely physical adsorption of Pd ions that cannot be easily released by reversing polarity of the carbon electrodes. SEM and EDS analysis further indicted the formation of a complex or crystal on both surfaces of cathode and cation exchange membrane which may be mitigated through proper physical and chemical cleanings.
- The study pointed out the potential for MCDI to be either integrated with the conventional electrowinning process to supplement Pd recovery from the plating industry. The other option is to apply MCDI using Pd ion selective electrode or ion-exchange membrane which could significantly enhance the MCDI energy efficiency.

CHAPTER 9

Conclusions and Recommendations

9.1 Summary of major outcomes

Owing to the rising global demand for depleting mineral resources and nutrients, recovering valuable resources from municipal wastewaters such as nitrogen, phosphorus, and mineral resources has been acknowledged as a significant environmental and social issue. MCDI is considered a potentially effective technology to recover mineral resources from wastewaters by selectively collecting minerals present in small amounts in low salinity waters. However, a full investigation of the MCDI technology as a resource recovery process from a practical perspective is required for demonstrating the application potential of MCDI.

This study aimed to explore its application potential in practical use for mineral recovery from wastewater resources. Carbon electrodes coated with a thin ion-exchange polymer layer were employed as advanced electrodes for better performance which induced lower membrane electrical resistance and inhibited the electrosorption of counter-ions during regeneration of electrodes. Synthetic feed water solutions were used to probe the effect of operating conditions and solution chemistries on the adsorption and desorption efficiency, whereas real wastewaters also were used as a feed solution to understand the complex nature of charged impurities. The major findings from each chapter in this dissertation are addressed as follows.

9.1.1 Ion discharging behavior during electrode regeneration and its implications on mineral recovery

As the MCDI process is rooted in ion separation from aqueous solutions, it effectively recovers charged compounds by collecting the ions present in small amounts from low salinity wastewater resources. This study (Chapter 4) aimed to understand the behavior of ion desorption during electrode regeneration of MCDI in mineral resource recovery, especially the ion discharging behavior into high concentration brine solution.

The experimental results implied the ions from the bulk brine can be reversely diffused to the carbon electrode or the electrochemical driving force from the applied potential difference be compensated by a reverse chemical gradient. The reverse-ionic strength built by different ions as brine, such as Mg^{2+} and K^{+}, confirmed the interruption of ion discharge from the EDL surface, which can be elucidated by the Gouy-Chapman theory. The retardation of ion desorption was more apparent when a small amount of ions was adsorbed on the electrode at lower feed concentration, which was due to the enhanced membrane resistance of the IX layer. The preferential desorption under a mixture of cations was related more to the diffusion transport kinetics of the adsorbed cations within the EDL rather than the permselectivity (ion mobility) trend through the CEM, whereas the electrostatic force induced by multivalent ions had an insignificant impact on ion discharge. Fitting the results with pseudo kinetic models could be a useful tool to understand the desorption kinetics in MCDI, particularly the preferential desorption order of different ions.

9.1.2 Selective nitrate and phosphate recovery from municipal wastewater

Chapters 5 and 6 present the applicability of MCDI using IX layer coated electrodes as a nutrient recovery process by investigating its advantages in terms of ion selectivity, efficiency of recovery, and long-term sustainability. The systematic investigation of the MCDI and its process optimization for enhanced electrosorptive performance were carried out considering the complex nature of the characteristics of real municipal wastewater.

The low resistance of the IX layer induced by the thinly coating and its low contact resistance with the carbon surface resulted in high SAC and charge efficiency. The removal efficiency of NO_3^- was much higher than that of different anions, owing to its fast diffusion and its strong hydrophobicity over the other anions, and was further adsorbed by substituting the other adsorbed anions. Increasing the feed flow rate gave rise to a shorter time for saturation of the electrode, and the adsorbed Cl^- and SO_4^{2-} were quickly replaced by the supplemented NO_3^- from the continually supplied wastewater feed. In contrast, applying a higher voltage induced a significant increase in the ion mobilities of Cl^- and SO_4^{2-} through the AEM compared to that of NO_3^-.

The overall adsorption capacity of phosphate was apparently higher in the lower pH, where $H_2PO_4^-$ was dominantly present in wastewater, owing to the smaller hydrated radii of monovalent ions occupying less space within the EDL for charge neutralization. Besides, the swift change between $H_2PO_4^-$ and HPO_4^{2-} to maintain the equilibrium system also influenced T-P removal. However, the equilibrium system of phosphate was insignificant because in reality, as the P concentration is much lower and the other anions are predominantly presented in real wastewater. The degradation of electrosorption performance caused by the organic substances was insignificant during longer operation,

as the flat surface of the coated IX layer with low roughness offered a smaller change for the organic substances to accumulate on the electrode surface.

9.1.3 Development of nitrate selective electrode for enhanced recovery

One of the major disadvantages of MCDI for mineral recovery is the inability of the electrodes to selectively remove the target ions. Therefore, in Chapter 7, a nitrate selective composite electrode was developed by coating a slurry of grounded A520E nitrate selective resin and anion exchange polymer on the surface of commercial activated carbon electrode.

The low contact resistance due to the tight adhesion between the IX layer and the carbon surface of the IX polymer layer coated MCDI enhanced electrosorption and reduced energy consumption. However, incorporating grounded NO_3^- selective resins in the IX layer rather increased the resistance, resulting in higher membrane resistance. More selective NO_3^- removal could be attained by using the NO_3—selective electrodes, since the selective electrode kept collecting NO_3^- even after the electrode reached saturation, which was attributed to the exchange between the Cl^- within the EDL and NO_3^- from the supplied feed stream. However, the longest time was needed for full desorption of NO_3^- from the NO_3—selective electrodes, because the NO_3^- passing through the resin embedded IX layer was exchanged with the Cl^- ions in the resin, thus temporarily being trapped at the IX layer.

9.1.4 Membrane capacitive deionization for recovery on palladium

waste

Assessing the potential application of MCDI on mineral recovery was expanded to the recovery of palladium waste from metal plating wastewater, which can be an economically viable precious metal that can be feasibly recovered (Chapter 8). This study showed the MCDI process can be utilized not only for reclaiming nutrients from domestic wastewater but also different mineral resources from a variety of industrial wastewaters.

The high adsorption of Pd from a single Pd solution, higher than 98.38% even at a low applied potential (0.3 V), was driven by both electrosorptive and physical adsorption. Its competitive removal was achieved even under co-existence of different cations because Pd ions in the plating solution possessed high concentrations and ionic charge valency. However, an incomplete discharge of Pd in the successive MCDI cycles was observed, owing to the reverse-ionic-strength gradient built between the bulk feed solution and electrode surface. The further decrease in Pd removal and desorption under the repetitive cycles was attributed to the surface physisorption or complexation of Pd metal ions, resulting in resulting in reduced available surface of area of electrode for further electrosorption.

9.2 Recommendations

This thesis demonstrated the application potential of MCDI for the recovery of wasted mineral resources from industrial and municipal wastewaters such as nutrients and precious elements. This study covers the behavior of ion transportr between the electrode and bulk feed solution across the IEM, recovery of nitrate and phosphorus from municipal water using ion-exchange polymer layer coated carbon electrodes, development of an ion

selective electrode for enhanced mineral recovery by incorporating grounded selective resins, and expanding its potential application to resource recovery from industrial wastewater. The recommendations based on the results in this dissertation are made as below to provide future insights into realizing the practical use of MCDI systems for the recovery of valuable resources.

1. This study addresses the concerns of the retarded electrode regeneration of MCDI and limited enrichment of the brine, constrained by the reverse-ionic-strength gradient induced by the highly enriched brine solutions. Especially, recovering minerals from low concentration water could be challenging due to the enhanced resistance of the IX layer. Reversing polarity at higher potential might work the best for overcoming the limited resource recovery by applying electrostatic repulsive force, whereas short-circuiting was revealed to be inefficient due to the lack of electrochemical repelling force.
2. Nitrate was preferentially recovered via MCDI, owing to its high permselectivity through the IX layer and strong affinity to the carbon surface. Lowering the potential and increasing the flow rate resulted in the enhanced selectivity of nitrate, whereas that of phosphate rather decreased. Therefore, the operating conditions needs to be adjusted based on the understandings of the transport (mobility) behavior of the specific target to achieve high selectivity. Besides the optimum condition have to be determined deliberately considering the total removal efficiency, as lowering potential or increasing flow rate for enhanced selectivity of nitrate may rather result in poor removal of total ions in the wastewater. Selective collection of phosphate was difficult at the current level of MCDI technology, due to its low permselectivity and low amount present in wastewater.

3. Although MCDI for recovery of mineral resources calls for selective and target removal of specific ions, this study demonstrated the carbon electrodes can be customized for adsorption of target species by coating an ion selective polymer layer. This aspect of electrode development is expected to lead MCDI to its practical application for the recovery of specific mineral resources. However, the intensified electrical resistivity caused by the grounded resins at the ion selective layer is challenging in fabricating the ion selective electrode. New coating techniques for a thinner selective layer incorporating micro-fine resins will further improve the performance of MCDI to attain both high charge efficiency and selective ion recovery.
4. MCDI is shown to have a potential for the selective removal and recovery of precious metals in this study. Multivalent metallic cations, such as Pd, can be competitively collected from wastewater, owing to their high ion valencies and permselectivities. However, the complexation or crystal formation of the metallic species on the IX layer surface in longer operation needs to be inhibited through implementing preventive maintenance or cleaning strategies. Still, future works on discovering new potential ionic resources (e.g., lithium or copper) from unconventional water sources and on designing optimized operation and configuration will further widen the applications of MCDI for the effective reclamation of specific valuable resources.

References

Ahn, Y., Hwang, Y.-H. & Shin, H.-S. 2011, 'Application of PTFE membrane for ammonia removal in a membrane contactor', *Water Science and Technology*, vol. 63, no. 12, pp. 2944-8.

Alklaibi, A.M. & Lior, N. 2005, 'Membrane-distillation desalination: status and potential', *Desalination*, vol. 171, no. 2, pp. 111-31.

Anderson, M.A., Cudero, A.L. & Palma, J. 2010, 'Capacitive deionization as an electrochemical means of saving energy and delivering clean water. Comparison to present desalination practices: will it compete?', *Electrochimica Acta*, vol. 55, no. 12, pp. 3845-56.

Ansari, A.J., Hai, F.I., Price, W.E., Drewes, J.E. & Nghiem, L.D. 2017, 'Forward osmosis as a platform for resource recovery from municipal wastewater - A critical assessment of the literature', *Journal of Membrane Science*, vol. 529, pp. 195-206.

Asano, T. & Levine, A.D. 1996, 'Wastewater reclamation, recycling and reuse: past, present, and future', *Water Science and Technology*, vol. 33, no. 10-11, pp. 1-14.

Aslani, P. & Kennedy, R.A. 1996, 'Studies on diffusion in alginate gels. I. Effect of cross-linking with calcium or zinc ions on diffusion of acetaminophen', *Journal of controlled release*, vol. 42, no. 1, pp. 75-82.

Ayala-Bribiesca, E., Araya-Farias, M., Pourcelly, G. & Bazinet, L. 2006, 'Effect of concentrate solution pH and mineral composition of a whey protein diluate solution on membrane fouling formation during conventional electrodialysis', *Journal of Membrane Science*, vol. 280, no. 1-2, pp. 790-801.

Bae, B.-U., Jung, Y.-H., Han, W.-W. & Shin, H.-S. 2002, 'Improved brine recycling during nitrate removal using ion exchange', *Water Research*, vol. 36, no. 13, pp. 3330-40.

Bahmani, P., Maleki, A., Rezaee, R., Khamforoush, M., Yetilmezsoy, K., Dehestani Athar, S. & Gharibi, F. 2019, 'Simultaneous removal of arsenate and nitrate from aqueous solutions using micellar-

enhanced ultrafiltration process', *Journal of Water Process Engineering*, vol. 27, pp. 24-31.

Barka, N., Abdennouri, M., El Makhfouk, M. & Qourzal, S. 2013, 'Biosorption characteristics of cadmium and lead onto eco-friendly dried cactus (Opuntia ficus indica) cladodes', *Journal of Environmental Chemical Engineering*, vol. 1, no. 3, pp. 144-9.

Batstone, D., Hülsen, T., Mehta, C. & Keller, J. 2015, 'Platforms for energy and nutrient recovery from domestic wastewater: A review', *Chemosphere*, vol. 140, pp. 2-11.

Bazant, M.Z., Thornton, K. & Ajdari, A. 2004, 'Diffuse-charge dynamics in electrochemical systems', *Physical review E*, vol. 70, no. 2, p. 021506.

Biesheuvel, P. 2009, 'Thermodynamic cycle analysis for capacitive deionization', *Journal of colloid and interface science*, vol. 332, no. 1, pp. 258-64.

Biesheuvel, P., Bazant, M., Cusick, R., Hatton, T., Hatzell, K., Hatzell, M., Liang, P., Lin, S., Porada, S. & Santiago, J. 2017, 'Capacitive Deionization--defining a class of desalination technologies', *arXiv preprint arXiv:1709.05925*.

Biesheuvel, P., Fu, Y. & Bazant, M. 2012, 'Electrochemistry and capacitive charging of porous electrodes in asymmetric multicomponent electrolytes', *Russian Journal of Electrochemistry*, vol. 48, no. 6, pp. 580-92.

Biesheuvel, P., Porada, S., Levi, M. & Bazant, M.Z. 2014, 'Attractive forces in microporous carbon electrodes for capacitive deionization', *Journal of solid state electrochemistry*, vol. 18, no. 5, pp. 1365-76.

Biesheuvel, P. & Van der Wal, A. 2010a, 'Membrane capacitive deionization', *Journal of Membrane Science*, vol. 346, no. 2, pp. 256-62.

Biesheuvel, P., Van Limpt, B. & Van der Wal, A. 2009, 'Dynamic adsorption/desorption process model for capacitive

deionization', *The journal of physical chemistry C*, vol. 113, no. 14, pp. 5636-40.

Biesheuvel, P., Van Soestbergen, M. & Bazant, M. 2009, 'Imposed currents in galvanic cells', *Electrochimica Acta*, vol. 54, no. 21, pp. 4857-71.

Biesheuvel, P., Zhao, R., Porada, S. & Van der Wal, A. 2011a, 'Theory of membrane capacitive deionization including the effect of the electrode pore space', *Journal of colloid and interface science*, vol. 360, no. 1, pp. 239-48.

Biesheuvel, P.M. & van der Wal, A. 2010b, 'Membrane capacitive deionization', *Journal of Membrane Science*, vol. 346, no. 2, pp. 256-62.

Biesheuvel, P.M., Zhao, R., Porada, S. & van der Wal, A. 2011b, 'Theory of membrane capacitive deionization including the effect of the electrode pore space', *Journal of Colloid and Interface Science*, vol. 360, no. 1, pp. 239-48.

Bijmans, M., Burheim, O., Bryjak, M., Delgado, A., Hack, P., Mantegazza, F., Tenisson, S. & Hamelers, H. 2012, 'Capmix-deploying capacitors for salt gradient power extraction', *Energy Procedia*, vol. 20, pp. 108-15.

Bixio, D., Thoeye, C., Wintgens, T., Ravazzini, A., Miska, V., Muston, M., Chikurel, H., Aharoni, A., Joksimovic, D. & Melin, T. 2008, 'Water reclamation and reuse: implementation and management issues', *Desalination*, vol. 218, no. 1-3, pp. 13-23.

Blair, J.W. & Murphy, G.W. 1960, 'Electrochemical demineralization of water with porous electrodes of large surface area'ACS Publications.

Blöcher, C., Niewersch, C. & Melin, T. 2012, 'Phosphorus recovery from sewage sludge with a hybrid process of low pressure wet oxidation and nanofiltration', *Water research*, vol. 46, no. 6, pp. 2009-19.

Boeije, G., Corstanje, R., Rottiers, A. & Schowanek, D. 1999, 'Adaptation of the CAS test system and synthetic sewage for biological

nutrient removal: Part I: Development of a new synthetic sewage', *Chemosphere*, vol. 38, no. 4, pp. 699-709.

Bradford-Hartke, Z., Lane, J., Lant, P. & Leslie, G. 2015, 'Environmental benefits and burdens of phosphorus recovery from municipal wastewater', *Environmental science & technology*, vol. 49, no. 14, pp. 8611-22.

Broséus, R., Cigana, J., Barbeau, B., Daines-Martinez, C. & Suty, H. 2009, 'Removal of total dissolved solids, nitrates and ammonium ions from drinking water using charge-barrier capacitive deionisation', *Desalination*, vol. 249, no. 1, pp. 217-23.

Chapman, D.L. 1913, 'LI. A contribution to the theory of electrocapillarity', *The London, Edinburgh, and Dublin philosophical magazine and journal of science*, vol. 25, no. 148, pp. 475-81.

Chen, J.P. & Lim, L. 2005, 'Recovery of precious metals by an electrochemical deposition method', *Chemosphere*, vol. 60, no. 10, pp. 1384-92.

Chen, L., Wang, C., Liu, S., Hu, Q., Zhu, L. & Cao, C. 2018, 'Investigation of the long-term desalination performance of membrane capacitive deionization at the presence of organic foulants', *Chemosphere*, vol. 193, pp. 989-97.

Chen, L., Yin, X., Zhu, L. & Qiu, Y. 2018, 'Energy recovery and electrode regeneration under different charge/discharge conditions in membrane capacitive deionization', *Desalination*, vol. 439, pp. 93-101.

Chen, Z., Zhang, H., Wu, C., Wang, Y. & Li, W. 2015, 'A study of electrosorption selectivity of anions by activated carbon electrodes in capacitive deionization', *Desalination*, vol. 369, pp. 46-50.

Chislock, M.F., Doster, E., Zitomer, R.A. & Wilson, A. 2013, 'Eutrophication: causes, consequences, and controls in aquatic ecosystems', *Nature Education Knowledge*, vol. 4, no. 4, p. 10.

Choi, J., Dorji, P., Shon, H.K. & Hong, S. 2019, 'Applications of capacitive deionization: Desalination, softening, selective removal, and energy efficiency', *Desalination*, vol. 449, pp. 118-30.

Choi, J., Lee, H. & Hong, S. 2016, 'Capacitive deionization (CDI) integrated with monovalent cation selective membrane for producing divalent cation-rich solution', *Desalination*, vol. 400, pp. 38-46.

Choy, E.M., Evans, D.F. & Cussler, E. 1974, 'Selective membrane for transporting sodium ion against its concentration gradient', *Journal of the American Chemical Society*, vol. 96, no. 22, pp. 7085-90.

Chrispim, M.C., Scholz, M. & Nolasco, M.A. 2019, 'Phosphorus recovery from municipal wastewater treatment: Critical review of challenges and opportunities for developing countries', *Journal of environmental management*, vol. 248, p. 109268.

Chung, T.-S., Li, X., Ong, R.C., Ge, Q., Wang, H. & Han, G. 2012, 'Emerging forward osmosis (FO) technologies and challenges ahead for clean water and clean energy applications', *Current Opinion in Chemical Engineering*, vol. 1, no. 3, pp. 246-57.

Chuntanalerg, P., Bureekaew, S., Klaysom, C., Lau, W.-J. & Faungnawakij, K. 2019, 'Nanomaterial-incorporated nanofiltration membranes for organic solvent recovery', *Advanced Nanomaterials for Membrane Synthesis and its Applications*, Elsevier, pp. 159-81.

Clara, M., Kreuzinger, N., Strenn, B., Gans, O. & Kroiss, H. 2005, 'The solids retention time—a suitable design parameter to evaluate the capacity of wastewater treatment plants to remove micropollutants', *Water Research*, vol. 39, no. 1, pp. 97-106.

Conley, D.J., Paerl, H.W., Howarth, R.W., Boesch, D.F., Seitzinger, S.P., Havens, K.E., Lancelot, C. & Likens, G.E. 2009, 'Controlling eutrophication: nitrogen and phosphorus', American Association for the Advancement of Science.

Connor, R. 2015, *The United Nations world water development report 2015: water for a sustainable world*, vol. 1, UNESCO Publishing.

Connor, R., Renata, A., Ortigara, C., Koncagül, E., Uhlenbrook, S., Lamizana-Diallo, B.M., Zadeh, S.M., Qadir, M., Kjellén, M. & Sjödin, J. 2017, 'The united nations world water development report 2017. wastewater: The untapped resource', *The United Nations World Water Development Report*.

Corapcioglu, M. & Huang, C. 1987, 'The adsorption of heavy metals onto hydrous activated carbon', *Water Research*, vol. 21, no. 9, pp. 1031-44.

Cordell, D., Drangert, J.-O. & White, S. 2009, 'The story of phosphorus: global food security and food for thought', *Global environmental change*, vol. 19, no. 2, pp. 292-305.

Cordell, D. & White, S. 2015, 'Tracking phosphorus security: indicators of phosphorus vulnerability in the global food system', *Food Security*, vol. 7, no. 2, pp. 337-50.

Cui, J. & Zhang, L. 2008, 'Metallurgical recovery of metals from electronic waste: A review', *Journal of hazardous materials*, vol. 158, no. 2, pp. 228-56.

Delahay, P. 1965, *Double layer and electrode kinetics*, John Wiley & Sons Inc.

Długołęcki, P., Anet, B., Metz, S.J., Nijmeijer, K. & Wessling, M. 2010, 'Transport limitations in ion exchange membranes at low salt concentrations', *Journal of Membrane Science*, vol. 346, no. 1, pp. 163-71.

Długołęcki, P. & van der Wal, A. 2013, 'Energy Recovery in Membrane Capacitive Deionization', *Environmental Science & Technology*, vol. 47, no. 9, pp. 4904-10.

Długołęcki, P. & van der Wal, A. 2013, 'Energy recovery in membrane capacitive deionization', *Environmental science & technology*, vol. 47, no. 9, pp. 4904-10.

Dong, Q., Guo, X., Huang, X., Liu, L., Tallon, R., Taylor, B. & Chen, J. 2019, 'Selective removal of lead ions through capacitive deionization: Role of ion-exchange membrane', *Chemical Engineering Journal*, vol. 361, pp. 1535-42.

Dorji, P., Choi, J., Kim, D.I., Phuntsho, S., Hong, S. & Shon, H.K. 2018, 'Membrane capacitive deionisation as an alternative to the 2nd pass for seawater reverse osmosis desalination plant for bromide removal', *Desalination*, vol. 433, pp. 113-9.

Duan, J. & Gregory, J. 2003, 'Coagulation by hydrolysing metal salts', *Advances in Colloid and Interface Science*, vol. 100-102, pp. 475-502.

Dykstra, J., Dijkstra, J., Van der Wal, A., Hamelers, H. & Porada, S. 2016, 'On-line method to study dynamics of ion adsorption from mixtures of salts in capacitive deionization', *Desalination*, vol. 390, pp. 47-52.

El-Bourawi, M., Khayet, M., Ma, R., Ding, Z., Li, Z. & Zhang, X. 2007, 'Application of vacuum membrane distillation for ammonia removal', *Journal of Membrane Science*, vol. 301, no. 1-2, pp. 200-9.

Elimelech, M., Gregory, J. & Jia, X. 2013, *Particle deposition and aggregation: measurement, modelling and simulation*, Butterworth-Heinemann.

Elimelech, M. & Phillip, W.A. 2011, 'The Future of Seawater Desalination: Energy, Technology, and the Environment', *Science*, vol. 333, no. 6043, pp. 712-7.

Epsztein, R., Nir, O., Lahav, O. & Green, M. 2015, 'Selective nitrate removal from groundwater using a hybrid nanofiltration–reverse osmosis filtration scheme', *Chemical Engineering Journal*, vol. 279, pp. 372-8.

EU 2002, 'Directive 2002/96/EC of the European parliament and of the council of 27 January 2003 on waste electrical and electronic equipment (WEEE) — joint declaration of the European parliament, the council and the commission relating to article 9', *Official Journal L 037, 13/02/2003*.

Evans, S., Accomazzo, M. & Accomazzo, J. 1969, 'Electrochemically Controlled Ion Exchange I. Mechanism', *Journal of the Electrochemical Society*, vol. 116, no. 2, pp. 307-9.

Evans, S. & Hamilton, W. 1966, 'The mechanism of demineralization at carbon electrodes', *Journal of the Electrochemical Society*, vol. 113, no. 12, pp. 1314-9.

Fan, C.-S., Liou, S.Y.H. & Hou, C.-H. 2017, 'Capacitive deionization of arsenic-contaminated groundwater in a single-pass mode', *Chemosphere*, vol. 184, pp. 924-31.

Fan, C.-S., Tseng, S.-C., Li, K.-C. & Hou, C.-H. 2016, 'Electro-removal of arsenic(III) and arsenic(V) from aqueous solutions by capacitive deionization', *Journal of Hazardous Materials*, vol. 312, pp. 208-15.

Fang, K., Gong, H., He, W., Peng, F., He, C. & Wang, K. 2018, 'Recovering ammonia from municipal wastewater by flow-electrode capacitive deionization', *Chemical Engineering Journal*, vol. 348, pp. 301-9.

Farmer, J.C., Bahowick, S.M., Harrar, J.E., Fix, D.V., Martinelli, R.E., Vu, A.K. & Carroll, K.L. 1997, 'Electrosorption of Chromium Ions on Carbon Aerogel Electrodes as a Means of Remediating Ground Water', *Energy & Fuels*, vol. 11, no. 2, pp. 337-47.

Feng, C., Tsai, C.-C., Ma, C.-Y., Yu, C.-P. & Hou, C.-H. 2017, 'Integrating cost-effective microbial fuel cells and energy-efficient capacitive deionization for advanced domestic wastewater treatment', *Chemical Engineering Journal*, vol. 330, pp. 1-10.

Filippelli, G.M. 2002, 'The Global Phosphorus Cycle', *Reviews in Mineralogy and Geochemistry*, vol. 48, no. 1, pp. 391-425.

Forum, W.E. 2015, 'Global Risks 2015–10th Edition'.

Fowler, D., Coyle, M., Skiba, U., Sutton, M.A., Cape, J.N., Reis, S., Sheppard, L.J., Jenkins, A., Grizzetti, B. & Galloway, J.N. 2013, 'The global nitrogen cycle in the twenty-first century', *Philosophical Transactions of the Royal Society B: Biological Sciences*, vol. 368, no. 1621, p. 20130164.

Gabelich, C.J., Tran, T.D. & Suffet, I.M. 2002, 'Electrosorption of inorganic salts from aqueous solution using carbon aerogels', *Environmental science & technology*, vol. 36, no. 13, pp. 3010-9.

Galama, A., Vermaas, D., Veerman, J., Saakes, M., Rijnaarts, H., Post, J. & Nijmeijer, K. 2014, 'Membrane resistance: The effect of salinity gradients over a cation exchange membrane', *Journal of membrane science*, vol. 467, pp. 279-91.

Gan, L., Wu, Y., Song, H., Zhang, S., Lu, C., Yang, S., Wang, Z., Jiang, B., Wang, C. & Li, A. 2019, 'Selective removal of nitrate ion using a novel activated carbon composite carbon electrode in capacitive deionization', *Separation and Purification Technology*, vol. 212, pp. 728-36.

Gao, Q., Wang, C.-Z., Liu, S., Hanigan, D., Liu, S.-T. & Zhao, H.-Z. 2019, 'Ultrafiltration membrane microreactor (MMR) for simultaneous removal of nitrate and phosphate from water', *Chemical Engineering Journal*, vol. 355, pp. 238-46.

García-Quismondo, E., Santos, C., Palma, J. & Anderson, M.A. 2016, 'On the challenge of developing wastewater treatment processes: capacitive deionization', *Desalination and Water Treatment*, vol. 57, no. 5, pp. 2315-24.

Ge, Z., Chen, X., Huang, X. & Ren, Z.J. 2018, 'Capacitive deionization for nutrient recovery from wastewater with disinfection capability', *Environmental Science: Water Research & Technology*, vol. 4, no. 1, pp. 33-9.

González, O., Bayarri, B., Aceña, J., Pérez, S. & Barceló, D. 2016, 'Treatment Technologies for Wastewater Reuse: Fate of Contaminants of Emerging Concern', in D. Fatta-Kassinos, D.D. Dionysiou & K. Kümmerer (eds), *Advanced Treatment Technologies for Urban Wastewater Reuse*, Springer International Publishing, Cham, pp. 5-37.

Gouy, M. 1910, 'Sur la constitution de la charge électrique à la surface d'un électrolyte', *J. Phys. Theor. Appl.*, vol. 9, no. 1, pp. 457-68.

Gude, V.G., Nirmalakhandan, N. & Deng, S. 2010, 'Renewable and sustainable approaches for desalination', *Renewable and Sustainable Energy Reviews*, vol. 14, no. 9, pp. 2641-54.

Guo, J., Lee, J.-G., Tan, T., Yeo, J., Wong, P.W., Ghaffour, N. & An, A.K. 2019, 'Enhanced ammonia recovery from wastewater by Nafion

membrane with highly porous honeycomb nanostructure and its mechanism in membrane distillation', *Journal of Membrane Science*, vol. 590, p. 117265.

Gwak, G., Jung, B., Han, S. & Hong, S. 2015, 'Evaluation of poly (aspartic acid sodium salt) as a draw solute for forward osmosis', *Water Research*, vol. 80, pp. 294-305.

Gwak, G., Kim, D.I. & Hong, S. 2018, 'New industrial application of forward osmosis (FO): Precious metal recovery from printed circuit board (PCB) plant wastewater', *Journal of Membrane Science*, vol. 552, pp. 234-42.

Gwak, G., Kim, D.I., Kim, J., Zhan, M. & Hong, S. 2019, 'An integrated system for CO2 capture and water treatment by forward osmosis driven by an amine-based draw solution', *Journal of Membrane Science*, vol. 581, pp. 9-17.

Hancock, N.T., Xu, P., Roby, M.J., Gomez, J.D. & Cath, T.Y. 2013, 'Towards direct potable reuse with forward osmosis: Technical assessment of long-term process performance at the pilot scale', *Journal of Membrane Science*, vol. 445, pp. 34-46.

Hanjra, M.A., Blackwell, J., Carr, G., Zhang, F. & Jackson, T.M. 2012, 'Wastewater irrigation and environmental health: Implications for water governance and public policy', *International journal of hygiene and environmental health*, vol. 215, no. 3, pp. 255-69.

Haruvy, N. 1998, 'Wastewater reuse—regional and economic considerations', *Resources, Conservation and Recycling*, vol. 23, no. 1-2, pp. 57-66.

Hassanvand, A., Chen, G.Q., Webley, P.A. & Kentish, S.E. 2017a, 'A comparison of multicomponent electrosorption in capacitive deionization and membrane capacitive deionization', *Water Res*, vol. 131, pp. 100-9.

Hassanvand, A., Chen, G.Q., Webley, P.A. & Kentish, S.E. 2017b, 'Improvement of MCDI operation and design through experiment and modelling: Regeneration with brine and optimum residence time', *Desalination*, vol. 417, pp. 36-51.

Hassanvand, A., Chen, G.Q., Webley, P.A. & Kentish, S.E. 2018, 'A comparison of multicomponent electrosorption in capacitive deionization and membrane capacitive deionization', *Water research*, vol. 131, pp. 100-9.

Hau, N.T., Chen, S.-S., Nguyen, N.C., Huang, K.Z., Ngo, H.H. & Guo, W. 2014, 'Exploration of EDTA sodium salt as novel draw solution in forward osmosis process for dewatering of high nutrient sludge', *Journal of Membrane Science*, vol. 455, pp. 305-11.

Haupt, A. & Lerch, A. 2018, 'Forward osmosis application in manufacturing industries: a short review', *Membranes*, vol. 8, no. 3, p. 47.

Hawks, S.A., Cerón, M.R., Oyarzun, D.I., Pham, T.A., Zhan, C., Loeb, C.K., Mew, D., Deinhart, A., Wood, B.C. & Santiago, J.G. 2019, 'Using ultramicroporous carbon for the selective removal of nitrate with capacitive deionization', *Environmental Science & Technology*, vol. 53, no. 18, pp. 10863-70.

Helmholtz, H.v. 1853, 'Ueber einige Gesetze der Vertheilung elektrischer Ströme in körperlichen Leitern, mit Anwendung auf die thierisch-elektrischen Versuche (Schluss.)', *Annalen der Physik*, vol. 165, no. 7, pp. 353-77.

Henze, M. & Comeau, Y. 2008, 'Wastewater characterization', *Biological wastewater treatment: Principles modelling and design*, pp. 33-52.

Hertz, H. & Franks, F. 1973, 'Water: A comprehensive treatise', *by F. Franks, Plenum Press, New York*, vol. 3.

Hoekstra, A.Y. & Wiedmann, T.O. 2014, 'Humanity's unsustainable environmental footprint', *Science*, vol. 344, no. 6188, pp. 1114-7.

Hou, C.-H. & Huang, C.-Y. 2013, 'A comparative study of electrosorption selectivity of ions by activated carbon electrodes in capacitive deionization', *Desalination*, vol. 314, pp. 124-9.

Hou, C.-H., Taboada-Serrano, P., Yiacoumi, S. & Tsouris, C. 2008a, 'Electrosorption selectivity of ions from mixtures of electrolytes inside nanopores', *The Journal of chemical physics*, vol. 129, no. 22, p. 224703.

Hou, C.-H., Taboada-Serrano, P., Yiacoumi, S. & Tsouris, C. 2008b, 'Monte Carlo simulation of electrical double-layer formation from mixtures of electrolytes inside nanopores', *The Journal of chemical physics*, vol. 128, no. 4, p. 044705.

Hu, C., Dong, J., Wang, T., Liu, R., Liu, H. & Qu, J. 2018, 'Nitrate electro-sorption/reduction in capacitive deionization using a novel Pd/NiAl-layered metal oxide film electrode', *Chemical Engineering Journal*, vol. 335, pp. 475-82.

Huang, C.-C. & He, J.-C. 2013, 'Electrosorptive removal of copper ions from wastewater by using ordered mesoporous carbon electrodes', *Chemical engineering journal*, vol. 221, pp. 469-75.

Huang, G.-H., Chen, T.-C., Hsu, S.-F., Huang, Y.-H. & Chuang, S.-H. 2014, 'Capacitive deionization (CDI) for removal of phosphate from aqueous solution', *Desalination and Water Treatment*, vol. 52, no. 4-6, pp. 759-65.

Huang, S.-Y., Fan, C.-S. & Hou, C.-H. 2014, 'Electro-enhanced removal of copper ions from aqueous solutions by capacitive deionization', *Journal of Hazardous Materials*, vol. 278, pp. 8-15.

Huang, X., He, D., Tang, W., Kovalsky, P. & Waite, T.D. 2017, 'Investigation of pH-dependent phosphate removal from wastewaters by membrane capacitive deionization (MCDI)', *Environmental Science: Water Research & Technology*, vol. 3, no. 5, pp. 875-82.

Huang, Z., Lu, L., Cai, Z. & Ren, Z.J. 2016, 'Individual and competitive removal of heavy metals using capacitive deionization', *Journal of Hazardous Materials*, vol. 302, pp. 323-31.

Huertas, E., Herzberg, M., Oron, G. & Elimelech, M. 2008, 'Influence of biofouling on boron removal by nanofiltration and reverse osmosis membranes', *Journal of Membrane Science*, vol. 318, no. 1-2, pp. 264-70.

Jande, Y.A.C., Minhas, M.B. & Kim, W.S. 2015, 'Ultrapure water from seawater using integrated reverse osmosis-capacitive deionization system', *Desalination and Water Treatment*, vol. 53, no. 13, pp. 3482-90.

Jeon, S.-i., Yeo, J.-g., Yang, S., Choi, J. & Kim, D.K. 2014, 'Ion storage and energy recovery of a flow-electrode capacitive deionization process', *Journal of Materials Chemistry A*, vol. 2, no. 18, pp. 6378-83.

Jia, B. & Zou, L. 2012, 'Graphene nanosheets reduced by a multi-step process as high-performance electrode material for capacitive deionisation', *Carbon*, vol. 50, no. 6, pp. 2315-21.

Jiang, J., Kim, D.I., Dorji, P., Phuntsho, S., Hong, S. & Shon, H.K. 2019a, 'Phosphorus removal mechanisms from domestic wastewater by membrane capacitive deionization and system optimization for enhanced phosphate removal', *Process Safety and Environmental Protection*, vol. 126, pp. 44-52.

Jiang, J., Kim, D.I., Dorji, P., Phuntsho, S., Hong, S. & Shon, H.K. 2019b, 'Phosphorus removal mechanisms from domestic wastewater by membrane capacitive deionization and system optimization for enhanced phosphate removal', *Process Safety and Environmental Protection*.

Johir, M., George, J., Vigneswaran, S., Kandasamy, J. & Grasmick, A. 2011, 'Removal and recovery of nutrients by ion exchange from high rate membrane bio-reactor (MBR) effluent', *Desalination*, vol. 275, no. 1-3, pp. 197-202.

Johnson, A. & Newman, J. 1971a, 'Desalting by means of porous carbon electrodes', *Journal of the Electrochemical Society*, vol. 118, no. 3, pp. 510-7.

Johnson, A., Venolia, A., Newman, J., Wilbourne, R., Wong, C., Gillam, W., Johnson, S. & Horowitz, R. 1970, 'Electrosorb process for desalting water, Office of Saline Water Research and Development', *Progress Report No 516, US Department of the Interior, Publication 200 056*.

Johnson, A.M. & Newman, J. 1971b, 'Desalting by Means of Porous Carbon Electrodes', *Journal of The Electrochemical Society*, vol. 118, no. 3, pp. 510-7.

Kang, C., Li, W., Tan, L., Li, H., Wei, C. & Tang, Y. 2013, 'Highly ordered metal ion imprinted mesoporous silica particles exhibiting

specific recognition and fast adsorption kinetics', *Journal of Materials Chemistry A*, vol. 1, no. 24, pp. 7147-53.

Kang, J., Kim, T., Shin, H., Lee, J., Ha, J.-I. & Yoon, J. 2016, 'Direct energy recovery system for membrane capacitive deionization', *Desalination*, vol. 398, pp. 144-50.

Karamati-Niaragh, E., Alavi Moghaddam, M.R., Emamjomeh, M.M. & Nazlabadi, E. 2019, 'Evaluation of direct and alternating current on nitrate removal using a continuous electrocoagulation process: Economical and environmental approaches through RSM', *Journal of Environmental Management*, vol. 230, pp. 245-54.

Kim, D., Dorji, P., Gwak, G., Phuntsho, S., Hong, S. & Shon, H. 2019a, 'Effect of Brine Water on Discharge of Cations in Membrane Capacitive Deionization and its Implications on Nitrogen Recovery from Wastewater', *ACS Sustainable Chemistry & Engineering*.

Kim, D., Gwak, G., Dorji, P., He, D., Phuntsho, S., Hong, S. & Shon, H. 2017a, 'Palladium recovery through membrane capacitive deionization (MCDI) from metal plating wastewater', *ACS Sustainable Chemistry & Engineering*.

Kim, D.I., Dorji, P., Gwak, G., Phuntsho, S., Hong, S. & Shon, H. 2019b, 'Reuse of municipal wastewater via membrane capacitive deionization using ion-selective polymer-coated carbon electrodes in pilot-scale', *Chemical Engineering Journal*, vol. 372, pp. 241-50.

Kim, D.I., Dorji, P., Gwak, G., Phuntsho, S., Hong, S. & Shon, H. 2019c, 'Reuse of municipal wastewater via membrane capacitive deionization using ion-selective polymer-coated carbon electrodes in pilot-scale', *Chemical Engineering Journal*.

Kim, D.I., Gwak, G., Dorji, P., He, D., Phuntsho, S., Hong, S. & Shon, H. 2017b, 'Palladium Recovery through Membrane Capacitive Deionization from Metal Plating Wastewater', *ACS Sustainable Chemistry & Engineering*, vol. 6, no. 2, pp. 1692-701.

Kim, D.I., Gwak, G., Dorji, P., He, D., Phuntsho, S., Hong, S. & Shon, H. 2018, 'Palladium Recovery through Membrane Capacitive Deionization from Metal Plating Wastewater', *ACS Sustainable Chemistry & Engineering*, vol. 6, no. 2, pp. 1692-701.

Kim, D.I., Kim, J. & Hong, S. 2016, 'Changing membrane orientation in pressure retarded osmosis for sustainable power generation with low fouling', *Desalination*, vol. 389, pp. 197-206.

Kim, J.-S. & Choi, J.-H. 2010a, 'Fabrication and characterization of a carbon electrode coated with cation-exchange polymer for the membrane capacitive deionization applications', *Journal of membrane science*, vol. 355, no. 1-2, pp. 85-90.

Kim, J.S., Kim, C.S., Shin, H.S. & Rhim, J.W. 2015, 'Application of synthesized anion and cation exchange polymers to membrane capacitive deionization (MCDI)', *Macromol. Res*, vol. 23, no. 4, pp. 360-6.

Kim, S., Eichhorn, P., Jensen, J.N., Weber, A.S. & Aga, D.S. 2005, 'Removal of Antibiotics in Wastewater: Effect of Hydraulic and Solid Retention Times on the Fate of Tetracycline in the Activated Sludge Process', *Environmental Science & Technology*, vol. 39, no. 15, pp. 5816-23.

Kim, S., Yoon, H., Shin, D., Lee, J. & Yoon, J. 2017, 'Electrochemical selective ion separation in capacitive deionization with sodium manganese oxide', *Journal of Colloid and Interface Science*, vol. 506, pp. 644-8.

Kim, Y.-J. & Choi, J.-H. 2010b, 'Enhanced desalination efficiency in capacitive deionization with an ion-selective membrane', *Separation and Purification Technology*, vol. 71, no. 1, pp. 70-5.

Kim, Y.-J. & Choi, J.-H. 2010c, 'Improvement of desalination efficiency in capacitive deionization using a carbon electrode coated with an ion-exchange polymer', *Water research*, vol. 44, no. 3, pp. 990-6.

Kim, Y.-J. & Choi, J.-H. 2012, 'Selective removal of nitrate ion using a novel composite carbon electrode in capacitive deionization', *Water research*, vol. 46, no. 18, pp. 6033-9.

Kim, Y.-J., Kim, J.-H. & Choi, J.-H. 2013, 'Selective removal of nitrate ions by controlling the applied current in membrane capacitive deionization (MCDI)', *Journal of membrane science*, vol. 429, pp. 52-7.

Kimura, K., Hara, H. & Watanabe, Y. 2007, 'Elimination of Selected Acidic Pharmaceuticals from Municipal Wastewater by an Activated Sludge System and Membrane Bioreactors', *Environmental Science & Technology*, vol. 41, no. 10, pp. 3708-14.

Koparal, A.S. & Öğütveren, Ü.B. 2002, 'Removal of nitrate from water by electroreduction and electrocoagulation', *Journal of Hazardous Materials*, vol. 89, no. 1, pp. 83-94.

Kotoski, J.E. 1997, *Information on Phosphorus Amounts & Water Quality*, viewed 03 January 2018, <http://osse.ssec.wisc.edu/curriculum/earth/Minifact2_Phosphorus.pdf>.

Lado, J.J., Pérez-Roa, R.E., Wouters, J.J., Isabel Tejedor-Tejedor, M. & Anderson, M.A. 2014, 'Evaluation of operational parameters for a capacitive deionization reactor employing asymmetric electrodes', *Separation and Purification Technology*, vol. 133, pp. 236-45.

Lado, J.J., Pérez-Roa, R.E., Wouters, J.J., Tejedor-Tejedor, M.I., Federspill, C., Ortiz, J.M. & Anderson, M.A. 2017, 'Removal of nitrate by asymmetric capacitive deionization', *Separation and Purification Technology*, vol. 183, pp. 145-52.

Lay, W.C., Chong, T.H., Tang, C.Y., Fane, A.G., Zhang, J. & Liu, Y. 2010, 'Fouling propensity of forward osmosis: investigation of the slower flux decline phenomenon', *Water science and technology*, vol. 61, no. 4, pp. 927-36.

Ledezma, P., Kuntke, P., Buisman, C.J., Keller, J. & Freguia, S. 2015, 'Source-separated urine opens golden opportunities for microbial electrochemical technologies', *Trends in Biotechnology*, vol. 33, no. 4, pp. 214-20.

Lee, J.-H., Bae, W.-S. & Choi, J.-H. 2010, 'Electrode reactions and adsorption/desorption performance related to the applied

potential in a capacitive deionization process', *Desalination*, vol. 258, no. 1, pp. 159-63.

Lee, J.-Y., Seo, S.-J., Yun, S.-H. & Moon, S.-H. 2011, 'Preparation of ion exchanger layered electrodes for advanced membrane capacitive deionization (MCDI)', *Water Research*, vol. 45, no. 17, pp. 5375-80.

Lee, S., Boo, C., Elimelech, M. & Hong, S. 2010, 'Comparison of fouling behavior in forward osmosis (FO) and reverse osmosis (RO)', *Journal of Membrane Science*, vol. 365, no. 1-2, pp. 34-9.

Levich, V.G.e. 1962, 'Physicochemical hydrodynamics'.

Li, H., Zou, L., Pan, L. & Sun, Z. 2010, 'Novel Graphene-Like Electrodes for Capacitive Deionization', *Environmental Science & Technology*, vol. 44, no. 22, pp. 8692-7.

Li, Y., Zhang, C., Jiang, Y., Wang, T.-J. & Wang, H. 2016, 'Effects of the hydration ratio on the electrosorption selectivity of ions during capacitive deionization', *Desalination*, vol. 399, pp. 171-7.

Liang, P., Sun, X., Bian, Y., Zhang, H., Yang, X., Jiang, Y., Liu, P. & Huang, X. 2017, 'Optimized desalination performance of high voltage flow-electrode capacitive deionization by adding carbon black in flow-electrode', *Desalination*, vol. 420, no. Supplement C, pp. 63-9.

Liang, P., Yuan, L., Yang, X., Zhou, S. & Huang, X. 2013, 'Coupling ion-exchangers with inexpensive activated carbon fiber electrodes to enhance the performance of capacitive deionization cells for domestic wastewater desalination', *Water research*, vol. 47, no. 7, pp. 2523-30.

Liberti, L., Boari, G., Petruzzelli, D. & Passino, R. 1981, 'Nutrient removal and recovery from wastewater by ion exchange', *Water Research*, vol. 15, no. 3, pp. 337-42.

Lindstrand, V., Sundström, G. & Jönsson, A.-S. 2000, 'Fouling of electrodialysis membranes by organic substances', *Desalination*, vol. 128, no. 1, pp. 91-102.

Liu, P., Yan, T., Zhang, J., Shi, L. & Zhang, D. 2017, 'Separation and recovery of heavy metal ions and salt ions from wastewater by

3D graphene-based asymmetric electrodes via capacitive deionization', *Journal of Materials Chemistry A*, vol. 5, no. 28, pp. 14748-57.

Liu, Y., Nie, C., Liu, X., Xu, X., Sun, Z. & Pan, L. 2015, 'Review on carbon-based composite materials for capacitive deionization', *Rsc Advances*, vol. 5, no. 20, pp. 15205-25.

Liu, Y., Pan, L., Xu, X., Lu, T., Sun, Z. & Chua, D.H. 2014, 'Enhanced desalination efficiency in modified membrane capacitive deionization by introducing ion-exchange polymers in carbon nanotubes electrodes', *Electrochimica Acta*, vol. 130, pp. 619-24.

Luo, T., Abdu, S. & Wessling, M. 2018a, 'Selectivity of ion exchange membranes: A review', *Journal of membrane science*, vol. 555, pp. 429-54.

Luo, T., Abdu, S. & Wessling, M. 2018b, 'Selectivity of ion exchange membranes: A review', *Journal of Membrane Science*.

Macías, C., Lavela, P., Rasines, G., Zafra, M., Tirado, J. & Ania, C. 2014, 'Improved electro-assisted removal of phosphates and nitrates using mesoporous carbon aerogels with controlled porosity', *Journal of Applied Electrochemistry*, vol. 44, no. 8, pp. 963-76.

Majumdar, D. & Gupta, N. 2000, 'Nitrate pollution of groundwater and associated human health disorders', *Indian journal of environmental health*, vol. 42, no. 1, pp. 28-39.

Mateo-Sagasta, J., Raschid-Sally, L. & Thebo, A. 2015, 'Global wastewater and sludge production, treatment and use', *Wastewater*, Springer, pp. 15-38.

Matsubae, K., Yamasue, E., Inazumi, T., Webeck, E., Miki, T. & Nagasaka, T. 2016, 'Innovations in steelmaking technology and hidden phosphorus flows', *Science of The Total Environment*, vol. 542, pp. 1162-8.

Maurer, M., Escher, B.I., Richle, P., Schaffner, C. & Alder, A.C. 2007, 'Elimination of β-blockers in sewage treatment plants', *Water Research*, vol. 41, no. 7, pp. 1614-22.

Maurer, M., Pronk, W. & Larsen, T. 2006, 'Treatment processes for source-separated urine', *Water research*, vol. 40, no. 17, pp. 3151-66.

Mayer, B.K., Baker, L.A., Boyer, T.H., Drechsel, P., Gifford, M., Hanjra, M.A., Parameswaran, P., Stoltzfus, J., Westerhoff, P. & Rittmann, B.E. 2016, 'Total value of phosphorus recovery', *Environmental science & technology*, vol. 50, no. 13, pp. 6606-20.

Mekonnen, M.M. & Hoekstra, A.Y. 2016, 'Four billion people facing severe water scarcity', *Science advances*, vol. 2, no. 2, p. e1500323.

Mendow, G., Veizaga, N.S., Querini, C.A. & Sánchez, B.S. 2019, 'A continuous process for the catalytic reduction of water nitrate', *Journal of Environmental Chemical Engineering*, vol. 7, no. 1, p. 102808.

Menkouchi Sahli, M.A., Annouar, S., Mountadar, M., Soufiane, A. & Elmidaoui, A. 2008, 'Nitrate removal of brackish underground water by chemical adsorption and by electrodialysis', *Desalination*, vol. 227, no. 1, pp. 327-33.

Mew, M. 2016, 'Phosphate rock costs, prices and resources interaction', *Science of the Total Environment*, vol. 542, pp. 1008-12.

Miller, G.W. 2006, 'Integrated concepts in water reuse: managing global water needs', *Desalination*, vol. 187, no. 1-3, pp. 65-75.

Minhas, M.B., Jande, Y.A.C. & Kim, W.S. 2014, 'Combined reverse osmosis and constant-current operated capacitive deionization system for seawater desalination', *Desalination*, vol. 344, pp. 299-305.

Mogens Henze, Y.C. 2008, '3-Wastewater Characterization ', *Biological Wastewater Treatment: Principles, Modelling and Design* IWA Publishing.

Mohammed, S.A. & Shanshool, H.A. 2009, 'Phosphorus removal from water and waste water by chemical precipitation using alum and calcium chloride', *Iraqi Journal of Chemical and Petroleum Engineering*, vol. 10, no. 2, pp. 35-42.

Molden, D. 2013, *Water for food water for life: A comprehensive assessment of water management in agriculture*, Routledge.

Mondor, M., Ippersiel, D., Lamarche, F. & Masse, L. 2009, 'Fouling characterization of electrodialysis membranes used for the recovery and concentration of ammonia from swine manure', *Bioresource technology*, vol. 100, no. 2, pp. 566-71.

Mossad, M. & Zou, L. 2012, 'A study of the capacitive deionisation performance under various operational conditions', *Journal of hazardous materials*, vol. 213, pp. 491-7.

Mossad, M. & Zou, L. 2013, 'Study of fouling and scaling in capacitive deionisation by using dissolved organic and inorganic salts', *Journal of hazardous materials*, vol. 244, pp. 387-93.

Murphy, G. & Caudle, D. 1967, 'Mathematical theory of electrochemical demineralization in flowing systems', *Electrochimica Acta*, vol. 12, no. 12, pp. 1655-64.

Musfique, A., Hasan, C.K., Hafizur, R., Hossain, M.A. & Uddin, S.A. 2015, 'Prospects of using wastewater as a resource-nutrient recovery and energy generation', *American Journal of Environmental Sciences*, vol. 11, no. 2, pp. 99-114.

Namasivayam, C. & Kadirvelu, K. 1997, 'Agricultural solid wastes for the removal of heavy metals: adsorption of Cu (II) by coirpith carbon', *Chemosphere*, vol. 34, no. 2, pp. 377-99.

Nations, U. 2015a, 'Transforming our world: The 2030 agenda for sustainable development', *Resolution adopted by the General Assembly*.

Nations, U. 2015b, 'World population prospects: The 2015 revision', *United Nations Econ Soc Aff*, vol. 33, no. 2, pp. 1-66.

Nghiem, L.D., Tadkaew, N. & Sivakumar, M. 2009, 'Removal of trace organic contaminants by submerged membrane bioreactors', *Desalination*, vol. 236, no. 1, pp. 127-34.

Nguyen, T.-T., Kook, S., Lee, C., Field, R.W. & Kim, I.S. 2019, 'Critical flux-based membrane fouling control of forward osmosis: Behavior,

sustainability, and reversibility', *Journal of membrane science*, vol. 570, pp. 380-93.

Nie, C., Pan, L., Liu, Y., Li, H., Chen, T., Lu, T. & Sun, Z. 2012, 'Electrophoretic deposition of carbon nanotubes–polyacrylic acid composite film electrode for capacitive deionization', *Electrochimica Acta*, vol. 66, pp. 106-9.

Niewersch, C., Bloch, A.B., Yüce, S., Melin, T. & Wessling, M. 2014, 'Nanofiltration for the recovery of phosphorus—Development of a mass transport model', *Desalination*, vol. 346, pp. 70-8.

Nightingale Jr, E. 1959, 'Phenomenological theory of ion solvation. Effective radii of hydrated ions', *The Journal of Physical Chemistry*, vol. 63, no. 9, pp. 1381-7.

O'Flaherty, E. & Gray, N. 2013, 'A comparative analysis of the characteristics of a range of real and synthetic wastewaters', *Environmental Science and Pollution Research*, vol. 20, no. 12, pp. 8813-30.

Oladunni, J., Zain, J., Hai, A., Banat, F., Bharath, G. & Alhseinat, E. 2018, 'A comprehensive review on recently developed carbon based nanocomposites for capacitive deionization: from theory to practice', *Separation and Purification Technology*.

Oren, Y. 2008a, 'Capacitive deionization (CDI) for desalination and water treatment—past, present and future (a review)', *Desalination*, vol. 228, no. 1-3, pp. 10-29.

Oren, Y. 2008b, 'Capacitive deionization (CDI) for desalination and water treatment — past, present and future (a review)', *Desalination*, vol. 228, no. 1, pp. 10-29.

Palakkal, V.M., Rubio, J.E., Lin, Y.J. & Arges, C.G. 2018, 'Low-Resistant Ion-Exchange Membranes for Energy Efficient Membrane Capacitive Deionization', *ACS Sustainable Chemistry & Engineering*, vol. 6, no. 11, pp. 13778-86.

Palko, J.W., Oyarzun, D.I., Ha, B., Stadermann, M. & Santiago, J.G. 2018, 'Nitrate removal from water using electrostatic regeneration of

functionalized adsorbent', *Chemical Engineering Journal*, vol. 334, pp. 1289-96.

Pan, L., Wang, X., Gao, Y., Zhang, Y., Chen, Y. & Sun, Z. 2009, 'Electrosorption of anions with carbon nanotube and nanofibre composite film electrodes', *Desalination*, vol. 244, no. 1, pp. 139-43.

Park, J.Y. & Yoo, Y.J. 2009, 'Biological nitrate removal in industrial wastewater treatment: which electron donor we can choose', *Applied Microbiology and Biotechnology*, vol. 82, no. 3, pp. 415-29.

Park, M.J., Gonzales, R.R., Abdel-Wahab, A., Phuntsho, S. & Shon, H.K. 2018, 'Hydrophilic polyvinyl alcohol coating on hydrophobic electrospun nanofiber membrane for high performance thin film composite forward osmosis membrane', *Desalination*, vol. 426, pp. 50-9.

Park, M.J., Lim, S., Gonzales, R.R., Phuntsho, S., Han, D.S., Abdel-Wahab, A., Adham, S. & Shon, H.K. 2019, 'Thin-film composite hollow fiber membranes incorporated with graphene oxide in polyethersulfone support layers for enhanced osmotic power density', *Desalination*, vol. 464, pp. 63-75.

Pekala, R., Farmer, J., Alviso, C., Tran, T., Mayer, S., Miller, J. & Dunn, B. 1998, 'Carbon aerogels for electrochemical applications', *Journal of non-crystalline solids*, vol. 225, pp. 74-80.

Penuelas, J., Poulter, B., Sardans, J., Ciais, P., Van Der Velde, M., Bopp, L., Boucher, O., Godderis, Y., Hinsinger, P. & Llusia, J. 2013, 'Human-induced nitrogen–phosphorus imbalances alter natural and managed ecosystems across the globe', *Nature Communications*, vol. 4.

Picioreanu, C., Van Loosdrecht, M. & Heijnen, J. 1997, 'Modelling the effect of oxygen concentration on nitrite accumulation in a biofilm airlift suspension reactor', *Water Science and Technology*, vol. 36, no. 1, pp. 147-56.

Pillai, K.C., Chung, S.J. & Moon, I.-S. 2008, 'Studies on electrochemical recovery of silver from simulated waste water from Ag (II)/Ag

(I) based mediated electrochemical oxidation process', *Chemosphere*, vol. 73, no. 9, pp. 1505-11.

Poisson, A. & Papaud, A. 1983, 'Diffusion coefficients of major ions in seawater', *Marine Chemistry*, vol. 13, no. 4, pp. 265-80.

Porada, S., Bryjak, M., Van Der Wal, A. & Biesheuvel, P. 2012a, 'Effect of electrode thickness variation on operation of capacitive deionization', *Electrochimica Acta*, vol. 75, pp. 148-56.

Porada, S., Bryjak, M., van der Wal, A. & Biesheuvel, P.M. 2012b, 'Effect of electrode thickness variation on operation of capacitive deionization', *Electrochimica Acta*, vol. 75, pp. 148-56.

Porada, S., Weinstein, L., Dash, R., Van Der Wal, A., Bryjak, M., Gogotsi, Y. & Biesheuvel, P. 2012, 'Water desalination using capacitive deionization with microporous carbon electrodes', *ACS applied materials & interfaces*, vol. 4, no. 3, pp. 1194-9.

Porada, S., Zhao, R., Van Der Wal, A., Presser, V. & Biesheuvel, P. 2013a, 'Review on the science and technology of water desalination by capacitive deionization', *Progress in Materials Science*, vol. 58, no. 8, pp. 1388-442.

Porada, S., Zhao, R., van der Wal, A., Presser, V. & Biesheuvel, P.M. 2013b, 'Review on the science and technology of water desalination by capacitive deionization', *Progress in Materials Science*, vol. 58, no. 8, pp. 1388-442.

Prior, T., Giurco, D., Mudd, G., Mason, L. & Behrisch, J. 2012, 'Resource depletion, peak minerals and the implications for sustainable resource management', *Global Environmental Change*, vol. 22, no. 3, pp. 577-87.

Pronk, W., Biebow, M. & Boller, M. 2006, 'Electrodialysis for recovering salts from a urine solution containing micropollutants', *Environmental science & technology*, vol. 40, no. 7, pp. 2414-20.

Pronk, W., Palmquist, H., Biebow, M. & Boller, M. 2006, 'Nanofiltration for the separation of pharmaceuticals from nutrients in source-separated urine', *Water Research*, vol. 40, no. 7, pp. 1405-12.

Qu, D., Sun, D., Wang, H. & Yun, Y. 2013, 'Experimental study of ammonia removal from water by modified direct contact membrane distillation', *Desalination*, vol. 326, pp. 135-40.

Rana-Madaria, P., Nagarajan, M., Rajagopal, C. & Garg, B.S. 2005, 'Removal of Chromium from Aqueous Solutions by Treatment with Carbon Aerogel Electrodes Using Response Surface Methodology', *Industrial & Engineering Chemistry Research*, vol. 44, no. 17, pp. 6549-59.

Ruiz, J., Álvarez-Díaz, P., Arbib, Z., Garrido-Pérez, C., Barragán, J. & Perales, J. 2013, 'Performance of a flat panel reactor in the continuous culture of microalgae in urban wastewater: prediction from a batch experiment', *Bioresource technology*, vol. 127, pp. 456-63.

Ryu, T., Lee, D.-H., Ryu, J.C., Shin, J., Chung, K.-S. & Kim, Y.H. 2015, 'Lithium recovery system using electrostatic field assistance', *Hydrometallurgy*, vol. 151, pp. 78-83.

Ryu, T., Ryu, J.C., Shin, J., Lee, D.H., Kim, Y.H. & Chung, K.-S. 2013, 'Recovery of lithium by an electrostatic field-assisted desorption process', *Industrial & Engineering Chemistry Research*, vol. 52, no. 38, pp. 13738-42.

Sales, B., Saakes, M., Post, J., Buisman, C., Biesheuvel, P. & Hamelers, H. 2010, 'Direct power production from a water salinity difference in a membrane-modified supercapacitor flow cell', *Environmental science & technology*, vol. 44, no. 14, pp. 5661-5.

Sata, T. 2000, 'Studies on anion exchange membranes having permselectivity for specific anions in electrodialysis—effect of hydrophilicity of anion exchange membranes on permselectivity of anions', *Journal of Membrane Science*, vol. 167, no. 1, pp. 1-31.

Sata, T. 2007, *Ion exchange membranes: preparation, characterization, modification and application*, Royal Society of chemistry.

Schoeman, J.J. & Steyn, A. 2003, 'Nitrate removal with reverse osmosis in a rural area in South Africa', *Desalination*, vol. 155, no. 1, pp. 15-26.

Senthil Kumar, P., Yaashikaa, P.R. & Ramalingam, S. 2019, 'Efficient Removal of Nitrate and Phosphate Using Graphene Nanocomposites', in M. Naushad (ed.), *A New Generation Material Graphene: Applications in Water Technology*, Springer International Publishing, Cham, pp. 287-307.

Seo, S.-J., Jeon, H., Lee, J.K., Kim, G.-Y., Park, D., Nojima, H., Lee, J. & Moon, S.-H. 2010, 'Investigation on removal of hardness ions by capacitive deionization (CDI) for water softening applications', *Water Research*, vol. 44, no. 7, pp. 2267-75.

Shanbhag, S., Bootwala, Y., Whitacre, J.F. & Mauter, M.S. 2017, 'Ion Transport and Competition Effects on NaTi2(PO4)3 and Na4Mn9O18 Selective Insertion Electrode Performance', *Langmuir*, vol. 33, no. 44, pp. 12580-91.

Shannon, M.A., Bohn, P.W., Elimelech, M., Georgiadis, J.G., Marinas, B.J. & Mayes, A.M. 2008, 'Science and technology for water purification in the coming decades', *Nature*, vol. 452, no. 7185, pp. 301-10.

Shirazi, A., Mahdi, M. & Kargari, A. 2015, 'A review on applications of membrane distillation (MD) process for wastewater treatment', *Journal of Membrane Science and Research*, vol. 1, no. 3, pp. 101-12.

Smith, D.P. & Smith, N.T. 2015, 'Anaerobic-ion exchange (AN-IX) process for local-scale nitrogen recovery from wastewater', *Bioresource technology*, vol. 196, pp. 324-31.

Stern, O. 1924, 'Zur theorie der elektrolytischen doppelschicht', *Zeitschrift für Elektrochemie und angewandte physikalische Chemie*, vol. 30, no. 21-22, pp. 508-16.

Strathmann, H. 2004, *Ion-exchange membrane separation processes*, Elsevier.

Strom, P.F. August 2006, *Technologies to Remove Phosphorus from Wastewater* viewed 3 January 2018, <http://www.water.rutgers.edu/Projects/trading/p-trt-lit-rev-2a.pdf>.

Suss, M., Porada, S., Sun, X., Biesheuvel, P., Yoon, J. & Presser, V. 2015, 'Water desalination via capacitive deionization: what is it and what can we expect from it?', *Energy & Environmental Science*, vol. 8, no. 8, pp. 2296-319.

Suss, M.E. 2017, 'Size-based ion selectivity of micropore electric double layers in capacitive deionization electrodes', *Journal of The Electrochemical Society*, vol. 164, no. 9, pp. E270-E5.

Suss, M.E., Baumann, T.F., Bourcier, W.L., Spadaccini, C.M., Rose, K.A., Santiago, J.G. & Stadermann, M. 2012, 'Capacitive desalination with flow-through electrodes', *Energy & Environmental Science*, vol. 5, no. 11, pp. 9511-9.

Tanaka, Y. 2007, 'Chapter 3 Bipolar Membrane Electrodialysis', in Y. Tanaka (ed.), *Membrane Science and Technology*, vol. 12, Elsevier, pp. 405-36.

Tang, W., He, D., Zhang, C., Kovalsky, P. & Waite, T.D. 2017, 'Comparison of Faradaic reactions in capacitive deionization (CDI) and membrane capacitive deionization (MCDI) water treatment processes', *Water research*, vol. 120, pp. 229-37.

Tang, W., He, D., Zhang, C. & Waite, T.D. 2017, 'Optimization of sulfate removal from brackish water by membrane capacitive deionization (MCDI)', *Water research*, vol. 121, pp. 302-10.

Tang, W., Kovalsky, P., He, D. & Waite, T.D. 2015, 'Fluoride and nitrate removal from brackish groundwaters by batch-mode capacitive deionization', *Water Research*, vol. 84, pp. 342-9.

Tilton, J.E. 2003, 'Assessing the threat of mineral depletion', *Minerals and Energy-Raw Materials Report*, vol. 18, no. 1, pp. 33-42.

Toifl, M., Bulteau, G., Diaper, C. & O'Halloran, R. 2014, 'Greywater recycling: Guidelines for safe adoption', *Alternative Water Supply Systems*, p. 217.

Tran, A.T., Zhang, Y., Lin, J., Mondal, P., Ye, W., Meesschaert, B., Pinoy, L. & Van der Bruggen, B. 2015, 'Phosphate pre-concentration from municipal wastewater by selectrodialysis: Effect of competing

components', *Separation and Purification Technology*, vol. 141, pp. 38-47.

Tuan, T.N., Chung, S., Lee, J.K. & Lee, J. 2015, 'Improvement of water softening efficiency in capacitive deionization by ultra purification process of reduced graphene oxide', *Current Applied Physics*, vol. 15, no. 11, pp. 1397-401.

Uzun, H.I. & Debik, E. 2019, 'Economical approach to nitrate removal via membrane capacitive deionization', *Separation and Purification Technology*, vol. 209, pp. 776-81.

van der Salm, C., Kros, J. & de Vries, W. 2016, 'Evaluation of different approaches to describe the sorption and desorption of phosphorus in soils on experimental data', *Science of the Total Environment*, vol. 571, pp. 292-306.

van Limpt, B. & van der Wal, A. 2014, 'Water and chemical savings in cooling towers by using membrane capacitive deionization', *Desalination*, vol. 342, pp. 148-55.

Vieno, N.M., Tuhkanen, T. & Kronberg, L. 2005, 'Seasonal Variation in the Occurrence of Pharmaceuticals in Effluents from a Sewage Treatment Plant and in the Recipient Water', *Environmental Science & Technology*, vol. 39, no. 21, pp. 8220-6.

Vörösmarty, C.J., Green, P., Salisbury, J. & Lammers, R.B. 2000, 'Global water resources: vulnerability from climate change and population growth', *science*, vol. 289, no. 5477, pp. 284-8.

Wang, C., Song, H., Zhang, Q., Wang, B. & Li, A. 2015, 'Parameter optimization based on capacitive deionization for highly efficient desalination of domestic wastewater biotreated effluent and the fouled electrode regeneration', *Desalination*, vol. 365, pp. 407-15.

Wang, H. & Na, C. 2014, 'Binder-free carbon nanotube electrode for electrochemical removal of chromium', *ACS applied materials & interfaces*, vol. 6, no. 22, pp. 20309-16.

WANG, L., YU, F. & MA, J. 2017, 'Design and Construction of Graphene-Based Electrode Materials for Capacitive Deionization', *Acta Physico-Chimica Sinica*, vol. 33, no. 7, pp. 1338-53.

Wang, X., Wang, Y., Zhang, X., Feng, H., Li, C. & Xu, T. 2013, 'Phosphate recovery from excess sludge by conventional electrodialysis (CED) and electrodialysis with bipolar membranes (EDBM)', *Industrial & Engineering Chemistry Research*, vol. 52, no. 45, pp. 15896-904.

Wang, Z., Gong, H., Zhang, Y., Liang, P. & Wang, K. 2017, 'Nitrogen recovery from low-strength wastewater by combined membrane capacitive deionization (MCDI) and ion exchange (IE) process', *Chemical Engineering Journal*, vol. 316, pp. 1-6.

Water, U. 2014, 'The United Nations world water development report 2014: water and energy', *United Nations, Paris*.

Watsuntorn, W., Ruangchainikom, C., Rene, E.R., Lens, P.N.L. & Chulalaksananukul, W. 2019, 'Comparison of sulphide and nitrate removal from synthetic wastewater by pure and mixed cultures of nitrate-reducing, sulphide-oxidizing bacteria', *Bioresource Technology*, vol. 272, pp. 40-7.

Wilkinson, G.M. 2017, 'Eutrophication of Freshwater and Coastal Ecosystems ', *Encyclopedia of Sustainable Technologies*, Elsevier, Oxford, pp. 145-52.

Wimalasiri, Y., Mossad, M. & Zou, L. 2015, 'Thermodynamics and kinetics of adsorption of ammonium ions by graphene laminate electrodes in capacitive deionization', *Desalination*, vol. 357, pp. 178-88.

Wouters, J.J., Tejedor-Tejedor, M.I., Lado, J.J., Perez-Roa, R. & Anderson, M.A. 2018, 'Influence of Metal Oxide Coatings, Carbon Materials and Potentials on Ion Removal in Capacitive Deionization', *Journal of The Electrochemical Society*, vol. 165, no. 5, pp. E148-E61.

WWAP, U. 2012, 'World Water Assessment Programme: The United Nations World Water Development Report 4: Managing Water under Uncertainty and Risk', Paris: UNESCO.

Xiao, K., Wang, X., Huang, X., Waite, T.D. & Wen, X. 2011, 'Combined effect of membrane and foulant hydrophobicity and surface

charge on adsorptive fouling during microfiltration', *Journal of Membrane Science*, vol. 373, no. 1-2, pp. 140-51.

Xie, M., Nghiem, L.D., Price, W.E. & Elimelech, M. 2013, 'A forward osmosis–membrane distillation hybrid process for direct sewer mining: system performance and limitations', *Environmental science & technology*, vol. 47, no. 23, pp. 13486-93.

Xie, M., Nghiem, L.D., Price, W.E. & Elimelech, M. 2014, 'Toward resource recovery from wastewater: extraction of phosphorus from digested sludge using a hybrid forward osmosis–membrane distillation process', *Environmental Science & Technology Letters*, vol. 1, no. 2, pp. 191-5.

Xie, Z., Duong, T., Hoang, M., Nguyen, C. & Bolto, B. 2009, 'Ammonia removal by sweep gas membrane distillation', *Water research*, vol. 43, no. 6, pp. 1693-9.

Xu, P., Drewes, J.E., Heil, D. & Wang, G. 2008, 'Treatment of brackish produced water using carbon aerogel-based capacitive deionization technology', *Water research*, vol. 42, no. 10-11, pp. 2605-17.

Yang, L., Shi, Z. & Yang, W. 2014, 'Enhanced capacitive deionization of lead ions using air-plasma treated carbon nanotube electrode', *Surface and Coatings Technology*, vol. 251, pp. 122-7.

Yao, Q. & Tang, H.L. 2017, 'Effect of Desorption Methods on Electrode Regeneration Performance of Capacitive Deionization', *Journal of Environmental Engineering*, vol. 143, no. 9, p. 04017047.

Yazici, E. & Deveci, H. 2009, 'Recovery of metals from E-wastes', *Madencilik*, vol. 48, no. 3, pp. 3-18.

Yeo, J.-H. & Choi, J.-H. 2013, 'Enhancement of nitrate removal from a solution of mixed nitrate, chloride and sulfate ions using a nitrate-selective carbon electrode', *Desalination*, vol. 320, pp. 10-6.

Yoon, H., Lee, J., Kim, S.-R., Kang, J., Kim, S., Kim, C. & Yoon, J. 2016, 'Capacitive deionization with Ca-alginate coated-carbon electrode for hardness control', *Desalination*, vol. 392, pp. 46-53.

Yu, J., Jo, K., Kim, T., Lee, J. & Yoon, J. 2018, 'Temporal and spatial distribution of pH in flow-mode capacitive deionization and membrane capacitive deionization', *Desalination*, vol. 439, pp. 188-95.

Yu, J., Qin, J., Kekre, K.A., Viswanath, B., Tao, G. & Seah, H. 2013, 'Impact of operating conditions on performance of capacitive deionisation for reverse osmosis brine recovery', *Journal of Water Reuse and Desalination*, vol. 4, no. 2, pp. 59-64.

Zarebska, A., Nieto, D.R., Christensen, K.V. & Norddahl, B. 2014, 'Ammonia recovery from agricultural wastes by membrane distillation: fouling characterization and mechanism', *Water research*, vol. 56, pp. 1-10.

Zarzo, D. & Prats, D. 2018, 'Desalination and energy consumption. What can we expect in the near future?', *Desalination*, vol. 427, pp. 1-9.

Zhang, C., He, D., Ma, J., Tang, W. & Waite, T.D. 2018, 'Faradaic reactions in capacitive deionization (CDI) - problems and possibilities: A review', *Water Research*, vol. 128, pp. 314-30.

Zhang, C., Ma, J., Song, J., He, C. & Waite, T.D. 2018, 'Continuous ammonia recovery from wastewaters using an integrated capacitive flow electrode membrane stripping system', *Environmental science & technology*, vol. 52, no. 24, pp. 14275-85.

Zhang, J., She, Q., Chang, V.W., Tang, C.Y. & Webster, R.D. 2014, 'Mining nutrients (N, K, P) from urban source-separated urine by forward osmosis dewatering', *Environmental science & technology*, vol. 48, no. 6, pp. 3386-94.

Zhang, W., Mossad, M., Yazdi, J.S. & Zou, L. 2016, 'A statistical experimental investigation on arsenic removal using capacitive deionization', *Desalination and Water Treatment*, vol. 57, no. 7, pp. 3254-60.

Zhang, W., Mossad, M. & Zou, L. 2013, 'A study of the long-term operation of capacitive deionisation in inland brackish water desalination', *Desalination*, vol. 320, pp. 80-5.

Zhang, Y., Desmidt, E., Van Looveren, A., Pinoy, L., Meesschaert, B. & Van der Bruggen, B. 2013, 'Phosphate separation and recovery from wastewater by novel electrodialysis', *Environmental science & technology*, vol. 47, no. 11, pp. 5888-95.

Zhang, Y., Paepen, S., Pinoy, L., Meesschaert, B. & Van der Bruggen, B. 2012, 'Selectrodialysis: fractionation of divalent ions from monovalent ions in a novel electrodialysis stack', *Separation and purification technology*, vol. 88, pp. 191-201.

Zhao, R., Biesheuvel, P., Miedema, H., Bruning, H. & Van der Wal, A. 2009, 'Charge efficiency: a functional tool to probe the double-layer structure inside of porous electrodes and application in the modeling of capacitive deionization', *The Journal of Physical Chemistry Letters*, vol. 1, no. 1, pp. 205-10.

Zhao, R., Biesheuvel, P. & Van der Wal, A. 2012, 'Energy consumption and constant current operation in membrane capacitive deionization', *Energy & Environmental Science*, vol. 5, no. 11, pp. 9520-7.

Zhao, R., Porada, S., Biesheuvel, P. & van der Wal, A. 2013, 'Energy consumption in membrane capacitive deionization for different water recoveries and flow rates, and comparison with reverse osmosis', *Desalination*, vol. 330, pp. 35-41.

Zhao, R., Satpradit, O., Rijnaarts, H., Biesheuvel, P. & Van der Wal, A. 2013, 'Optimization of salt adsorption rate in membrane capacitive deionization', *Water research*, vol. 47, no. 5, pp. 1941-52.

Zhao, R., Van Soestbergen, M., Rijnaarts, H., Van der Wal, A., Bazant, M. & Biesheuvel, P. 2012, 'Time-dependent ion selectivity in capacitive charging of porous electrodes', *Journal of colloid and interface science*, vol. 384, no. 1, pp. 38-44.

Zhao, Y., Wang, Y., Wang, R., Wu, Y., Xu, S. & Wang, J. 2013, 'Performance comparison and energy consumption analysis of capacitive deionization and membrane capacitive deionization processes', *Desalination*, vol. 324, pp. 127-33.

Zhao, Z.-P., Xu, L., Shang, X. & Chen, K. 2013, 'Water regeneration from human urine by vacuum membrane distillation and analysis of membrane fouling characteristics', *Separation and Purification Technology*, vol. 118, pp. 369-76.

Zhao, Z., Cao, H., Shi, S., Li, Y. & Yao, L. 2016, 'Characterization of anion exchange membrane modified by electrodeposition of polyelectrolyte containing different functional groups', *Desalination*, vol. 386, pp. 58-66.

Zhao, Z., Shi, S., Cao, H., Shan, B. & Sheng, Y. 2018, 'Property characterization and mechanism analysis on organic fouling of structurally different anion exchange membranes in electrodialysis', *Desalination*, vol. 428, pp. 199-206.

Zhu, E., Hong, X., Ye, Z., Hui, K. & Hui, K. 2019, 'Influence of various experimental parameters on the capacitive removal of phosphate from aqueous solutions using LDHs/AC composite electrodes', *Separation and Purification Technology*, vol. 215, pp. 454-62.

Zhu, S., Kingsbury, R.S., Call, D.F. & Coronell, O. 2018, 'Impact of solution composition on the resistance of ion exchange membranes', *Journal of membrane science*, vol. 554, pp. 39-47.

Zornitta, R.L. & Ruotolo, L.A. 2018, 'Simultaneous analysis of electrosorption capacity and kinetics for CDI desalination using different electrode configurations', *Chemical Engineering Journal*, vol. 332, pp. 33-41.

Zou, S., Wang, Y.-N., Wicaksana, F., Aung, T., Wong, P.C.Y., Fane, A.G. & Tang, C.Y. 2013, 'Direct microscopic observation of forward osmosis membrane fouling by microalgae: Critical flux and the role of operational conditions', *Journal of membrane science*, vol. 436, pp. 174-85.